



Fate of antibiotic resistance genes and bacteria under sequential redox conditions within biofilm reactors

Mui Choo Jong BSc (Hons), MSc

A thesis submitted to Newcastle University in partial fulfilment of the requirements of the degree of Doctor of Philosophy within the Faculty of Science, Agriculture and Engineering

School of Engineering
Newcastle University
Newcastle upon Tyne
NE1 7RU

February 2020

Declaration

I hereby certify that the work presented in this thesis is my original research work. Due reference is given to literature and any research collaborations where appropriate. No part of this thesis has been submitted previously for a degree at this or any university.

Mui Choo Jong

Abstract

Antibiotic resistance (AR) is a major health threat to global populations. However, mortal infections are most profound in Low-Middle-Income Countries (LMICs) where wastewater treatment is not universal and rarely precedes urbanisation. Therefore, reducing waste- and water-borne AR exposures through improved wastewater treatment is a high priority; however, few small-scale and economical technologies are available for application in LMICs.

This thesis studied low-energy, sponge-core bioreactors, called Denitrifying Downflow Hanging Sponge (DDHS) systems, as a technology reducing AR genes and bacteria from domestic wastewater. The technology uses sequential redox conditions (i.e., aerobic-anoxic), an option previously shown to enhance AR reduction in wastewater ecosystems. Here, DDHS systems were co-optimised for total nitrogen (TN) and AR genes removal, using a 20% influent wastewater bypass (by volume of total influent) to enhance denitrification in the second-stage anoxic unit. Under such conditions, removals of 2.0 to 3.0 log AR genes, >79% carbon and 71% TN were achieved. Subsequent 16S rRNA amplicon sequencing and microbiome characterisation indicated the wastewater bypass positively influenced resident microbial communities, especially increasing reactor biodiversity (Shannon diversity index for 0% bypass = 5.92 ± 0.05 and 20% bypass = 6.15 ± 0.03), which in turn, translated to improved overall treatment performance.

To better explain AR fate in the DDHS reactors, independent experiments assessed the impact of different redox conditions on relative transmission of AR gene-bearing plasmids. Biofilm and liquid phase samples from aerobic, anoxic and anaerobic bioreactors were collected and assessed for *in situ* horizontal gene transfer, tracked using a fluorescent-labelled AR plasmid assay (developed here) from a recombinant *E. coli* host added to the systems at seeding concentrations of 10^6 cells/mL. Overall, plasmid hosts disappeared more rapidly in the aerobic bioreactors (2.0 log net reduction; final concentrations = $4.4 \sim 4.7 \times 10^4$ cells/mL after 72 hours) and survived much longer in oxygen-free systems, especially in anaerobic biofilms (1.0 log net reduction; final concentrations = $1.6 \sim 2.7 \times 10^5$ cells/mL after 72 hours). However, evident conjugal transfer of the AR plasmid was limited in native biofilm communities.

Final work tested DDHS systems at pilot-scale in Southern Malaysia to operationalise and validate the technology for field application. A semi-optimised configuration was developed, effectively removing C and TN (respective percentage load removal at 55% and 53%; satisfying local discharge standards), micropollutants, and reducing AR genes by 1.0 to 2.0 log from the wastewater community. Promising field results warrant further development of future prototypes to fuel the uptake of the DDHS technology, especially for LMIC applications.

Acknowledgements

This PhD has been one of the most challenging and the best things I have ever done. I am deeply and forever grateful to my three supervisors: Prof. David Graham, Prof. Colin Harwood and Prof. Jason Snape, for their kindest patience, intellectual guidance and moral support throughout my doctoral journey. Each has nurtured me to develop and grow in every research and life aspects, and helped me to establish strong network. Your faith means a lot to me and my family.

I greatly appreciate AstraZeneca UK and the 'Engineering and Physical Sciences Research Council' (EPSRC) for providing financial support and funding, which has allowed me to undertake this doctorate: to conduct my experimental work and to travel to conferences. Mega thanks to Stephen Edward, Marcos Quintela, David Race, David Early and Lisa, for all their professional and laboratory support over the years, and to Susie for her invaluable help during one of my toughest experiments.

My sincerest thanks to all the lab buddies and colleagues I've met at Newcastle University, especially to Josh, Carl, Pani, Andy, Carolina, Aizat, Nur, Ismatul, and Burhan, for all your wonderful chats, motivation, and unselfish advice. You have made this journey enjoyable and less daunting. I also would like to thank Prof. Tom Curtis, for his continued encouragements, even though I am not one of his PhD flocs.

I have been extremely fortunate to forge long-lasting collaborations and lifetime friendships while I was in Malaysia running the field work. To Izah, Daniel, Mardhiah, Jia-Yee and Sylvia, I cannot thank you enough for your care and assistance. To Prof. Christ Baldwin, Dr. Michaela Goodson, and also to all staffs at NUMed, thank you for your support and being so welcoming. Also at NUS, I am grateful to Prof. Karina, and Dr. Ngoc Han Tran for kindly supporting the UHPLC/MS-MS training and analysis.

To my beloved parents, sisters: Olivia and Winnie, and brother-in-law, Kian Huat, thank you for being my number one supporters, my source of emotional strength and happiness. To my dearest husband, Robert, thank you for being there with me every step of the way, your unceasing love and care (and often your delicious cooking) are the most important stabilising factors that have helped me through tough moments. Needless to mention all the sacrifices you have made. I feel truly blessed to have you in my life and I praise Almighty God for '**ALL**' His work in me. Hallelujah! I did it!

Table of Contents

Declaration	iii
Abstract	v
Acknowledgements	vii
Table of Contents	ix
List of Figures	xiii
List of Tables	xx
List of Equations	xxi
List of Abbreviations	xxii
Chapter 1 Introduction	1
1.1 Aims and objectives	3
1.2 Overview of experimental chapters	4
Chapter 2 Literature review	5
2.1 The antibiotic resistance crisis	5
2.2 Disseminations of AR in the environment	8
2.3 Human activities and AR in the aquatic environment	11
2.4 Horizontal gene transfer (HGT) in environmental ecosystems	13
2.5 Environmental AR: A water, sanitation and hygiene (WASH) issue	14
2.6 WASH actions and guidance on AR control	15
2.7 Improving sanitation to combat environmental AR	16
2.8 Wastewater treatment technologies and AR removal	18
2.9 Strategic approach and practical technological solutions	19
2.10 Knowledge gaps	21
Chapter 3 Denitrifying Downflow Hanging Sponge (DDHS) bioreactors for reducing total nitrogen and antibiotic resistance genes in domestic wastewater	23
3.1 Introduction	23
3.1.1 Downflow Hanging Sponge (DHS) systems	25
3.1.2 Denitrifying Downflow Hanging Sponge (DDHS) systems	26
3.2 Materials and methods	27
3.2.1 Laboratory DDHS bioreactors for domestic wastewater treatment	27
3.2.2 Wastewater bypass for the optimisation of effluent nitrates removal	30
3.2.3 Influent source, routine sample analysis and monitoring	30
3.2.4 Sample collection, DNA extraction and ARB enumeration	31
3.2.5 High-throughput quantitative PCR (HTH-qPCR)	32

3.2.6	Genomic data screening and analysis	33
3.3	Results and discussion	34
3.3.1	Enhanced denitrification for decentralised wastewater treatment.....	34
3.3.2	Total abundances and patterns of ARGs and MGEs.....	35
3.3.3	Relative ARG and MGE abundances.....	37
3.3.4	Broader observations on ARG removal across DDHS bioreactors.....	38
3.3.5	Persistent and unique ARG and MGE subtypes, and practical implications	39
3.4	Conclusions	41
Chapter 4 Microbiomes within sponge biofilm reactors as a function of operating regime and local redox conditions		43
4.1	Introduction.....	43
4.1.1	Molecular microbial ecology.....	45
4.2	Materials and methods.....	46
4.2.1	Experimental background	46
4.2.2	Extraction of genomic DNA from Sponge biofilm	47
4.2.3	Amplicon preparation and Illumina Miseq 16S rRNA sequencing.....	47
4.2.4	Phylogenetic analysis workflow.....	48
4.2.5	Bioinformatics and statistics.....	49
4.2.6	Quantitative polymerase chain reaction (qPCR)	51
4.3	Results and Discussion.....	53
4.3.1	16S rRNA amplicon sequencing and abundances	53
4.3.2	Microbial α -diversity versus local redox	55
4.3.3	Microbiomes within sponge biofilms.....	58
4.3.4	Core microbial communities.....	60
4.3.5	Impact of wastewater bypass on β -diversity and relationships with process variables	63
4.3.6	Nitrogen transforming genes abundances	67
4.3.7	Abundance of faecal organisms and potential pathogens	70
4.4	Implications.....	72
4.4.1	DDHS microbial community diversity differs with operating regime.....	72
4.4.2	Dominant genera	73
4.4.3	DDHS diversity and overall reactor performances.....	74
4.5	Conclusions	75
Chapter 5 Impact of redox conditions on the fate of a resistance host and conjugative plasmid in biofilm reactors		77
5.1	Introduction.....	77

5.1.1	IncP-1 plasmids	79
5.1.2	Green fluorescent protein (GFP) marker and flow cytometry	80
5.1.3	Experimental systems and specific objectives	81
5.2	Materials and methods.....	81
5.2.1	Experimental design	81
5.2.2	Sequencing batch reactors set up.....	84
5.2.3	Operating conditions.....	86
5.2.4	Inoculum and start up	87
5.2.5	Routine sample collection and monitoring.....	88
5.2.6	GFP tagged pRP4	88
5.2.7	Fluorescence microscopy	89
5.2.8	Transformation of reporter E. coli.....	89
5.2.9	Seeding procedures.....	92
5.2.10	Sampling procedures.....	93
5.2.11	Extended seeding and sampling regimes (Phase 2)	94
5.2.12	Sample preparations for fluorescence cytometry analysis.....	95
5.2.13	Fluorescence cytometry quantification	97
5.2.14	Enumeration of the seeded E. coli reporter strain and presumptive transconjugants	97
5.2.15	DNA extraction and detection of gfpmut3b genes	101
5.2.16	16S sequencing for identification of transconjugants	102
5.2.17	Protozoa counts.....	102
5.2.18	Data analysis	103
5.3	Results and Discussion.....	104
5.3.1	Phase 1: Preliminary seeding tests	104
5.3.2	Phase 2: Seeding frequencies versus spatial and temporal patterns of pRP4- gfp hosts in SBBR.....	108
5.3.3	Transfer frequencies estimated by selective plate count	112
5.3.4	Identification and phylogenetic analysis of transconjugants	115
5.3.5	Elevated predation: a possible explanation for the reduced transfer frequencies observed under aerobic conditions	117
5.4	Implications.....	122
5.4.1	Tracing AR plasmids in bioreactors	122
5.4.2	Influence of redox and local niches	123
5.4.3	Removal of pRP4 hosts	124
5.4.4	Putative HGT in bioreactor.....	125
5.5	Conclusions	126

Chapter 6	Operating and optimising DDHS prototype as a small-scale domestic wastewater treatment technology, in Southern Malaysia	129
6.1	Introduction.....	129
6.2	Materials and methods.....	130
6.2.1	DDHS prototype design	130
6.2.2	Bioreactor installation	132
6.2.3	Operating regimes	133
6.2.4	Sample collection and analysis	136
6.2.5	Data analysis	140
6.3	Results and Discussion.....	141
6.3.1	Acclimatisation of the pilot DDHS system and operational challenges	141
6.3.2	Operational performance: Wastewater bypass versus recirculation regimes.	142
6.3.3	Richness and relative abundance of ARGs and MGEs in wastewater and DDHS effluents	146
6.3.4	Bacterial and ARBs removals	149
6.3.5	Unique removal patterns and persistent genes	151
6.3.6	DDHS core resistome: Diversity and abundance in biofilms.....	152
6.3.7	Micropollutants: Fate of antimicrobial agents and other personal care products in DDHS 155	
6.4	Conclusions	159
Chapter 7	Conclusions and future research.....	163
7.1	Conclusions	163
7.2	Potential future work	166
7.2.1	Sponge-core at molecular scale.....	167
7.2.2	Understanding the role and extent of horizontal gene transfer	167
7.2.3	Understanding ARG removal mechanisms	168
7.2.4	Reiterating prototype: modularity in design	168
7.3	Final thoughts	169
Appendices	171
Appendix A	172
Appendix B	191
Appendix C	194
Appendix D	206
References	219

List of Figures

- Figure 2-1** Consumption rate of four most-consumed therapeutic classes of antibiotics (DDDs per 1,000 inhabitants per day) by country income classification: High-income countries (HIC), Upper-Middle-Income countries (LMIC-UM) and Low-Middle-Income Countries (LMICs) (Klein et al., 2018). Specific area of usage was not defined..... 8
- Figure 2-2** An exemplary anthropogenic sources and distribution pathways of antibiotic resistance in the environment, where the aquatic environment is the interface between human, animals and the environment (EAWAG, 2015). 10
- Figure 2-3** Faecal-oral disease transmission pathways and interventions to break them (Yates et al., 2017)..... 17
- Figure 2-4** Locations in a waste management system highlighted in red where AR mitigation interventions might occur, aligned with Sustainable Development Goal 6.0; including SDG 6.2 via improved basic sanitation; SDG 6.3 via secondary treatment; and SDG 6.5 via advanced tertiary treatments (Graham et al., 2019b). 20
- Figure 3-1** Assembly of laboratory-scale DDHS bioreactors. (A) Reactor column made from PVC cylinder with side holes. (B) Starting from the left the bypass amendments were as follows: 0% bypass (Control; R-S0); 10% bypass (R-S10); 20% bypass (R-S20); and 30% bypass (R-S30). All reactors were configured with 30% internal recirculation of the final effluent (percentage by volume of total influent rate). (C) Schematic diagram showing sponge media and hydraulic configurations. 29
- Figure 3-2** DDHS reactors mean performance as a function of wastewater bypass. Stacked bars present mean COD levels (particulate and soluble fractions) and nitrogen constituents (Ammonium; Nitrate; Nitrite; and Organic-N) in raw wastewater and the reactor effluents (n = 12 per reactor). Error bars show standard deviation around the mean; R-S10, R-S20 and R-S30 had minor standard errors. 34
- Figure 3-3** Total abundance of ARGs and MGEs detected in the raw wastewater and DDHS reactor effluent samples conferring resistance to specific class of antibiotics. (A) Absolute gene copy numbers per mL of wastewater; (B) Relative gene copy numbers normalised to bacterial cell numbers derived from ambient 16S-rRNA gene abundances; (C) Relative percentages of ARG abundances across samples. The line shows absolute bacterial cell levels in the influent and effluents, which reflects eubacterial abundances (error bars ~ small deviations concealed by marker). The blow-up insert shows subtle differences among ARGs and MGEs in different DDHS reactor effluents. FCA = fluoroquinolone, quinolone, florfenicol,

chloramphenicol, and amphenicol ARGs; MLSB = Macrolide-Lincosamide-Streptogramin B ARGs. 36

Figure 3-4 Venn diagram showing overlap of ARGs among influent and effluent samples from different DDHS configurations. Subsets represent number of genes detected in the wastewater influent (59 ARGs); R-S0 (35 ARGs); R-S10 (35 ARGs); R-S20 (28 ARGs) and R-S30 (30 ARGs). The central overlap represents the number of persistent ARGs..... 40

Figure 3-5 Persistent ARGs not removed in any DDHS reactor configuration. Relative abundances of persistent ARGs in the influent and effluents of each reactor (top panel; ARGs noted in the legend), and corresponding relative percentages of ARGs in reactor influent and effluent based on proportion of total ARG copy numbers (bottom panel). 41

Figure 4-1 Workflow for microbiome data analysis using a combination of Qiime2 (Caporaso, 2018) and R statistical software 3.5.0 (R Core Team, 2013) DADA2: from raw reads to community analyses (Callahan et al., 2016a). Grey boxes denote upstream data processing using Qiime2; green boxes denote downstream statistical analysis in R. 48

Figure 4-2 qPCR quantification of 16S rRNA abundances of the sponge biofilms, as indicated by sponge layers, along sponge columns of the R-S0 and R-S20 bioreactors (n = 4; two technical replicates per biological replicate)..... 54

Figure 4-3 Comparisons of α -diversity between local biofilms, by sponge layers, within each bioreactor showing (A) Shannon and (B) Simpson indices and analysis of variance (ANOVA). Asterisks indicate the p significant values comparing mean diversity index per sponge layer to the group mean for that reactor. * denotes $p \leq 0.05$; ** denotes $p \leq 0.01$; *** denotes $p \leq 0.001$; **** denotes $p \leq 0.0001$ 55

Figure 4-4 Shannon and Simpson indices between DDHS biofilm samples and paired samples T-tests; A) & B) Shannon and Simpson indices comparisons by reactors; C) & D) Shannon and Simpson indices comparisons by redox environments within individual reactor. Asterisk * denotes $p \leq 0.05$; ** denotes $p \leq 0.01$; ns denotes $p > 0.05$ 57

Figure 4-5 Microbial compositions identified along sponge column where each section represents 11 sponge layers for the Control (R-S0) and Co-optimal (R-S20) bioreactors. (A) Bacterial relative abundance >3% at phylum level. (B) Relative abundances of the archaeal community belonging to phylum Euryarchaeota..... 59

Figure 4-6 Relative abundance of major genera (> 3% relative abundance) in the bioreactors. Each section represents 11 sponge layers for Control (R-S0) and Co-optimal (R-S20) bioreactor, including wastewater influent and treated effluents (Eff). 61

Figure 4-7 PCoA plot based on Unweighted Unifrac distances of all samples showing clustering of biofilm microbiomes together with wastewater and reactor effluents spanning 69% of total variations.....	64
Figure 4-8 CCA tri-plot of major genera (> 3% relative abundance) and locations for biofilm samples from all sponge layers of the DDHS bioreactors showing the correlation of environmental process variables. Shared-core genera were coloured black and other genera were shown by other colours.	66
Figure 4-9 Nitrogen-transforming gene levels across biofilms from all sponge layers, classified based on sequential steps preceded by nitrification and followed by denitrification in the second step. (A) Nitrifying gene abundances; (B) Denitrifying gene abundances showing differences in both bioreactors.	68
Figure 5-1 Bacterial gene transfer. (A) A bacterium containing chromosomal DNA and plasmids. Bacteria carry more than one type of plasmid, representing additional but optional genetic elements. Such plasmids are not considered as part of the cell's genome because the same plasmid may exist in two different species and be transferred across species (Clark and Pazdernik, 2013); (B) Transmission electron micrograph of bacterial plasmids (Bennett, 2008). (C) Overview of conjugation instigated by the formation of the pilus appendages.	78
Figure 5-2 Summary of experimental work plan for (A) Phase 1 and (B) Phase 2 seeding experiments. Three redox conditions were contrasted in parallel in both phases using sequencing batch bioreactors whereby Phase 1 compared liquid phase and biofilm systems under single-pulse seeding while Phase 2 compared biofilm systems under both single-pulse and semi-continuous seeding.	83
Figure 5-3 (A) Clean polyurethane sponge cut into 1cm x 1cm x 1cm cubes for use as immobilisers to support biofilm growth in bioreactors; (B) Sponge cubes containing biofilms taken from SBBR during pseudo-steady state.....	84
Figure 5-4 Laboratory assembly of sequencing batch reactors (SBR) used in seeding experiments; (A) Series of bioreactors consisting three contrasting redox in duplicate; (B) Schematic overview of the SBBR vessels containing sponge cubes for biofilm attachment. Starting from the left: aerobic biofilm reactors in duplicate, anoxic biofilm reactors (duplicates), and anaerobic biofilm reactors (duplicates). The temperature and circulation of water in the heating water baths were regulated by titanium aquarium heaters with water circulators (Ab Aqua Medic Ltd., UK) to provide constant temperature at 25 ± 2 °C.	85
Figure 5-5 (A) Phase contrast; and (B) epifluorescence micrograph of <i>Pseudomonas putida</i> KT2442 encoding pRP4-gfp. Visualisation of the overnight cell culture grown in LB broth	

supplemented with 12.5 µg/mL kanamycin at 30°C was performed using a Nikon Eclipse Ti fluorescent microscope as detailed in the next section. 89

Figure 5-6 Enumeration and screening of *E. coli* donor derivative strain, EcoFJ2, encoding Nal resistance and the pRP4-gfp plasmid. (A) UV illuminated colonies of the EcoFJ2 strain showing fluorescing GFP (left) and non-fluorescing colonies of the original unmodified environmental *E. coli* strain, EcoFJ1-Nal^r without pRP4-gfp (right), as a negative control. Plates were irradiated at a wavelength of 366 nm from a benchtop UV-transilluminator. (B) Phase contrast and (C) epifluorescence micrographs of the EcoFJ2 donor strain showing green fluorescent colonies on a Nikon Eclipse Ti fluorescence microscope. 92

Figure 5-7 Step-by-step workflow for sample preparation prior to flow cytometry analysis using the Attune NxT flow cytometer (ThermoFisher Scientific). 96

Figure 5-8 Enumeration of samples taken at different times from the bioreactors. Agar dishes illustrating the spot plating technique selecting for cells carrying the pRP4-gfp plasmids. Samples (10-µL) were plated neat (10^0) and as increasing dilutions (10^{-1} to 10^{-5}) and incubated over night at 30°C. The following day the plates were placed on a UV transilluminator to detect fluorescence and the colonies counted. (A) Selective agar containing antibiotics selecting for the *E. coli* EcoFJ2 donor strain (i.e. Amp, Kan, Tet, Nal); (B) Selective agar containing antibiotics selecting for all strains containing pRP4-gfp (i.e. Amp, Kan, Tet). The control strain was *E. coli* harbouring the original unmodified pRP4 plasmid with no GFP (not fluorescing under UV illumination) which was a gift from Professor C.M. Thomas, University of Birmingham, UK. Results with countable colonies and corresponding dilution factor was recorded. 98

Figure 5-9 Bacterial colonies on a selective and differentiation agar plate containing antibiotics selective for pRP4-based plasmids (i.e. Amp, Kan, Tc) and containing X-Gluc. *E. coli* strains produce blue colonies in the presence of X-gluc while other microbes will produce white or colourless (red arrows). *E. coli* strains were predominant bacteria in all samples. .. 99

Figure 5-10 Decision tree for the screening and isolation of presumptive transconjugants from sub-samples using selective media. 100

Figure 5-11 Trend of pRP4-gfp levels across Phase 1 bioreactors over 72 hours. The top row represents the flow cytometry data from biofilm and suspended samples in (A) aerobic, (B) anoxic and (C) anaerobic conditions. The bottom row (D-F) presents corresponding relative pRP4-gfp population within biofilm and suspended samples. Error bars indicate the standard deviation of biological replicates. 105

Figure 5-12 Spatial and temporal pattern of relative GFP population across contrasting redox conditions in biofilms and liquid phase samples. Error bars indicate the standard deviation of biological replicates.....	107
Figure 5-13 Spatial and temporal pattern of pRP4-gfp cell densities across contrasting redox conditions in biofilms and liquid phase samples during the pulse influx and continuous influx. Error bars indicate the standard deviation of biological replicates.	109
Figure 5-14 Estimated plasmid transfer frequency on recipients (T/R; putative transconjugant/total recipient cells), in biofilms and the liquid phase during pulse seeding and continuous seeding, taken after each cycle of 24 hours exposure.....	114
Figure 5-15 Phylogenetic tree based on neighbour-joining (NJ) method showing relationships between the EcoFJ2 seed strain and transconjugants isolated from difference samples.	117
Figure 5-16 Microscopic analysis of samples abstracted from (A) liquid phase; and (B) sponge biofilm from the aerobic SBBR before any seeding. Samples specimens were viewed at 400x magnification and predators were indicated by red arrows.	118
Figure 5-17 Protozoa numbers in samples abstracted from aerobic and anaerobic sponge biofilm and the liquid phase. Error bars indicate standard deviations.	119
Figure 5-18 Correlations between pRP4-gfp levels and protozoa count in liquid phase and biofilm samples. Shaded areas represent the 95% confidence level of the correlation coefficients.....	120
Figure 5-19 Microscopy analysis showing (A & C) Phase contrast, and (B & D) epifluorescence images of food vacuoles expressing GFP fluorescence suggesting pRP4 host cells potentially engulfed by predacious eukaryotes.	121
Figure 6-1 A schematic view of the pilot DDHS prototype showing configurations of treatment tanks with major components.....	131
Figure 6-2 Photographs of pilot plant installation at Taman Selesa STW, Johor Bahru. (A) DDHS apparatus were manufactured locally according to designed specifications; (B) designated space cleared and levelled for the installation of the pilot; and (C) onsite assembly of the pilot plant by the local contractor.	132
Figure 6-3 Pilot plant set up at Taman Selesa, Johor Bahru. Reactor consisted separate aerobic and anoxic tank with hydraulic operations controlled by pumps and a control panel. Aerobic tank was raised and mounted on a platform supported by steel frame structure with the anoxic tank located at the bottom to create a gravity flow within the system.	134

Figure 6-4 Retrofits to improve system operation in the field. (A) A stainless steel filter; and (B) additional clarifier installed upstream of the influent storage tank at Taman Selesa STW which were designed to prevent clogging of the hydraulic system of the pilot DDHS. 142

Figure 6-5 Comparisons of pollutants load removals (kg pollutants/m³-sponge/day) through four operating conditions OP1-OP4 using the pilot DDHS. Boxplot (n = 11 per operation, except for n = 8 for OP3) showing ranges of load removals for (A-B) carbon and (C-F) nitrogen pollutants, with the points inside boxes representing means of removal rates per operation..... 144

Figure 6-6 Comparisons between OP2 (20% bypass; aerobic recirculation) and OP4 (20% bypass; complete recirculation) over three independent sampling weeks showing (A) absolute gene copies per mL (GC/mL); (B) relative abundance normalised per bacterial genome (GC/cell); and (C) relative percentages of ARG and MGE abundances across samples. Abundance of ARGs and MGEs detected in the raw wastewater and DDHS reactor effluent samples conferring resistance to specific class of antibiotics, including, for ARGs, aminoglycosides, b-lactams, FCA (fluoroquinolone, quinolone, florfenicol, chloramphenicol and amphenicol resistance genes), MLSB (macrolide-lincosamide-streptogramin B), other/efflux (multidrug-efflux pumps or others), sulphonamides; tetracyclines; and vancomycin. Error bars show standard deviation (n = 6 per sample per operating regime).147

Figure 6-7 Bacterial levels quantified at redox treatment steps during OP2 and OP4, with (A) bacterial cell number estimated from quantified total 16S concentrations of individual sample using the average16S rRNA-encoding genes per bacteria genome (4.1 copies per genome; RrnDB database); (B) count of enterobacteriaceae colonies cultured on Hicrome coliform media with and without antibiotic supplements (n = 6). Error bars show standard deviation around the mean..... 150

Figure 6-8 Venn diagram showing distribution of detected ARGs and MGEs among influent, post-aerobic effluent and final effluent samples from contrasting operating DDHS configurations, OP2 and OP4. Subsets represent number of unique genes detected in aqueous samples with the central overlap represents the number of persistent ARGs. 152

Figure 6-9 Diversity and relative abundance of sponge biofilms abstracted from the aerobic core (Top and Middle) and the anoxic core (Bottom) during operating regimes OP2 and OP4. (A) Relative gene copy per cell (GC/cell) of ARGs and MGEs normalised to bacterial cell numbers derived from 16S-rRNA gene abundances for each sample; (B) number of antibiotic resistance genes (ARGs); and (C) mobile genetic elements (MGEs) at different sites along reactor depths. Error bars show standard deviation around the mean (n = 3). 154

Figure 6-10 Concentrations of the target pharmaceuticals and personal care products (PPCPs) in raw influent, post-aerobic treated effluent and final effluent of DDHS operated at OP2 and OP4, with (A) array of detected antimicrobial agents; (B) other personal care products and caffeine. Error bars show standard deviation around the mean (n = 6 per sample per sampling location). 157

Figure 6-11 Boxplot for antibiotics, antiseptics and personal care products (PCPs) measured and detected in the final effluents of OP2 and OP4. Light purple area represents method detection limit of the SPE-HPLC/MSMS; red lines mark the PNEC (predicted no effect concentration) as proposed by Bengtsson-Palme and Larsson (2016); *no PNEC defined (Bengtsson-Palme and Larsson, 2016). 159

List of Tables

Table 2-1 New antibacterial drugs launched since 2000 divided into natural-product (NP) and synthetically-derived listed by antibiotic classes (Butler and Cooper, 2011).	7
Table 3-1 Influent flow rates to the top of bioreactors and bypass points of each bioreactor.	30
Table 4-1 Primer sets used for qPCR assays of all samples including their sequences and appropriate reaction conditions.	52
Table 4-2 Relative abundance of faecal indicators throughout sponge layers.	71
Table 5-1 Antibiotic susceptibility tests results of an environmental strain of <i>E. coli</i> , EcoFJ1, performed at the Department of Pathology (Freeman Hospital, Newcastle upon Tyne).	90
Table 5-2 Sampling time points designated for Phase 1 and Phase 2.	94
Table 5-3 Screening of bacterial colonies from redox samples for isolating presumptive transconjugants.	101
Table 5-4 P-values, showing significant differences for comparisons between the liquid phase and biofilm samples at different redox conditions in sequencing batch reactors seeded with pRP4-gfp EcoFJ2.	106
Table 5-5 P-values, showing significant differences of pRP4-gfp levels for comparisons between suspended and biofilm samples at different redox conditions in sequencing batch reactors during Phase 2 experiments.	111
Table 5-6 Significant species detected based on sample DNA sequencing and database sequences in the NCBI nucleotide database.	116
Table 6-1 Testing of pilot reactor at four hydraulic operating conditions to assess the impact of bypass and recirculation regimes.	135
Table 6-2 Array of monitored pharmaceuticals and personal care products (PPCPs) in aqueous phase of reactor samples, during pseudo-steady state sampling campaigns for OP2 and OP4.	156

List of Equations

Equation 4-1 The equation used to determine species diversity which takes into account both richness and evenness.....	56
Equation 5-1 The equation used to determine the daily liquid exchange volume based on designed hydraulic retention time.....	87
Equation 5-2 The equation used to determine the volume of sludge wasting based on designed solid retention time.....	87
Equation 5-3 The equation used to determine the transfer frequency from original seed organism to potential recipient cells present in the bioreactors (Yang et al., 2013a).....	113
Equation 6-1 The equation used to determine percentage of load removal rate based on pollutants loading onto sponge media.	143

List of Abbreviations

AMR	Antimicrobial resistance
ANOVA	Analysis of variance
AR	Antibiotic resistance
ARB	Antibiotic resistant bacteria
ARG	Antibiotic resistance genes
ASV	Amplicon sequence variant
CRE	Carbapenem resistant Enterobacteriaceae
DDHS	Denitrifying downflow hanging sponge
DHS	Downflow hanging sponge
DNA	Deoxyribonucleic acid
DO	Dissolved oxygen
ESBL	Extended-spectrum beta-lactamase
FCM	Flow cytometry
GFP	Green fluorescent protein
HGT	Horizontal gene transfer
HIC	High-Income country
UHPLC	Ultrahigh performance liquid chromatography
HRT	Hydraulic retention time
HTH-qPCR	High-throughput quantitative polymerase chain reaction
LMIC	Low-Middle-Income country
MCR-1	Mobilized colistin resistance
MDR	Multi-drug resistance
MGE	Mobile genetic element
MIC	Minimum inhibitory concentration
MS	Mass spectrometry
NDM-1	New Delhi metallo- β -lactamase (<i>bla</i> NDM-1)
OLR	Organic loading rate
PCR	Polymerase chain reaction
PPCP	Pharmaceutical and personal care products
PU	Polyurethane
QPCR	Quantitative polymerase chain reaction

SBR	Sequencing batch reactor
SBBR	Sequencing batch biofilm reactor
SRT	Sludge retention time
TN	Total nitrogen
UK	United Kingdom
USA	United States of America
WASH	Water, sanitation and hygiene
WWTP	Wastewater treatment plant

Chapter 1 Introduction

Antibiotics had truly transformed the treatment against deadly bacterial infections, which has saved millions of lives around the world since the post-war years. Despite mainly being used to treat infections, they also have enabled health services in the ways (e.g., advanced surgeries), allowing modern medicine to enhance the quality of life and prolong life expectancy (Gould and Bal, 2013; Wright, 2014). However, the rise of antimicrobial resistance (AMR) in recent decades has hugely eroded treatment efficiencies, causing the global emergence and dispersal of antibiotic resistant bacteria, both in natural and clinical settings (Davies and Davies, 2010).

Antibiotic resistance (AR) happens when bacteria develop the ability to defeat the antibacterial drug designed to kill them. AMR is a broader term encompassing resistance to drugs used to treat infections caused by other microorganisms as well, such as viruses and parasites. Initially, AR was more prevalent in the clinical settings, where hospitals were the foci of resistance incidents and contagions. As such, clinical AR was better understood. However, since around 2000, evidence of “environmental” AR was increasing, with elevated resistance in bacteria being reported away from hospitals in different natural environments, including soils (Wright, 2010; Knapp *et al.*, 2011), water (Baquero *et al.*, 2008; Zhang *et al.*, 2009a) and river sediments (Pruden *et al.*, 2006; Knapp *et al.*, 2012). For example, clinically relevant AR genes and mobile genetic elements (MGEs) were found on farms (Smith *et al.*, 2004; Zhu *et al.*, 2013), with highly diverse and abundant AR levels being detected in feedlot soils and lagoons, and across the food chain (Horton *et al.*, 2011; Founou *et al.*, 2016). In parallel, clinical AR continued to grow. Medical practices were increasingly challenged by growing treatment complications, sequelae and mortality, including multidrug resistant pathogens; more infamously called ‘superbugs’ (Walsh *et al.*, 2011; Liu *et al.*, 2015). Since then, AR has become topical, and is now studied by clinical, environmental and trans-disciplinary scientists (Cantas *et al.*, 2013).

Increasing AR is the result of a complex web of events. It is comprised of many sources, drivers, and distribution pathways, interlaced among human, animal and

environmental factors (Section 2.2), which is a ‘One Health’ issue (AVMA, 2008). The AR epidemiology coincided with the dramatic growth in world population since 1950s (Hawkey and Jones, 2009), which has seen an upsurge in food and water demand (Roura *et al.*, 1992; Vaz-Moreira *et al.*, 2011), and also the globalisation of human movements and their food products (Cantas *et al.*, 2013). In summary, although AR in microbes occurs naturally in the environment (originally intrinsic for survival and colonisation), the rise of antibiotics usage, i.e., misuse and often overuse, and improper downstream waste disposal have accelerated bacterial AR in the recent decades. It has become one of the most urgent health threats of our time.

AR is a societal problem. Particularly, greater infection mortality and morbidity exist in Low-Middle-Income Countries (LMICs), especially in emerging nations, where populations are rising and urbanising (e.g., Asia and Africa), but plagued with poor sanitation and waste management (Pimentel *et al.*, 2007; Ayukekbong *et al.*, 2017). Elevated AR and the infectious disease burden appear to be linked to chronically polluted water bodies because emissions of inadequately treated or even untreated wastewater into the environment is common and widespread (Graham *et al.*, 2011; Ahammad *et al.*, 2014). Moreover, aquatic ecosystems contaminated with wastewater-borne AR genes and bacteria also are impacted by organic pollutants (e.g., nutrients) and other co-contaminants (e.g. antibiotics, heavy metals, biocides), which have been implicated to select or co-select for AR in exposed environments (Baker-Austin *et al.*, 2006; Wales and Davies, 2015; Singer *et al.*, 2016).

Regardless of growing evidence, the key role of regionally poor water quality in global AR transmission is still underappreciated in the AR discourse (Graham *et al.*, 2014), despite resistance strains that have emerged in LMICs linked to polluted water (Ahammad *et al.*, 2014) and spread rapidly across the globe (Kumarasamy *et al.*, 2010). It is important to recognize that although antibiotic use is the major cause of the emergence and maintenance of AR, other factors contribute to its prevalence and transmission, for example, poor sanitation (Collignon *et al.*, 2018). Therefore, improving local water quality through the treatment of wastewater is a priority if we want to reverse the present trend of increasing global AR (Burgmann *et al.*, 2018; Graham *et al.*, 2019b). However, most conventional wastewater treatment options are expensive, mainly due to elevated energy demands and costly sewerage infrastructure. Therefore, they are usually unaffordable in LMICs. As such,

developing alternative treatment technologies suitable for local and smaller scale implementation is a strategic approach for such locations (Graham *et al.*, 2019b). For this purpose, the basic strategy here is to increase local wastewater treatment in regions with limited civil infrastructure, using smaller-scale technical options to curb AR release, its exposures and spread across the environment.

This thesis assesses a novel low-energy treatment option ideally suited for the treatment of domestic wastewater at smaller scales. This biofilm-based sponge-core technology, called Denitrifying Downflow Hanging Sponge (DDHS) reactors, is designed to purify wastewater through sequential redox steps (i.e., aerobic-anoxic) and hydraulic schemes, which has been shown to effectively remove primary organic pollutants, i.e., carbon (C) and nitrogen (N). The root of the new work here was that sequential redox exposures also may be effective at mitigating AR genes (ARG) and bacteria (ARB) spread (Christgen *et al.*, 2015). However, more research is needed to better explain the primary removal mechanisms of ARG and ARB in such systems. And such essential knowledge is also needed to improve designs, optimise AR removal rates, and ensure process reliability into the future. It is envisioned that as new DDHS designs evolve, the technology will translate to the real world scenarios, such as decentralised wastewater treatment in LMICs and-or other AMR hotspots.

1.1 Aims and objectives

The central goal of this thesis is to evaluate the rates and mechanisms of ARG and ARB removal in sponge-core DDHS bioreactors. This goal was met by performing the following key objective tasks:

1. Assessing antibiotic resistance profiles in and out of DDHS systems treating settled domestic wastewater using different wastewater bypass schemes
2. Elucidating microbial community structure within sponge reactor biofilms as a function of sequential redox habitat and bypass schemes, especially as they related to different levels of TN removal and AR treatment success.
3. Investigating the impact of redox conditions on the spatial and temporal fate of an AR host and plasmid in biofilms and the liquid phase in a series of experimental bioreactors.
4. Examining ARGs and other treatment targets in pilot-scale DDHS systems in Malaysia to test how operational lab data is translated to field applications.

1.2 Overview of experimental chapters

A series of sub-studies were conducted to evaluate DDHS systems using lab bioreactors and then pilot-scale reactors in Malaysia. The first study described in Chapter 3 examined the resistomes of influent and effluents from four sponge-core bioreactors with varying hydraulic regimes, with the aim to co-optimize the bioreactor for total nitrogen and ARG removal. Here, we used high-throughput quantification to screen and quantify the fate of ARGs and mobile genetic elements (MGEs) in raw wastewater and treated effluents in four reactor designs. This work also led to the microbiome analysis of contrasting bioreactors (i.e., the 'most' versus the 'least' effective in terms of ARG removal) to characterise microbial communities in the sponge biofilms relative to local redox habitats and hydraulic regimes (Chapter 4). It is essential to understand how different operating designs influence microbial communities to explain relative bioreactor performance in terms of nutrients (C and N), total bacteria, and AR genes removal.

In the next sub-study (Chapter 5), targeted experiments were performed on the fate of a recombinant *E. coli* host, which had been inserted with a genetically modified AR plasmid (green-fluorescent-labelled), in independent sequencing batch biofilm reactors sustained under different redox conditions. The bioreactors were seeded with the fluorescent-labelled reporter strain to track AR plasmid and host migration and putative gene exchange as a function of redox conditions and biofilm conditions. We focused on the changes in biofilm and liquid phase using combined classical microbiology and molecular fluorescent cytometry to determine the spatial and temporal patterns of host fate and gene transfer in the different reactors.

Finally, a pilot-scale DDHS reactor system was built, operated, and monitored in peri-urban Malaysia to assess whether the technology could translate to application in a LMIC. Different hydraulic configurations were tested and semi-optimal design was developed (Chapter 6). Laboratory groundwork did translate well to the field, which shows the technology may be an effective option for reducing AR spread via wastewater in a LMIC scenario.

Chapter 2 Literature review

2.1 The antibiotic resistance crisis

The discovery and subsequent utilisation of antibiotics in healthcare since the 1940s is one of the most successful medical achievements. Antimicrobial medications to treat infectious diseases have had profound impacts on human health by enabling rapid treatment of infected patients, which has substantially reduced the burden of infectious disease and mortality worldwide, both in the developed and developing world (Davies and Davies, 2010). However, the recent global rise of antimicrobial resistance (AMR) has caused a setback in modern medicine because drug regimens are becoming ineffective against previously susceptible target microorganisms, resulting in chronic and incurable infections.

Antimicrobial resistance (AMR) refers to the development of resistance in microbes; e.g., bacteria, virus, fungi, and parasites to antimicrobial medicines, such as antiparasitic, antivirals, and antifungals to which they were previously sensitive (WHO, 2001). Antibiotic resistance (AR) is one type of AMR, and happens when bacteria no longer respond to antibacterial agents designed to stop or kill them. As cautioned by Sir Alexander Fleming (the discoverer of penicillin in 1928) in the Nobel Prize lecture, AR is the ability of a bacteria to defend itself from antibiotics targeted against them (Davies, 1994). Such resistance to antibiotics can either be intrinsic or acquired (James, 1999), which result from “natural” cellular mechanisms in a given bacterial species (Munita and Arias, 2016) or the acquisition of new, specific mechanisms of resistance via bacterial gene exchange or mutations (van Hoek *et al.*, 2011), respectively. Although resistance occurs naturally in bacteria since ancient times (Martínez, 2008), anthropogenic influences due to mass use and casual administration of antibiotics have fuelled globally increasing AR in the recent decades (Ventola, 2015).

Broadly speaking, current acquired AR is driven by combinations of: (i) overuse and misuse of antibiotics; (ii) global dissemination due to international travel (e.g., tourism, migration, food imports, wildlife); and (iii) environmental emissions of AR

bacteria and genes, and antibiotics themselves (Hawkey and Jones, 2009; Canica *et al.*, 2015). Particularly in the environmental domain, Collignon *et al.* (2018) showed factors such as poorer infrastructure (e.g., health, sanitation), poorer governance (e.g., corruption), and even climate shift are contributing to the rise and prevalence of AR. These factors, together with the bacteria world's ever evolving defence features to sense and adapt antibiotic assault (William *et al.*, 2013), make AR and AMR very difficult to eliminate and even control.

Our worry is real because even the 'last line' antibiotics, such as broad-spectrum carbapenems and colistin, are becoming incapable of treating infections. The distribution of carbapenem-resistant Enterobacteriaceae (CRE) since 1990s has reached epidemic levels in recent years, affecting populations across the world (Logan and Weinstein, 2017). This has led to the reintroduction of colistin, a toxic but potent antibiotic that can cure infections due to CRE. Unfortunately, colistin resistance has now been spotted in China (Liu *et al.*, 2015) and has quickly spread to other countries, such as Spain, Germany and the United States (Prim *et al.*, 2016; Wang *et al.*, 2018). Besides, other 'priority pathogens' (WHO, 2017a), such as extended-spectrum-beta-lactamase (ESBL) producing Enterobacteriaceae and vancomycin resistant *Enterococcus* spp., are becoming widespread in the environment around the world (Shaikh *et al.*, 2015; Nishiyama *et al.*, 2017). Evidence shows that up to 46% of human populations in the West Pacific and 22% in Africa have fecal colonization by ESBL-producing Enterobacteriaceae (Karanika *et al.*, 2016). Further, a recent report suggests '*...the risk of the emergence and spread of antibiotic resistance in South East Asia is the highest of the World Health Organization regions...*' (Chereau *et al.*, 2017). Here, higher AR risks exist because a majority of communities live with inadequate sanitation and contaminated water supply (Singh, 2017). Similar to the scenario in Africa, 22% of its population have fecal colonization with ESBL-producing Enterobacteriaceae (Karanika *et al.*, 2016). In short, AR is more prevalent in Low-Middle-Income Countries (LMICs), which seeds regional AR and fuels the further spread of AR to the wider globe.

Drug-resistant infections already cost too many lives; i.e., 700,000 people die worldwide every year (likely underestimated; Review on AMR (2014)) due to AR infections. This pattern, which is bad enough, is predicted to increase to 10 million annual deaths by year 2050 if we do not become more proactive and holistic in our

interventions (Review on AMR, 2016b). Moreover, there are increasing multidrug resistant (MDR) pathogens in parallel with limited new antibiotic discovery, which has become growingly apparent in the pharmaceutical industry since late 1980s (Silver, 2011). Antibiotic development demands high costs and long times, and there are also increasing pressure to curtail antibiotic usage to reduce emergence of resistance; antibacterial research and development stagnates (Nelson, 2003). Since 2000, only 20 new antibiotics have been launched worldwide (Table 2-1), with another six undergoing Phase-III clinical trials. Today, however, resistance has been reported to almost all drugs implemented since. For example, carbapenem resistance as discussed earlier (Leavitt *et al.*, 2009; Li *et al.*, 2015).

Table 2-1 New antibacterial drugs launched since 2000 divided into natural-product (NP) and synthetically-derived listed by antibiotic classes (Butler and Cooper, 2011).

Year	Name	Class
NP-derived		
2002	Biapenem	β -Lactam (carbapenem)
2002	Ertapenem	β -Lactam (carbapenem)
2005	Doripenem	β -Lactam (carbapenem)
2009	Tebipenem pivoxil	β -Lactam (carbapenem)
2008	Ceftobiprole medocaril	β -Lactam (cephalosporin)
2010	Ceftaroline fosamil	β -Lactam (cephalosporin)
2001	Telithromycin	Macrolide (ketolide)
2003	Daptomycin	Lipopeptide
2005	Tigecycline	Tetracycline
2007	Retapamulin	Pleuromutilin
2009	Telavancin	Glycopeptide
Synthetically-derived		
2000	Linezolid	Oxazolidinone
2002	Prulifloxacin	Fluoroquinolone
2002	Pazufloxacin	Fluoroquinolone
2002	Balofloxacin	Fluoroquinolone
2004	Gemifloxacin	Fluoroquinolone
2007	Garenoxacin	Quinolone
2008	Sitafloxacin	Fluoroquinolone
2009	Antofloxacin	Fluoroquinolone
2009	Besifloxacin	Fluoroquinolone

It seems that we will soon (or perhaps already) have as many antibiotics as we will ever have. In summary, the worldwide increase of AR is rapidly exhausting available drugs for infections treatment due to decreased therapeutic effectiveness in antibiotics; common bacterial infections can be fatal again.

2.2 Disseminations of AR in the environment

Antibiotics use anywhere can lead to resistance and antibiotics have not only been used in human medicine (Laxminarayan *et al.*, 2013). The use of antibiotics is diverse and global consumption has increased by 65% between 2000 and 2015 (21.1-34.8 billion defined daily doses; DDDs) (Figure 2-1).

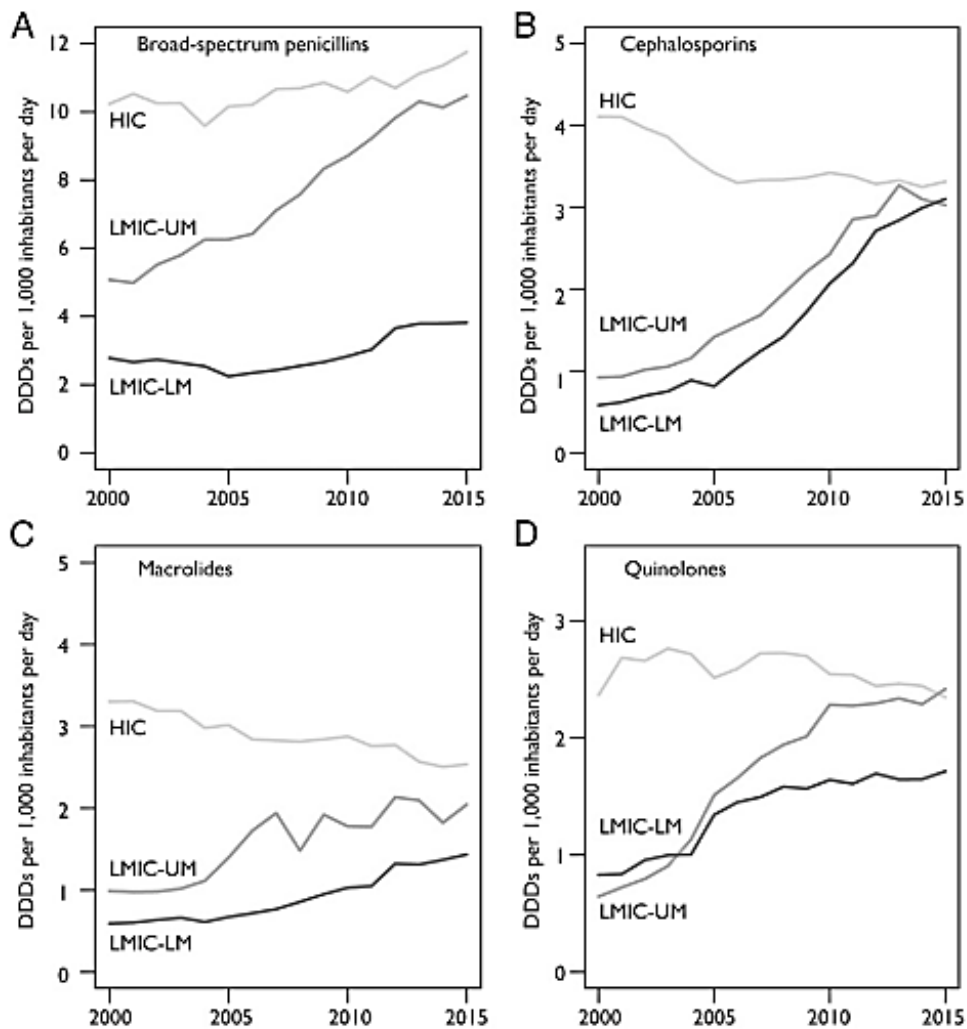


Figure 2-1 Consumption rate of four most-consumed therapeutic classes of antibiotics (DDDs per 1,000 inhabitants per day) by country income classification: High-income countries (HIC), Upper-Middle-Income countries (LMIC-UM) and Low-Middle-Income Countries (LMICs) (Klein *et al.*, 2018). Specific area of usage was not defined.

As the world population boomed after the World War II, increasing food demand had transformed traditional farming to large-scale commercial farming, with antibiotics being used increasingly for growth promotion and prophylactic measures to boost production (Verraes *et al.*, 2013). This led to the misuse and often overuse of antibiotics in livestock and aquaculture, which fosters the emergence and maintenance of AR in animal's gut microflora (FAO, 2016). Antibiotics together with commensal AR bacteria eventually pass into the environment through animal wastes (e.g., manure, slurry and sludge), and via the reuse of biological residues in agricultural soils as fertiliser (Review on AMR, 2015). It also was more common for farmers to add antibiotics directly into fish and shrimp farming ponds, which is a huge industry in developing and emerging economies (e.g., Philippines, Thailand). Therefore, AR bacteria and even MDR bacteria now have been isolated from aquaculture products, water, and sediment (Tendencia and de la Peña, 2001; Akinbowale *et al.*, 2006). Given this, waste-borne AR bacteria and antibiotics are now pervasive in food farming, soils, agricultural run-off, and even crops that end up with consumers (Founou *et al.*, 2016).

Human waste also is a problem because humans, livestock, fish farms, and even our pets are being treated with similar or even the same classes of antibacterial agents to treat infectious diseases (De Briyne *et al.*, 2014; Graham *et al.*, 2019a). Waste-borne AR bacteria of human origin can be released into natural ecosystems through different routes (Figure 2-2), which are then spread via environmental exposures, the food chain, and drinking water. AR in the environment converges people, animals and their mutual surrounding environment, therefore, it is a quintessential One Health issue, which AVMA (2008) defines as “...*the collaborative effort of multiple disciplines-working locally, nationally, and globally – to attain optimal health for people, animals and our environment...*”.

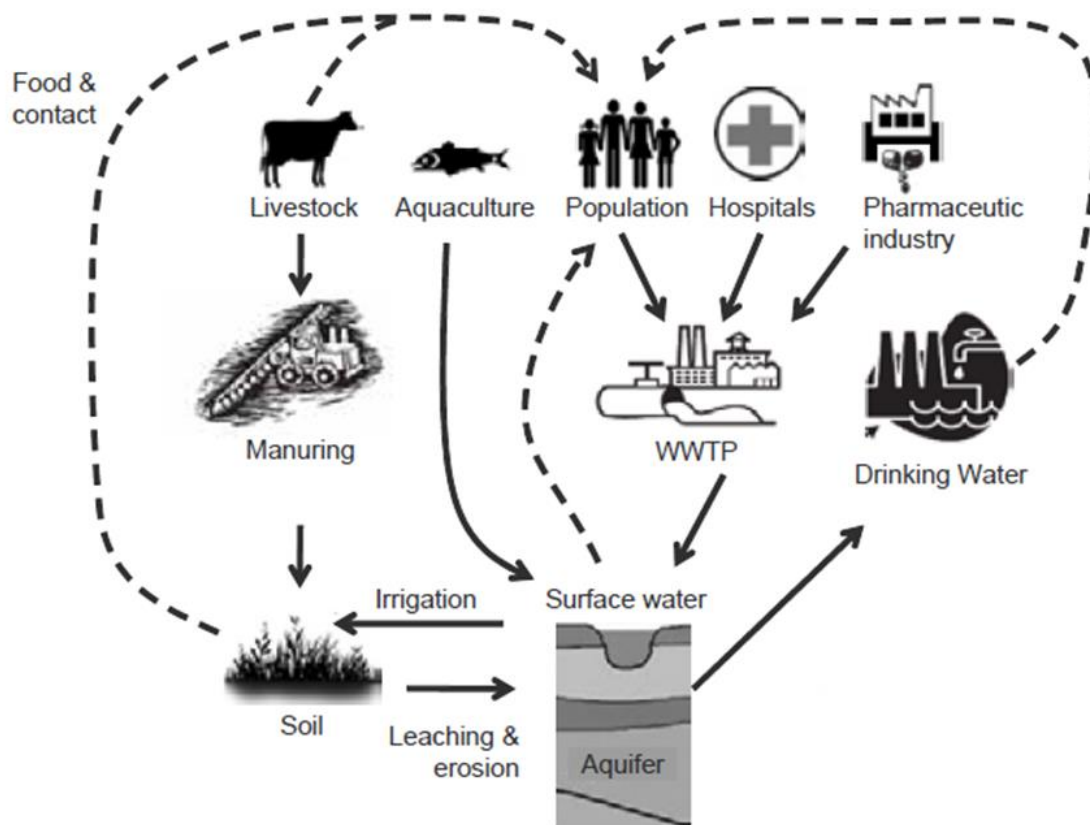


Figure 2-2 An exemplary anthropogenic sources and distribution pathways of antibiotic resistance in the environment, where the aquatic environment is the interface between human, animals and the environment (EAWAG, 2015).

Further, reports recently stated that earth's climate change could worsen global AR, whereby differences in ambient temperatures of 10 °C in the United States (USA) was stochastically associated with increases in AR of 4.2%, 2.2%, and 2.7% for the common pathogens *Escherichia coli*, *Klebsiella pneumoniae* and *Staphylococcus aureus*, respectively across USA (MacFadden *et al.*, 2018). Similar temperature relationships were seen in India related to CRE exposures in urban drains (Lamba *et al.*, 2018). This relationship is plausible as commensal bacteria thrive in the intestine of warm-blooded animals, including healthy humans (Blaak *et al.*, 2014), therefore temperature is a strong abiotic factor which affects their survival and growth. For example, in a five-year review of infections in burns intensive care units, researchers for infectious diseases in Singapore suggested that high incidence of *Acinetobacter baumannii* occurred in tropical, warm climate (Chim *et al.*, 2007), which also was evident in Indian surface waters (Lamba *et al.*, 2018).

In addition, more extreme weather caused by global warming (e.g., torrential rain and flooding) might further lead to outbreaks of infectious water-borne diseases and AR, as water and soils move in mass and can disperse biohazardous pollutants, including fecal contaminants, especially in places with open sewers and open defecation (Brown and Murray, 2013; Okaka and Odhiambo, 2018). Very recently, the Chief Medical Officer in the United Kingdom, Professor Dame Sally Davies, warned that the AR crisis paralleled climate emergency as a global concern, whereby it may soon become irreversible if we do not act quickly to reverse the trend (The Guardian, 2019).

2.3 Human activities and AR in the aquatic environment

AR bacteria (ARB) and AR genes (ARG) in the environments are diverse and abundant (Lu *et al.*, 2010; Amos *et al.*, 2014; Ghaderpour *et al.*, 2015), which can promote the evolution and dispersal of new resistant strains (William *et al.*, 2013). As discussed earlier, AR can enter the environment via wastewater streams, whereby water is an important transport medium for the proliferation and carriage of ARB in the environment (Quintela-Baluja *et al.*, 2015). MDR pathogens have been detected in various water sources around the world due to disposal of human wastes into the aquatic systems (Graham *et al.*, 2011; Finley *et al.*, 2013). In seminal work, Ahammad *et al.* (2014) show that excreta-related wastes released during seasonal pilgrim influxes in the famous Upper Ganges River significantly increased the levels of MDR *bla*_{NDM-1} genes across sampling sites. When pilgrims were absent, the concentrations of fecal coliform and *bla*_{NDM-1} genes dropped, suggesting that the migration of largely urban pilgrims increased MDR in pseudo-pristine sites during temporary visits. Resistant Gram-positive bacteria also are ubiquitous in freshwaters, where greater numbers of vancomycin resistant enterococci (VRE) were increasingly detected in urban rivers, especially downstream of densely populated areas (Lata *et al.*, 2009; Nishiyama *et al.*, 2017).

Studies analysing ARGs in the recreational aquatic environment, showed that beach and river waters are contaminated with MDR faecal bacteria (de Oliveira and Watanabe Pinhata, 2008; Blaak *et al.*, 2015), both Gram-positive and Gram-negative, which are of evident human origin. For example, an extensive monitoring programme along the River Danube (Joint Danube Survey 2013) by Kittinger and co-workers

found MDR ESBL-producing Enterobacteriaceae, including *E. coli* and *Klebsiella pneumoniae* which are resistant to clinically important drugs like carbapenem (Kittinger *et al.*, 2016). Moreover, elevated ARGs also were detected in lake waters which linked to increased human activities in a lake Geneva catchment as shown by Czekalski *et al.* (2012), and by Koczura *et al.* (2015) who assessed recreational lakes in Poland. In both studies, MDR strains of apparent faecal bacteria were identified from lake water and sediment samples. This shows an apparent public health risk of the spread of infectious illness through direct exposure to contaminated water and even ingestion of resistant pathogens during water sports, such as swimming and surfing (Leonard *et al.*, 2015).

In Southeast Asia (SEA), water is central to many economic activities, which supports securing industry, a water-food nexus, and transportation, and hence, regional socioeconomic progress over the last decades (El-Hifnawi, 2014; Pangare *et al.*, 2014). Here, thousands of local communities are relying on river water for sustaining livelihood, mainly through fisheries, coastal farming and tourism (Pangare *et al.*, 2014; Viswanathan and Bahinipati, 2016). However, regional water also suffers from chronic pollution that means people are at greater risk of AR exposures from aquatic environments. Tropical waters are often polluted with diverse MDR bacteria and genes, for example in mangrove fishing villages in Malaysia (Ghaderpour *et al.*, 2015) and across aquaculture systems in the Mekong Delta (Brunton *et al.*, 2019). It is becoming clear that environmental AR scenarios in the developing nations and the fully developed nations are similar; resistance determinants are everywhere in the water environment due to various human activities.

Overall, the increasing AR burden in aquatic environments is mainly caused by microbial contamination from point and non-point sources, such as agricultural run-off, infiltration of poorly maintained septic systems, and disposal of inadequately treated wastewater (Graham *et al.*, 2011; Knapp *et al.*, 2012; Ahammad *et al.*, 2014). Effluents discharge from wastewater treatment plants is one avenue of emissions, which caused elevated ARGs in freshwater lakes, for example across 21 lakes in Switzerland as shown in studies by Czekalski *et al.* (2015), in rivers (Taucer-Kapteijn *et al.*, 2016; Yang *et al.*, 2016) and in coastal waters (Zhu *et al.*, 2017).

These emissions often contain trace levels of antibiotics and their transformation products, metals, and biocides (Singer *et al.*, 2016; Tran *et al.*, 2016a), which may exert further selective pressure on environmental microbiota (Seiler and Berendonk, 2012; Wales and Davies, 2015). Although quantity may be lower than minimum inhibitory concentrations, they may become pseudo-persistent when discharge continuously into the environment (Daughton, 2003; Bu *et al.*, 2016). Furthermore, most bacteria carry mobile genetic elements (MGEs), e.g., plasmids, transposons and integrons, which can harbor transmissible ARGs (White *et al.*, 2001; Mazel, 2006; Partridge *et al.*, 2009). As a result, any impacted water might become a focus for the emergence of pan-resistant strains via horizontal gene transfer and possibly by mutation (Baquero *et al.*, 2008; Graham *et al.*, 2014; Farkas *et al.*, 2016).

2.4 Horizontal gene transfer (HGT) in environmental ecosystems

It is becoming clear that aquatic environments and other ecosystems are common sites for AR transmission and spread. Once in the environment, AR bacteria and genes can persist in soil and water due to genetic plasticity. However, problems can become more serious when a bacteria gains multiple ARGs in their genome through HGT (Fletcher, 2015), which underlie genetic diversity; studies have shown broad dissemination of a variety of resistance plasmids and integrons (i.e., mobilome) in the aquatic environment (Rahube and Yost, 2010; Gillings *et al.*, 2015). Expansion of the AR mobilome and positive selective determinants in polluted aquatic systems is especially concerning when MGEs are recruited into pathogenic strains (Stokes *et al.*, 2001; Stokes and Gillings, 2011). The plasmid-borne MCR-1 and *bla*_{NDM-1} genes encoding resistance towards colistin and carbapenem, respectively (Section 2.1), are examples of the international dispersal of resistant strains hosting these genes in different environmental matrices (Khan *et al.*, 2017).

Bacteria procure and accumulate foreign resistance genes from their surroundings through gene exchange. Three distinct processes are known to be responsible for HGT in natural and engineered environments, namely, i) transformation (uptake of ambient naked DNA), ii) transduction (mediated by bacteriophage) and, iii) conjugation (transfer of plasmid DNA between bacteria via cell-to-cell contact) (Munita and Arias, 2016). In most cases the transferred genes are located on MGEs

such as plasmids, transposons, phage DNA and pathogenicity islands, but occasionally fragments of chromosomal DNA are transferred (Hanssen *et al.*, 2004).

HGT have been suggested in various environmental habitats where bacteria prevail, including transformation of extracellular DNA in river sediments bacteria (Mao *et al.*, 2014), conjugative plasmid transfers in soils (Musovic *et al.*, 2006) and wastewater ecosystems (Del Casale *et al.*, 2011; Yang *et al.*, 2013a). Consequently, HGT accelerates the global spread of environmental AR including pathogenic commensal bacteria (Johnson *et al.*, 2007; Liu *et al.*, 2015). However, these biological ecosystems are complex and constantly changing, which could influence *in situ* HGT (Aminov, 2011). Ecological and habitat factors are also critical (Quintela-Baluja *et al.*, 2019). Therefore, studying the movement of genes mediated by MGEs in any environmental conditions is key to understanding and addressing the horizontal spread of resistance across species and habitats.

2.5 Environmental AR: A water, sanitation and hygiene (WASH) issue

Water pollution causes environmental degradation and contributes to the spread of a myriad human diseases due to waterborne infections linked to excreta-related waste and unsanitary living conditions (Pimentel *et al.*, 2007). Waterborne diarrhoeal diseases, for example, are responsible for two million deaths each year, with the majority occurring amongst children under five (roughly 500,000 deaths) in the poorest third-world regions (UNICEF, 2012). A case study in Nigeria recently indicated that inadequate sanitation is a major cause of diarrhoea (Yaya *et al.*, 2018), as well as other infectious diseases specially in LMICs (Fletcher, 2015). For example, typhoid disease caused by *Salmonella enterica* is spreading in South Asia and only two antibiotics remain effective against the strain, i.e., azithromycin and fluoroquinolone (Cousins, 2018). Experts in tropical disease believe this infectious agent is released in sewage systems and is spreading through unclean water. Such water- and wastewater-borne infectious diseases are preventable thorough sanitation barriers and clean water access.

Unfortunately, billions of people worldwide live without access to even basic sanitation. Despite some progress, the UN Millennium Development Goal of halving the proportion of people with reliable waste treatment has not been achieved,

especially in Sub-Saharan Africa and South-East Asia (WHO, 2015b). This is partly because of rapidly growing peri-urban populations, which are remote from central sewage collection networks and a dearth of effective small-scale wastewater treatment options amenable to decentralised applications (Mara, 2003; Jong *et al.*, 2018). By 2050, some five million people could die each year in Asia alone due to AMR related illnesses, according to UN agencies and the UK's AMR review commission (Review on AMR, 2014).

Poor sanitation infrastructure can lead to the spread of infectious agents and leads to greater use of antibiotics to treat them. Intriguingly, a study conducted by Review on AMR (2016a) revealed that around 70% of diarrhoeal illness are caused by virus, rather than bacteria, against which antibiotics are ineffective – and yet antibiotics are frequently used as a treatment. The UK's Review on AMR estimated that across four middle-income countries, namely India, Indonesia, Nigeria and Brazil, close to 500 million courses of antibiotics are used per year to treat diarrhoea from unclean water. With universal access to improved water and sanitation, though, this would be reduced by some 60% (Review on AMR, 2016b).

2.6 WASH actions and guidance on AR control

The World Health Organisation (WHO) has recently started to prioritise AR control within the water and sanitation systems (Graham *et al.*, 2019b), when AR was declared a water, sanitation and hygiene (WASH) issue in 2014 (WHO, 2014). Particularly, WHO highlighted research needs to identify water and wastewater treatment technologies to minimise antibiotics and AR bacteria in human and animal wastes in environmental media. Later in its Global Action Plan on AMR, the WHO delineated in five specific objectives, which includes Objective 3 to “*Reduce the incidence of infection through effective sanitation, hygiene and infection prevention measures*” (WHO, 2015a). However, there seems to be absence of a clear framework for action within the water and sanitation context, whereby more focus is being placed on vaccination, antibiotic-free agricultural practices, and training and education in hygiene for infection prevention. In the final UK Review on AMR entitled “Tackling drug-resistant infections globally: Final report and recommendations”, Review on AMR (2016b) recommended nine interventions which highlighted the need to improve community sanitation especially in LMICs, i.e., Intervention 2.

The WHO/UNICEF Joint Monitoring Programme (JMP) classifies ‘improved’ sanitation as a connection to a sewerage system, septic tanks, pour-flush toilets, ventilated improved pit latrines, and pit latrines with a concrete slab (WHO and UNICEF, 2006). In 2015, data suggested that the progress for improved sanitation has not been met, as almost 2.5 billions world population still lack sanitation services and up to 80% of wastewater resulting from human activities is discharged into rivers or sea without any major treatment (WHO, 2015b). Therefore, the United Nations included Target 6 in the 2030 agenda for Sustainable Development Goals (SDG), which targets clean water and sanitation (United Nations, 2015b). Specifically, Target 6.3 calls for an improvement in water quality by halving the proportion of untreated wastewater, which challenges countries to increase wastewater collection and treatment by 2030 so that effluent consistently meets national standards.

Although clean water and sanitation are adequate in High-Income Countries (HICs), AR is also a One World issue (Robinson *et al.*, 2016), which means AR occurring in the developing world will eventually affect everyone in the world. Improving water and sanitation represent an important work to be done globally, especially in LMICs to overcome increasing AR.

2.7 Improving sanitation to combat environmental AR

Effective sanitation aims to block human excreta from entering the environment using treatment and safe disposal. It is a critical step in public health protection by preventing the spread of enteric pathogens because human faeces can contain enumerable known bacterial, viral, protozoan and helminthic pathogens (Brown *et al.*, 2013). In work to provide a public health guidance for the World Bank, Crowdy (1984) revealed that one gram of fresh faeces from an infected person can contain around $10^6 - 10^8$ bacterial pathogens. WASH-related illnesses and mortality rate are high in many LMICs due to poor sanitation and access to contaminated water (Section 2.5).

Excreta-related infections can travel from one host to another through various routes, including direct fecal-oral transmission or by indirect transmission via contaminated water, soil, food, and vectors, as illustrated in the “F-Diagram” (Figure 2-3). The F-Diagram represents the bona fide situation in LMICs settings where billions of people are not connected to improved sanitation while many still practice open defecation (WHO, 2017). This also means opportunities exist to intervene at targeted sites, as

defined by the 1) toilet barrier; 2) safe water barrier; and 3) personal hygiene barrier (Yates *et al.*, 2017). Furthermore, in many LMICs, wastewater is either directly release without treatment or being treated to varying levels and discharged into the rivers, which means barriers are needed to obstruct the spread of infectious disease (Mara *et al.*, 2010).

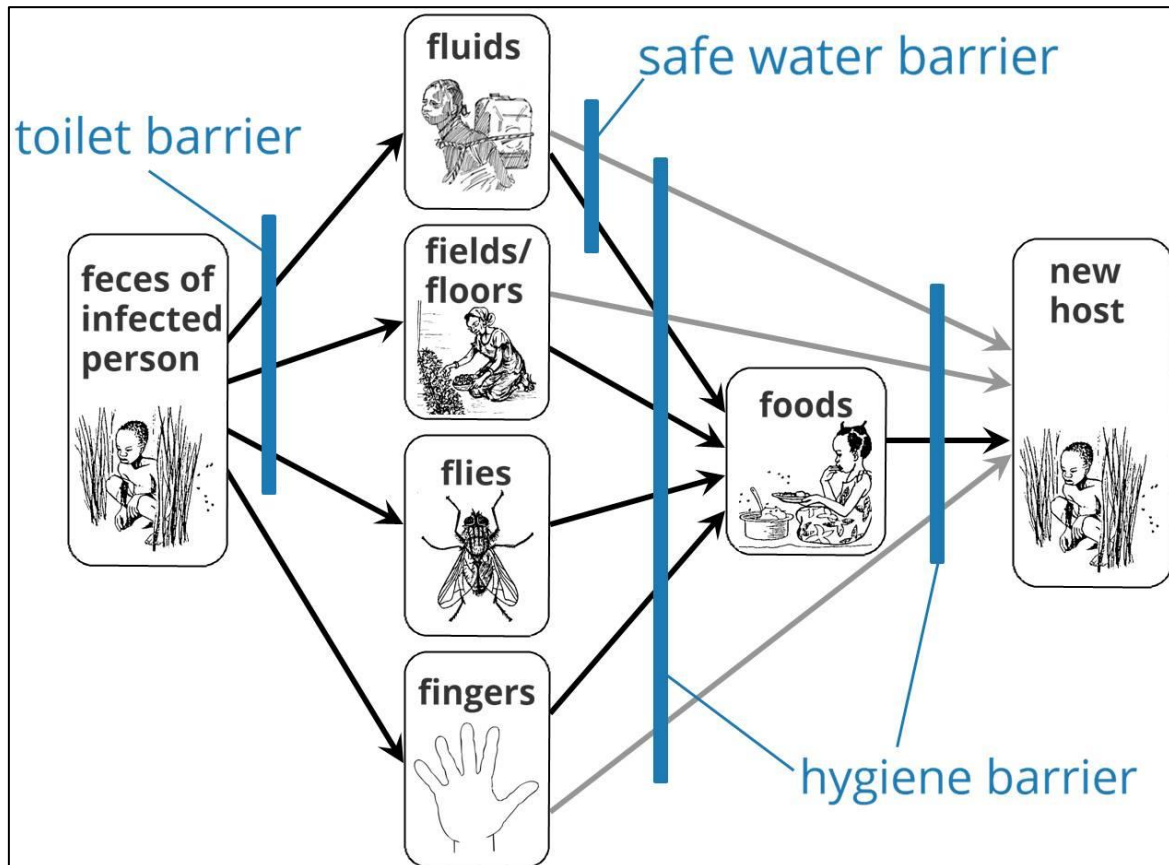


Figure 2-3 Faecal-oral disease transmission pathways and interventions to break them (Yates *et al.*, 2017).

Untreated sewage and poorly treated wastewater also contain nutrients and organic pollutants, which degrade the overall quality of water and damage ecosystems. For example, high nutrient inputs, such as nitrogen and phosphorus, can cause eutrophication and algal blooms. Eutrophication is harmful to the natural waterways and human health with implications, including depleted dissolved oxygen levels and altered microbial community structure (Yang *et al.*, 2008). One example is the Taihu Lake basin in China, where discharge of untreated and poorly treated domestic wastewater contributes to 46% of nitrogen in the lake and severe eutrophication (Liu *et al.*, 2013), which also correlates with prevalence of AR enteric bacteria containing ARGs against β -lactams and carbapenems (Zhang *et al.*, 2015). Therefore,

wastewater treatment technologies should also target nutrient removal for ensuring overall water safety and community health outcome.

2.8 Wastewater treatment technologies and AR removal

In developed countries, wastewater treatment facilities are identified as point sources for the “redistribution” of ARGs because such facilities were not devised to reduce genetic and micropollutants (Zhang *et al.*, 2009c; Quintela-Baluja *et al.*, 2015). Moreover, most waste treatment protocols were not designed specifically to address antimicrobial residues, therefore their efficacy to mitigate these residues is highly variable depending on the treatment process and the specific antimicrobial in question (United Nations, 2018). However, a world without wastewater treatment will be worse as seen in many of the developing countries.

Evidence show propagation of some AR genes and bacteria after biological wastewater treatment (Luo *et al.*, 2014; Ju *et al.*, 2016), however they were also frequently reduced following treatment for example via peat biofiltration (Park *et al.*, 2016) and thermophilic anaerobic treatment (Wu *et al.*, 2016). Besides, Yuan *et al.* (2016) found that membrane bioreactor was highly effective at removing ARGs from domestic wastewater (~2.80-3.54 log reductions), while removal by an integrated constructed wetland was possible (>99%) through combinations of adsorption, phytoremediation and photoremediation as shown by (Chen *et al.*, 2016a).

In a study using advanced oxidation, Zhang *et al.* (2016) discovered that oxidation by the Fenton process was slightly better at removing ARGs (2.58-3.79 log) than the ultraviolet/hydrogen peroxide (UV/H₂O₂; 2.26-3.35 log) under the optimal conditions wherein molarity and pH were carefully designed at reaction time of 2 hours. Several other studies also reported substantial reduction in ARGs using ozonation combined with filtration methods (Lüddecke *et al.*, 2015), and chlorination and ultraviolet (Zhuang *et al.*, 2015). Degradation and deactivation of ARGs via such advanced oxidation processes were achieved by chemical oxidation, photolysis and photocatalysis (Quote). Thus far, little is known about how biological treatment technologies remove ARGs (Manaia *et al.*, 2016). It is believed that the capacity of the treatment to remove bacteria is crucial to removing ARGs from wastewater (Novo and Manaia, 2010; Manaia *et al.*, 2016), and removal efficiencies may vary by operating factors such as organic loading rate, temperature, hydraulic residence

time, pH, et cetera (Kim *et al.*, 2007; Bouki *et al.*, 2013; Burch *et al.*, 2016). Further, spatial ecology of biotreatment processes such as bacterial biosolids-liquid phase separation and specific waste sources may be key influencers to AR fate and downstream resistomes in wastewater networks (Quintela-Baluja *et al.*, 2019).

2.9 Strategic approach and practical technological solutions

Waste- and wastewater treatment represent an important mitigation option for AR control and our battlefront against AR in the environment (Pruden *et al.*, 2013; Burgmann *et al.*, 2018). Effective waste collection and treatment can protect community health and a wide range of technologies exists to achieve this, which include sophisticated and high-cost methods like centralised sewage systems and tertiary treatment such as advanced oxidation and ozonation. However, such services have to be feasible and accessible for LMICs (Graham *et al.*, 2019b). Most of the wastewater technologies that have developed in the developed countries are less feasible for the 2.5 billion people needing adequate sanitation by the end of 2050 because they are too expensive to use in developing countries and require high skills to operate and maintain (Mara, 2003). More often than not, conventional centralised approaches failed to address the needs for peri-urban and rural communities due to disproportionately large investments and disconnection from sewerage systems (Parkinson and Tayler, 2003; Parkinson, 2005).

Importantly, the technologies for use in LMIC scenarios should be affordable in that majority of the populations who are needing them are in poverty, especially in East Asia and Pacific and Sub-Saharan Africa, where people live on less than US\$ 1.90 per day (World Bank, 2018). In brief, wastewater treatment technologies should be sustainable, which means, economically viable, socially acceptable, technically appropriate, and it should also protect the environment and natural resources (Sustainable sanitation alliance, 2008).

Given that sanitation problems in the LMICs are diverse (e.g., open defecation, religions, socio-cultural factors) with inequitable resources between urban versus sub-urban and rural areas, using smaller and tiered (incremental) sanitation mitigations may be a more practical approach to bridge the gap (Figure 2-4), as proposed by Graham *et al.* (2019b). The key purpose is to make wastewater

treatment universal. Particularly, the strategy proposes locations in the waste management system where AR mitigations might occur and smaller scale secondary treatment technologies might be more feasible for LMICs as an affordable intermediate step. Graham *et al.* (2019b) argue, using a quasi-cost–benefit analysis, that “next-most-cost-effective” AR mitigation options exist, which better fit the resources and existing infrastructure in a country.

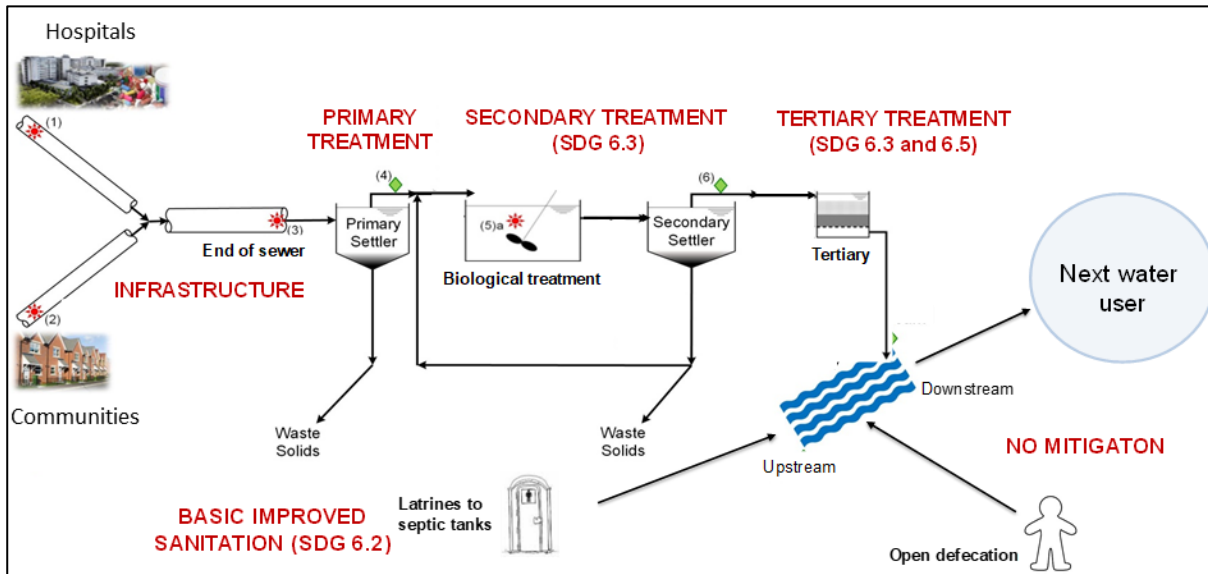


Figure 2-4 Locations in a waste management system highlighted in red where AR mitigation interventions might occur, aligned with Sustainable Development Goal 6.0; including SDG 6.2 via improved basic sanitation; SDG 6.3 via secondary treatment; and SDG 6.5 via advanced tertiary treatments (Graham *et al.*, 2019b).

Small-scale decentralised schemes keep waste collection at minimal cost and focus mainly on necessary treatment and disposal or reuse. Specifically, smaller scale technologies do not require the same level of sewerage infrastructure as it aims to treat wastewater at a community scale, using less costly condominial sewerage collection (decentralised) systems. Decentralisation can circumnavigate the high cost required to construct sewerage network with large distances and pumping, therefore is better suited for peri-urban and rural communities in LMICs. As significant progress has been made for wastewater treatment in the urban cities using centralised approaches (Massoud *et al.*, 2009), it is positive that reliable decentralised systems can reduce waste loading burden in conventional systems due to rapid urbanisation by equipping peri-urban communities with independent local waste treatment and

disposal. Hence, water is protected at more local scales from pollution, and AR burden and exposure through reducing untreated waste emissions.

2.10 Knowledge gaps

Decentralised scheme is practical for LMICs and other underserved communities in need of sanitation coverage, which can help deliver the Sustainable Development Goal 6 of universal access to wastewater treatment by 2030, and controlling the spread of AR in the environment. Future AR mitigation strategy in relation to environmental release and exposure should focus on the reduction of waste- and wastewater-borne AR sources and emissions, particularly across LMICs, which can be achieved by using small scale systems. Developing a simple secondary treatment technology that can be used at small local scales is urgently needed, but also a deeper understanding of AR removal mechanisms in such systems, such that they can be made sustainable under the LMIC conditions. Furthermore, treatment technologies should be effective and reliable at removing organic pollutants (e.g., enforced by discharge standards), to attract the uptake from local water firms.

Crucially, understanding the mechanisms and the microbial ecology of prospective technologies can help optimise removal efficiencies and ensure process reliability. Associated with that, we need to know whether technologies can be scaled up and elaborated to become a sustainable option for meeting public health and water quality goals in LMICs. As such, technology selection should include low-energy considerations, minimal maintenance and systems that rely on natural ecological principles rather than expensive advanced technologies so that wastewater treatment is cost effective for LMICs communities in the long run.

Chapter 3 Denitrifying Downflow Hanging Sponge (DDHS) bioreactors for reducing total nitrogen and antibiotic resistance genes in domestic wastewater

Parts of this chapter have been published as Jong, M.-C., Su, J.-Q., Bunce, J.T., Harwood, C.R., Snape, J.R., Zhu, Y.-G., Graham, D.W. 2018. Co-optimization of sponge-core bioreactors for removing total nitrogen and antibiotic resistance genes from domestic wastewater. Science of The Total Environment, 634, 1417-1423.

3.1 Introduction

Clean water and sanitation are critical for human and environmental health because water is essential for earth ecosystems (United Nations, 2015a), and effective wastewater treatment can protect water resources from pollutions (Metcalf & Eddy, 2003). With adequate sanitation, safe ambient water quality can be ensured which helps control the spread of water-borne and excreta-related diseases (Mara *et al.*, 2010; Burgmann *et al.*, 2018).

Exposure to antibiotic resistant organisms in the aquatic environment is both detrimental to public health and economic productivity (Review on AMR, 2015; United Nations, 2018). This impact is most profound in Low-Middle-Income Countries (LMICs) because the AR burden is greater due to less sanitary living conditions, causing much increased mortality relative to High-Income Countries (HICs) (Ayukekbong *et al.*, 2017; Chereau *et al.*, 2017; Collignon *et al.*, 2018). Specifically, waste management systems in LMICs struggle to keep up with growing urbanisation, leading to contaminated water and declining environmental quality. Improving community sanitation, therefore, is crucial to help improve personal hygiene by limiting the spread of AR bacteria through water. Accordingly, the United Nations has committed to halve the lack of “improved basic sanitation” by 2030 (United Nations, 2016) and is promoting a One Health approach to combat AR spread in the environment (Robinson *et al.*, 2016; Singh, 2017).

Worldwide, sanitation problems are particularly evident in rapidly expanding peri-urban environments in LMICs because such locations often lack centralised sewage collection and treatment. In such locations, conventional wastewater treatment options are less feasible due to excess cost, as it requires major sewerage infrastructures for wastes collection and substantial energy inputs to drive the intensive aeration needed for the activated sludge process (Graham *et al.*, 2019b). As such, smaller, local-scale treatment options are needed to increase wastewater treatment coverage, however, few reliable “small-scale” technologies exist that are able to reduce carbon (C) and total nitrogen (TN) levels as well as mitigate against the release of waterborne pathogens and antibiotic resistant bacteria (ARB).

Denitrifying Downflow Hanging Sponge (DDHS) reactors are a low cost and low maintenance wastewater treatment option that is ideally suited for smaller or decentralised applications (Bundy *et al.*, 2017), which is an alternate design of traditional Downflow Hanging Sponge (DHS; Section 3.1.1) systems. Briefly, it employs porous sponge matrix for biofilm growth and passive aeration to purify domestic wastewater in a two-stage aerobic-anoxic treatment step, configured with a raw wastewater bypass (wastewater bypassing the upper aerobic sponge; Section 3.1.2) to supply extra carbon to the lower anoxic sponge section to promote denitrification (Isaacs and Henze, 1995; Schipper *et al.*, 2010). It can effectively remove suspended solids, organic carbon and nitrogen pollutants from domestic wastewater (Uemura *et al.*, 2010; Bundy *et al.*, 2017). However, the removal of antibiotic resistance genes (ARGs) and mobile genetic elements (MGEs) via DDHS treatment has yet to be investigated. There are reasons to believe that DDHS systems may be effective because sequenced changes in redox conditions have been shown previously to enhance ARG removal (Christgen *et al.*, 2015). Whereas there are also concerns about how a wastewater bypass might impact on the ARG and ARB levels in effluent, which is a critical issue in LMICs where this technology would be most valuable.

Therefore, this chapter assesses ARG levels in both the inflowing wastewater and released effluents in DDHS bioreactors during sewage treatment. Four parallel laboratory-scale DDHS bioreactors with varying wastewater distribution regimes designed to optimise TN removal were examined using a combination of chemical

and molecular biological methods. Comparing fate of ARG and MGE pre- and post-DDHS treatment can provide key data for process optimisation, especially where TN and ARG reductions are both desired, such as places where improved decentralised treatment is urgently needed (e.g. Mexico, China, India, Cambodia). The objectives of work in this chapter were as follows:

- a) To monitor treatment performance of prospective DDHS bioreactors under varying wastewater bypass conditions.
- b) To obtain quasi-resistome data for comparing influent and effluent ARGs and MGEs in DDHS bioreactors, using high-throughput qPCR (HTH-qPCR) quantification.
- c) To contrast ARG and MGE profiles under different wastewater bypass regimes.

3.1.1 Downflow Hanging Sponge (DHS) systems

DHS is a wastewater treatment technology that has existed for over 20 years and is well suited for decentralised use. DHS bioreactors are passively aerated systems composed of a series of porous sponge media, which are used in the treatment of wastewater (Agrawal *et al.*, 1997). In principle, microbes develop biofilms within the sponges that act as a support matrix for biofilm growth, facilitating metabolism and the transformation of organic carbon (C) and secondary nutrients in the wastewater to water, biomass and evolved gases (Uemura *et al.*, 2010). The use of sponges in DHS biofiltration technology often offers higher surface-to-volume ratios compared to more traditional media, such as stone or plastic (Lessard and Le Bihan, 2003). Traditional DHS systems have generally performed well at simultaneous C-removal and nitrification (Machdar *et al.*, 1997; Araki *et al.*, 1999; Tandukar *et al.*, 2005; Chuang *et al.*, 2007).

Originally, DHS systems were developed as complimentary treatment units to polish Upflow Anaerobic Sludge Blanket (UASB) effluents during wastewater treatment. Subsequently, DHS was visualised for stand-alone decentralised use (Onodera *et al.*, 2014), and also for treating other types of wastewater, including rubber processing waste (Watari *et al.*, 2016; Watari *et al.*, 2017), agricultural drainage water (Fleifle *et al.*, 2013a; Fleifle *et al.*, 2013b), high-strength soft-drink wastewater (Liao *et al.*,

2017), and most recently, treatment of septic sludge (Machdar *et al.*, 2018). Although previous DHS designs have been effective at chemical oxygen demand (COD) and ammonia (NH_3) removal, previous designs were less able to also denitrify because they have tended to expose the sponge matrix entirely to air in order to maximise passive aeration. Hence, treated effluent from DHS systems often contains high levels of nitrates (NO_3^-). Here, denitrification is key to reducing the nitrates and overall nitrogen burden on the receiving aquatic environment, and to achieve compliance with strict TN discharge consents where they exist. For example, some emerging countries, such as China and Thailand, have developed increasingly stringent laws on effluent discharges to the environment, particularly related to TN releases (Chan *et al.*, 2009). Therefore, an alternate to DHS reactors was conceived at Newcastle University.

3.1.2 Denitrifying Downflow Hanging Sponge (DDHS) systems

DDHS systems overcome poor denitrification in traditional DHS systems by providing a further anoxic treatment step in the process train. Essentially, DDHS systems are a bipartite wastewater treatment apparatus that consists of sequential redox compartments for combined aerobic-anoxic biological treatment. Specifically, the anoxic compartments were made submerged in aerobically treated (nitrified) effluent from the preceding aerobic step. Here, the anoxic compartments were supplied with additional wastewater at a bypass influent point located at the top of the anoxic sponge section.

The “bypass” is a portion of “raw” wastewater bypassing the upstream aerobic sponge core and fed directly to the anoxic zone, which is designed to encourage anoxia and to supplement carbon in the lower submerged layers to promote denitrification (Isaacs and Henze, 1995; Shackle *et al.*, 2000; Schipper *et al.*, 2010). Here, wastewater bypass is crucial to DDHS systems because the majority of bio-available carbon is removed from the wastewater in the upper aerobic section before it passes through the subsequent anoxic section. As a result, in the absence of bypass, the anoxic section becomes C-limited, restricting the conversion of nitrate to N_2 . This is critical for implementation in places such as China and Thailand which have tight TN discharge standards (Ministry of Natural Resources and Environment, 1992; Ministry of Environmental Protection, 2002).

Many previous studies have used external carbon source such as acetate and methanol (Osaka *et al.*, 2008; Song *et al.*, 2015) as substrates to ensure denitrification during wastewater treatment. However, this is not practical for decentralised implementation of DDHS in LMICs, especially for remote and-or sub-urban communities, where chemicals such as acetate and methanol are not readily available, and have on-site storage and safety issues. In contrast, untreated wastewater is a more economical and readily available carbon source, especially suitable for decentralised application in developing and rural locations.

DDHS systems use minimal energy because they use passive aeration within porous sponge matrix and also provide design flexibility in the sponge core (e.g. varying redox zones, reactor volumes and density ratios) that can be customised to local conditions. Polyurethane (PU) foam sponges are used in DDHS because they are the most amendable form of packing media since they can be designed to fit any configuration with respective desired surface-to-volume capacity (Ahammad *et al.*, 2013). In addition, its multicellular structure with high void space is an advantage for both aeration and higher surface areas for biofilm adherence (Stephenson *et al.*, 2013). In particular, PU foam with two different pore sizes were employed in the DDHS design. The characteristics of the sponges with different pore sizes are defined by their specific pore numbers per area, i.e. pore per inch. Coarse sponges (20 pores per inch; ppi) were used in the aerobic sponge layers as larger pore size increases ventilation across the matrix while fine sponges (45 ppi) were used in the anoxic section to increase surface area (fine sponge consists higher specific area as compared to the coarse sponge with the same density).

3.2 Materials and methods

3.2.1 Laboratory DDHS bioreactors for domestic wastewater treatment

Four physically identical bench-scale DDHS bioreactors were assembled and operated in parallel for 210 days, as described previously in Bundy *et al.* (2017). Figure 3.1 provides an overview of the reactors and their main components. In brief, each bioreactor was made from a PVC cylinder (0.5 m tall x 0.14 m internal diameter; working volumes = 3 L), and configured to include internal recirculation and a wastewater bypass (also called a “shunt”) to the submerged layer.

The cores of the DDHS reactor consisted of:

- i) the upper hanging sponge layers exposed to air from above, below, and through side vents, which provide maximal passive aeration for C-removal and nitrification, and;
- ii) the bottom anoxic sponge layers, submerged in partially treated (nitrified) wastewater from the preceding aerobic section for denitrification, conditionally enhanced by wastewater bypass.

Cylindrical sponge discs of 20 ppi and 45 ppi were cut to tightly fit within the reactor columns, with four stacked 20 ppi sponges in the top section and six stacked 45 ppi sponges in the bottom section (see Figure 3-1). The reactors were inoculated with nitrifying return activated sludge (RAS) to encourage biofilm growth within the sponge matrix, and were operated in continuous-flow mode at an organic loading rate of 0.4 kg COD/m³-sponge/day (HRT = 0.6 days) and under ambient room temperature (22-23 °C) (Bundy *et al.*, 2017).

The columns were designed to be flexible in terms of water depth and aeration, with holes every 30 mm along the entire height of the reactor on two sides. These holes can be left open for aeration, sealed with water-tight Suba-Seal closures, or fitted with a tap for sampling or bypass introduction. Watson Marlow 520S peristaltic pumps were used to:

- i) supply settled wastewater across the four bioreactors:
 - a. to each influent point at the top sponge layer,
 - b. to each bypass point at the submerged sponge layer,
- ii) facilitate recirculation of effluent from the base to the top of each reactor, where recirculated effluent was mixed with inputted wastewater.

Liquid was distributed as evenly as possible over the top sponge layer via a passive sprinkler system constructed with a plastic plate perforated with tiny holes hanging above the first layer of sponge. Wastewater was moved through the reactors and into effluent collection jars by gravity flow.

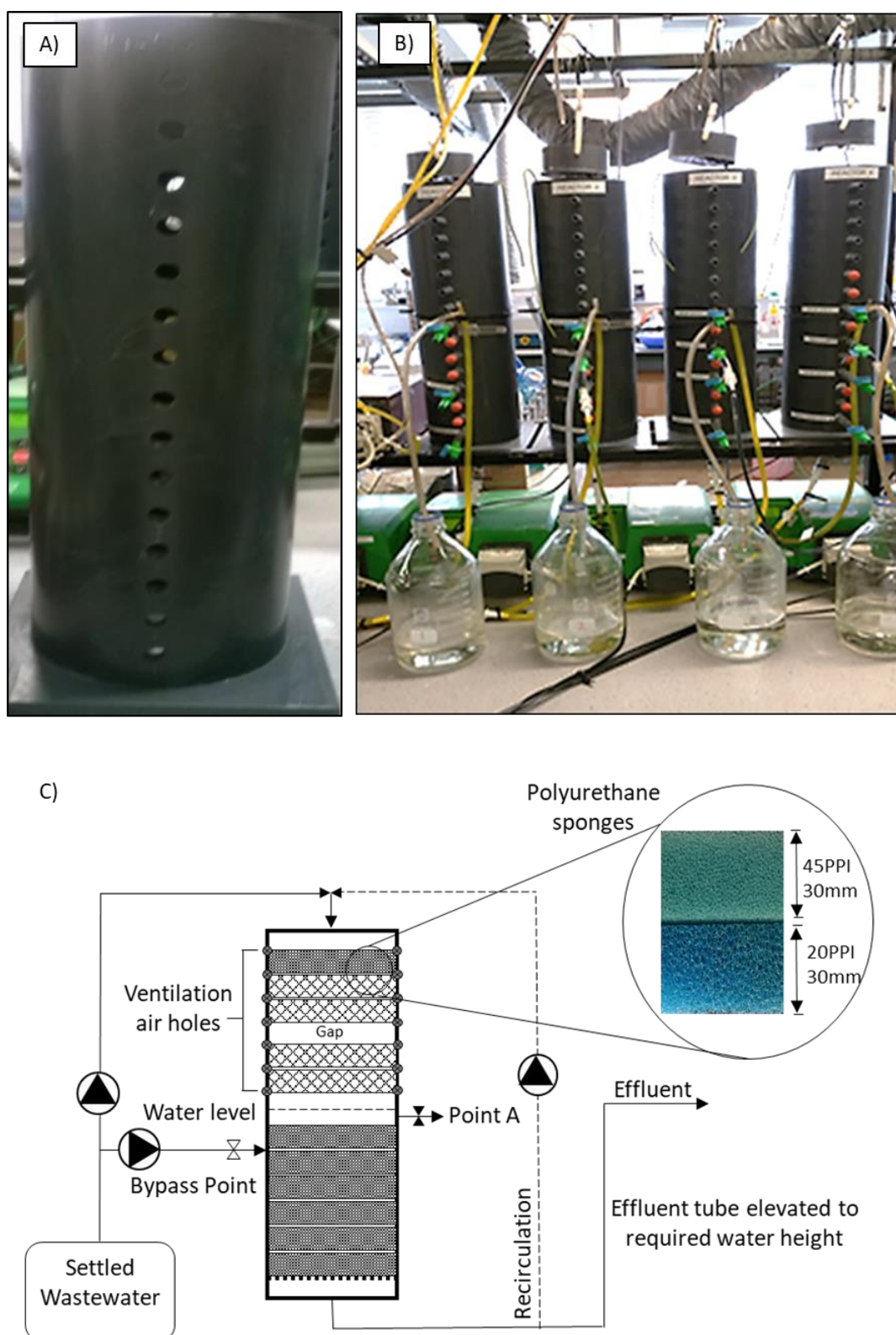


Figure 3-1 Assembly of laboratory-scale DDHS bioreactors. (A) Reactor column made from PVC cylinder with side holes. (B) Starting from the left the bypass amendments were as follows: 0% bypass (Control; R-S0); 10% bypass (R-S10); 20% bypass (R-S20); and 30% bypass (R-S30). All reactors were configured with 30% internal recirculation of the final effluent (percentage by volume of total influent rate). (C) Schematic diagram showing sponge media and hydraulic configurations.

3.2.2 Wastewater bypass for the optimisation of effluent nitrates removal

The principal variable that was investigated in the initial experiment, reported by Bundy *et al.* (2017), was the effect of percent bypass on the quality of the effluent produced by the bioreactors; specifically on their ability to remove nitrate from the partially treated wastewater from the preceding aerobic treatment step. As such, incrementally increasing bypasses percentages (by 10%) were applied for the four reactors, ranging zero to 30%. The goal was to optimise total nitrogen (TN) removal in the DDHS reactors. All reactors were fed at the same total flowrate; however, the proportion of bypass-to-raw wastewater supplied to the anoxic zone varied (percent bypass; see Table 3-1). The reactors were designated R-S0, R-S10, R-S20 and R-S30, being defined by different bypass percentages; 0%, 10%, 20% and 30% (% of total wastewater by volume), respectively. R-S0 with no bypass was the control unit. Previous work showed TN removals were most efficient at bypass levels of 20 to 30% (Bundy *et al.*, 2017).

Table 3-1 Influent flow rates to the top of bioreactors and bypass points of each bioreactor.

Flow regimes (mL/min)	R-S0	R-S10	R-S20	R-S30
Total flowrate	2.14	2.11	2.15	2.14
Upper influent flowrate	2.14	1.92	1.77	1.47
By-pass flowrate	0	0.19	0.37	0.67
Actual percent shunting (%)	0	9.10	18.00	31.40
OLR ^a aerobic sponges	0.34	0.30	0.28	0.25
OLR anoxic sponges	0.04	0.07	0.1	0.2
Total OLR	0.38	0.37	0.38	0.37

Notes: ^aOLR is organic loading rate defined as kg COD/m³-sponge/day and calculated using COD loading and working sponge volume.

3.2.3 Influent source, routine sample analysis and monitoring

Bioreactor influent and effluent samples were collected and analysed to monitor treatment performance over space and time, i.e., from inlet and outlet of bioreactors, once every week. Fresh settled wastewater (post primary settling; called 'raw' here) was collected weekly from a municipal wastewater treatment plant in northern England and stored at 4 °C prior to use as reactor influent. Raw wastewater was fed in parallel via influent pumps to all reactors from an 18-L carboy retained in a fridge

located next to the reactors. Analyses on influent and effluents included Soluble COD ($\text{COD}_{\text{Soluble}}$), Total COD ($\text{COD}_{\text{Total}}$), Total Suspended Solids (TSS), Volatile Suspended Solids (VSS), Total Kjeldahl Nitrogen (TKN), Ammonium-Nitrogen ($\text{NH}_4\text{-N}$), Nitrite ($\text{NO}_2\text{-N}$) and Nitrate ($\text{NO}_3\text{-N}$). All samples were collected and analysed in triplicates.

TSS and VSS measurements were undertaken in accordance to the APHA Standard method for the examination of water and wastewater. Total ($\text{COD}_{\text{Total}}$) and soluble COD ($\text{COD}_{\text{Soluble}}$) were determined using calorimetric COD test kit (25-1500 mg COD/L, Merck & Co. Inc., USA) on a Spectroquant Pharo 300 spectrophotometer, in line with manufacturer's instructions (Merck & Co. Inc., USA). Ammoniacal nitrogen was determined using Spectroquant ammonium test kit (2.0 - 150 mg/L $\text{NH}_4\text{-N}$), with the manufacturer's bar-coded autoselector on a Spectroquant Pharo 300 spectrophotometer. Anion analysis was performed using Ion Chromatography on a Dionex ICS-1000 fitted with an AS40 auto sampler (ThermoFisher Scientific, UK). Samples were filtered using 0.20- μm PES syringe filters (VWR, UK) prior to analysis (in duplicate). Total nitrogen (TN) is defined as the sum of TKN and nitrogenous anions ($\text{NO}_3\text{-N}$ and $\text{NO}_2\text{-N}$). Mean wastewater and effluent characteristics are summarised in Table A-1 (see Appendix A).

3.2.4 Sample collection, DNA extraction and ARB enumeration

Sample collection for ARG, MGE, and antibiotic resistant bacteria (ARB; i.e., Extended Spectrum Beta Lactamase (ESBL)-producing isolates) quantification was conducted during quasi-steady-state conditions (based on C and TN removal data) during three biweekly sampling regimes. Altogether, 15 samples were collected for AR-related analyses, consisting of five samples per sampling week: one influent from parallel feeding points and four DDHS final effluents from the respective final discharge points.

For ARG and MGE quantification, samples were collected in sterilised 0.5-L Schott bottles and concentrated to obtain adequate biomass for DNA extraction. Effluent samples (e.g., 500 mL each) were collected, stored on ice (for 2 to 4 hours), and then filtered through 0.20- μm pore-sized polyethersulfone filters (Pall Corporation, USA) to harvest the cells, whereas influent samples (e.g., 100 mL each) were collected and concentrated by centrifugation at 4000 x g for 10 minutes. Filtrates and centrates

were discarded, respectively, and filter paper and pellets were stored at -20°C prior to subsequent DNA extraction, using the FastDNA SPIN Kit for Soil and a FastPrep-24 Homogeniser (MP Biomedicals, Santa Ana, CA, USA). Following extraction, DNA samples were checked for purity using a NanoDrop 1000 Spectrophotometer (ThermoFisher Scientific, UK) and DNA concentrations were quantified by using the Qubit 2.0 Fluorometer (Invitrogen, UK). DNA samples were stored at -80°C prior to downstream analysis.

In parallel, influent and effluent samples were screened for ESBL-producing Enterobacteriaceae, using ChromID ESBL selective chromogenic media (Biomérieux, UK). The selective agar contains a mixture of antibiotics, including cefpodoxime as the marker antibiotic for the selective growth of ESBL-producing Enterobacteria. Simultaneous detection and isolation of presumptive ESBL-positive *E. coli* and KESC group (i.e., *Klebsiella/Enterobacter/Serratia/Citrobacter* spp.) bacteria were recorded according to chromogenic characteristics provided by manufacturer (*E. coli* pink/burgundy; KESC group blue/green). Raw wastewater samples were serially diluted in 1 x sterile phosphate buffer saline (PBS) solution and 100- μ L aliquots were plated in triplicate per dilution per sample. Viable ESBL-producing *E. coli* and KESC isolates were counted after 24 hours of incubation at 37°C and reported as CFUs/100 mL.

3.2.5 High-throughput quantitative PCR (HTH-qPCR)

Abundance and diversity of ARGs and MGEs were quantified by HTH-qPCR using the SmartChip Real-time PCR (Warfergen Inc. USA) (Su *et al.*, 2015). A total of 296 primer sets (Table A-2) were used to screen for ARGs and MGEs, including 293 validated primer sets targeting 284 ARGs, representing potential resistance to nine major classes of antibiotics. Eight transposase genes, two integron-associated genes (universal class I integron-integrase gene, *intl*; and the clinical class 1 integron-integrase gene, *cintI*); and one eubacterial 16S rRNA gene are also included. Target genes were originally identified with BLAST on the Antibiotic Resistance Genes Database (ARDB) or the National Center for Biotechnology Information (NCBI) database.

HTH-qPCR amplification was conducted as follows: 100- μ L reaction containing (final concentration) 1 \times LightCycler 480 SYBR® Green I Master Mix (Roche Inc., USA),

nuclease-free PCR-grade water, 1 ng/μL BSA, 9 ng/μL DNA template, and 1 μM of each forward and reverse primer. The thermal cycle was as follows: initial denaturation at 95 °C for 10 min, followed by 40 cycles of denaturation at 95 °C for 30 s, annealing at 60 °C for 30 s, and finally with a melting curve analysis auto-generated by the programme. Corroborating 16S rRNA quantification targeting universal eubacteria for the same samples was performed using conventional qPCR. Standard curves and the same 16S rRNA primer sequences were used to quantify 16S gene copies for sample normalisation (Looft *et al.*, 2012; Ouyang *et al.*, 2015).

3.2.6 Genomic data screening and analysis

Raw HTH-qPCR data was cleaned using SmartChip qPCR Software (V 2.7.0.1), which removes data from wells with multiple melting peaks or inefficient amplification (i.e., outside 90% to 110%). Cleaned data from three independent samples (one per week per sampling location) were then screened according to their threshold cycle value (C_T). Samples with a $C_T > 31$ were removed, which previous experience suggested are probable false positives (i.e., $C_T = 31$ was the detection limit).

Normalised gene copy numbers of ARGs and MGEs were calculated as described in previous studies (Ouyang *et al.*, 2015; Chen *et al.*, 2016b). Bacterial cell numbers were estimated by dividing quantified 16S rRNA copy numbers by the average number of 16S rRNA per bacterium (estimated at 4.1 based on the Ribosomal RNA Operon Copy Number Database, rrnDB version 4.3.3) (Klappenbach *et al.*, 2001).

All statistical analysis was performed using SPSS (V19.0, IBM, USA). One-way analysis of variance (ANOVA) test was used to determine the difference between parameter means, for example, One-way ANOVA tests were performed on the three biweekly ARG datasets and metadata, and statistical comparisons confirmed no significant variations existed among biweekly sampling events (i.e. p -value > 0.05). ARG and MGE levels from the three biweekly datasets were used for subsequent comparisons among influent and reactors effluents. Comparisons of treatment efficiencies relative to untreated influent were performed using Paired-samples T-tests to examine bioreactors' performance. Non-parametric statistical methods were employed when data were not normally distributed. Statistical significance always was defined to within 95% confidence limits (i.e., p -value < 0.05).

3.3 Results and discussion

3.3.1 Enhanced denitrification for decentralised wastewater treatment

Reactor performance of the DDHS units is shown in Figure 3-2 and shows differences among bypass schemes. COD_{Soluble} and COD_{Total} removal efficiencies always were over 79% and 83%, respectively, and NH₄-N and solids (TSS and VSS; see Table A1) removals were consistently over 84% and 90%, respectively. Despite the addition of bypass wastewater in R-S10, R-S20 and R-S30, COD removal efficiencies did not significantly differ versus bypass levels (ANOVA; p-value > 0.05), indicative of carbon utilisation in the anoxic sponge layers.

However, TN removal rates improved dramatically with increasing bypass with significantly lower effluent NO₃-N levels in higher bypass units (see Table A-1, paired T-test; p-value < 0.001). Gross TN% removals were 28.5%, 37.6%, 64.5% and 71.0% for R-S0, R-S10, R-S20 and R-S30, respectively, indicating wastewater bypass does enhance denitrification. Greater COD reductions in R-S20 and R-S30, and lower effluent NO₃-N levels (presumed converted to N₂) suggest increased denitrification is occurring as designed (Bundy *et al.*, 2017).

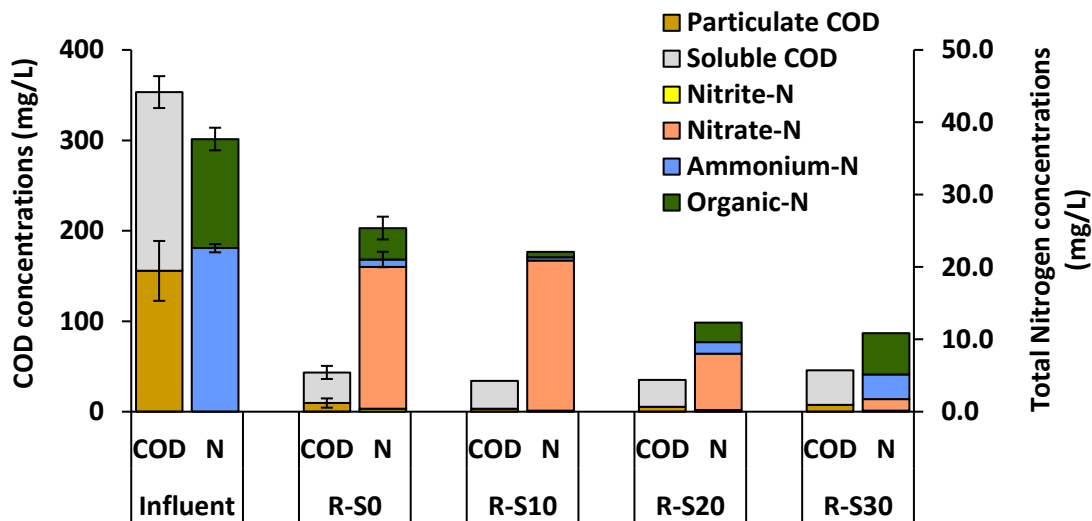


Figure 3-2 DDHS reactors mean performance as a function of wastewater bypass. Stacked bars present mean COD levels (particulate and soluble fractions) and nitrogen constituents (Ammonium; Nitrate; Nitrite; and Organic-N) in raw wastewater and the reactor effluents ($n = 12$ per reactor). Error bars show standard deviation around the mean; R-S10, R-S20 and R-S30 had minor standard errors.

3.3.2 Total abundances and patterns of ARGs and MGEs

HTH-qPCR quantifies both ARGs and MGEs, including ARGs associated with nine different antibiotic classes, different resistance mechanisms (deactivation, protection, efflux pump, and unknown), and two MGE groups (transposases and integrons). A total of 59 unique ARGs ($2.2 \times 10^{10} \pm 3.7 \times 10^9$ copies/mL) and seven MGEs ($1.4 \times 10^{10} \pm 2.2 \times 10^9$ copies/mL) were detected in influent samples as shown in Figure 3-3, with “multidrug” ARGs being most abundant (MDR; 33.8%), followed by aminoglycoside (23.2%), tetracycline (19.6%), Macrolide-Lincosamide-Streptogramin B (MLSB; 12.9%) and β -lactam (9.5%). Detected influent MGEs were 58% and 42% for transposase and integrase genes, respectively. As DNA was extracted from biomass concentrated from samples by filtering through 0.2- μ m membrane filters, therefore ARG levels reported here are presumed to be cell-associated. Extra-cellular ARGs were not included in this study.

Absolute ARG abundances significantly declined in all DDHS reactors (see Figure 3-3A), consistently achieving 2.0 to 3.0 log reductions (influent vs effluent paired T-test; p -value < 0.05). Effluent ARG levels ranged from 2.5×10^7 to 4.5×10^8 ARG copies/mL. Highest absolute ARG removals were seen in the reactors with 10 and 20% bypass as compared with no bypass (R-S0) and 30% bypass (R-S30). R-S30 had the highest effluent ARG levels, suggesting “excess” bypass negatively impacts ARG removal. MGE levels also significantly declined in all reactors following similar patterns as for ARGs (Figure 3-3A). Overall, the wastewater bypass improves TN removal and achieves efficient ARG removal, which is co-optimized at ~20% bypass. Highest TN removals were seen at a 30% bypass, but results shows ARG removals decline, presumably because greater quantities of raw wastewater are bypassing the aerobic layer, suggesting the aerobic layer may be particularly important to ARG removal as suggested previously by Christgen *et al.* (2015), and also confirmed in Chapter 5 here (see later).

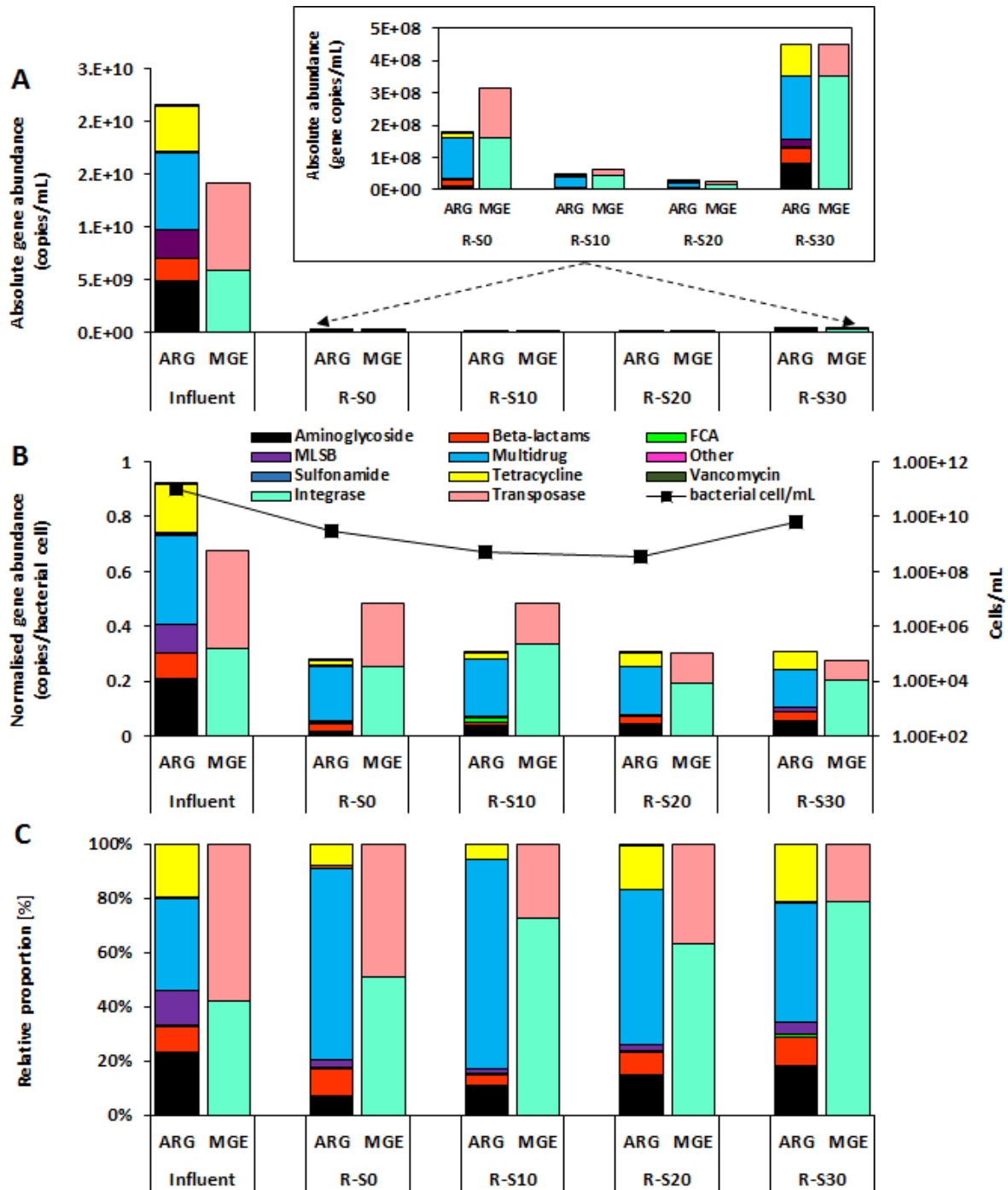


Figure 3-3 Total abundance of ARGs and MGEs detected in the raw wastewater and DDHS reactor effluent samples conferring resistance to specific class of antibiotics. (A) Absolute gene copy numbers per mL of wastewater; (B) Relative gene copy numbers normalised to bacterial cell numbers derived from ambient 16S-rRNA gene abundances; (C) Relative percentages of ARG abundances across samples. The line shows absolute bacterial cell levels in the influent and effluents, which reflects eubacterial abundances (error bars ~ small deviations concealed by marker). The blow-up insert shows subtle differences among ARGs and MGEs in different DDHS reactor effluents. FCA = fluoroquinolone, quinolone, florfenicol, chloramphenicol, and amphenicol ARGs; MLSB = Macrolide-Lincosamide-Streptogramin B ARGs.

Overall, Figure 3-3 shows DDHS reactors are “efficient” at reducing both ARG and MGE levels. This is encouraging because DDHS systems use minimal energy compared to other available options for ARG and MGE removal (Bundy *et al.*, 2017). For example, UV, advanced oxidation, and membrane bioreactor processes can effectively reduce ARGs (Zhang *et al.*, 2016; Wen *et al.*, 2018), but they use copious energy and often operationally complex for the majority of application where basic sanitation is lacking, such as in many LMICs.

3.3.3 *Relative ARG and MGE abundances*

Relative effluent ARG and MGE levels (normalised to bacterial cell abundances) display different removal patterns compared with absolute abundance data (Figure 3-3B). Relative ARG levels declined by ~70% in all four DDHS reactors, although dominant ARGs in effluents differed among bypass schemes. Specifically, relative effluent tetracycline and aminoglycoside ARG levels increased and MDR genes decreased with increased bypass, suggesting the aerobic top layer particularly enhances tetracycline and aminoglycoside ARG removal. In contrast, relative effluent MGE levels generally declined with increasing percent bypass, suggesting the anoxic layer may enhance MGE removal in DDHS systems.

DDHS reactors appear to be particularly effective at reducing medically important β -lactam and aminoglycoside ARGs. As examples, all DDHS configurations significantly removed ESBL- (e.g., *bla*_{CTX-M}, *bla*_{SHV}, *bla*_{TEM}, *bla*_{SFO}) and cephalosporin-resistance (e.g., *bla*_{cepa} and *bla*_{AmpC}) ARGs, which are often associated with Gram (-) enteric bacteria (Alouache *et al.*, 2014; Blaak *et al.*, 2015; Willemsen *et al.*, 2015). Further, 2.0 to 4.0 log reductions in culturable ESBL-producing *E. coli* and KESC group bacteria were observed in DDHS units (see Figure A-1). Effluent ESBL-resistant isolate numbers increased with greater percent bypass, which is consistent with the ARG removal data.

DDHS reactors clearly reduce absolute ARG abundances from domestic wastewater. Estimated bacterial cell numbers in treated effluents showed 1.0 to 2.0 log reductions relative to influent levels (Figure 3-3B), with highest bacterial removals observed in R-S20. Further, bacterial removals parallel ARG removals, suggesting ARG reductions may be simply due to the removal of bacteria, which is greatest at the intermediate bypass levels. This implies that ARG removal in DDHS systems may be

primarily an ecological phenomenon, possibly including predation, which has been suggested previously for this type of reactor (Onodera *et al.*, 2013) and supported by new observations in Chapter 5 (see later). Conversely, TN removal increases with greater bypass, therefore an operational trade-off is needed to co-optimize TN and ARG removal for any application.

3.3.4 **Broader observations on ARG removal across DDHS bioreactors**

Differences in ARG, MGE and bacterial removals across our DDHS systems permit some general observations about ARG removal in bioreactors. For example, data here suggest removal of common ARGs from wastewater is largely associated with removing bacteria, which in the case of DDHS systems, imply the aerobic layer is particularly key to ARG removal. Previous work has shown aerobic processes may be better for ARG removal (Christgen *et al.*, 2015), which data here suggest this may be due to greater bacteria removal. Specifically, as percent bypass is increased to a certain threshold (30% here), more influent bacteria (often anaerobes and facultative strains) “avoid” the aerobic treatment step, carrying and-or possibly exchanging ARGs in and through the lower anoxic layer. Therefore, although increasing percent bypass enhances denitrification, it allows bacteria to circumnavigate the aerobic layer. This is supported by the fact that relative ARG abundances are similar among effluents (Figure 3-3B), suggesting absolute ARG in the effluents is mostly related to bacterial numbers.

In contrast, relative ‘MDR’ ARGs and also MGE abundances were lower in effluents when bypass is included (Figure 3-3B). Here, in general, the abundance of ARGs in reactor effluents increased very slightly as bypass percent was increased, whereas the opposite was apparent for MGEs. The dominant ARG subclass in R-S0 effluent is MDR genes (~73%), whereas MDR only represents 44% of ARGs in R-S30 effluent (Figure 3-3C). Further, although absolute MGE levels increase with increasing bypass, relative MGE levels were highest in R-S0 and R-S10 with no or low bypass. This implies bacteria that survived both the aerobic and denitrifying layers tend to have greater genetic plasticity (i.e., higher MGEs per cell and potential for horizontal gene transfer, HGT), which may partially explain why such bacteria survive both redox environments.

An increase in MDR in aerobic processes has been seen previously (Pal *et al.*, 2005; Yang *et al.*, 2013b), although a definitive explanation has not been provided. Higher MDR was previously explained by the presence of many micro-stressors in wastewater (e.g., metals, biocides etc.), which select for bacteria with multiple defence mechanisms (Christgen *et al.*, 2015). However, our DDHS reactors had the same influent. Therefore, a better explanation is a change from anoxic sewage to the aerobic treatment unit influences HGT, potentially driving the emergence of MDR genotypes (Pal *et al.*, 2005; Poole, 2012). This explanation is possible because bacterial SOS stress responses cue HGT (Baharoglu *et al.*, 2010) and a change in redox conditions might increase bacterial stress. However, a third explanation is that higher rates of HGT prevail under aerobic reactor conditions, possibly due to higher growth rates and greater bacterial densities. Suggesting aerobic units increase gross HGT is mildly controversial because others have found greater ARG HGT under anaerobic conditions (Rysz *et al.*, 2013). However, data here imply the aerobic step in DDHS systems is key to ARG removal, which is consistent with observations in other studies (Leverstein-van Hall *et al.*, 2003; Tennstedt *et al.*, 2003; Zhang *et al.*, 2009b; Mokracka *et al.*, 2012; Farkas *et al.*, 2016). Such questions will be examined in greater detail in Chapter 5.

3.3.5 Persistent and unique ARG and MGE subtypes, and practical implications

A Venn diagram of ARGs present in the influent and effluents is provided as Figure 3-4. It shows 10 “persistent” ARGs (i.e., not removed by any configuration) across all reactors and also unique ARGs among different effluents (see Table A-4 for specific ARGs). Overall, effluent from R-S0 had the highest number of unique ARGs (10), whereas R-S30 effluents had lowest number of unique ARG numbers (2), although R-S30 also had the highest absolute bacterial and ARG abundances. ARGs in the central overlap were persistent in all effluents (see Table A-3; Appendix A), including *tetQ*, *tetM*, *tetX*, *bl2d_oxa10*, and *qacEdelta1*; ARGs often associated with acquired resistance (van Hoek *et al.*, 2011).

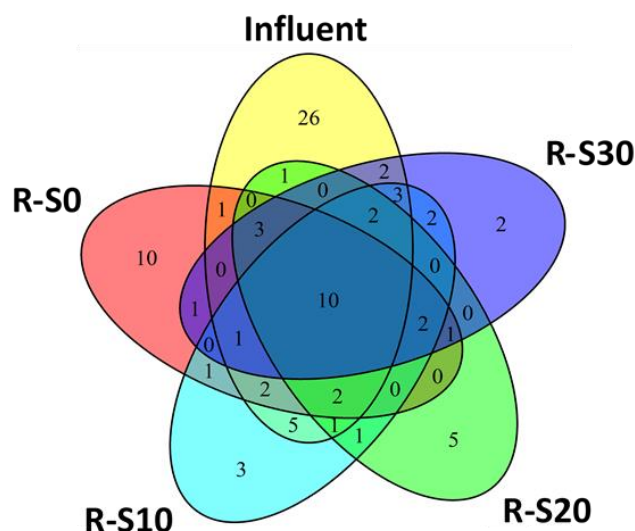


Figure 3-4 Venn diagram showing overlap of ARGs among influent and effluent samples from different DDHS configurations. Subsets represent number of genes detected in the wastewater influent (59 ARGs); R-S0 (35 ARGs); R-S10 (35 ARGs); R-S20 (28 ARGs) and R-S30 (30 ARGs). The central overlap represents the number of persistent ARGs.

All persistent ARGs are summarised in Figure 3-5 and statistical associations with persistent MGEs are provided in Table A-5 (Appendix A). First, persistence appears strongly associated with MDR genes, especially in no or low bypass reactors.

However, if one looks at the implied MDR signal, only one ARG is apparent, *qacEdelta1*, which is closely associated with integron cassettes (Partridge *et al.*, 2009) and only correlates with *int1* and *Cint1* (Table A-5). In data here, more of the persistent ARGs statistically correlate with *tp614* (especially tetracyclines and ESBL ARGs), which codes for a transposable element often linked to carbapenem resistance (Soki *et al.*, 2006). This does not mean *tp614* is carrying these ARGs, but implies integron genes are not directly associated with the most persistent ARGs in DDHS effluents.

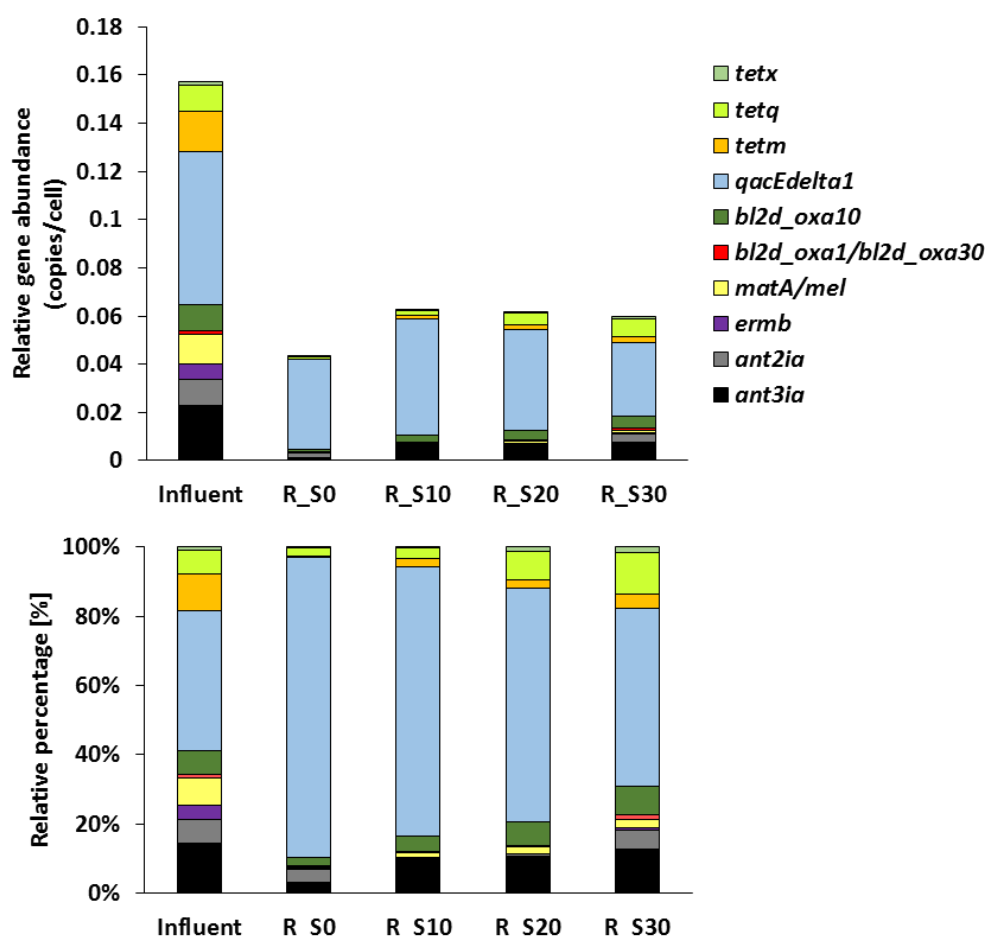


Figure 3-5 Persistent ARGs not removed in any DDHS reactor configuration. Relative abundances of persistent ARGs in the influent and effluents of each reactor (top panel; ARGs noted in the legend), and corresponding relative percentages of ARGs in reactor influent and effluent based on proportion of total ARG copy numbers (bottom panel).

3.4 Conclusions

This study assessed the flux of ARG and MGE level across DDHS configurations consisting of increasing bypass portion from the upper sponge biofilm, during domestic wastewater treatment. Resistome data showed that DDHS reactors are “efficient” at reducing both ARGs and MGEs from domestic wastewater. Fifty-nine targeted ARGs and seven MGEs including exemplary ESBL-producing determinants were detected in untreated wastewater and were reduced by 50% in the co-optimised R-S20 DDHS, to undetected levels.

DDHS and other sponge reactors are an attractive option for small-scale wastewater treatment. Kobayashi *et al.* (2017) reported sponge systems effectively remove pathogenic viruses (1.5 to 3.7 log reduction for aichivirus, novovirus and enterovirus),

which complements results here on ARG removal. In particular, DDHS systems can reduce both TN and ARGs from domestic wastewater (contrary to other sponge designs) and are suitable for small-scale applications due to low energy and maintenance needs.

Although optimization is still required, early results indicate that ARG and MGE removal is especially high at 20% wastewater bypass, which we suspect is due to sequential exposure of resistance organisms to aerobic and the stronger anoxic conditions. Based on positive ARG removal, the potential for TN removal, and low energy demands, DDHS systems show great promise at reducing environmental and health impacts of wastewater discharge on local scales. As such, they should be considered in locations where centralised treatment does not exist or would be costly, although co-optimization is needed to satisfy local priorities relative to ARG versus TN removal. However, complex microbial food chain and redox ecology warrant further investigations to characterise DDHS for bioengineering optimisation. These topics will be examined in greater detail in Chapters 4 and 5.

Acknowledgement

I would like to thank Stephen Edward, who trained me when I first started working in the lab as a master's student, and assisted with the set-up of the bioreactors. I would like to thank Cathy Bundy, who monitored the bioreactors in the initial stage. I would like to thank David Early and David Race for their continuous lab assistance, Marcos Quintela for teaching me how to do DNA extraction, and Cara Wray for showing me how to do basic microbiology. Finally, thanks to JianQiang and XinYuan from Chinese Academy of science for performing the HtH-qPCR.

Chapter 4 Microbiomes within sponge biofilm reactors as a function of operating regime and local redox conditions

4.1 Introduction

Ever since the activated sludge technology emerged in England around 1913, this approach of biological wastewater treatment has become global because it is effective and achieves good effluent quality, although it also requires intensive energy for active aeration. The high cost of power to operate conventional treatment facilities is making wastewater treatment inaccessible for under-resourced communities, especially those in rural and peri-urban LMICs. This compromises sanitary improvements to protect water quality aimed at reducing the spread of waterborne illnesses in these locations.

Denitrifying Downflow Hanging Sponge (DDHS) bioreactors are promising low-energy option which can remove pollutants from household wastewater effectively through sequential aerobic-anoxic sponge biofilms, and without any further tertiary treatment (Bundy *et al.*, 2017). In Chapter 3, DDHS bioreactors were assessed using high-throughput ARG quantification and showed simultaneous TN and antibiotic resistance genes (ARGs) removal. The effectiveness of this removal could be enhanced using a co-optimal wastewater bypass regime (Jong *et al.*, 2018). Resistome data suggest DDHS bioreactors can remove ARGs from domestic sewage, however, there is a percent bypass threshold whereby a high percent bypass (e.g., 30% bypass by volume of total influent) improves TN removal, but at the expense of ARG reduction.

The co-optimised bypass ratio was around 20%, which had the advantage of an effective level of TN and ARG removal from domestic wastewater without impacting on ARG levels in the effluent. Overall effluent quality was significantly better than the effluent treated without any wastewater bypass (i.e., Control bioreactor; 0% bypass). Such a treatment outcome was accomplished by the sequential passage of

wastewater through the aerobic and anoxic sponge cores, which support ARG removal and nitrification-denitrification reactions. This configuration is different from a traditional trickling filter, where DDHS bioreactors are comprised of two distinct redox environments; the upper aerobic hanging sponge layers and the lower anoxic sponge layers submerged in effluent wastewater from the top layers providing specialised redox niches.

Characterising biofilm microbial assemblages and the locations where bacterial diversity fluctuates can help explain how microbial communities function, including in biological treatment systems. For example, Kubota *et al.* (2014) and Mac Conell *et al.* (2015) detected differing abundances of ammonium- and nitrite-oxidizing bacteria (AOB and NOB) and Anammox bacteria (*Candidatus brocadia*) at different locations along traditional Downflow hanging sponge (DHS) post-treatment bioreactor columns, which contributed to a reduction in ammonia and total organic carbon over a range of operational organic loading rates (OLRs). Furthermore, unique differences in the composition of the wider microflora has been noted in DHS-type systems (Kim *et al.*, 2016). Reticulated sponges act as a support matrix for biofilm growth, including both eukaryotes and prokaryotes and have been used to explain minimised sludge production through predation (Uemura *et al.*, 2012; Ikeda *et al.*, 2013). Some background is provided later (Section 4.1.1).

Despite the above, the microbial communities in sponge biofilms within two-stage aerobic-anoxic DDHS systems has not yet been characterised. Nor has the effect of wastewater bypass on the microbial composition within sponge cores. Given the unique sponge stratum, redox environments and resultant treatment quality, studying microbial communities along the sponge column can help answers questions about the microbial ecology of the reactors, especially between reactors that are performing well versus less-well in relation to nitrogen processing. It is hypothesized that discrepancies in effluent quality versus bypass regime can be explained by differences in microbial composition, which this chapter aims to assess.

Specifically, the microbial composition of DDHS bioreactors with and without bypass were compared, especially related to differing community compositions along the reaction pathway in the varying redox layers. These studies were performed using high-throughput amplicon sequencing and a model-based Divisive Amplicon

Denoising Algorithm 2 (DADA2). The work aimed to answer the following questions: 1) does wastewater bypass alter “sponge microbiomes” (e.g. ‘who’ and ‘where’ in the reactors) and explain contrasting performance of ARG and TN removals between different bioreactors; and 2) does bypass influence the abundance of faecal organisms and potential pathogens within the sponge biofilms and treated effluents? These aims were accomplished by satisfying the following actions:

- a) Performing Illumina MiSeq 16S rRNA amplicon sequencing for characterising the microbiomes within the sponge biofilms, as a function of redox habitats and wastewater bypass.
- b) Determining how wastewater bypass impacts on the composition of the microbial communities along sponge column.
- c) Quantifying the 16s rRNA and nitrogen-transforming genotypes using real-time quantitative polymerase chain reaction (qPCR).

4.1.1 Molecular microbial ecology

Characterizing microbial populations in natural and engineered ecosystems is essential to understand their roles and how they work together in biogeochemical cycling. The complexity and composition of microbial ecology varies across biological systems and environmental niches. Classical microbial culturing of environmental samples, including wastewater, is hugely constrained by the low cultivability (as little as 0.01-1% of the total cell population) of environmental bacteria (Amann *et al.*, 1995). Early microbial molecular tools such as fluorescence in situ hybridisation (FISH) (Amann *et al.*, 2001) and denaturing gradient gel electrophoresis (DGGE) (Muyzer, 1999) were initially developed to target the identification of representative bacteria. However, the advent of quantitative PCR and next generation sequencing (NGS) have totally changed how microbial ecology is performed. These are the methods use in the current study.

NGS allows the exploration of bacterial diversity in the environment and semi-quantification of relative abundances of taxa of various ranks (Hugenholtz *et al.*, 1998), hence now driving most environmental genomic studies (Joly and Faure, 2015). Within NGS, high-throughput Illumina MiSeq sequencing has enabled the study of microbial diversity at a greater depth by using 16S rRNA as a taxonomic

marker genes to estimate biodiversity and to identify the microbial phylotypes present in complex samples, such as gut microbiomes, soil, wastewater and biofilms (Hong *et al.*, 2015; Dong *et al.*, 2016; Byerley *et al.*, 2017).

4.2 Materials and methods

4.2.1 *Experimental background*

As described in Chapter 3, the performance of four bench-scale DDHS bioreactors were assessed for TN, COD and ARG removal as a function of different operating regimes. Different wastewater bypass percentages were compared (i.e., 0%, 10%, 20% and 30% of total wastewater by volume) to determine the optimum quantity of wastewater required to promote denitrification in the anoxic sponge layers. This was done in tandem with how these regimes impacted the fate of ARG. Chapter 3 showed that the reactor performance without a wastewater bypass was very different from those with a bypass, with a 20% bypass being the most effective for TN and ARG removal.

For the molecular microbial work in Chapter 4, the laboratory-scale DDHS bioreactors (Chapter 3; Section 3.2.1) were decommissioned after 206 days of continuous operation. Specifically, liquid was drained slowly from each bioreactor via the effluent port located at the bottom of the units. This was performed carefully in order to not lose key biomass from the sponge media. Sponges were allowed to stand for one hour to allow retained liquid within sponge media to drain. The semi-dried sponge discs were then aseptically retrieved from each column (11 sponge discs per bioreactor; see Figure B-1, Appendix B), individually wrapped in pre-sterilised aluminium foil, and stored at -80 °C prior to DNA extraction. Sponge discs were labelled in order, from top to bottom; i.e. 'Sponge 1' for the topmost sponge and 'Sponge 11' for the bottommost sponge

For the purpose of characterising and contrasting microbial communities with and without bypass, only sponge discs from the control bioreactor (R-S0; 0% bypass) and the co-optimised bioreactor (R-S20; 20% bypass) were used for DNA extraction and reported analysis in Chapter 4. This was due to time constraints, although all of the other core sponges are still available for further analysis. Within this context, cells

and DNA were extracted with the 11 sponge discs per reactor, spanning the aerobic and anoxic layers.

4.2.2 Extraction of genomic DNA from Sponge biofilm

All sponge discs from the 0% and 20% bypass reactors were thawed and dried at room temperature for an hour. The dried discs were weighed individually and the average weights of the clean discs (measured before the reactors were operated) were subtracted to estimate the weight of biomass formed in each disc. Each sponge disc was then diced into smaller sections and homogenised in a pre-sterilised mixer at high speed.

Approximately 200 mL of sterile phosphate buffer solution (PBS; Sigma Aldrich, UK) then was added to the mixer content to release/elute biomass from the diced sponges. Sponge pieces were squeezed to transfer cell biomass into the PBS, which was collected in sterile polypropylene (PP) centrifuge bottles (Fisher Scientific, UK). The PBS suspension containing eluted sponge biomass was centrifuged at 12000 rpm for 30 minutes and the pelleted biomass was recovered for DNA extraction, using the Fast DNA Spin Kit for Soils (MP Biomedical, USA) according to the manufacturer's instructions. Subsequent pure DNA extracts were recovered using the QIAquick Nucleotide Spin columns (QIAGEN, UK), removing salts and other inhibitory contaminants to ensure good DNA quality for downstream sequencing on the Illumina MiSeq platform. The quality of DNA samples was determined using a Denovix DS-11 Spectrophotometer and the nucleic acid absorbance programme according to the instrument operating manual (Denovix, UK). DNA extracts were stored at -20 °C prior to subsequent analysis.

DNA also was extracted from samples of the reactor influent and effluent wastewater, streams collected during the time-window associated with the sampling and analysis reported in Chapter 3. In total, 50 DNA samples were obtained for sequencing and qPCR.

4.2.3 Amplicon preparation and Illumina Miseq 16S rRNA sequencing

Approximately 10 µL of pure, undiluted DNA extract per sample were aliquoted into a 96-well plate, which were sealed and shipped for DNA sequencing at the NU-OMICS research facility (Northumbria University, UK). The V4 hyper variable region of the

16S rRNA-encoding gene, which can detect both bacteria and archaea, was amplified from the DNA template using the barcoded dual-index 515f and 806r primers developed by Kozich *et al.* (2013). PCR products were then checked by gel electrophoresis, cleaned, normalised, and finally pooled to construct a 16S rRNA gene library that was used for paired-end (2x250bp) amplicon sequencing on the Illumina MiSeq V3 platform, in accordance to the 16S sequencing Illumina MiSeq Personal Sequencer protocol described by Kozich *et al.* (2013). The 500 cycle MiSeq V2 chemistry kit was used to generate up to 12-13 million cluster reads. Demultiplexed FASTQ files containing completed amplicon sequences were delivered via the Cloud and were used for subsequent microbiome data analysis.

4.2.4 Phylogenetic analysis workflow

The Illumina amplicon dataset was processed and analysed using a dual combination of QIIME2 (Caporaso *et al.*, 2010; Caporaso, 2018) for upstream data preparation, and R statistical software 3.5.0 (R Core Team, 2013) for downstream statistical computing and visualisation. The workflow employs the Divisive Amplicon Denoising Algorithm 2 (DADA2) package (Callahan *et al.*, 2016a), tailored for analysing Illumina-sequenced amplicon data to provide high-resolution microbiomes. An overview of the workflow of microbiome analysis is outlined in Figure 4-1.

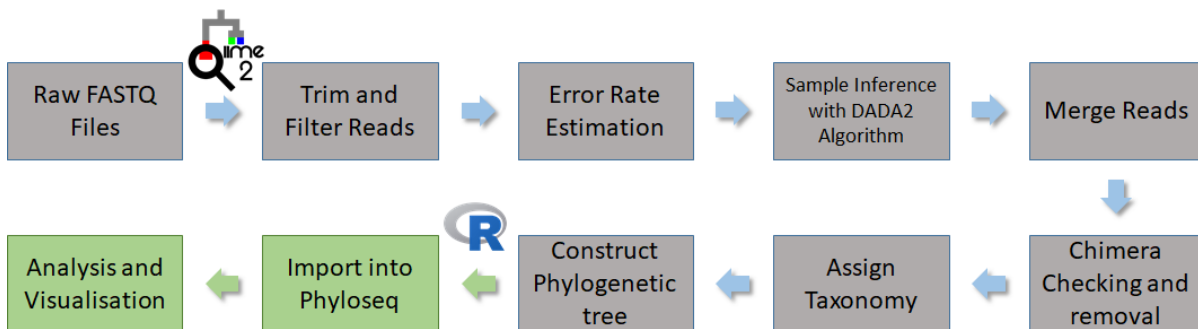


Figure 4-1 Workflow for microbiome data analysis using a combination of Qiime2 (Caporaso, 2018) and R statistical software 3.5.0 (R Core Team, 2013) DADA2: from raw reads to community analyses (Callahan *et al.*, 2016a). Grey boxes denote upstream data processing using Qiime2; green boxes denote downstream statistical analysis in R.

Upstream sequencing data processing was preceded by importing demultiplexed FASTQ files from the Illumina MiSeq run into QIIME2. Here, the DADA2 pipeline was implemented. Low quality sequencing reads were trimmed and filtered by inspecting the quality profile: the forward reads maintained high quality throughout for all

samples (Phred score ≥ 30), while reverse reads for bases greater than the 200th nucleotide had a Phred score that dipped below 30. Therefore, reverse reads at position 200 and onwards were truncated and rejected from analysis together with the first 10 nucleotides for both forward and reverse reads, which were also truncated. Previous observations across many Illumina datasets have suggested that these bases often have a high error frequency (Callahan *et al.*, 2016b). Then, error-corrected and chimeric-removed output sequences were assembled into highly distinguishable amplicon sequence variants (ASV), and were assigned taxonomy by comparisons with the Silva132 reference database. A multiple sequence alignment then was conducted and a phylogenetic tree was built using the MAFFT (Katoh *et al.*, 2002) and FastTree packages (Price *et al.*, 2010), respectively.

Subsequent downstream bioinformatics were carried out entirely in the R open-source software environment via the Rstudio interface. In R, Phyloseq (McMurdie and Holmes, 2013) was used to create a phyloseq object that combined the ASV sequence table, the taxonomy table, the metadata table, and phylogenetic trees for use in downstream phylogenetic comparisons and multivariate analysis.

4.2.5 Bioinformatics and statistics

Microbial community diversity in the sponge biofilms from both bioreactors were computed in R using the taxonomically filtered dataset generated in the upstream processing. R was chosen for downstream statistical procedures as it allows curated analysis of complex molecular microbial datasets; numerically and visually.

Specifically, the microbial diversities (i.e., Alpha diversity, see later) of biofilms from individual bioreactor sites, comprising 11 individual sponge layers per bioreactor, spanning the aerobic and anoxic section, were compared as follows:

- i) across local sponge layers within each bioreactor (i.e., Sponges 1 to 11 of each bioreactor);
- ii) crosswise across parallel sponge layers between the two bioreactors (i.e., Sponges 1 R-S0 vs. Sponge 1 R-S20);
- iii) crosswise across parallel redox zones between the two bioreactors (i.e., aerobic zone sponges R-S0 vs. aerobic zone sponges R-S20).

The purpose was to assess where and how bacterial diversity might fluctuate within individual bioreactor, and between the contrasting operating regimes.

Alpha (α -) diversity within the sponge biofilms was measured using the Shannon and Simpson indices (diversity estimators), which statistically quantify sample richness (number of species; i.e., who is there?) and evenness (number of individuals per species; i.e., how many are there?). Observed Simpson's and Shannon's indexes from contrasting bioreactors were plotted, and statistically compared using the parametric independent T-test and ANOVA (analysis of variance) for normally distributed samples to determine paired group and multiple groups differences, as defined above. When data distributions were not normal, Kruskal-Wallis and Wilcoxon test were used as non-parametric alternatives for the ANOVA and T-test, respectively. Significance was defined at the 95% confidence level (i.e., p -value < 0.05). Changes in relative abundances (>3% of overall abundance) were analysed to assess the compositions of the microbial communities and the distributions of major genera across the sponge biofilms.

Beta (β -) diversity based on Unweighted Unifrac distance matrices (i.e., among samples; i.e., how similar are groupings of samples?) was used to visualise patterns and differences (dissimilarities) between sample clusters resulting from phylogenetic variation. These are displayed in a principal coordinate analysis (PCoA) plot. Permutational multivariate analysis of variance (PERMANOVA) tests were used to assess phylogenetic differences between sample groups in β -diversity and the Canonical correspondence analysis (CCA) was used to assess the impact of process variables on the diversity patterns, as a function of measured local environmental parameters.

Correlations were examined in an ordination map consisting of candidate environmental variables, the microbial compositions via individual genera (top 30 most abundant genera), and arrows (\rightarrow), using the Vegan R package. Microbial community responses to particular environmental parameters can be revealed via perpendicular projections of samples or species points along an environmental variable's arrow, hence, explaining possible relationships that may exist.

4.2.6 Quantitative polymerase chain reaction (qPCR)

The abundance of total bacteria (as estimated via 16S rRNA) and nitrogen-transforming microorganisms, including those performing nitrification (ammonia oxidation and nitrite oxidation; for both bacterial and archaeal populations), denitrification, and nitrogen fixation were quantified using qPCR on DNA samples extracted from all sponge layers abstracted from R-S0 and R-S20. Accordingly, the 16S-rRNA, *amoA* (bacterial and archaea), *nirS*, *nirK*, *nifH* genes and *nitrobacter* and *nitrospira spp.* were detected and amplified using probes and primers summarised in Table 4-1.

Before quantification, samples were assayed for possible inhibition of the PCR. Six samples were randomly selected and serially diluted from 10^1 to 10^5 with molecular-grade water and analysed with primers to quantify 16S-rRNA (see Table 4-1). The resulting trend lines were compared with those of 'neat' standards; the lowest dilutions that had comparable slopes between test samples and the standards were selected for subsequent use. Optimal dilution series were selected based on the strength of PCR amplification (i.e., curve slopes), regular CT-spacing (3.3 cycles) of subsequent dilutions, and minimal intra-sample variable. As such, all samples were diluted 1:100 to minimise any inhibitory effects on the PCR polymerase enzyme.

Each 10- μ L reaction comprised of 5 μ L GoTaq® qPCR Master Mix with dsDNA-binding dye (Promega™), 1 μ L primer solution (500nM final concentration; Sigma-Aldrich; Haverhill, UK), 7 μ L molecular-grade water (Qiagen, Hilden, Germany), and 2 μ L of sample (or standard or blank). Temperature cycles involved 10 min at 95 °C for initial denaturation; 40 cycles of denaturation (20 s, 95 °C); primer annealing (20 s at primer-specific temperatures; see Table 4-1); and elongation and fluorescence detection (10 sec, 72 °C) on a BioRad iCycler with an iQ fluorescence detector (BioRad). Gene-containing plasmids, each diluted in yeast tRNA solution (10^1 to 10^7 copies per micro-litre) were used as standard controls (Smith, et al., 2004). Post-analytical quality control included a temperature-melt curve of PCR products to verify reaction quality (50-95 °C, $\Delta T = 0.1$ °C/sec).

Table 4-1 Primer sets used for qPCR assays of all samples including their sequences and appropriate reaction conditions.

Target gene/micro-organisms	Primer/probe	Sequence (5' - 3')	Annealing, Ta (°C)	Reference(s)
16S-rRNA; total bacteria	515F	GTGCCAGCAGCCGCGGTAA	58 °C	Dorn-In <i>et al.</i> , 2015
	805R	GACTACCAGGGTATCTAATC		
<i>nirS</i> : haeme-based nitrite reductase; denitrifiers	nirSCD3aF	AACGYSAAGGARACSGG	57 °C	Kandeler <i>et al.</i> , 2006; Throbäck <i>et al.</i> , 2004
	nirSR3cd	GA(C/G)TTCGG(A/G)TG(C/G)GTCTTG A		
<i>nirK</i> : copper-based nitrite reductase; denitrifiers	F1aCu	ATCATGGT(C/G)CTGCCGCG	57 °C	Hallin <i>et al.</i> , 1999; Throbäck <i>et al.</i> , 2004
	R3Cu	GCCTCGATCAG(A/G)TTGTGGTT		
<i>NifH</i> : Nitrogenase iron protein; nitrogen fixers	PolF	TGCGAYCCSAARGCBGACTC	55 °C	Poly <i>et al.</i> , 2001
	PolR	ATSGCCATCATYTCRCCGGA		
<i>amoA</i> : ammonia mono-oxygenase (bacterial): AOB	amoA-1F	GGGGTTTCTACTGGTGGT	60 °C	Rotthauwe <i>et al.</i> , 1999
	amoA-2R	CCCCTCKGSAAAGCCTTCTTC		
<i>amoA</i> : ammonia mono-oxygenase (crenarchaeal): AOA	crenamoA23F	ATGGTCTGGCTWAGACG	55 °C	Tournai <i>et al.</i> , 2008
	crenamoA616R	GCCATCCATCTGTATGTCCA		
<i>Nitrobacter</i> spp. 16S-rRNA	Nitro-1198f	ACCCCTAGCAAATCTCAAAAAACCG	58 °C	Knapp & Graham, 2007; Graham <i>et al.</i> , 2007
	Nitro-1423r	CTTCACCCCAGTCGCTGACC		
<i>Nitrospira</i> spp. 16S-rRNA	Nspra-675f	GCGGTGAAATGCGTAGAKATCG	58 °C	Knapp & Graham, 2007; Graham <i>et al.</i> , 2007
	Nspra746r	TCAGCGTCAGRWAYGTTCCAGAG		

4.3 Results and Discussion

4.3.1 16S rRNA amplicon sequencing and abundances

Illumina MiSeq V3 amplicon sequencing yielded a total of four million 16S rRNA sequence reads, equivalent to mean reads of 90,000 per sample after quality filtering. Retained sequences containing overlapping paired-end reads with an average length of 253 bases were inferred in the DADA2 algorithm, and generated 14,613 unique amplicon sequence variants (ASVs). The assembled ASVs were subsequently assigned taxonomy and classified using the Silva 132 reference database.

Different from previous QIIME workflow (Schloss *et al.*, 2009; Caporaso *et al.*, 2010), which classifies amplicons by picking Operational Taxonomic Unit (OTU) based on 97% radius similarity (underutilising high throughput sequencing data and tends outputting erroneous inferences), DADA2 uses de novo read data and infers sample sequences precisely (Callahan *et al.*, 2016a). This reduces false positives.

Limitations still occur when classifying bacteria at the species level because of relatively short read lengths generated from Illumina sequencing (Cole *et al.*, 2010).

Overall, both bioreactors had similar unique ASV counts across biofilm samples, with mean observed counts of 1467.1 ± 228 and 1459.5 ± 212 ASVs per sponge layer for R-S0 and R-S20, respectively. Bacteria identified from the samples were classified into 41 and 39 phyla, respectively. Further taxonomic level data (e.g. class, order, family, genus and species) revealed microbiome profiles that differed between the two bioreactors. The R-S20 reactor biofilms exhibited a greater diversity at the class level. For example, a total of 587 bacterial genera was identified to genus level in the R-S20 biofilms, whereas 520 genera were identified in R-S0. R-S20 biofilms had generally greater microbial diversity.

DDHS biofilm communities had comparable bacterial densities with conventional activated sludge aeration tanks, which typically range from 10^8 to 10^9 cells/mL (Manti *et al.*, 2008). Real-time PCR showed similar bacterial abundances (as 16S rRNA) throughout the sponge column and for both bioreactors (Figure 4-2) with the average value of 9.75×10^8 16S copies/g biofilm per sponge layer, equated to approximately 2.4×10^8 cells/g biofilm when average 16S copy numbers are taken into account.

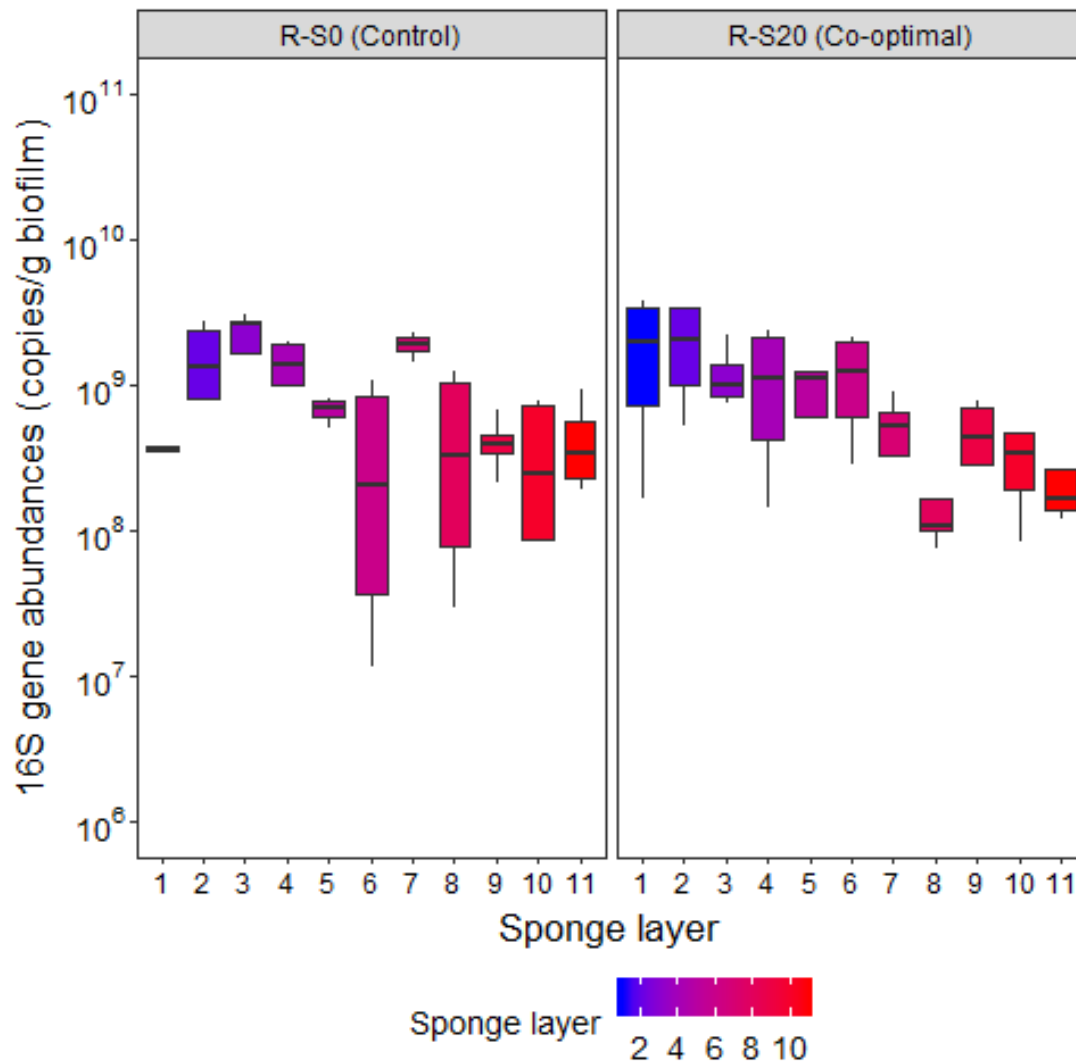


Figure 4-2 qPCR quantification of 16S rRNA abundances of the sponge biofilms, as indicated by sponge layers, along sponge columns of the R-S0 and R-S20 bioreactors ($n = 4$; two technical replicates per biological replicate).

Despite similar abundances, significant variations were seen between the sponge layers within the R-S0 bioreactor (Kruskal-Wallis; p -value = 0.005) while less variations were observed between the sponge layers within the R-S20 bioreactor (Kruskal-Wallis; p -value = 0.031; i.e., better evenness), implying that R-S20 had a less spatially varied biofilm development. Further, vertical profiles of bacterial levels show gradually decreasing abundances as sponge depth increases, which may reflect the filtration effects through the sponge media and the reductions in the availability of organic compounds at the lower depths of the reactor, especially in the R-S0 bioreactor due to the absence of a bypass.

4.3.2 Microbial α -diversity versus local redox

Shannon and Simpson indexes (Shannon, 1948; Simpson, 1949) were used to evaluate α -diversity of DDHS sponge biofilm communities. Analysis of variance (ANOVA; p -value < 0.05) shows significant differences in the majority of local biofilms (i.e., by sponge layers) within the individual bioreactor.

Figure 4-3 provides an overview of the α -diversity pattern across sponge depths of R-S0 and R-S20.

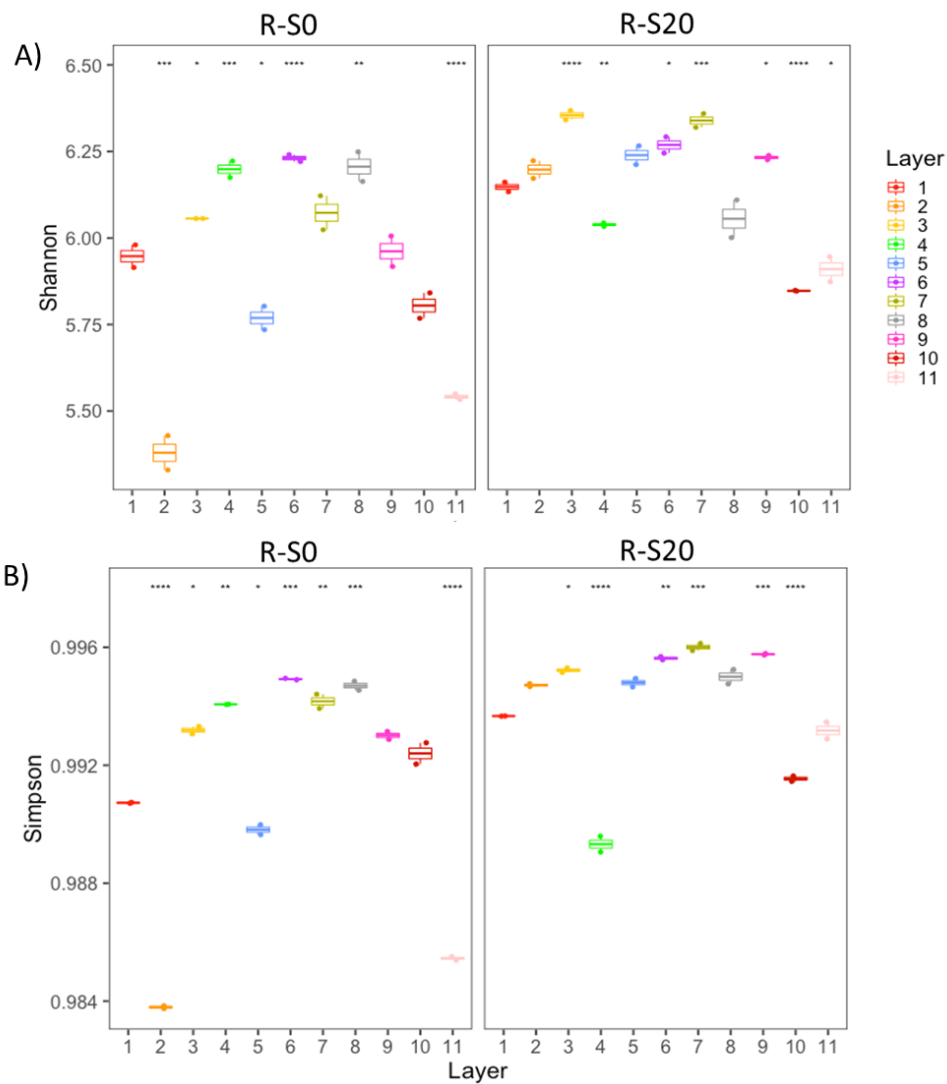


Figure 4-3 Comparisons of α -diversity between local biofilms, by sponge layers, within each bioreactor showing (A) Shannon and (B) Simpson indices and analysis of variance (ANOVA). Asterisks indicate the p significant values comparing mean diversity index per sponge layer to the group mean for that reactor. * denotes $p \leq 0.05$; ** denotes $p \leq 0.01$; *** denotes $p \leq 0.001$; **** denotes $p \leq 0.0001$.

Overall, biofilm diversity varied throughout the depths of the sponge layers in both bioreactors with slightly greater fluctuations observed in R-S0. For example, a noticeably lower Shannon and Simpson indices were seen in Sponge 2 of R-S0. In contrast, biofilm diversities in R-S20 were more evenly spread across sponge layers.

Further comparisons of the indices were performed using a paired-samples T-test to examine differences in biofilm community diversity between the bioreactors. Shannon and Simpsons indices (Figure 4-4A and Figure 4-4B) suggest significantly greater taxonomic diversity (i.e., richness and evenness) in the R-S20 biofilms compared with the R-S0 biofilms (T-tests for Shannon and Simpson indexes; both p-values < 0.01). It had been hypothesised that the differences of bacterial diversity between bioreactors might occur when bypass was used, in particular to the potentially richer denitrifying guild. However, crosswise comparisons of the microbial diversities between “aerobic R-S0” vs “aerobic R-S20” layers and “anoxic R-S0” vs “anoxic R-S20” layers showed that this was not the case.

Instead, differences in diversity between the R-S20 and R-S0 bioreactors were apparent in the aerobic sponge layers (Figure 4-4C and Figure 4-4D) with the aerobic layers in R-S20 displaying higher in α -diversity (T-tests for Shannon and Simpsons indexes; both p-values < 0.05). Differences in community diversity between the two anoxic sponge layers were not significant, although the R-S20 bioreactor did have a higher level of diversity overall. Such observations may be explained by the Simpson index (D), which measures richness and also accounts for the proportions of species within the measured population; i.e., relative abundance (Simpson, 1949). It is determined by summing the relative abundance of each species, as described in Equation 4-1; the Evenness is calculated by expressing index (D) as a proportion of the maximum possible value. Values range between 0 and 1; the higher the value, the greater the richness and evenness, with 1 being infinite diversity.

Equation 4-1 The equation used to determine species diversity which takes into account both richness and evenness.

$$D = \frac{\sum n(n-1)}{N(N-1)}$$

Where:

N = the total number of organisms of all species and

n = the total number of organisms of a particular species from which Simpson's index of diversity, $1 - D$, is found.

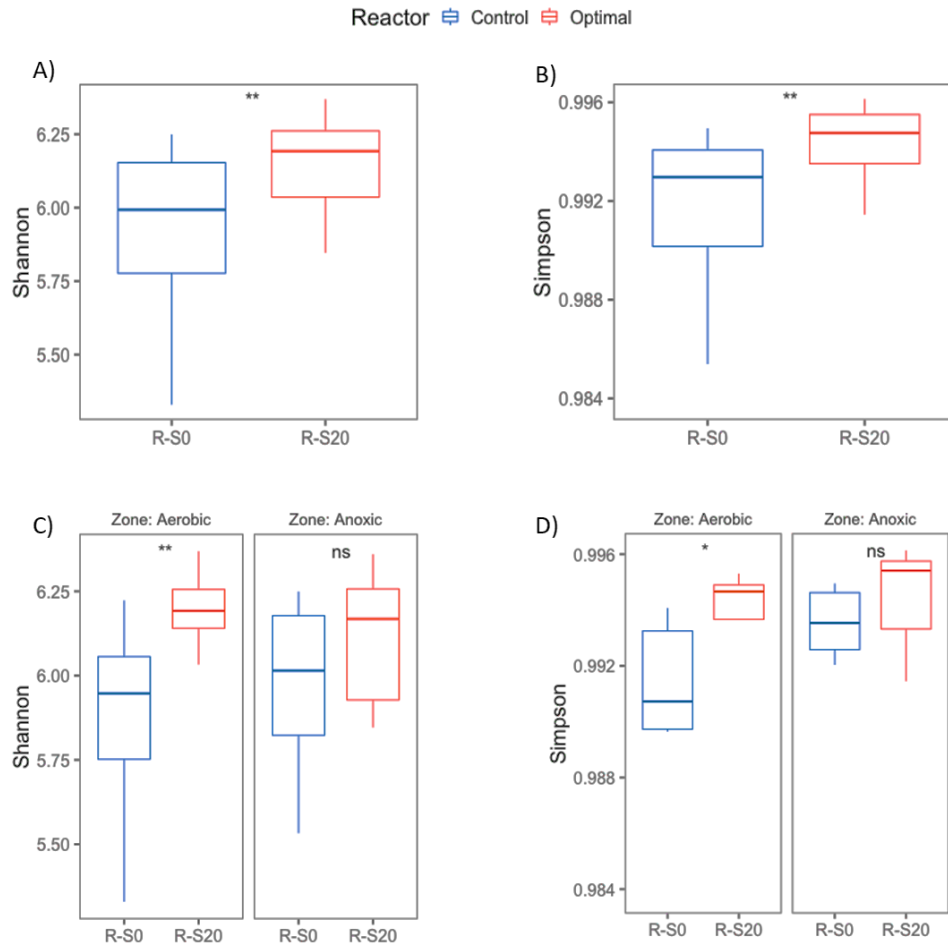


Figure 4-4 Shannon and Simpson indices between DDHS biofilm samples and paired samples T-tests; A) & B) Shannon and Simpson indices comparisons by reactors; C) & D) Shannon and Simpson indices comparisons by redox environments within individual reactor. Asterisk * denotes $p \leq 0.05$; ** denotes $p \leq 0.01$; ns denotes $p > 0.05$.

In the aerobic biofilms, the relatively lower Simpson indices observed in the R-S0 bioreactor suggest the presence of dominant species, hence affecting the evenness of its population. A detailed look into the α -diversity across sponge layers (see Figure B-2; Appendix B) confirmed lower community evenness in the biofilms of the R-S0 bioreactor, especially in the aerobic sponges, where greater richness and evenness were observed in majority of the R-S20 sponge biofilms.

4.3.3 Microbiomes within sponge biofilms

Microbial communities in the DDHS sponge biofilms display considerable diversity, especially between the different redox environments. The major phyla (> 3% relative abundance), encompassing Proteobacteria, Planctomycetes, Chloroflexi, Bacteroidetes, Verrumicrobia, and Actinobacteria formed the core biofilm community across all sponge layers (Figure 4-5). Proteobacteria was the most abundant phylum in all of the sponge layers, which is similar to that found in other biological wastewater treatment systems (Wagner *et al.*, 2002; Jiang *et al.*, 2008; Wang *et al.*, 2017a); with an average abundance of 36% (SD \pm 10) and 30% (SD \pm 4), respectively, in R-S0 and R-S20 biofilms. Although samples from both bioreactors were quite similar in community composition, differences in relative abundances were apparent. For example, Proteobacteria was very dominant in the top five layers of the R-S0 bioreactor (~42-50%), but lower (28-38%) in R-S20. Statistics confirmed that the relative abundance of Proteobacteria in the R-S0 aerobic biofilms was significantly greater than in the R-S20 aerobic biofilms (T-test; p-value = 0.00028).

As reactor depth extended to the anoxic sponges (bottom six layers), the dominance of Proteobacteria was reduced in R-S0 (~21-28%), which was more similar to that of R-S20 (~22-30%). The resultant changes in Proteobacteria within R-S0 was more dramatic and significantly different when switching from aerobic to anoxic biofilms (ANOVA; p-value=0.00048), as compared to R-S20 (ANOVA; p-value = 0.17). The majority of Proteobacteria are fast growing heterotrophs (Gray, 2004) with higher affinity towards organic substrate, and as a result are more likely to be sensitive to changes in the availability of carbon sources. This shift of Proteobacteria in R-S0 was probably caused by the lowering of the wastewater COD with increasing sponge depth as it gets utilised by microbes in the upper sponges. R-S0 had higher OLR in the upper aerobic biofilms due to the absence of a bypass. A corresponding absence of Verrumicrobia and lower abundances of Plantomycetes and Chloroflexi within the top five sponge layers in R-S0 suggests they were likely to be outgrown by Proteobacteria.

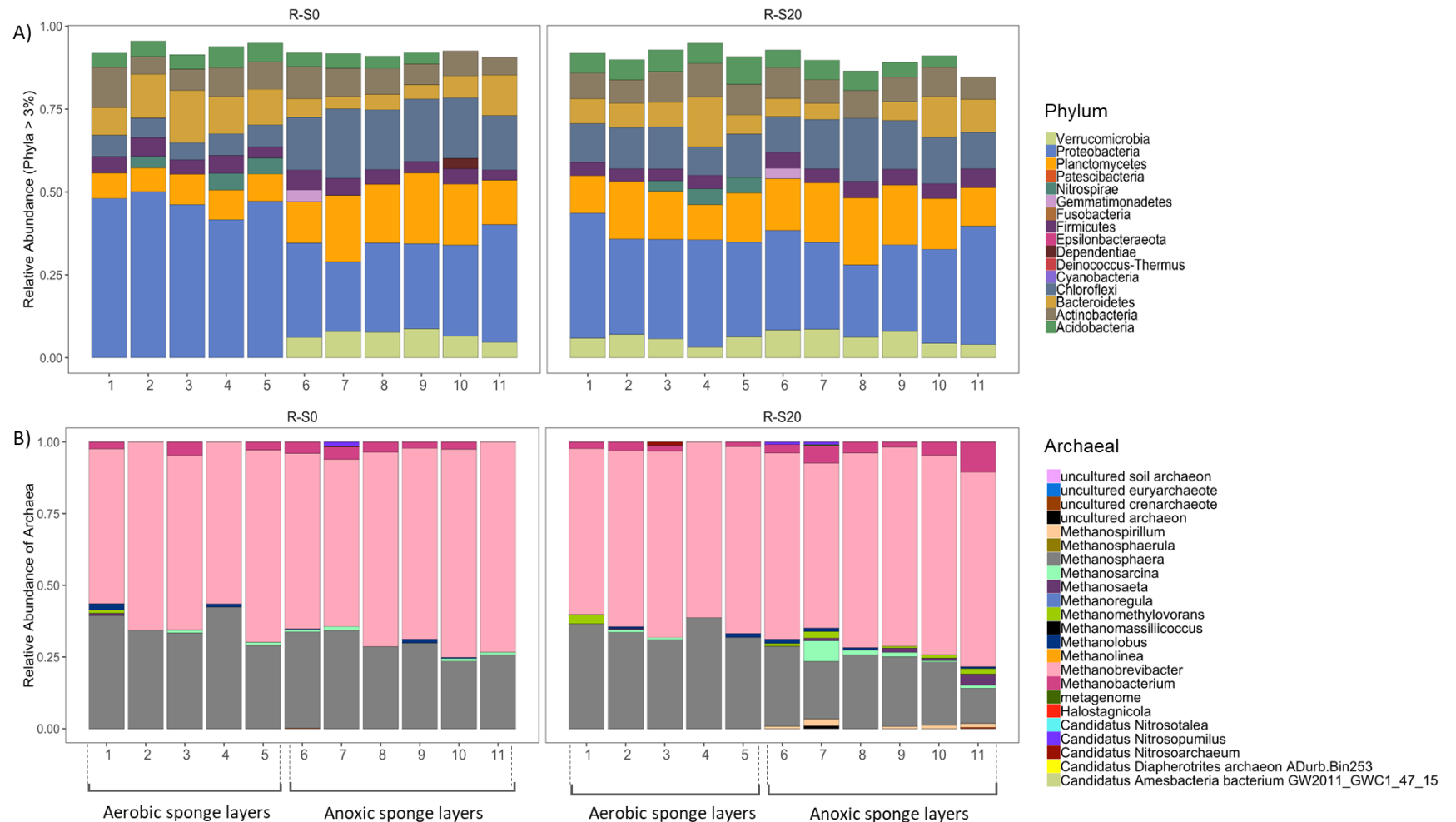


Figure 4-5 Microbial compositions identified along sponge column where each section represents 11 sponge layers for the Control (R-S0) and Co-optimal (R-S20) bioreactors. (A) Bacterial relative abundance >3% at phylum level. (B) Relative abundances of the archaeal community belonging to phylum Euryarchaeota.

Liao *et al.* (2017) reported that the higher abundance of Proteobacteria in the upper part of their DHS bioreactor was responsible for total organic carbon, which in turn they also attributed to a higher OLR. Apparently in our R-S20 bioreactor, the bypass appears to even out the distribution of Proteobacteria because 20% less wastewater was applied to the aerobic sponges. Interestingly, the final sponge layer located at the bottom of both reactors saw a slight increase in Proteobacteria abundance (35% and 36%, respectively), although it is not clear why. It might be due to a general shortage of nutrients and metabolic versatility of these organisms.

Archaea were present in all sponge biofilms at low abundances, constituting only 0.4% of the total microbial population in the R-S0 bioreactor and 0.8% in R-S20 bioreactor. This is not surprising given that neither system was evidently methanogenic. In both reactors, the archaeal population was dominated by *Methanobrevibacter* and *Methanosphaera* with a greater level of archaeal diversity observed in the R-S20 bioreactor.

4.3.4 Core microbial communities

Figure 4-6 illustrates the top 26 most abundant genera in both bioreactors. Common bacterial flora (> 3% relative abundance) includes genera *Acinetobacter*, *Pseudomonas*, *Nitrosomonas*, *Nitrospira*, and *Flavobacterium*. These are similar to other fixed-film systems (Saminathan *et al.*, 2013; Blázquez *et al.*, 2017), including DHS bioreactors (Kubota *et al.*, 2014; Kim *et al.*, 2016; Liao *et al.*, 2017). The distribution of microbial communities across sponge biofilms was similar for both bioreactors, excepting for the evident dominance of *Acinetobacter* and *Chryseobacterium* in the aerobic biofilms of R-S0. The relative abundances of genera is indicated by the size of bubbles in the figure.

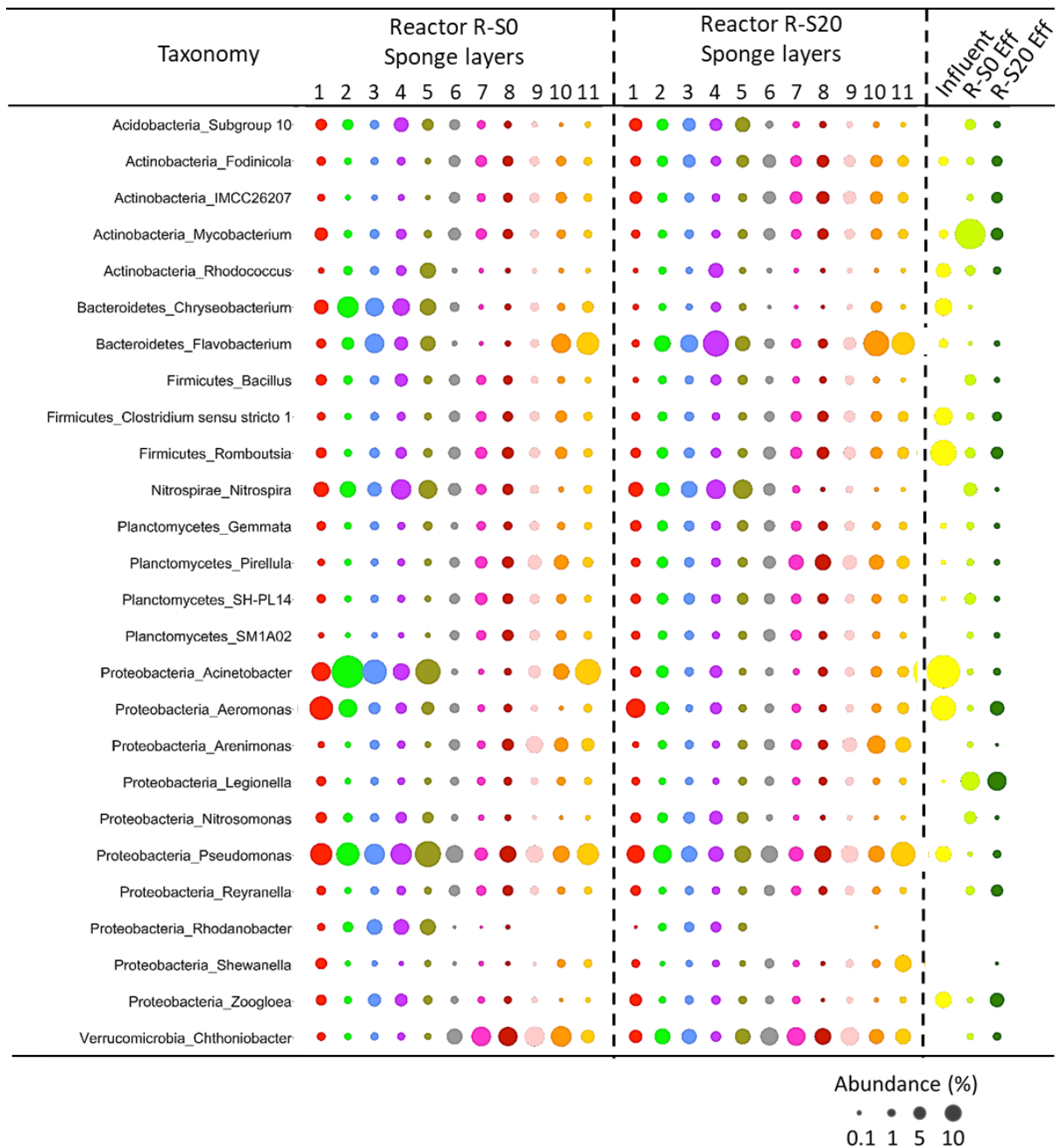


Figure 4-6 Relative abundance of major genera (> 3% relative abundance) in the bioreactors. Each section represents 11 sponge layers for Control (R-S0) and Co-optimal (R-S20) bioreactor, including wastewater influent and treated effluents (Eff).

Under the higher OLR conditions of the aerobic biofilms in R-S0, *Acinetobacter* and *Chryseobacterium* were the dominant bacteria. They were significantly more abundant than in the anoxic biofilms (T-test, p-values = 0.05 and 0.004, respectively). In contrast, these genera were more evenly distributed throughout upper and lower biofilms in R-S20 with no significant differences detected (T-tests; p-values = 0.35

and 0.5). As example, the sum of relative abundance of these genera accounted for up to 37% of the total abundance in the second sponge layer in the R-S0 bioreactor, but only accounted for 3% in the same location in R-S20 (Table B-1; Appendix B). Such dominance affirms the aforementioned putative dominant taxa (α -diversity; Section 4.3.2), which is likely to affect the evenness and diversity in the R-S0 aerobic biofilms. It is suspected that they are the primary phylotypes (i.e., Proteobacteria) responsible for organic carbon degradation in the upper aerobic layers, which are receiving greater organics and resulting in higher biomass yields.

The more dramatic spatial variation (aerobic versus anoxic) within R-S0 was evidenced by the preponderance of *Acinetobacter* and *Chryseobacterium*, a major difference between the two bioreactors. During the change from aerobic to anoxic environments in R-S0, abundances of both *Acinetobacter* (T-test; p-value = 0.05) and *Chryseobacterium* (T-test; p-value = 0.004) dropped significantly. However, their abundance did not significantly vary between redox environments in R-S20 (T-tests; p-values < 0.05 for both). It was noticeable that *Acinetobacter* had an increased abundance in the lowest anoxic sponge layer in R-S0. This may be due to the presence of traces of organic compounds released as a result of the turnover of microbes in the biofilms due to death and cell lysis. *Acinetobacter* in particular relies on external carbon source and there was no additional carbon was supplied in R-S0.

Pseudomonas species were abundant throughout all sponges in both bioreactors, implying that they are not influenced significantly by the local redox conditions. They were slightly more abundant in R-S0 aerobic biofilms, probably due to higher availability of carbon. In contrast, *Nitrospira* was apparently selected by redox conditions, where it was significantly higher in the aerobic biofilms than in the anoxic in R-S0 (T-test; p-value = 0.005) and in R-S20 (T-test; p-value = 0.003). *Nitrospira* was especially enriched in sponge layers four and five in both reactors (R-S0; p-value = 0.024) and (R-S20; p = 0.00005). It is suspected this is because the dominant heterotrophs were less competitive due to lower available of nutrients at this depth, allowing ammonia- and nitrite-oxidising to succeed.

R-S20 had generally greater *Flavobacterium* abundances. *Flavobacterium* strains are often strict aerobes (Whitman *et al.*, 2015), although some can be facultative and carry out anoxic denitrification (Horn *et al.*, 2005). For example, they have been

found to be dominant in denitrifying granular sludge bioreactors at low COD/N ratios (Cydzik-Kwiatkowska *et al.*, 2014) and in polymer biofilms (Xu and Chai, 2017). Another bacterium that denitrifies is *Shewanella* (Yoon *et al.*, 2013; Chen and Wang, 2015), and members of this genus were found to increase towards the bottom of R-S20. Given optimal TN removal in R-S20 and increased abundance in the bypassed bioreactor, it is possible that *Flavobacterium* and *Shewanella* may be primarily responsible for the observed removal of nitrate in the R-S20 bioreactor.

4.3.5 Impact of wastewater bypass on β -diversity and relationships with process variables

The results of a principal coordinate analysis (PCoA) based on Unweighted Unifrac clustering were plotted (Figure 4-7). The data were used to visualise differences and clustering between sponge biofilms from both bioreactors. The distances between the points reflect sample dissimilarity (Ramette, 2007).

The first two components from the scree plot analyses account for 69% of the total variation observed between samples. This is explained by the organic substrate loading rate as principal component 1 (PC1), which represents 46% of variations, whereas PC2 separates group centroids based on apparent redox conditions and represents 23% of the variation. It is clear that the influent wastewater and reactor effluents were phylogenetically different that the reactor biofilm communities as they are separated from the sponge communities. However, distinct biofilm communities were apparent in different locations. Samples were grouped into two major clusters according to those receiving higher organic loadings (left centroid; aerobic biofilm R-S0) and lower organic loadings (right centroid; anoxic biofilms). A subpopulation was also apparent, presumably related to intermediate loadings (middle centroid; aerobic biofilms in R-S20) associated with the raw wastewater diverted in the bypass.

There was a significant difference between aerobic and anoxic biofilms within the DDHS sequential redox settings (PERMANOVA; p-value = 0.001). Distances between aerobic biofilm communities taken from the R-S0 bioreactor were larger than those taken from aerobic and anoxic biofilms of the R-S20 bioreactor. While the microbial communities in most of the anoxic biofilms were similar between bioreactors, a noticeable community displacement in sponge layer 11 of R-S0 is

evident from the rest of the anoxic samples. This may be associated with the marked increase in *Acinetobacter* in sponge 11 as discussed in Section 4.3.4.

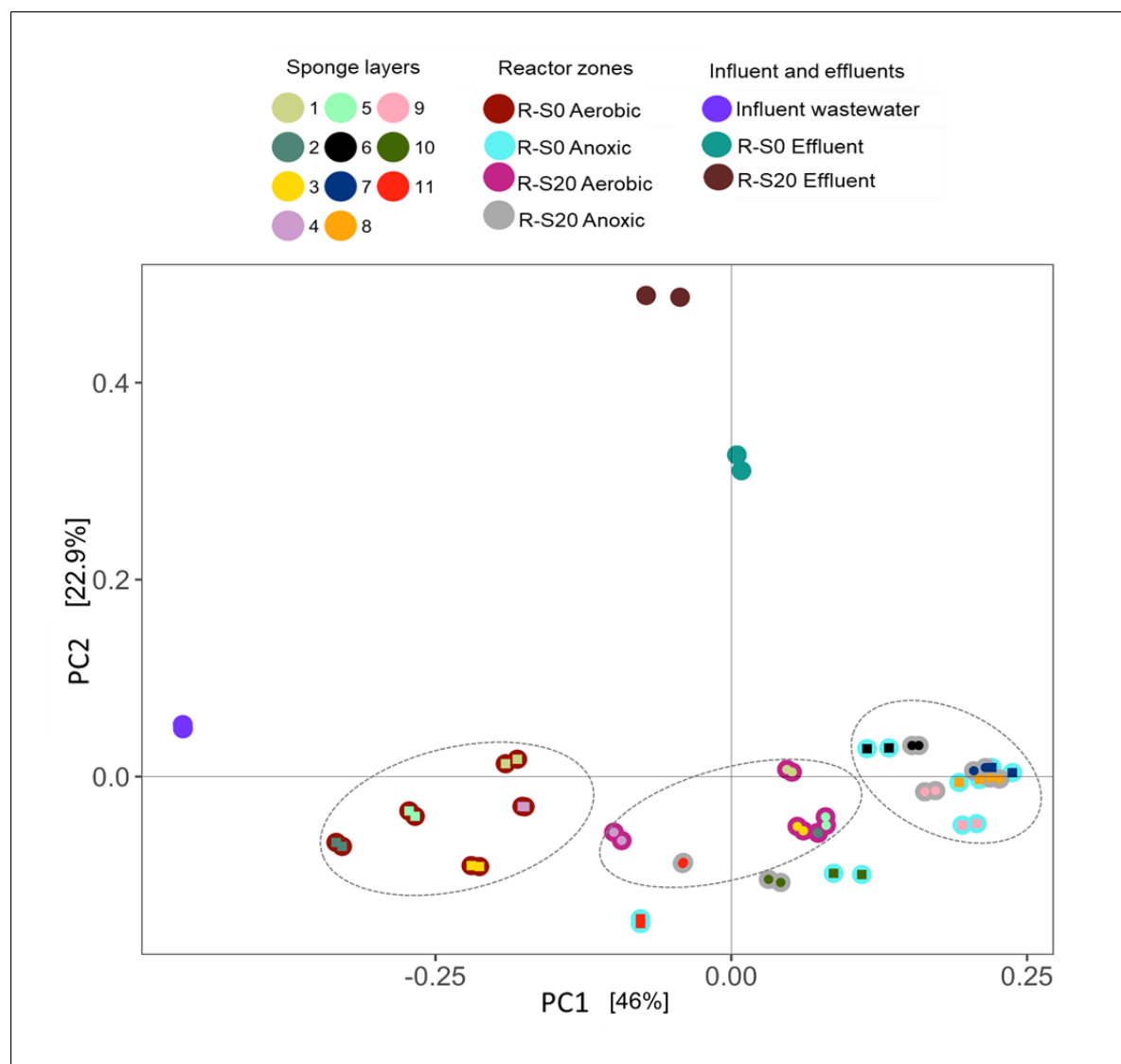


Figure 4-7 PCoA plot based on Unweighted Unifrac distances of all samples showing clustering of biofilm microbiomes together with wastewater and reactor effluents spanning 69% of total variations.

Interestingly, samples were less separated by wastewater bypass itself, but more by the indirect effect of the bypass; for example, differences in OLRs into the aerobic treatment step. Samples within the R-S20 bioreactor (20% bypass) showed smaller differences between the aerobic and anoxic biofilms; more even diversities across sponge transects. The microbiomes in the R-S0 bioreactor (no bypass) was consequentially altered by greater organic substrate loadings at their top where a distinct heterotrophic community is suggested.

To determine the factors influencing the spatial differences in the microbial communities observed above, canonical correspondence analysis (CCA) was applied to the top 30 most prevalent genera in the upper and lower biofilms, superimposed with measured environmental variables. Figure 4-8 shows the CCA tri-plot of shared common genera (black dots) and the top 30 most abundant bacterial genera together with sample locations shown in other colours and their interactions with abiotic parameters indicated by the arrows. The length of arrows is related to the rate of responses to changes in parameters. Eighty-one percent of the observed phylogenetic differences between redox conditions and community assembly are explained by sponge depth, OLR, apparent DO, and sponge density. There was a significant correlation of the canonical axes with these variables (p -value < 0.001).

CCA analysis further confirmed that the composition of biofilms formed in the DDHS aerobic sponges were phylogenetically different between bypass schemes. The analysis shows that the upper biofilm communities in R-S0 were highly influenced by OLR and DO, with *Acinetobacter*, *Pseudomonas*, *Aeromonas* and *Chryseobacterium* positively correlated with these parameters. The distinct groupings can be seen by colours, with the locations of dots and the arrows indicating the parameters that most influenced the groupings. Samples from the anoxic sponge layers had negative correlations (ordinated further away) with respect to high DO and OLR, corroborating that denitrifying bacteria thrive better under anoxic conditions. A moderate carbon supply (e.g., 20% bypass) encouraged denitrification and responded less to OLR. As consequence of the bypass, communities from the R-S20 aerobic biofilms grouped in the middle of the plot and were inclined towards a more moderate OLR. Conversely, the anoxic communities were positively correlated with reactor depth and sponge porosity, but responded less to the TN levels (short arrow).

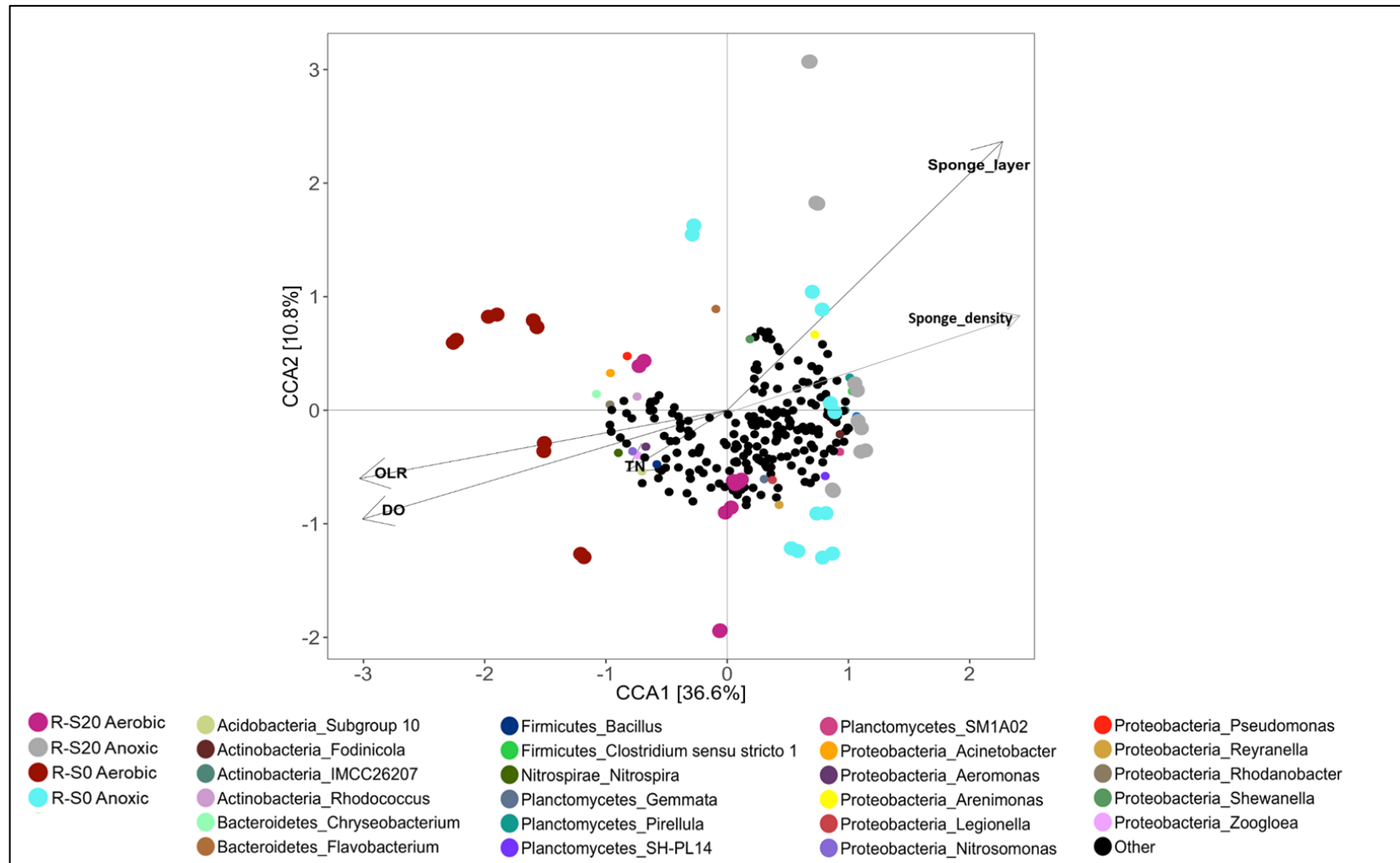


Figure 4-8 CCA tri-plot of major genera (> 3% relative abundance) and locations for biofilm samples from all sponge layers of the DDHS bioreactors showing the correlation of environmental process variables. Shared-core genera were coloured black and other genera were shown by other colours.

4.3.6 Nitrogen transforming genes abundances

Bacteria responsible for denitrification belong to a wide range of subclasses of Proteobacteria (Ambus and Zechmeister-Boltenstern, 2007), including *Pseudomonas*, which was ubiquitous throughout both DDHS biofilms (Figure 4-6). It might have been expected that certain denitrifying groups would be enriched in R-S20, particularly in the anoxic biofilms, because of significantly improved TN removal in those locations (Bundy *et al.*, 2017). However, given that *Pseudomonas* were present in all of the sponge layers at similar concentration between both reactors (T-test; p-value = 0.68), they do not appear to play a visible or substantial role in DDHS denitrification. Besides, anoxic biofilms from both DDHS bioreactors were phylogenetically similar (Section 4.3.4), with the bacterial groups selected against high DO and OLR, but based on sponge depth and porosity. It therefore seems likely that nitrate reduction in the DDHS bioreactors was performed by a narrower group of bacteria, potentially by two putative groups of *Flavobacterium* and *Shewanella*, which increase in abundance in the anoxic biofilm communities in the R-S20 bioreactor (Section 4.3.4).

To determine whether there was an increase in known denitrifying gene levels enriched by wastewater bypass, functional *nir* genes (*nirS*, *nirK*) were quantified by qPCR, together with nitrogen fixation gene *nifH* and the nitrifying genotypes (*amoA*, *Nitrobacter* and *Nitrospira*) for further characterising the nitrogen genes pool in both bypass conditions to compliment the overall microbiome data.

In the preceding nitrification reaction (Figure 4-9A), the R-S20 bioreactor consisted a significantly greater number of ammonia oxidizing bacteria (AOB) than the R-S0 bioreactor (T-test; p-value = 0.002). The *AmoA* gene was in an approximately four-fold excess in the aerobic biofilms of the R-S20 (1.2×10^7 copies g⁻¹ biofilm; SD $\pm 9.6 \times 10^6$) than those of the R-S0 (3.0×10^6 copies g⁻¹ biofilm; SD $\pm 3.0 \times 10^6$). There was co-presence of ammonia oxidising archaeal (AOA) in DDHS biofilms at varying levels across sponge layers, with an average of $1.0 - 1.7 \times 10^6$ copies g⁻¹ biofilm, consistently detected in aerobic locations in the R-S20 bioreactor.

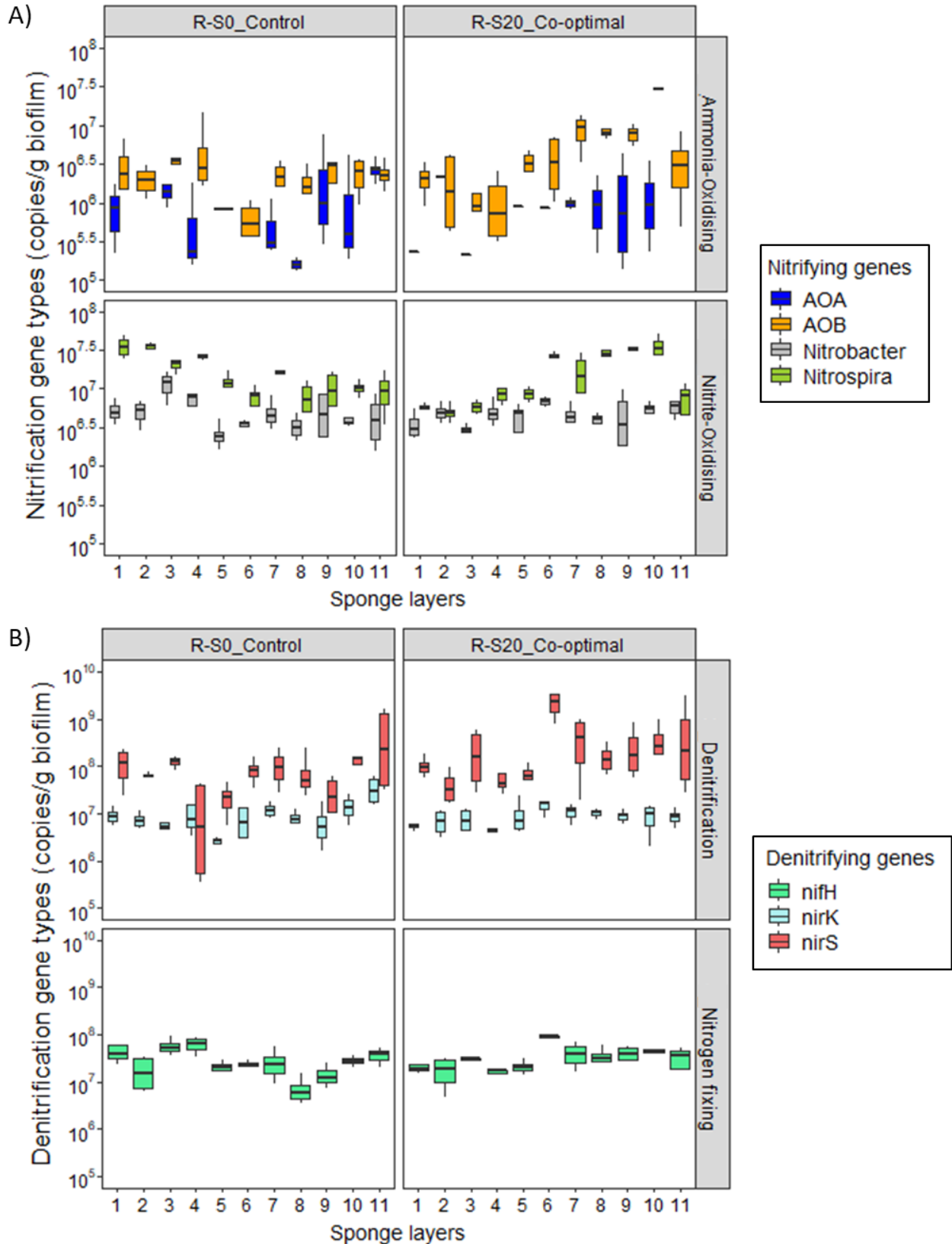


Figure 4-9 Nitrogen-transforming gene levels across biofilms from all sponge layers, classified based on sequential steps preceded by nitrification and followed by denitrification in the second step. (A) Nitrifying gene abundances; (B) Denitrifying gene abundances showing differences in both bioreactors.

One reason for this increased abundance of AOB and AOA observed in the upper aerobic biofilms of the R-S20 bioreactor could be the reduced OLR in the upper layers ($0.28 \text{ kg m}^3\text{-sponge}^{-1} \text{ day}^{-1}$; Chapter 3 Table 3-1) compared with that of the R-S0 bioreactor ($0.34 \text{ kg COD m}^3\text{-sponge}^{-1} \text{ day}^{-1}$). The reduced OLR probably have suppressed the normally dominant species in the aerobic biofilms (e.g. *Acinetobacter*, *Aeromonas*, and *Pseudomonas* etc.) thus allowing slower growing nitrifying organisms to prevail.

Similarly for nitrite oxidation, *Nitrospira* and *Nitrobacter* co-existed in all sponge biofilms, with *Nitrospira* (average 1.8×10^7 copies g^{-1} biofilm; $\text{SD} \pm 9.7 \times 10^6$) significantly outnumbering *Nitrobacter* (average 5.1×10^6 copies g^{-1} biofilm; $\text{SD} \pm 8.3 \times 10^5$) in both reactors (T-test; both p-values = 0.000). Overall, a more uniform nitrifying community was observed in the R-S20 bioreactor, with higher abundances in the upper biofilms, which is consistent with the design of sequential aerobic-anoxic treatment steps.

In relation to denitrification, the concentration of the *nirS* gene was ten-fold greater than the *nirK* gene in both reactors (T-test; R-S0 and R-S20; p-values = 0.006 and 0.0005), suggestive of the *nirS* gene being the more important gene driving denitrification (Figure 4-9B). As previously shown in Chapter 3, gross TN% removals were 28.5% versus 64.5% for R-S0 and R-S20. Here, the *nirS* gene concentrations in biofilms were significantly higher in the R-S20 reactor than the R-S0 reactor, by approximately one log (T-test; p-value = 0.014). This matched the same general patterns for TN removal in the respective bioreactors. Moreover, there was a significant difference in the apparent *nirS* gene concentrations between the aerobic vs anoxic layers in R-S20. Here, the *nirS* abundances were significantly higher in the anoxic biofilms (T-test; p-value = 0.014), starting at Sponge layer 6, the level at which the bypass occurred. In contrast, no significant difference was observed in the R-S0 reactor between the upper and lower biofilms (T-test; p-value = 0.13). The data strongly suggest that the *nirS* gene was enriched by wastewater bypass in the anoxic treatment step, possibly associated with an increase in the growth of *Flavobacterium* and *Shewanella*, who supported denitrification in R-S20. Strains of both these genera encode *nirS* genes in their genomes (Nogales *et al.*, 2002; Chen and Wang, 2015; Fang *et al.*, 2018)

Additionally, simultaneous nitrate reduction and nitrogen fixation also existed in DDHS reactors. There was a consistently high abundance of *nifH* gene (average 3.6×10^7 copies g^{-1} biofilm; $\text{SD} \pm 7.5 \times 10^7$), possibly returning the various species of nitrogen compounds to biomass and completing the nitrogen cycling with the emission of reduced N_2 from the DDHS treatment. However, this remains to be confirmed. It was recently shown by Tanikawa *et al.* (2019) that nitrogen-fixing *Xanthobacter* (Gomez *et al.*, 2005) was enriched in a traditional DHS bioreactor after dosing the lower biofilms with acetate (as an exogenous carbon source), which had not been seen in older DHS systems. This confirms the significance of supplying a bypass as a substrate to drive denitrification and subsequently nitrogen fixation in the Downflow sponge column.

4.3.7 Abundance of faecal organisms and potential pathogens

As a fraction of wastewater was treated directly in the anoxic step of the R-S20 bioreactor, there is a possible concern about how the bypass might impact the levels of faecal bacteria and other potential pathogens in the reactor effluent. Table 4-2 shows the relative abundance of standard faecal indicators used by World Health Organisation for checking water quality (Ashbolt *et al.*, 2001).

All three faecal indicators, Gram-negative *Escherichia-Shigella* (coliform) and Gram-positives *Enterococcus* and *Streptococcus* were detected in raw wastewater at 0.5%, 0.1%, and 0.8%, respectively. However, the data indicated relatively few faecal bacteria were present in the sponge biofilms and were additionally undetectable in most biofilms along DDHS column. Further, levels were significantly reduced in bioreactor effluents (T-tests influent vs effluents; $0 \leq \text{all p-values} \leq 0.03$). For *E. coli*, levels were reduced to 0.01% and 0.2% in the R-S0 and R-S20 reactors, respectively. While *Enterococcus* was completely eliminated in R-S0 and reduced to 0.02% in R-S20, *Streptococcus* survive better in R-S0 biofilm communities, which was reduced overall to 0.01% in the R-S0 effluent and undetected in R-S20 effluent.

Although slightly higher levels of *E. coli* and *Enterococcus* were seen in the effluent from R-S20 reactor compared with the R-S0 reactor, the overall pattern showed a net reduction in the DDHS reactors. The data show that the bypass did not seem to impact on the levels of faecal organism in the sponge biofilms. Moreover, members of the Enterobacteriaceae family, which are often associated waterborne pathogens,

were present at 2% in the influent wastewater, but reduced to 0.1% in the effluents of the R-S0 reactor and to 0.4% in the R-S20 reactor.

Table 4-2 Relative abundance of faecal indicators throughout sponge layers.

		Relative abundance (%)		
		Escherichia-Shigella	Enterococcus	Streptococcus
R-S0 ^a Aerobic biofilm	Raw wastewater	0.50	0.11	0.77
	Sponge 1	ND	0.014	0.019
	Sponge 2	ND	0.026	ND
	Sponge 3	ND	0.009	0.003
	Sponge 4	ND	ND	0.013
	Sponge 5	ND	0.016	0.019
R-S0 ^a Anoxic biofilm	Sponge 6	ND	ND	0.013
	Sponge 7	ND	ND	0.012
	Sponge 8	ND	ND	0.009
	Sponge 9	ND	ND	ND
	Sponge 10	ND	0.007	ND
	Sponge 11	ND	0.005	0.005
	Effluent	0.011	ND	0.013
R-S0 ^b Aerobic biofilm	Sponge 1	ND	0.007	ND
	Sponge 2	ND	ND	ND
	Sponge 3	ND	ND	ND
	Sponge 4	ND	ND	ND
	Sponge 5	ND	ND	ND
R-S20 ^b Anoxic biofilm	Sponge 6	ND	ND	ND
	Sponge 7	ND	ND	ND
	Sponge 8	ND	ND	ND
	Sponge 9	0.002	ND	ND
	Sponge 10	ND	ND	ND
	Sponge 11	0.007	ND	ND
	Effluent	0.178	0.015	ND

Notes: ^aR-S0 = Biofilm samples from Control reactor without any bypass; ^bR-S20 = Biofilm samples from Co-optimal reactor with 20% wastewater bypass (grey shading); ND defines not detected.

In general, the wastewater bypass may result in slightly higher levels of faecal organisms in the effluents, but the effect did not appear to relate to differences in ARGs and MGEs levels (Chapter 3). This could be offset by recirculating effluent back to the top of reactor, sequentially exposing effluent bacteria to aerobic and anoxic steps. Such bacteria might die off in aerobic step, possibly by selective predation (see Chapter 5). Further, raw wastewater and effluent samples were

phylogenetically separate from biofilm communities (Section 4.3.5), suggestive of differences in biofilm and effluent communities.

4.4 Implications

4.4.1 *DDHS microbial community diversity differs with operating regime*

The biofilms in DDHS reactors consist of a wide diversity of bacteria, the composition of which are primarily shaped by receiving OLR, the dissolved oxygen at the various depths of the reactor and the presence or absence of bypass. For example, a detectable shift in microbial composition was apparent in the aerobic layers based on the presence or absence of a 20% wastewater bypass, which altered the loading rate to the top sponges. The higher OLR in the upper region of the R-S0 bioreactor resulted in reduced microbial diversity in the aerobic layers and an apparent selection of opportunist carbon-removing phylotypes, most likely associated with faster growing aerobic heterotrophs commonly dominating biological wastewater treatment (Gray, 2004). This caused a less diverse community throughout the reactor, which affected the overall reactor performance. In contrast, the upper aerobic community in the R-S20 reactor had a more even distribution and was not dominated by heterotrophs with a growth advantage in the presence of higher OLR concentrations. Such trends were also observed in traditional DHS reactors, where Mac Conell *et al.* (2015) found the predominance of Proteobacteria (53%) at higher OLR concentrations ($0.45 \text{ kg COD m}^{-3}\text{-sponge}^{-1} \text{ day}^{-1}$) was reduced to 38% when a lower OLR ($0.37 \text{ kg COD m}^{-3}\text{-Sponge}^{-1} \text{ d}^{-1}$) was applied. Lower OLR concentrations resulted in a more diverse community and improved reactor performance.

Microbial composition also varied with sponge depth within the aerobic layer, and between the R-S0 and R-S20 bioreactors. In the R-S20 reactor, the upper aerobic layers were dominated by apparent heterotrophs, whereas lower layers had higher abundances of nitrifying bacteria, suggesting reduced competition for nutrients and greater success of the slower growing organisms (Table B-1; Appendix B). Such a pattern was not observed in the R-S0 reactor, which displayed much lower levels of TN removal and a less evidence of a nitrifying community. Finally, the anoxic layers in R-S20 were enriched with putative denitrifying bacteria, suggesting that the bypassed carbon in raw wastewater, and increased nitrate formed by the previous

nitrification allowed more efficient denitrification. As such, TN removals were much higher, which was the intent of the bypass.

Therefore, separation of microbial habitats throughout the bioreactors created organic (Kubota *et al.*, 2014) and redox gradients along the reactor column, which explains why TN and ARG removal were superior in R-S20 relative to R-S0. Specifically, co-optimal ARG and TN removal resulted from distinct microbial communities created by the bypass, which in tandem explain the improved performance.

4.4.2 Dominant genera

The design of DDHS reactors aims for complete C and N (simultaneous nitrification-denitrification) removal from the influent wastewater. Unlike conventional trickling filters or traditional DHS bioreactors, DDHS systems include an intentional submerged anoxic layer, which is supplemented with organic substrate to drive the reduction of nitrate produced by the upstream nitrification step (Bundy *et al.*, 2017). As noted above, the lower layers of the aerobic zone in the R-S20 reactor had elevated nitrifiers abundances (e.g., Sponge 3, 4 and 5; total = 8%), especially AOB (e.g., *Nitrosomonas* spp.) and NOB, despite their much slower growth rates compared with heterotrophic bacteria. AOB and NOB were less abundant in R-S0, presumably because they were out-competed by the more rapidly growing heterotrophs under higher OLR concentration.

Relative to specific bacterial groups, *Pseudomonas* spp. dominated the microbial sponge communities at all depths in both reactors (Figure 4-6), probably due to their highly diverse metabolic lifestyle. TN removal in the R-S0 reactor was lower than that of the R-S20 reactor. Given the higher abundance of *Pseudomonas* spp. in the aerobic biofilms of the R-S0 bioreactor, but similar abundances in the anoxic layers of both reactors, it is unlikely that they play a major role in denitrification. In contrast, the higher abundance of *Flavobacterium* in the anoxic sponge layers in the R-S20 (cf. the R-S0 reactor) could account for its increased level of denitrification. While more evidence is required to confirm this, it is notable that *Flavobacterium* spp. are also elevated in lower layers of the R-S20 reactor (e.g., Sponge layers 10 and 11), which is suggestive of their role in denitrification. From an ecological perspective this

makes sense because they are present at the bottom of the anoxic zone, and the low DO is unlikely to impeding denitrification (Oh and Silverstein, 1999). Presumably, the upper anoxic sponges contribute to the reduction of DO levels to those desirable denitrification, i.e., below 1 mg/L (Metcalf & Eddy, 2003). Finally, elevated levels of *Shewanella* was found in sponge layer 11 of the R-S20, suggesting they may also contribute to the observed reduction in nitrate. *Shewanella* spp. are well known denitrifiers (Fredrickson *et al.*, 2008; Yoon *et al.*, 2013), and their presence indicates that the design of the DDHS reactors provides a range of local niches that are suitable for different groups of denitrifiers. It is noteworthy that *Flavobacterium* also was detected in sponge layers 10 and 11 in the R-S0 reactor. However, despite their presence, it is suspected only partial denitrification was occurring (i.e. there was some TN removal; see Chapter 3 Section 3.3.1), probably due a combination of carbon limitation or low nitrate because of limited nitrate production by previous nitrification.

4.4.3 DDHS diversity and overall reactor performances

Here we show that the positive effects of bypass are manifest at the microbial scale. The bioinformatics analyses indicate that the wastewater bypass enhanced DDHS biofilm ecology through the co-optimal allocation of OLR in the sequential redox environment. Higher receiving OLR in the aerobic biofilms most likely created unstable biofilms in the R-S0 reactor, with uneven abundances due to the presence of dominant species. By shunting 20% of wastewater from upper aerobic biofilms to the lower biofilms, a greater biodiversity and evenness emerged in R-S20. Lower OLR (due to bypass) shifted the dominant taxa in aerobic biofilms to more even communities throughout the R-S20 reactor, and denitrifying selection in the bottom of the anoxic zone.

The diversity and evenness of the biofilm microbial community reported in this chapter helps explain the greater removal of TN, and reductions in ARGs and MGEs of the R-S20 reactors reported in Chapter 3. The combination of elevated nitrification in the bottom aerobic layers (producing nitrate) and additional raw wastewater at the top of the anoxic zone, created conditions that select for denitrifying bacteria and functional genes (i.e., *nirS*) in lower layers of the anoxic zone. In contrast, the lack of nitrification in the aerobic zone in the R-S0 reactor and C-limitation in the anoxic zone

resulted in limited TN removal. These conditions were mirrored by their respective microbial communities; specific selection and community evenness in the R-S20 reactor, and limited selection (except for opportunistic heterotrophs in the top aerobic layers) poorer evenness and diversity. This is true because a stable and diverse biofilm ecology almost certainly perform more efficiently (Fernández *et al.*, 1999; Valentín-Vargas *et al.*, 2012).

Slightly higher levels of faecal bacteria were observed in the effluent of the R-S20 reactor, as compared with R-S0. However, in both cases, levels were significantly reduced compared to the influent stream. Such patterns are consistent with reductions in the resistome; ARGs and MGEs also were significantly reduced. It should be noted the highest bypass ratio used in Chapter 3, namely 30% was not examined here and it would be useful to establish whether the presumptive faecal organism counts were higher than that of R-S20. The fact that biofilm communities were phylogenetically unrelated to the wastewater influent bacteria means that bypass did not greatly influence the compositions of the sponge native microbiomes. The phylogenies of the organisms in the wastewater influents and reactor effluents were significantly separated, implying that most influent ARGs, MGEs, and their hosts were removed by sequential exposure in DDHS, and bypass had, at most, only a minor negative effect on ARG removal.

Additionally, Onodera and co-workers characterised sponge “sludge” and showed they included diverse protozoa and macro-fauna (Onodera *et al.*, 2013; Onodera *et al.*, 2015). They suggested this was probably due to DHS systems having long sludge retention times and stable communities. As shown later (Chapter 5; Section 5.3.5), it appears that predation could play an important role in ARG removal in DDHS systems (Pauli *et al.*, 2001; Madoni, 2011).

4.5 Conclusions

The microbiomes and habitat data reported in this chapter are crucial for process improvements of DDHS bioreactors. Bacterial communities in the sponge biofilms show a rich microbial abundance and diversity, primarily dominated by Proteobacteria, Planctomycetes, and Chloflexi. However, they are clearly enriched further when a bypass is included in the process, especially with nitrifying and

denitrifying genera. There were clear differences between the microbiomes of the reactors with and without bypass regime. In general, the R-S20 reactor had a more uniform diversity throughout sponge layers, whereas R-S0 had less evenness.

Biofilms composition, especially in the aerobic zone, was sensitive to OLR and shifted hugely when higher loading was applied, especially in the upper layers of the aerobic zone. The R-S0 reactor had a lower level of microbial diversity due to the presence of dominant heterotrophic species influenced by higher OLR, whereas R-S20 had greater level of diversity and more evenness throughout the sponge layers. Also, key nitrifying bacteria were present at higher levels towards the bottom of the aerobic section (sponge layers 4 and 5), where OLR levels become reduced. Therefore, adequate sponge depth (i.e., a long enough sponge core) and contact time (i.e., hydraulic loading rate) are crucial for effective nitrification, hence the ultimate DDHS treatment objectives because it is the pre-reaction step for the downstream denitrification. The same also true for the anoxic section, where key denitrifying genotypes were more abundant at the bottom layers. These observations indicate that a clear spatial distribution of key genera is required for the N-cycle, and that the engineering of DDHS reactors need to optimise the depth of the sponge layers relative to the flowrate.

Taken together, a wastewater bypass may be an economical source of carbon for enhanced denitrification of DDHS reactors (or other bioreactors), that are designed to meet the demand for improved overall effluent quality, including TN and ARG removal. However, the bypass ratio needs to be chosen carefully to facilitate the optimal removal of C and N, and co-optimize the removal of ARGs and AR bacteria themselves. Removal mechanisms of ARGs and AR bacteria is the focus of Chapter 5.

Acknowledgement

I would like to thank Joshua Bunce and Aidan Robson for the upstream processing of the raw sequencing data using the supercomputer. I am deeply grateful to Carl Samuel for his patience and assistance in undertaking the diversity analysis. I also would like to thank Charles Knapp (Strathclyde University) for running the qPCR analysis.

Chapter 5 Impact of redox conditions on the fate of a resistance host and conjugative plasmid in biofilm reactors

5.1 Introduction

Bacteria can exist and thrive in hugely varying habitats owing to their genetic plasticity (Munita and Arias, 2016). One specific cell function related to plasticity is the gaining of extraneous antibiotic resistance (AR) determinants from surrounding environments via horizontal gene transfer (HGT); a bacterial strategy designed to optimise survival when exposed to antibiotics and other stressor compounds (Davies and Davies, 2010; van Hoek *et al.*, 2011).

HGT classically takes place via conjugative and other gene transfer mechanisms, mediated by gene vectors, such as plasmids and viruses, which can populate by self-replication and transmission between bacteria (Figure 5-1). Given plasmids usually carry multiple genes, including DNA sequences encoding resistance; they form the extrinsic resistome and mobilome in microbial communities, frequently associated with the emergence of multidrug resistance strains in natural and clinical environments (Nikaido, 2009; Huang *et al.*, 2012). Moreover, plasmids can mobilise other co-resistance genes through genetic linkages on mutual plasmids, such as resistance to heavy metals and biocides (Baker-Austin *et al.*, 2006; Wales and Davies, 2015), which allow the maintenance of AR without direct exposure to antibiotics (Huysman *et al.*, 1994; Alonso *et al.*, 2001)

It is also believed that HGT often occurs in environmental ecosystems with high bacterial densities, such as in biofilms (Davison, 1999) or in wastewater treatment plants (WWTPs) that contain abundant mobile genetic elements (MGEs); i.e., plasmids, viruses, transposons and integrons (Tennstedt *et al.*, 2003; Moura *et al.*, 2012; Wang *et al.*, 2013). Unfortunately, conventional WWTPs were never designed to remove AR genes and MGEs. In fact, some bio-based processes, such as activated sludge and biofilm systems, may be conducive to cell-to-cell contact and gene exchange (Schluter *et al.*, 2007; Novo and Manaia, 2010), providing a

resistance gene pool for microbial HGT and subsequent release into nature through effluent discharges. However, Munck *et al.* (2015) and Quintela-Baluja *et al.* (2019) both showed limited dissemination of WWTP resistomes into receiving water environments, i.e., the biosolids community and core resistome, were highly stable and unique to the WWTP environment, implying less frequent HGT occurred in WWTPs than previously believed.

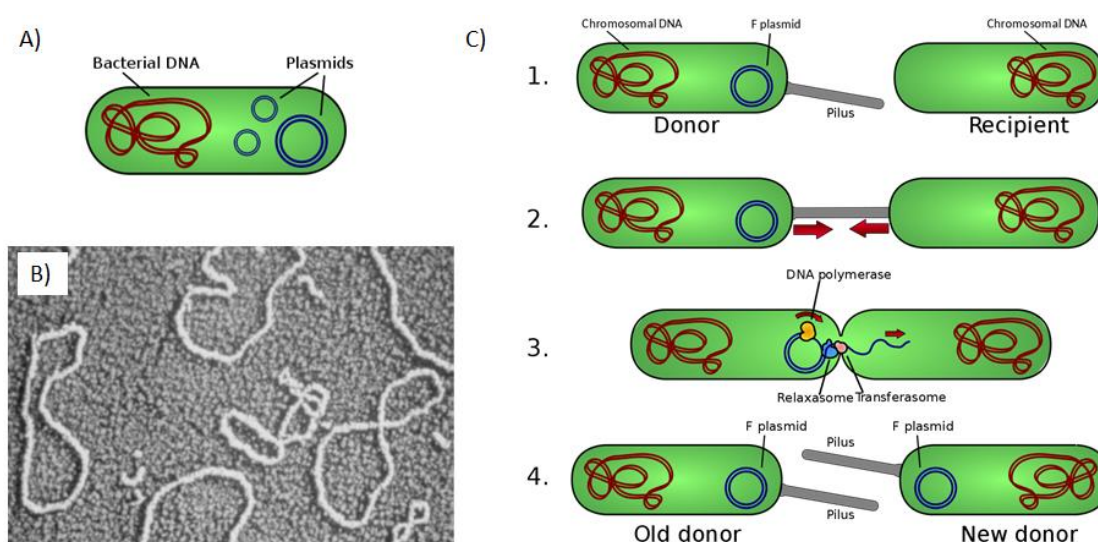


Figure 5-1 Bacterial gene transfer. (A) A bacterium containing chromosomal DNA and plasmids. Bacteria carry more than one type of plasmid, representing additional but optional genetic elements. Such plasmids are not considered as part of the cell's genome because the same plasmid may exist in two different species and be transferred across species (Clark and Pazdernik, 2013); (B) Transmission electron micrograph of bacterial plasmids (Bennett, 2008). (C) Overview of conjugation instigated by the formation of the pilus appendages.

These new observations suggest that the kinetics and underlying mechanisms of HGT within complex wastewater ecosystems are still poorly understood. This chapter aims to examine and understand ecological HGT within wastewater bioreactors under different biological redox conditions. It was shown in previous chapters that MGE abundances were reduced in domestic wastewater when exposed to sequential redox environments in sponge-core bioreactors (Chapter 3). Further, stable biofilm communities with higher diversity and abundances (Chapter 4) reduced total bacteria, AR gene and MGE levels in final effluents. Data in Chapter 3 also showed reduced treatment efficiencies for total bacterial and AR genes when excess wastewater was introduced at the anoxic step, bypassing the preceding aerobic step. This suggests the fate of AR genes, MGEs, and their associated hosts may vary as a

function of different redox regimes. Finally, both ecological and physical interactions might impact the uptake and maintenance of AR plasmids within an environment, which has been rarely considered previously.

Therefore, to better understand AR transmission in DDHS (Chapters 3 & 4) and other bioreactors, this chapter quantifies the fate of a traceable AR plasmid under different redox conditions. In particular, the influence of aerobic, anoxic and anaerobic exposures on the permissiveness of conjugal transfer are evaluated within biofilms and liquid phase niches. This was done by monitoring the presence of an AR reporter plasmid cloned into an environmental *E. coli* strain (i.e., donor), which was seeded in the influent stream feeding different bioreactors. Additionally, the *E. coli* donor strain was genetically modified to express constitutive nalidixic acid resistance to help distinguish it from the indigenous flora in the bioreactors.

Specifically, the *E. coli* donor strain was designed to carry a copy of the *IncP-1* conjugative plasmid RP4 (pRP4) into which the gene encoding a green fluorescent protein (GFP) had been cloned. The plasmid will be referred to here as pRP4-*gfp*. Tracking of the target GFP signal through fluorescence cell cytometry facilitated the measurement of the tagged pRP4 plasmid. Mass balances of GFP-labelled pRP4-*gfp* were used to estimate transfer kinetics of the plasmid between bacteria, hence, estimating putative horizontal gene exchange among reactor microbiota. Background is provided here.

5.1.1 *IncP-1* plasmids

Plasmids classified in the incompatibility (Inc) group, also called *IncP-1*, were first identified in antibiotic resistant *Pseudomonas aeruginosa* isolated from burn patients at the Birmingham Accident Hospital, England, UK (Lowbury *et al.*, 1969). The best studied *IncP-1* plasmids are pRP1, pRK2, and pRP4, which are relatively large (56kb) broad-host-range plasmids, widely distributed in many Gram-negative bacteria (Thomas, 1981). These are conjugative plasmids carrying genetic determinants conferring resistance against three antibiotics, namely ampicillin, kanamycin and tetracycline, plus additional resistance determinants against heavy metals (mercury and chromate) and also quaternary ammonium compounds (frequently used in disinfectants). These resistance traits maximise bacterial fitness and persistence under the presence of these selection pressures (Popowska and Krawczyk-Balska,

2013). A variant of the *IncP-1* conjugal plasmid RP4, namely PRP4-*gfp*, carried in a *Pseudomonas putida* strain (Section 5.2.6) was used in this study, which was later transformed into an environmental *E.coli* strain suited for this study (Section 5.2.8). The *Pseudomonas putida* strain was kindly provided by Professor Barth F. Smets from the Danish Technical University (Musovic *et al.*, 2010).

In recent years, *IncP*-like replicons have been detected in various environmental samples and bacterial species, including manure, soil and wastewater (Bahl *et al.*, 2009a; Jechalke *et al.*, 2013). Promiscuous horizontal mobility of *IncP-1* plasmids can occur in environmental soil communities (Klumper *et al.*, 2015) and wastewater activated sludge (Soda *et al.*, 2008; Li *et al.*, 2019), and their ability to replicate and be maintained in a broad spectrum of hosts make them a useful vehicle for assessing possible transmission of environmental antibiotic resistance among microbes, including spread to pathogenic bacteria.

5.1.2 Green fluorescent protein (GFP) marker and flow cytometry

Green Fluorescent Protein (GFP), isolated from the jellyfish *Aequorea victoria*, naturally exhibits a bright green fluorescence when exposed to blue or ultraviolet light (Chalfie *et al.*, 1994). The stable bioluminescent property makes GFP a versatile biological marker that is widely used in cell and molecular biology for reporting expression (Kain *et al.*, 1995), monitoring physiological processes and visualizing protein localization (Marshall *et al.*, 1995; Tsien, 1998).

Fluorescence cytometry (FCM) measures cell characteristics (cell size, cell count, cell cycle) and the volume of cells in a rapidly flowing fluid stream as they passed in front of a viewing aperture (Givan, 2011), thus facilitating high-throughput counting of bacterial cells based on the detection of stained fluorophores. Modern FCM can detect multiple fluorescent parameters simultaneously. Coupling FCM and GFP biosensing is a powerful tool for ecological studies in complex microbial ecosystems, such as marine (Stretton *et al.*, 1998) and wastewater systems (Eberl *et al.*, 2006). In this study, FCM allowed single-cell detection and discrimination between green and non-green fluorescent cells, hence differentially quantifying prospective target populations (Bahl *et al.*, 2009b).

5.1.3 *Experimental systems and specific objectives*

An array of six sequencing batch bioreactors providing aerobic, anoxic and anaerobic conditions in duplicate were examined to compare the fate and migration of pRP4-*gfp* across redox conditions and spatial ecologies; i.e. biofilm versus liquid phase samples. Two phases of experimental work were performed (see experimental design) to satisfy the following objectives:

- a) To quantify bacteria carrying the pRP4-*gfp* plasmid within the biofilm and liquid phase environments over a time series, using flow cytometry-based detection.
- b) To determine the spatial and temporal fate of pRP4-*gfp* host across redox bioreactors.
- c) To detect and assess the pathways of putative horizontal gene transfer within bioreactor environments.
- d) To explore ecological predation in contrasting bioreactors as possible removal mechanism of pRP4-*gfp* plasmid host during biological treatment.

The ultimate goal is to determine the extent to which the HGT of plasmid-borne AR genes might occur in different bioreactors and determine how redox conditions impacts the extent to which it occurs. This is key to understanding and optimising future bioreactors designed to reduce AR determinants and MGEs in their effluents.

5.2 **Materials and methods**

5.2.1 *Experimental design*

Two sets of bioreactor experiments were undertaken over two different phases in this work. Phase 1 involved preliminary tests to gain baseline data, including how to sustain stable redox conditions and to develop appropriate seeding and sampling protocols. This led to the Phase 2 experiments, which were more focused on the biofilm systems, comparing how seeding regime and redox conditions impacted on the fate of the *E. coli* donor strain and pRP4-*gfp* plasmid. Both Phases used sequencing batch reactors (SBR) to simulate different redox conditions presumed to prevail in the DDHS reactors. This approach was taken because it was impossible to perform such experiments in the DDHS systems themselves due to the difficulty of obtaining “undisturbed” samples over time. To create liquid-solid phase environments

equivalent to DDHS systems, polyurethane sponge cubes were “floated” in the batch reactors for use as attachment surfaces (see Section 5.2.2).

Prior to both seeding experiments, samples from bioreactors and the influent source were screened for the presence of pRP4-like plasmids by using selective agar media containing a combination of the three antibiotic markers; i.e., ampicillin (100 µg/mL), kanamycin (12.5 µg/mL) and tetracycline (50 µg/mL). Results were negative in all bioreactors, indicating the absence of background pRP4-like plasmids in the experimental bioreactors and wastewater source. Figure 5-2 displays the overview of the experimental works.

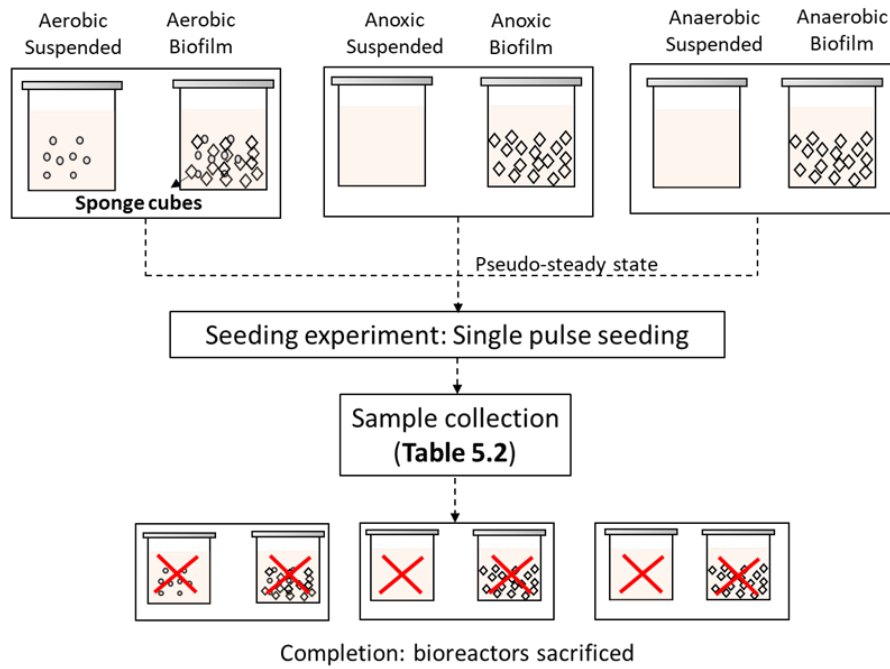
5.2.1.1 Phase 1: Preliminary experiments

Sequencing batch bioreactors, reflecting three different redox environments (i.e., aerobic, anoxic and anaerobic) were set up in a 3 x 2 matrix to examine suspended culture versus biofilm systems relative to HGT. Bioreactors were run according to the operating procedures described in Section 5.2.3 to stabilise redox conditions, which were followed by the seeding experiment. A series of tests were performed to determine suitable starting concentrations of *E. coli* pRP4-*gfp* donor strain (GFP-fluorescent donor *E. coli*), and the sampling regime and sample preparations for downstream flow cytometry analysis, including GFP sample fixation and pre-treatment. Single-pulse seeding was employed in Phase 1 experiments.

5.2.1.2 Phase 2: Extended experiments

After completion of the Phase 1 experiments, the bioreactors were deconstructed and a new set of bioreactors was assembled to operate under conditions identical to those in Phase 1. For Phase 2, the biological core from the same inoculum source (See Section 5.2.4) was used to initiate the new reactors and establish similar starting communities as Phase 1. Phase 2 experiments focused on the biofilm systems and involved two stages to compare the fate of the *E. coli* pRP4-*gfp* donor strain under different seeding conditions and also to examine its ecological fate. Specifically, the fate of pRP4-*gfp* hosts (i.e., the *E. coli* donor strain, *EcoFJ2*, and-or putative transconjugants) was studied using microbial culturing methods, whereas protozoan predation was explored as one of the underlying mechanisms affecting the host survival.

Phase 1



Phase 2

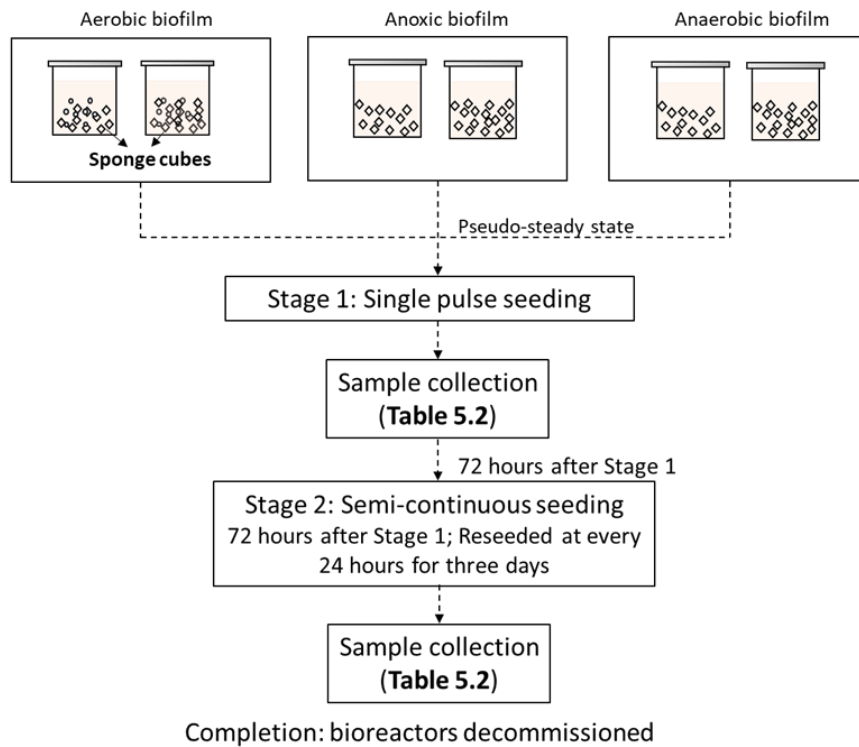


Figure 5-2 Summary of experimental work plan for (A) Phase 1 and (B) Phase 2 seeding experiments. Three redox conditions were contrasted in parallel in both phases using sequencing batch bioreactors whereby Phase 1 compared liquid phase and biofilm systems under single-pulse seeding while Phase 2 compared biofilm systems under both single-pulse and semi-continuous seeding.

5.2.2 Sequencing batch reactors set up

The bioreactor systems were sequencing batch reactors (SBR) that included suspended cultures and physical surfaces for biofilm growth (sequencing batch biofilm reactors; SBBR). Six identical 1-L glass vessels (GPE Scientific Ltd, UK) equipped with submersible magnetic stirrers (2mag AG, Germany) for mixing were placed in a heated water bath (Grant Instruments Ltd, UK). Each bioreactor was covered with a Quickfit flat flange lid with five ports (VWR, UK) secured by a retaining clip. Two hundred cubes of 1 cm x 1 cm x 1 cm polyurethane sponge (Figure 5-3), comprising total sponge volume equivalent to 0.2 L, were added into each of biofilm bioreactor, to act as supporting media for biofilm development and growth.

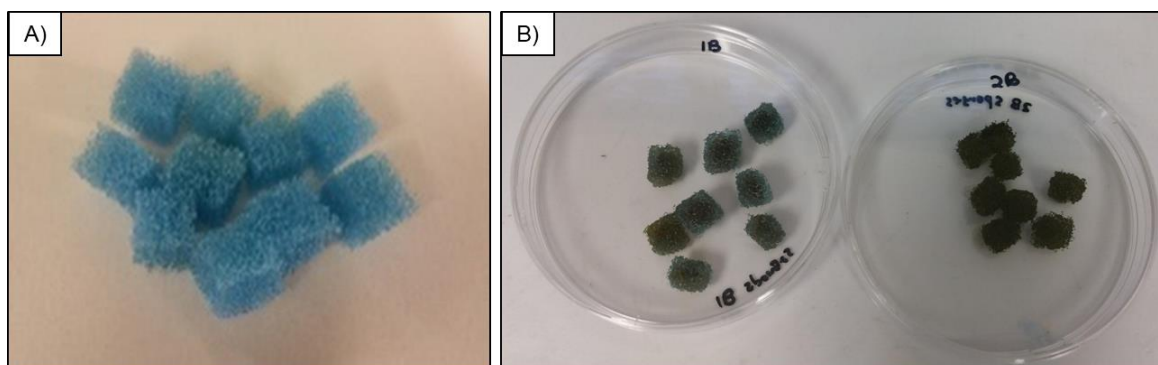


Figure 5-3 (A) Clean polyurethane sponge cut into 1cm x 1cm x 1cm cubes for use as immobilisers to support biofilm growth in bioreactors; (B) Sponge cubes containing biofilms taken from SBBR during pseudo-steady state.

Thermocouple sensors (Pico Technology, UK) and fibre-optic oxygen probes (FireSting O₂ Pyroscience, Germany) were connected to each bioreactor through dedicated ports to allow continuous measurement of temperature and dissolved oxygen (DO). Data were logged on the connecting laptop, with all cables carefully affixed on the metal supporting frame. Figure 5-4 shows the complete set up in the laboratory.

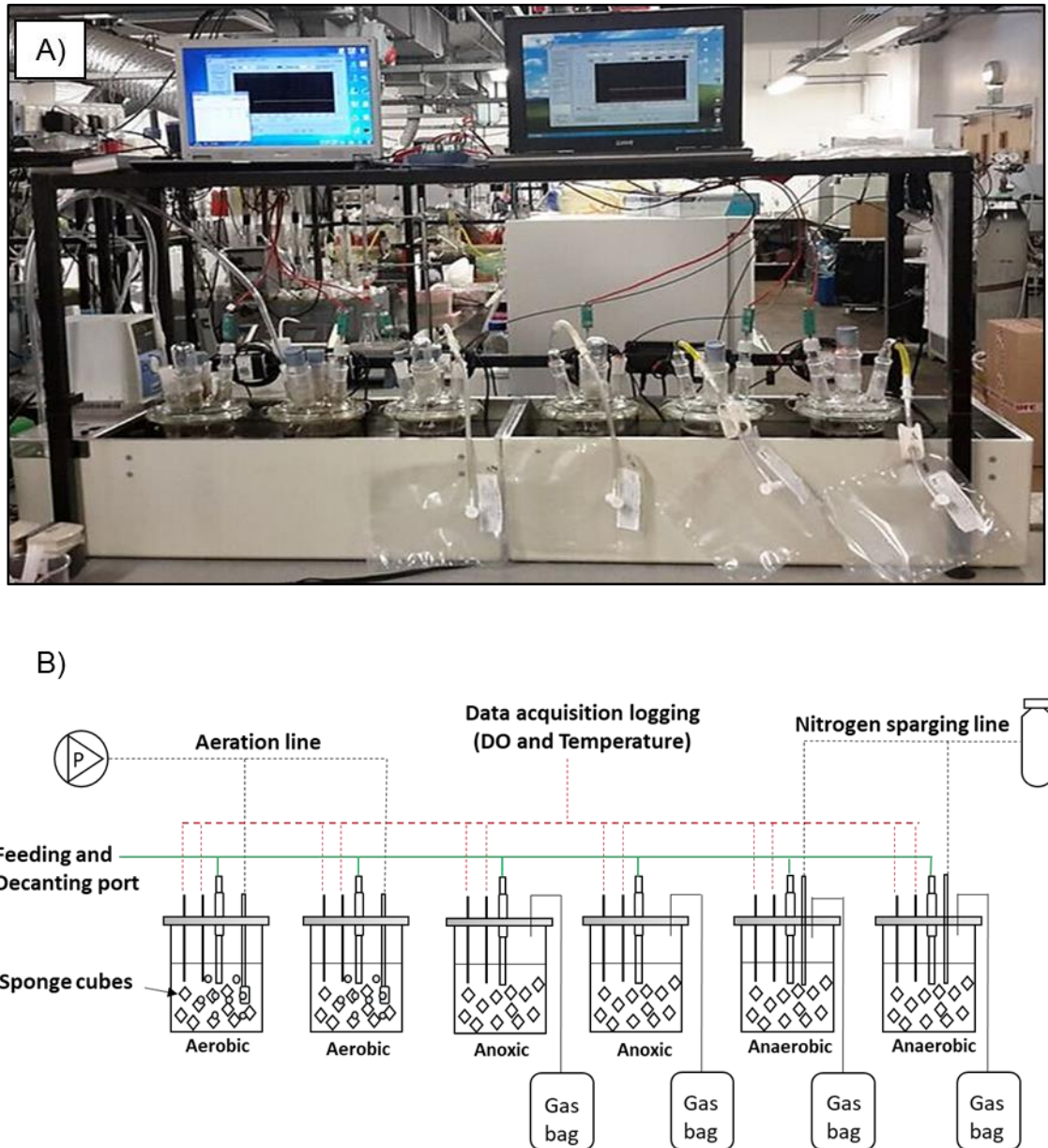


Figure 5-4 Laboratory assembly of sequencing batch reactors (SBR) used in seeding experiments; (A) Series of bioreactors consisting three contrasting redox in duplicate; (B) Schematic overview of the SBR vessels containing sponge cubes for biofilm attachment. Starting from the left: aerobic biofilm reactors in duplicate, anoxic biofilm reactors (duplicates), and anaerobic biofilm reactors (duplicates). The temperature and circulation of water in the heating water baths were regulated by titanium aquarium heaters with water circulators (Ab Aqua Medic Ltd., UK) to provide constant temperature at 25 ± 2 °C.

5.2.3 Operating conditions

The six bioreactors in both phases were operated in parallel, treating domestic wastewater in sequencing batch mode under aerobic, anoxic and anaerobic conditions (duplicate per redox condition). Conditions were as follows:

1. “Aerobic” conditions were maintained by pumping ambient air through air stone diffusers using a peristaltic pump (Watson Marlow, Cornwall UK). The pumping rate was adjusted at 120 mL/min to supply aeration that achieved a DO concentration of 4 ± 2 mg/L.
2. “Anoxic” conditions were ensured airtight by applying a layer of silicone grease sealant to prevent the intrusion of air and adding sodium nitrate stock solution to a final concentration at 25 mg/L $\text{NO}_3\text{-N}$, which past work showed was adequate to sustain denitrification (Loosdrecht *et al.*, 2016).
3. “Anaerobic” reactors were sealed similar to anoxic units, but no additional sodium nitrate was added and they were regularly sparged with N_2 gas.

Anoxic and anaerobic bioreactors were installed with a 0.5-L off-gas collection bags attached to the port via rubber tubing. These were intended to equalise the pressure in the airtight system during liquid exchange. While decanting, the gas bag decreased in volume and refilled again during feeding due to the changes in head space. This especially prevented the entry of oxygen into the anaerobic reactors. Overall, distinct redox potentials were developed and maintained as a descending gradient: aerobic > anoxic > anaerobic; 195 ± 25 millivolts (mV) > -15 ± 50 mV > -195 ± 15 mV, which were ideal contrasting conditions for the experiment.

All reactors had actual working volumes of 0.9 L, with designed hydraulic (HRT) and sludge retention times (SRT) of 3 days and 10 days, respectively, and were stirred at 200rpm for homogenous mixing during treatment cycle. Mixed liquor suspended solids (MLSS) concentrations were maintained between 2750 ± 205 mg/L across systems, as recommended by Metcalf & Eddy (2003) for sequencing batch reactors (with 10-15 day biomass retention times).

Daily feeding and decanting routines were performed manually using the following sequence: (i) stop mixing, (ii) settle, (iii) decant, (iv) refill, and (v) re-commence mixing. The settling time was one hour to allow the biosolids to settle before

decanting the settled liquid from each bioreactor by siphoning using silicone tubes. The frequency of HRT was calculated by dividing the volume of the biological reactor (V_P), here 0.9-L by the daily average influent flow rate (Q_I) (Equation 5-1) (Henze *et al.*, 2008).

Equation 5-1 The equation used to determine the daily liquid exchange volume based on designed hydraulic retention time.

$$HRT (d) = \frac{V_P (L)}{Q_I \left(\frac{L}{d}\right)}$$

SRT is equal to the volume of the biological reactor (V_P) divided by waste flow rate from the reactor (Q_W) (Equation 5-2), which assumes that the loss of solids with the effluent is negligible (Henze *et al.*, 2008).

Equation 5-2 The equation used to determine the volume of sludge wasting based on designed solid retention time.

$$SRT (d) = \frac{V_P (L)}{Q_W \left(\frac{L}{d}\right)}$$

Therefore, an HRT of 3 days was achieved by removing 0.3 L of settled bulk solution (Q_E) from the bioreactors, which was followed by refilling with 0.3 L of fresh primary settled sewage. For controlling an SRT of 15 days, a volume (0.12-L) of mixed liquor was withdrawn (wasting) from each reactor every two days during mixing (Q_W). During sludge wasting days, the decanted volume was calculated by subtracting Q_W from Q_E , therefore 0.18 L of settled liquid was withdrawn from the system after settling.

5.2.4 Inoculum and start up

Activated sludge (AS), anaerobic sludge, and primary settled wastewater were collected from two local waste treatment facilities in the Northeast of England, UK, for use as inoculum. AS and primary settled wastewater were collected from the nitrifying aeration tank and the holding chamber downstream of a primary clarifier in Tudhoe Mill (Northumbrian Water Ltd., Durham), which treats domestic wastewater

from the surrounding community (~22,500 population equivalents). Thickened anaerobic sludge was collected from the Howdon anaerobic digester (Northumbrian Water Ltd., Tyne and Wear), which primarily treats domestic biosolids from the region.

To ensure a uniform starting inoculum across the bioreactors, equal volumes of freshly collected aerobic sludge (settled and thickened AS) and anaerobic sludge were mixed (at 1:1 ratio) prior to inoculation. Each 1-L reactor was seeded with 0.4 L of the inoculum mixture and 0.5-L settled wastewater, which was then placed in the heated water bath on a submersed magnetic stirring plate for continuous mixing. Air was immediately introduced to the aerobic bioreactors while the anaerobic reactors were sparged with N₂ gas for 10 minutes to remove oxygen. Sodium nitrate (NaNO₃) stock solution was added into the anoxic bioreactors to promote nitrate as the dominant electron acceptor. Primary settled sewage for use as bioreactor feed was collected weekly from Tudhoe Mill throughout the experiment and stored at 4 °C prior to use.

5.2.5 Routine sample collection and monitoring

After inoculation, the reactors were operated for approximately 120 days to allow them acclimatise and establish a microbial community specific to each redox condition. pH and redox potential (ORP) were measured and monitored daily according to APHA standard method 4500-H+B (APHA 2005), using a 3010 pH-meter (Jenway, UK) and a HI-991002 ORP meter (Hanna Instruments, UK). All probes were regularly calibrated according to the manufacturer's instructions, using commercial certified standard solutions. Reactor performance was monitored by collecting untreated settled sewage and effluent samples twice weekly throughout the operation, and analysed in accordance with methods describe in Chapter 3 (Section 3.2.3).

5.2.6 GFP tagged pRP4

A previously constructed GFP tagged *IncP-1* pRP4 (RP4::*Plac::gfp*; renamed here as pRP4-*gfp*) was kindly provided by Professor Barth F. Smets from the Department of Environmental Engineering, Danish Technical University. pRP4-*gfp* has a molecular size 56.4 kb, and encodes resistance against the antibiotics ampicillin, kanamycin and tetracycline. In their work, the plasmid was tagged with *Tn5* insertion of the

gfpmut3b gene, and transferred to *Pseudomonas putida* KT2442 to act as donor strain (Musovic *et al.*, 2010). The GFP was constitutively expressed in the donor strain (Figure 5-5) and in recipient cells upon transfer.

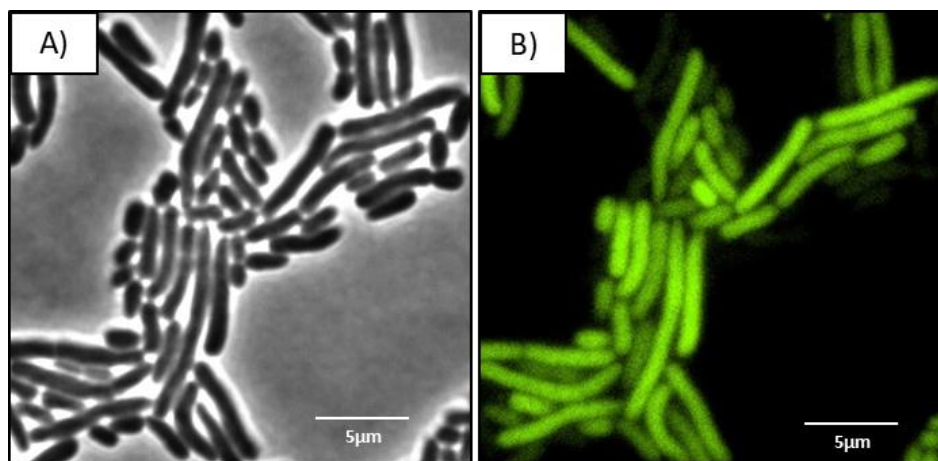


Figure 5-5 (A) Phase contrast; and (B) epifluorescence micrograph of *Pseudomonas putida* KT2442 encoding pRP4-gfp. Visualisation of the overnight cell culture grown in LB broth supplemented with 12.5 $\mu\text{g/mL}$ kanamycin at 30°C was performed using a Nikon Eclipse Ti fluorescent microscope as detailed in the next section.

5.2.7 Fluorescence microscopy

Fluorescence microscopy was used to detect GFP fluorescence in bacterial cell cultures. Microscope slides with reaction wells (ThermoFisher Scientific) were used to prepare samples for microscopy viewing at 1000x magnification. Approximately 500 μL of 1% of agarose in PBS were pipetted into each well, and when set, 1 μL of the overnight bacterial culture was spotted on the surface. For microscopy, a Nikon Eclipse Ti with a built-in perfect focus system was used in combination with a CoolSNAP HQ² CCD camera (Photometrics®) and MetaMorph software (Molecular Devices). The excitation/emission wavelengths and exposure time for the GFP fluorophore were 460-500 nm/510-560 nm for 1500 ms. Acquired images were analysed using the ImageJ software.

5.2.8 Transformation of reporter *E. coli*

An “environmental” *E. coli* was isolated using the Hicrome coliform agar (Sigma Aldrich, UK) from domestic wastewater samples taken from an existing lab-scale SBBR. Presumptive *E. coli* isolates were selected on the basis of colour differentiation by the chromogenic substrates in the Hicrome media, and were

repeatedly sub-cultured and streaked on the Hicrome agar. A pure isolate was obtained from cultivating a single colony and tested for the indole reaction using Kovac's reagent to confirm *E. coli*. Then, the isolated pure *E. coli* (named *EcoFJ1*; the original unmodified environmental *E. coli*) was subjected to routine antibiotic susceptibility testing, performed at the Department of Pathology (Freeman Hospital, Newcastle upon Tyne). Serotyping confirmed that the isolate is a non-serotype strain and therefore classified to ACDP Hazard Group 2. The isolate was susceptible to 21 clinical antibiotics including the three resistance phenotype markers encoded by *pRP4-gfp* (i.e., ampicillin, kanamycin and tetracycline; see Table 5-1).

Table 5-1 Antibiotic susceptibility tests results of an environmental strain of *E. coli*, *EcoFJ1*, performed at the Department of Pathology (Freeman Hospital, Newcastle upon Tyne).

Antibiotics	Susceptibility
Amoxicillin	Susceptible
Ampicilin	Susceptible
Aztreonam	Susceptible
Cefpodoxime	Susceptible
Ceftazidime	Susceptible
Cefuroxime	Susceptible
Cephalexin	Susceptible
Chloramphenicol	Susceptible
Ciprofloxacin	Susceptible
Co-amoxyclov	Susceptible
Co-trimoxazole	Susceptible
Ertapenem	Susceptible
Fosfomycin	Susceptible
Gentamicin	Susceptible
Kanamycin	Susceptible
Meropenem	Susceptible
Piperacillin-tazobactam	Susceptible
Temocillin	Susceptible
Tetracycline	Susceptible
Trimethoprim	Susceptible

The antibiotic susceptibility results also confirmed that there was no evidence of acquired resistance in this *EcoFJ1* strain and, therefore, that it was deemed suitable for use as a donor strain. To facilitate this, and to allow this strain to be detected against a background of *E. coli* strains in the bioreactors, a nalidixic acid (Nal) resistant chromosomal variant was isolated. To do this, the strain *EcoFJ1* was plated

onto a Luria-Bertani (LB) agar plate containing nalidixic acid (25µg/mL) and incubated for 48 hours at 30°C. A spontaneously resistant mutant was isolated, which was used for subsequent experiments. The isolated Nal-resistant strain was used as the donor organism to examine putative HGT. To this end, the genetically modified pRP4-*gfp* was transferred into this strain. Before this could be done, an authorisation was sought from the Health and Safety Executive Department (HSE, UK) via the university Biosafety Sub Committee (GM number: GM 540; Appendix C).

Plasmid pRP4-*gfp* was transferred to the Nal-resistant variant of *EcoFJ1* (*EcoFJ1-Nal^r*) via a conjugative plate mating technique. The *P. putida* KT2442 donor and the *EcoFJ1-Nal^r* recipient strains were grown overnight in LB medium at 30°C and 37 °C, respectively, with shaking at 165 rpm on an Innova 2300 platform shaker (New Brunswick Scientific). The LB medium used to grow *P. putida* KT2442 was supplemented with kanamycin (12.5 µg/mL). Overnight cultures were harvested and the optical density of each bacterial suspension was determined and adjusted with sterile saline solution (1 x PBS) to approximately 5×10^7 CFU/ml (optical density at 600 nm [OD₆₀₀] = 0.5).

Mating was initiated by mixing equal volumes of the *P. putida* plasmid donor (D) and *EcoFJ1-Nal^r* recipient (R) bacterial suspensions. A sample (30-µL) of the mixed suspension was transferred to a LB agar plate and incubated at 30°C for 48 hours after the liquid was completely absorbed. Following incubation, the cell mass was harvested by scrapping and resuspending in sterile PBS. Samples of the resulting bacterial suspensions were then streaked onto Hicrome chromogenic agar, supplemented with the combination of the three plasmid antibiotics to select for plasmid host. Presumptive *E. coli* transconjugants (blue colonies on the chromogenic medium) were isolated and further purified. The colonies were viewed under UV-light using a transilluminator and epifluorescent microscope (Figure 5-6) to confirm the presence of the *gfp* gene.

The final donor organism, named *EcoFJ2*, had a chromosomal resistance marker to nalidixic acid and a pRP4-*gfp* plasmid encoding resistance to ampicillin, kanamycin and tetracycline, and GFP fluorescence.

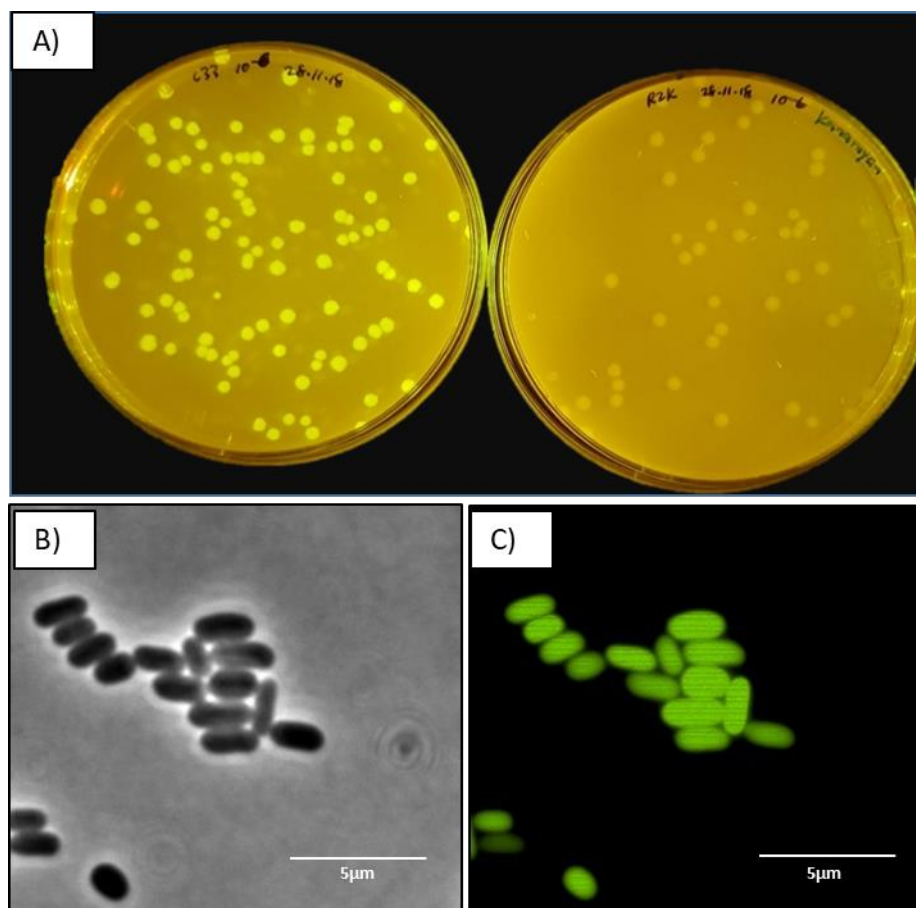


Figure 5-6 Enumeration and screening of *E. coli* donor derivative strain, *EcoFJ2*, encoding *Nal* resistance and the *pRP4-gfp* plasmid. (A) UV illuminated colonies of the *EcoFJ2* strain showing fluorescing GFP (left) and non-fluorescing colonies of the original unmodified environmental *E. coli* strain, *EcoFJ1-Nal^r* without *pRP4-gfp* (right), as a negative control. Plates were irradiated at a wavelength of 366 nm from a benchtop UV-transilluminator. (B) Phase contrast and (C) epifluorescence micrographs of the *EcoFJ2* donor strain showing green fluorescent colonies on a Nikon Eclipse Ti fluorescence microscope.

5.2.9 Seeding procedures

Inoculation of the GFP-expressing *EcoFJ2* donor was performed during pseudo-steady state reactor operations. Prior to using *EcoFJ2* in seeding experiments, its growth was determined by monitoring optical density to establish suitable timing for harvesting and to estimate the concentration of cells required for seeding. When inoculated from an overnight culture and then grown in LB medium at 37°C with shaking at 165 rpm, the fresh culture reached the end of exponential growth phase after around four hours of incubation. At this point, the viable cell count was approximately 9×10^8 CFU/mL. The cell densities in the bioreactors then were quantified by FCM, which indicated a bacterial count ranging from 10^8 to 10^9 cells/mL;

a range typical of biological wastewater treatment systems (Manti *et al.*, 2008). The target seeding concentration was selected based on a donor to recipient ratio of 1:100; i.e., the seeded *EcoFJ2* donor cells represented 1% of the total cell population. On the day of seeding, a fresh culture of *EcoFJ2* was grown and harvested towards the end of exponential phase and the number of cells required to achieve a final concentration of 1×10^6 cells/mL within bioreactors was determined. To avoid adding a large volume of liquid to the reactors, the volume of the inoculum was reduced by centrifuging at $4000 \times g$ for 15 minutes and re-suspended in 10-mL sterile PBS before being added to each reactor vessel following the daily feeding routine.

5.2.10 Sampling procedures

After inoculation, samples were systematically collected (in quadruplicate) from the seeded bioreactors, including both liquid phase and sponge biofilm samples. Samples at time zero were collected immediately after inoculation and subsequent sampling was carried out over designated time intervals as described in Table 5-2. All samplings were carried out during the mixing mode of bioreactors operation. To note, as each biofilm system (SBBR) consists of two sample environments, i.e., sponge biofilms and the liquid phase, both fractions were sampled and compared during the Phase 2 experiments.

Quadruplicate samples were divided into two sets (i.e., each set was duplicated): one set for use in the FCM analyses; and one for microbial culturing as described in Section 5.2.14. For FCM, all samples were immediately fixed using prepared sterile formaldehyde stock (Sigma Aldrich, UK) at a final concentration of 1% to preserve GFP activity. Here, formaldehyde acts a cross-linking fixing agent to effectively preserve cell structures and the GFP protein without dehydrating the cells and denaturing its proteins, as happens during fixation with alcohol. For biofilms, sponge cubes were sampled using a sampling coil made with galvanised wire, which was sterilised with 70% ethanol between uses. Sponge cubes were squeezed and washed using sterile PBS to recover cells from the biofilms from each sponge. Again, the recovered cells were fixed with 1% formaldehyde. All fixed samples were stored in dark at 4 °C until subsequent FCM analysis.

Table 5-2 Sampling time points designated for Phase 1 and Phase 2.

Redox	Aerobic		Anoxic		Anaerobic	
Sample matrix	Sponge biofilm	Liquid phase	Sponge biofilm	Liquid phase	Sponge biofilm	Liquid phase
Phase 1						
Sampling time (h)	0, 1, 3, 5, 7, 24, 48, 72		0, 1, 3, 5, 7, 24, 48, 72		0, 1, 3, 5, 7, 24, 48, 72	
Phase 2						
Stage 1 Sampling time (h)	0, 3, 6, 9, 12, 24, 48, 72		0, 3, 6, 9, 12, 24, 48, 72		0, 3, 6, 9, 12, 24, 48, 72	
Stage 2 Sampling time (h)	0, 24 (S1_0, S1_24); 0, 24 (S2_0, S2_24); 0, 24 (S3_0, S3_24); 168 (S3_168)		0, 24 (S1_0, S1_24); 0, 24 (S2_0, S2_24); 0, 24 (S3_0, S3_24); 168 (S3_168)		0, 24 (S1_0, S1_24); 0, 24 (S2_0, S2_24); 0, 24 (S3_0, S3_24); 168 (S3_168)	

5.2.11 Extended seeding and sampling regimes (Phase 2)

During the Phase 1 experiment, the bioreactors were seeded once at the beginning (a single pulse seeding) with the *E. coli* donor strain (*EcoFJ2*) and their abundance was monitored over 72 hours. In the Phase 2 experiments, an alternate seeding regime was introduced after 72 hours. The bioreactors underwent a Stage 1 single-pulse seeding and sampling at designed time points as for the Phase 1 experiment. However, after three days of sampling, each bioreactor was reseeded with *EcoFJ2* (final concentration = 1×10^6 cells/mL) at every hydraulic exchange cycle, i.e., every 24 hours during daily reactor feeding routine, for three days. This additional regime was designed to create a semi-continuous influx of the donor strain *EcoFJ2*. Samples were taken at 24-hour time interval after each seeding and routinely fixed for downstream analysis by FCM. The purpose was to evaluate pRP4-*gfp* profiles across the bioreactors in response to a semi-continuing influx. A final sample was collected at 168 hours (seven days) after the final semi-continuous seeding.

5.2.12 Sample preparations for fluorescence cytometry analysis

Pre-treatment methods for the preparation of cells for analysis by flow cytometry were adapted from past studies and further optimised for samples collected in this study. Pre-treatment is essential to ensure optimal passage of individual cells (rather than clumps) within cytometer's fluidic flow cell. A combination of sonication and treatment with surfactant (Brown *et al.*, 2015) were applied to optimise the disaggregation of the bacterial cells from the sludge and biofilm specimens, which tends to exist as biological flocs. The complete routine for FCM sample preparation is shown in Figure 5-7, which involves sample dilution, surfactant dispersal, ultrasound sonication, and filtration.

Samples dilution. The cells present in the formaldehyde-preserved samples were too concentrated for FCM analysis and, therefore, were diluted to adjust sample suspensions to avoid congestion of the fluidic flow cell during cell acquisition on the FCM. Samples that are too dense tend to mask GFP signal while excess dilution will result in missing the detection of rare populations.

Surfactant dispersion. Diluted samples were subjected to treatment with the surfactant Tween 80 (5%) in a solution of sodium pyrophosphate (10 mM) to disperse and disaggregate biofilm agglomerates. Samples were mixed with magnetic spin vanes (for stirring in V-vials) on a magnetic stirring plate at 200 rpm for 15 minutes in the dark.

Sonication and filtration. After chemical treatment, samples underwent sonication in an ultrasound sonicating bath to further dislodge floc-bound bacterial cells. Sonication was performed for four minutes with one-minute intervals. Subsequent samples were filtered through a 20- μ m sterile cell strainer (ThermoFisher Scientific, UK) to separate out the large particles that are often present in wastewater samples.

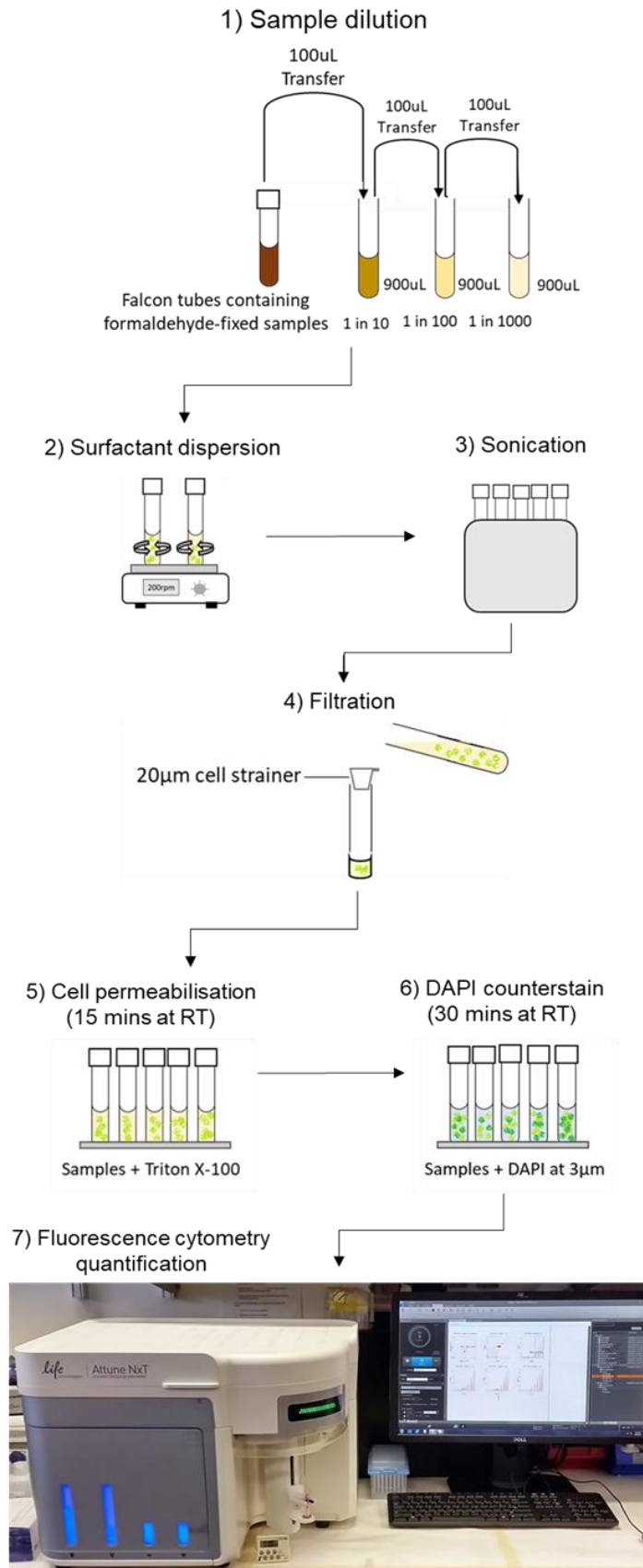


Figure 5-7 Step-by-step workflow for sample preparation prior to flow cytometry analysis using the Attune NxT flow cytometer (ThermoFisher Scientific).

5.2.13 Fluorescence cytometry quantification

Pre-treated uniformly suspended samples were counterstained with the blue-fluorescent nucleic acid stain (DAPI) to quantify total cell number within individual samples. DAPI was chosen as it has high affinity to dsDNA and has an emission spectrum that overlaps minimally with that of GFP, meaning that both signals could be quantified simultaneously. The process was as follows.

The samples (formaldehyde-fixed) were firstly permeabilised to allow DAPI to gain access to the interior of the cells by treatment with Triton X-100 (Sigma Aldrich, UK) at 0.1% for 15 minutes at room temperature. DAPI (ThermoFisher Scientific) was added into permeabilised bacterial suspension to a final concentration of 3 μM and incubated at room temperature for 30 minutes, in accordance to manufacturer's guidelines. DAPI counter-stained samples were immediately run through the Attune NxT flow cytometer equipped with acoustic assisted hydrodynamic focusing system (ThermoFisher Scientific), using the blue and violet laser with excitation/emission wavelength of 488/530 nm and 405/610 nm for GFP and DAPI, respectively. All samples were run at low flowrates (25 $\mu\text{L}/\text{min}$), and forward and side scattered light was used to measure cell volume and morphology, respectively. A threshold was set at the forward scattered light to eliminate background noise arising from the instrument. The FCS Express 6 software was used for the evaluation of flow cytometry data.

5.2.14 Enumeration of the seeded *E. coli* reporter strain and presumptive transconjugants

Beyond FCM, the relative fate of pRP4-*gfp* also was determined using plate culturing on selective media during the Phase 2 experiments. Time-series samples were serially diluted (10^0 to 10^5) in sterile PBS and 10 μL of diluted samples were spotted on solid LB nutrient agar medium supplemented with either:

- i) the three pRP4-*gfp* antibiotic markers (100 $\mu\text{g}/\text{mL}$ Amp, 12.5 $\mu\text{g}/\text{mL}$ Km and 50 $\mu\text{g}/\text{mL}$ Tc), or
- ii) the three pRP4-*gfp* antibiotic markers plus nalidixic acid (25 $\mu\text{g}/\text{mL}$) to counter-select for recipient cells that have acquired pRP4-*gfp* from the *E. coli* donor organism, *EcoFJ2*.

Quantitation on these plates allowed the proportion of the original seeded *EcoFJ2* donor cells with the pRP4-*gfp* plasmid and the proportion of cells that had received this plasmid by putative HGT to be determined. The spot plating method was used to screen many samples with unknown dilution range, given the time constraint of three-hour intervals (all serially diluted samples were enumerated). Resulting agar plates were inverted and incubated at 30°C for 24 hours before colony counting and viewing on a UV transilluminator to detect fluorescence (Figure 5-8). Remaining samples in PBS solutions were stored in dark at 4 °C. Such selective enumeration was used to estimate putative HGT, whereby the gross transfer frequency was calculated from the difference of total pRP4-*gfp* host number (i.e., bacteria resistant to Amp, Km and Tc) and pRP4-*gfp* donor *E. coli EcoFJ2* (i.e., *E. coli* resistant to Amp, Km, Tc and Nal).

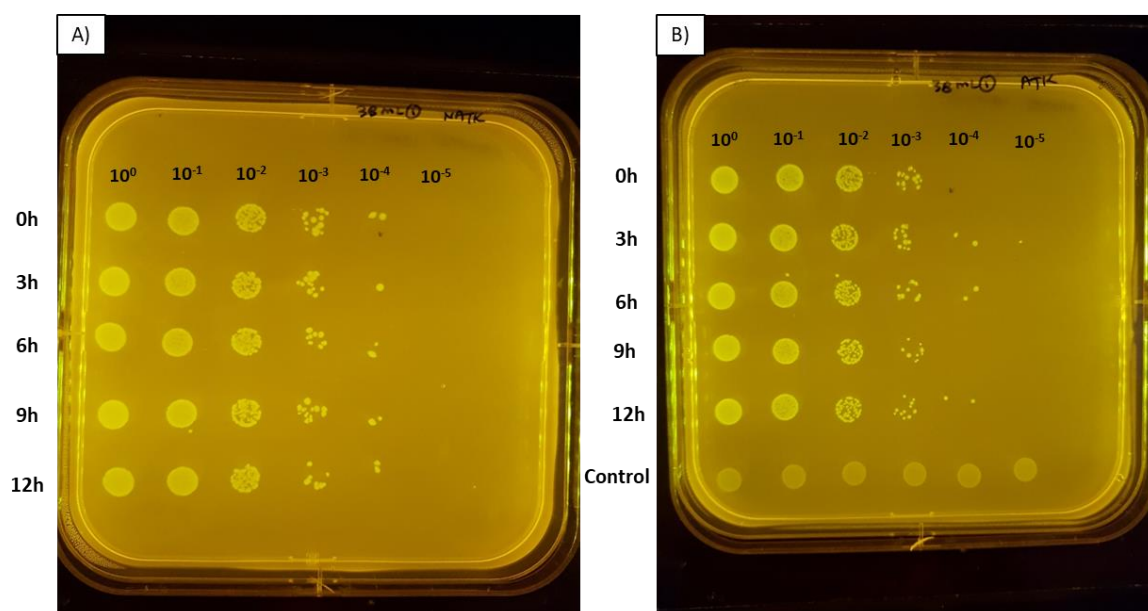


Figure 5-8 Enumeration of samples taken at different times from the bioreactors. Agar dishes illustrating the spot plating technique selecting for cells carrying the pRP4-*gfp* plasmids. Samples (10- μ L) were plated neat (10^0) and as increasing dilutions (10^{-1} to 10^{-5}) and incubated over night at 30°C. The following day the plates were placed on a UV transilluminator to detect fluorescence and the colonies counted. (A) Selective agar containing antibiotics selecting for the *E. coli EcoFJ2* donor strain (i.e. Amp, Kan, Tet, Nal); (B) Selective agar containing antibiotics selecting for all strains containing pRP4-*gfp* (i.e. Amp, Kan, Tet). The control strain was *E. coli* harbouring the original unmodified pRP4 plasmid with no GFP (not fluorescing under UV illumination) which was a gift from Professor C.M. Thomas, University of Birmingham, UK. Results with countable colonies and corresponding dilution factor was recorded.

Beyond the above, samples stored in PBS were sub-sampled and enumerated the next day on nutrient agar supplemented with X-gluc (ThermoFisher Scientific) and the

three antibiotics for the pRP4-based plasmid. Cleavage of X-gluc by the *E. coli* glucuronidase produce an intense blue precipitate of chloro-bromindigo, and the resulting blue colonies distinguish colonies of *E. coli* from other species (Figure 5-9). Only samples at 24 h were chosen to screen for putative transconjugants. Appropriate dilutions for plating were based on the spot plating results and 100 μ L aliquots were plated evenly on prepared agar plates and incubated at 30 °C for 24 hours.

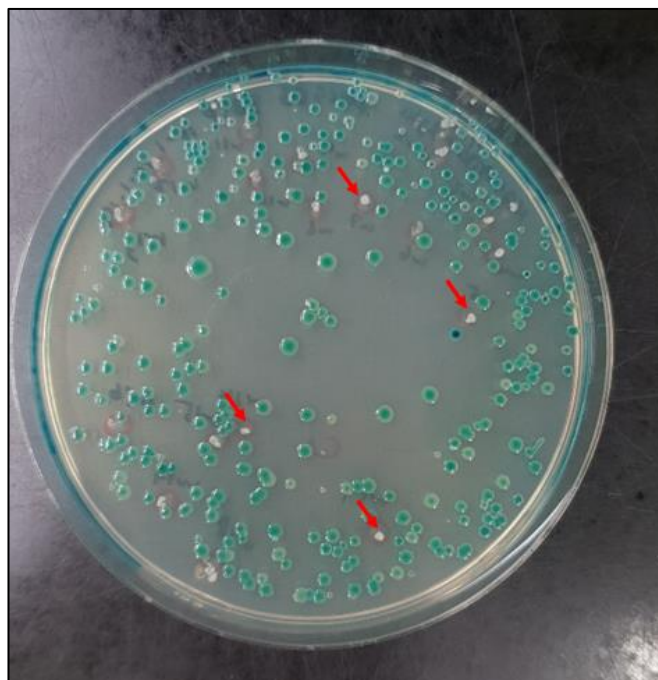


Figure 5-9 Bacterial colonies on a selective and differentiation agar plate containing antibiotics selective for pRP4-based plasmids (i.e. Amp, Kan, Tc) and containing X-Gluc. *E. coli* strains produce blue colonies in the presence of X-gluc while other microbes will produce white or colourless (red arrows). *E. coli* strains were predominant bacteria in all samples.

Incubated plates were examined and single colonies from each sample were randomly selected for subsequent screening on agar with appropriate amendments following the decision tree in Figure 5-10. Colonies that grew in the presence of nalidixic acid were presumably derived from the original seed culture while those that were nalidixic acid sensitive were presumed to have acquired pRP4-*gfp* by putative HGT from the seeded strain via conjugation. Presumptive transconjugants were isolated, sub-cultured and purified on selective plates. Pure bacterial cultures were stored in 25% glycerol at -80 °C.

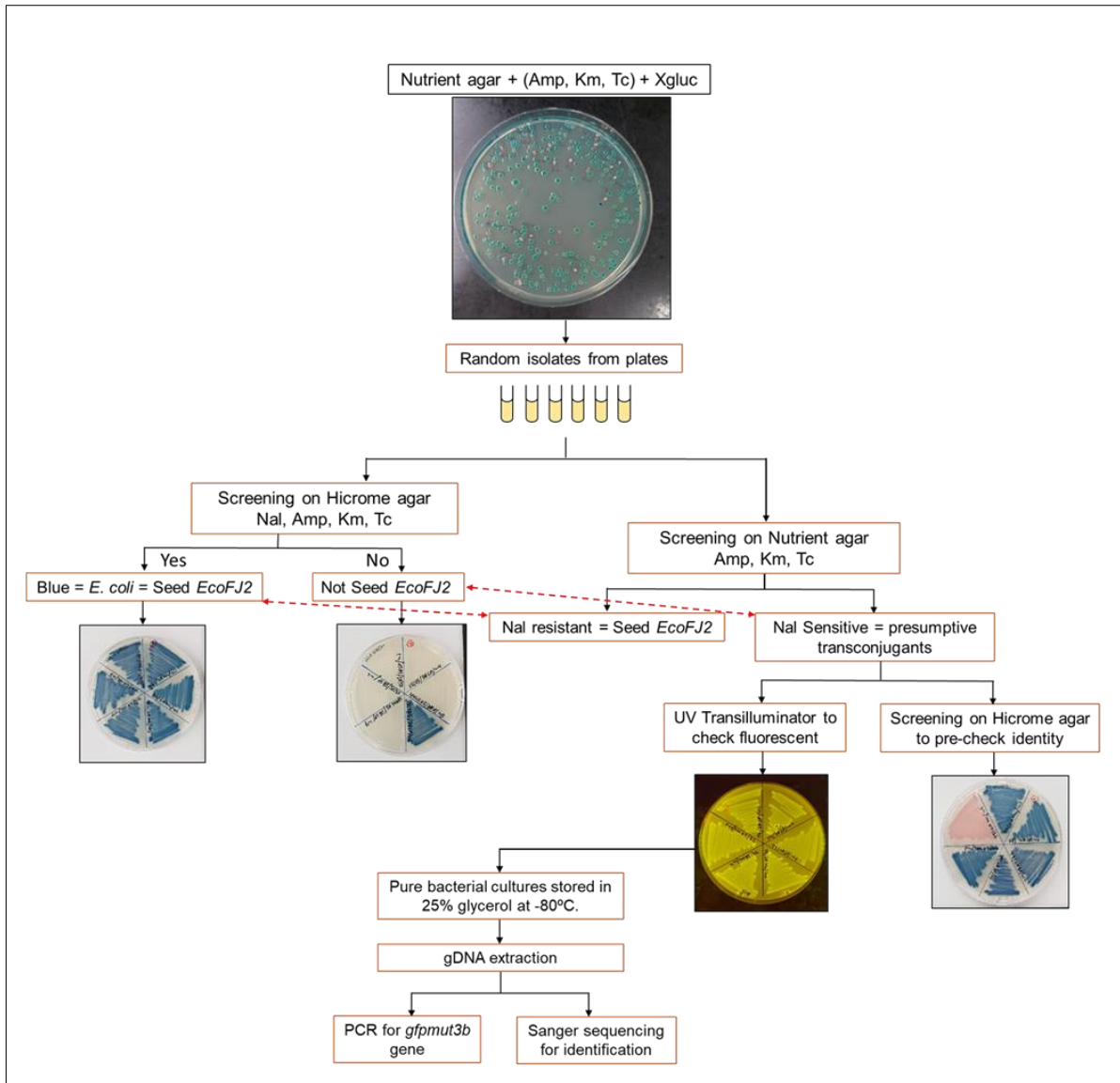


Figure 5-10 Decision tree for the screening and isolation of presumptive transconjugants from sub-samples using selective media.

5.2.15 DNA extraction and detection of *gfpmut3b* genes

A total of 191 isolates were screened and 24 stable presumptive transconjugants were isolated from different samples collected within biofilm and liquid phase samples (Table 5-3; see later for detailed results).

Table 5-3 Screening of bacterial colonies from redox samples for isolating presumptive transconjugants.

Samples	Aerobic	Anoxic	Anaerobic
Liquid phase	30	30	31
Biofilm	34	33	33
Total isolate screened	64	63	64
Total presumptive transconjugant	2	2	20

Genomic DNA from the isolates was extracted using the GenElute Bacterial Genomic DNA (Sigma Aldrich, UK) according to the manufacturer's protocols. Following extraction, DNA samples were checked for purity using a NanoDrop 1000 spectrophotometer (ThermoFisher Scientific, UK). To further confirm the presence of receiving pRP4-*gfp* in these isolates, detection of the *gfpmut3b* gene which is located on the plasmid was performed by PCR using the forward primer P*gfp(up)* (5'-CACTGGAGTTGTCCCAATTCTTG-3') and reverse primer P*gfp(down)* (5'-CAGATTGTGTGGACAGGTAATGG-3') (Andersen *et al.*, 1998).

The *Taq* DNA polymerase with standard *Taq* buffer (New England Biolabs, UK) was used for the PCR reactions. PCR amplifications of target DNA was performed from genomic DNA samples in 50- μ L reaction mixtures made up of 47 μ L prepared PCR master mix (containing 1 μ L of 10 mM dNTPs, 5 μ L of 10X standard *Taq* reaction buffer and 0.25 μ L of *Taq* DNA polymerase (1.25 U/50 μ L) and 40.75 μ L nuclease free water), 1 μ L of purified DNA template, and 1 μ L of each primer (10 μ M). The PCR reaction procedures were as follows: initial denaturation at 95 °C for 30 seconds, 30 amplification cycles of denaturation at 95 °C for 1 min, annealing at 53 °C for 1 min, and elongation at 68 °C for 1 min, and final extension at 68 °C for 1 min.

PCR products with an expected band size 593bp were confirmed by electrophoretic analysis of 8 μ L of the PCR product mixture with 2 μ L loading dye on a 1.5% agarose gel (See Figure C-1; Appendix C). A 1 kb DNA ladder (ThermoFisher Scientific, UK)

was used as the molecular size marker. Positive and negative controls were included in all PCR experiments, where positive controls contained 1 µl of *EcoFJ2* DNA extract, that contained the cloned *gfpmut3b* gene fragment and negative controls contained 1 µl of unmodified *EcoFJ1-Nal^r* DNA extract in place of the sample DNA.

5.2.16 16S sequencing for identification of transconjugants

Following the confirmation of presence of pRP4-*gfp* in transconjugants, DNA samples were subjected to 16S rRNA gene PCR amplification using the 16S universal primers 27F (5'-AGAGTTTGATCCTGGCTCAG-3') and 1492R (5'-GGTTACCTTGTACGACTT-3') (Yang *et al.*, 2016). PCR assays using the Q5 High-Fidelity DNA polymerase (New England Biolabs, UK) were conducted in a 100-µl volume reaction system containing 1 µl diluted DNA extract as the template, and 2.5 µl of each primer (10 µM), 10 µl of the 5x Q5 reaction buffer, 1 µl of 10 mM dNTPs, 0.5 µl Q5 DNA polymerase (0.02 U/µL) and 82.5 µl nuclease free water.

Prior to sequencing, the PCR products were purified using the QIAquick PCR purification kit (QIAGEN, UK) and sent for Sanger sequencing of both the forward and reverse reactions at GATC Biotech, UK. The same primers used for PCR were also employed to sequence both strands of the PCR products. Quality of nucleotide sequences were viewed and cleaned using the FinchTV chromatogram viewer program. Cleaned and edited sequences were queried against the National Centre for Biotechnology Information (NCBI) 16S rRNA gene database for archaea and bacteria to identify the species of transconjugants. Finally, DNA nucleotide sequences were aligned and phylogenetic analysis was conducted with the MEGA software using the neighbour-joining (NJ) method, to construct a distance-based tree.

5.2.17 Protozoa counts

We were interested in knowing whether bacterial cell numbers were significantly affected by predation by protozoa. Therefore, formaldehyde-fixed samples from the Phase 2 experiments were sub-sampled and analysed in a cell counting chamber (Haemocytometer; ThermoFisher Scientific, UK) for the presence of protozoa. This was done to provide metadata for the HGT experiment, assessing whether possible predation for pRP4-*gfp* host might differ under different redox environment. In particular, we wanted to enumerate the presence of eukaryotic organisms in the

biofilms and in suspension in contrasting environments, namely aerobic and anaerobic conditions. Samples were analysed at 0 h, 12 h, 24 h, 48 h and 72 h following Stage 1 seeding.

Biological samples were concentrated two-fold by centrifuging 100 μL of uniform suspensions at 4000 $\times g$ for 1 minute and resuspended in 50 μL PBS. A sample of the concentrate (10- μL) was loaded on the Haemocytometer, overlaid with a glass cover slide, and viewed on the microscope at 400x magnification. For counting, the number of protozoa on the four outer corner squares within the 9 mm^2 grid were recorded and the final protozoa concentrations were calculated according to the known volume of the chamber, following the manufacturer's guidelines.

5.2.18 Data analysis

All data were analysed using R statistical software 3.5.0 (R Core Team, 2013). The flow cytometry counts of pRP4-*gfp* and the relative abundance data were checked for normality prior to statistical analysis. One-way analysis of variance (ANOVA) sample tests followed by multiple pairwise-comparisons using post-hoc Tukey test were performed to compare the differences in GFP levels between contrasting redox conditions and time points.

Given the resulting data distributions were not consistently normal, Kruskal-Wallis and Games-Howell post-hoc tests were used as non-parametric alternatives for the ANOVA and Tukey tests, respectively. GFP abundance data were assessed using the unpaired two-sample Wilcoxon test to compare abundances between biofilm and liquid phase samples. Additionally, a two-way ANOVA test was performed to simultaneously evaluate the effect of time against redox conditions versus the changes in relative numbers of the pRP4-*gfp* abundances. Unless otherwise noted, differences between data groups with p-values less than or equal to 0.05 were defined as significant.

5.3 Results and Discussion

5.3.1 Phase 1: Preliminary seeding tests

E. coli *EcoFJ2* donor strain was seeded into each reactor vessel at a concentration of 10^6 cells/mL to attain the desired starting concentration of 1% of the total cell population. In the Phase 1 experiment, samples were collected after one hour and then at two-hour sample intervals over the first seven hours (i.e., 0 h, 1 h, 3 h, 5 h, 7 h; Table 5.3) to establish the suitable sample timings needed to detect temporal changes in pRP4-*gfp* concentrations.

Phase 1 data showed that temporal changes in pRP4-*gfp* levels differed among redox conditions. In general, percentages of pRP4-*gfp* *EcoFJ2* at time zero ranged from 0.2 to 2% giving suitable starting densities. The concentration in the aerobic biofilm samples was approximately two-log lower at time zero, which may be due to lack of overall cell attachment to sponge cubes. However, more homogeneous biomass concentrations were measured in subsequent suspension and biofilm samples, as indicated by standard deviation (Figure 5-11).

Data indicate that pRP4-*gfp* levels only changed slightly in all samples during the first three hours, whereas levels gradually increased by times 5 h and 7 h. This may reflect the need for the seed culture to acclimatise following exposure to the environment of the bioreactors. The increase was generally more obvious in the aerobic biofilm samples at around 3 h and 5 h, which was expected as aerobic conditions should support more rapid growth rates. Similar trends for pRP4-*gfp* signals were observed in the suspended bioreactors across redox conditions.

Overall, GFP signals within biofilms versus the liquid phase declined 24 hours after inoculation, with a more acute trend seen in the aerobic systems, which continued to decline over the following days (i.e., 48 h and 72 h). Analysis of variance show that temporal changes of pRP4-*gfp* abundances varied differently between redox conditions, where significant differences over time were detected in aerobic conditions, but no significance differences were observed in the anoxic and anaerobic conditions (Kruskal-Wallis; $0.038 < p\text{-value} < 0.43$).

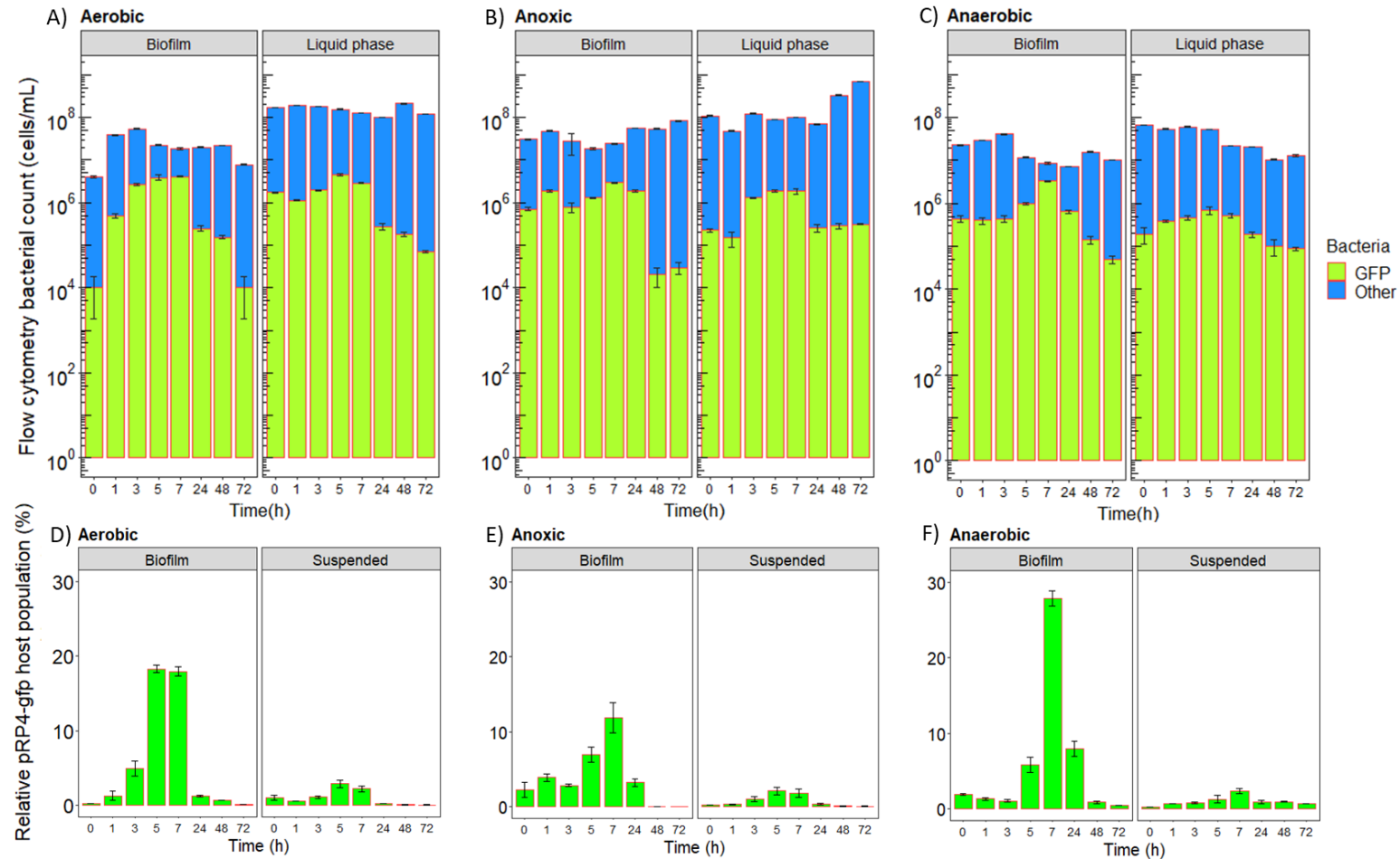


Figure 5-11 Trend of pRP4-gfp levels across Phase 1 bioreactors over 72 hours. The top row represents the flow cytometry data from biofilm and suspended samples in (A) aerobic, (B) anoxic and (C) anaerobic conditions. The bottom row (D-F) presents corresponding relative pRP4-gfp population within biofilm and suspended samples. Error bars indicate the standard deviation of biological replicates.

Levels of the pRP4-*gfp* in aerobic samples were significantly lower after 24 hours and longer (i.e., 24 h, 48 h and 72 h) compared with the initial concentration at time zero (both biofilm and liquid phase; Games-Howell post-hoc; both p-values = 0.047).

Whereas, pRP4-*gfp* levels over the same period did not significantly differ in both anoxic and anaerobic conditions (biofilm and liquid phase; Games-Howell post-hoc; both p-values = 0.072). The data suggest that the numbers of pRP4-*gfp* host (i.e., donor strain, *EcoFJ2* and-or putative transconjugants) declined much faster under aerobic conditions than under parallel anoxic and anaerobic conditions, especially in the first 24 hours.

Across bioreactors, pRP4-*gfp* concentrations were significantly different between redox conditions in the liquid phase samples (Kruskal-Wallis; p-values = 0.02), but not significantly different in the biofilm samples (Kruskal-Wallis; p-values = 0.47). Similar pRP4-*gfp* levels in all biofilm samples suggest that the fate of pRP4-*gfp* host is less different in biofilms, regardless of redox conditions. Further, multiple pairwise comparison (Games-Howell post-hoc tests) of the mean concentrations within redox conditions confirmed a strong contrast in the liquid phase samples as opposed to the biofilm samples (Table 5-4).

Table 5-4 P-values, showing significant differences for comparisons between the liquid phase and biofilm samples at different redox conditions in sequencing batch reactors seeded with pRP4-*gfp* *EcoFJ2*.

Bioreactor	Samples	Games-Howell post-hoc test
Aerobic - Anaerobic	Liquid phase	< 0.01**
Aerobic - Anoxic	Liquid phase	0.05*
Anaerobic - Anoxic	Liquid phase	0.02*
Aerobic - Anaerobic	Biofilm	0.26
Aerobic – Anoxic	Biofilm	0.8
Anaerobic – Anoxic	Biofilm	0.37

Note: Asterisks represent p-values; * denotes $p \leq 0.05$; ** denotes $p \leq 0.01$.

By transforming pRP4-*gfp* abundances into relative abundances, a clearer picture emerges. From ~1% starting concentration, the relative abundance of pRP4-*gfp* positive bacteria increase with time, peaking between 5 and 7 hours after seeding (Figure 5-11D-F). The peak in the aerobic biofilms occurs earliest, at 5 h. However,

the greatest relative abundances were seen in anaerobic biofilms (Figure 5-12). Relative abundances were greater in all biofilm samples, suggesting selective migration of the *EcoFJ2* donor strain into biofilms soon after seeding.

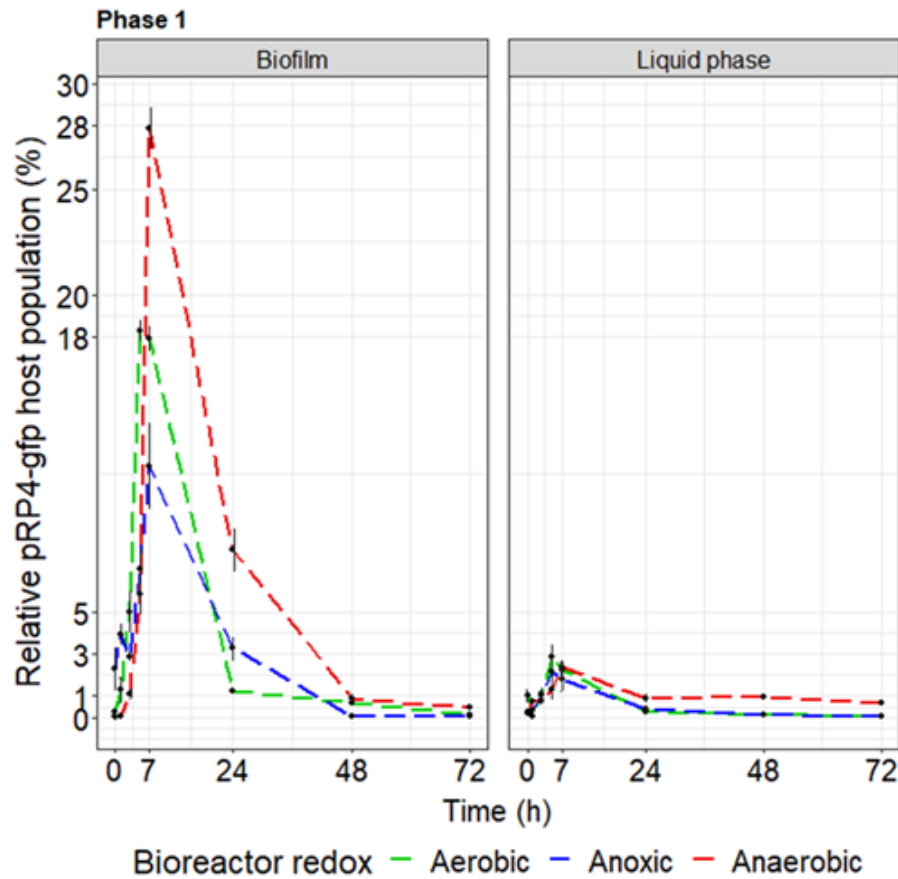


Figure 5-12 Spatial and temporal pattern of relative GFP population across contrasting redox conditions in biofilms and liquid phase samples. Error bars indicate the standard deviation of biological replicates.

In contrast, all relative abundances dramatically declined after 24 hours, although the relative rates of decline were much lower in the anoxic and anaerobic systems. Data indicate movement of the *EcoFJ2* into the biofilms was rapid under all conditions, and seemed to reside longer in anaerobic biofilms relative to aerobic and anoxic conditions.

Statistics show relative pRP4-*gfp* levels in biofilms were significantly higher than the liquid phase under aerobic (unpaired two-sample Wilcoxon test; p-value = 0.009) and anoxic conditions (unpaired two-sample Wilcoxon test; p-value = 0.03). Although the same general pattern was seen under anaerobic conditions, the relative difference

between biofilm and liquid phase samples were not significantly different (unpaired two-sample Wilcoxon test; p-value = 0.58).

The two-way ANOVA test was used to evaluate the effect of grouping the parameters of time and redox conditions on the changes in relative pRP4-*gfp* abundance.

Although differences were apparent among redox conditions, the results indicate that “time” was the more significant factor influencing changes in pRP4-*gfp* abundance in both biofilm (p-value = 0.005) and liquid phase samples (p-value = 0.0004).

5.3.2 Phase 2: Seeding frequencies versus spatial and temporal patterns of pRP4-*gfp* hosts in SBBR

The preliminary (Phase 1) study showed that major relative changes in the abundance of the donor strain *EcoFJ2* levels occurred within the first 12 hours after seeding and diminished after 24 hours, becoming almost undetectable after three days. Time following inoculation was the major factor influencing changes in plasmid abundance within the reactors, although differences were seen among different redox environments.

To examine more closely the effect of time and seeding, the Phase 2 experiment assessed both a single seeding event (Stage 1) and semi-intermittent seeding over time (Stage 2; more typical of an actual operating bioreactor). Phase 2 experiments used three-hour sampling intervals to more easily quantify donor's fate between 9 and 24 hours (Figure 5-13) and also capture seed fate over much longer periods with and without additional seeding of the systems.

Under Stage 1 single-pulse seeding, pRP4-*gfp* densities generally decreased during the first three hours in all the bioreactors, presumably reflecting initial acclimation as seen in the Phase 1 experiment. The pRP4-*gfp* levels experienced more dramatic drops in absolute levels in the aerobic samples taken from the Phase 2 experiment compared with the Phase 1 experiment, both in biofilm and liquid phase samples. Notably, aerobic samples displayed a distinctly different pattern than the anoxic and anaerobic systems. Despite small rises in pRP4-*gfp* host levels at some time points (e.g. 6 h and 24 h), the GFP signals continued to decline overtime with a two-log net reduction over 72 hours, which was significantly lower than starting levels (Games-Howell post-hoc; p-value < 0.001).

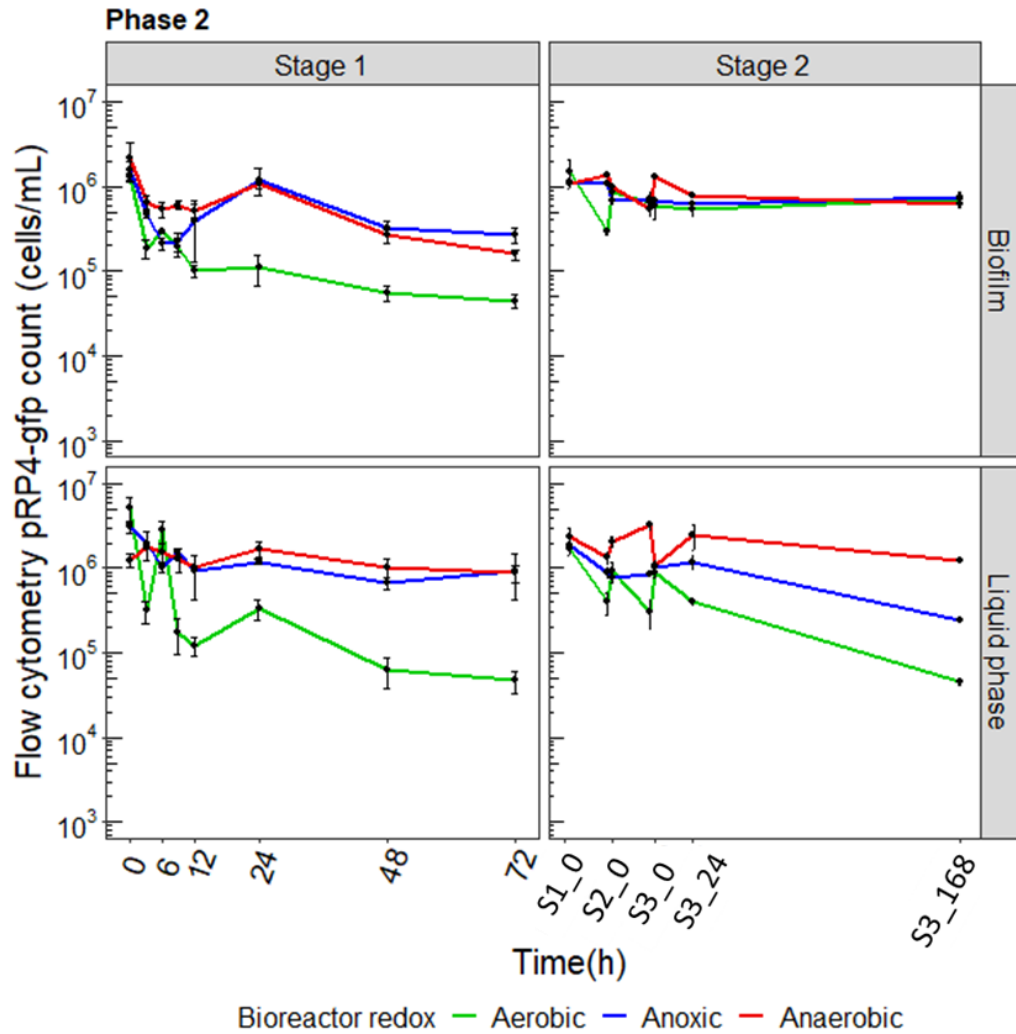


Figure 5-13 Spatial and temporal pattern of pRP4-gfp cell densities across contrasting redox conditions in biofilms and liquid phase samples during the pulse influx and continuous influx. Error bars indicate the standard deviation of biological replicates.

Although pRP4-gfp levels gradually declined during the first six hours in the anoxic and anaerobic systems, the GFP signals did not change dramatically through 24 h, equating roughly to the initial concentrations in both systems ($1 \sim 1.2 \times 10^6$ cells/mL). Host numbers subsequently declined to $2.6 \sim 3.3 \times 10^5$ cells/mL at 48 h (Games-Howell post-hoc; $p < 0.01$) and $1.6 \sim 2.7 \times 10^5$ cells/mL at 72 h (Games-Howell post-hoc; $p < 0.01$). Overall, similar to Phase 1, pRP4-gfp levels declined more rapidly in the aerobic systems. It is apparent that host cells are consistently declining under aerobic conditions, suggesting a systematic driver related to oxygen is probably impacting on the disappearance of the pRP4-gfp hosts (i.e., *E. coli* EcoFJ2 donor

strain and-or pRP4-*gfp* recipient cells). Specifically, pRP4-*gfp* hosts were retained longer under the anoxic and anaerobic conditions in both biofilm and liquid phase samples. By the end of sampling at 72 h, pRP4-*gfp* host numbers were similar in the anaerobic and anoxic samples ($1.6 \sim 8.7 \times 10^5$ cells/mL) and the host numbers aerobic samples were $4 \sim 4.4 \times 10^4$ cells/mL; one order of magnitude lower than the anaerobic and anoxic conditions.

During semi-continuous seeding, the pRP4-*gfp* levels were fairly similar in biofilms under the three redox conditions. Host populations were relatively constant after the second seeding (S2), even in the aerobic biofilms, which suggest possible colonisation or pseudo-equilibrium under semi-continuous seeding. On the other hand, in the liquid phase, pRP4-*gfp* levels exhibited different patterns among redox conditions. Although host numbers increased after each seeding (by $\sim 10^6$), abundances always declined in the aerobic systems after one day (\sim one log), but not as dramatically under the anoxic systems. In contrast, there was an increasing trend in the pRP4-*gfp* levels in the anaerobic liquid phase, eventually surpassing initial seeding concentrations. This suggests either the original seed strain is growing, either by actual growth and death avoidance, and-or actual transmission of pRP4-*gfp* is occurring to other bacteria; i.e., the *E. coli* EcoFJ2 donor strain is surviving better under these conditions and transmitting their plasmids.

Final samples were collected after 168 hrs of semi-continuous seeding (S3_168). The pRP4-*gfp* plasmid was retained equally in all biofilm samples ($\sim 10^5$ cells/mL), while the numbers in the liquid phase varied versus redox condition; i.e., anaerobic > anoxic > aerobic. The pRP4-*gfp* host numbers were two orders of magnitude greater in the anaerobic (1.3×10^6 cells/mL) versus aerobic systems (4.5×10^4 cells/mL). Once again, a factor associated with oxygen levels appears to be impacting the fate of the plasmid or its host strain, although the relative impact differs in the biofilm and liquid phase, depending on single versus semi-continuous seeding.

In the Phase 2 experiments, more data points were collected and statistics of the pRP4-*gfp* mean concentrations show significant difference between redox conditions in both the liquid phase and biofilm samples during Stage 1 pulse seeding (Kruskal-Wallis; both p-values < 0.01). Specifically, pRP4-*gfp* levels were significantly lower in aerobic samples than in the anaerobic samples (Tukey's comparisons for liquid

phase and biofilm samples; both p -values < 0.05) (Table 5-5). However, during Stage 2 semi-continuous seeding experiment, the levels of pRP4-*gfp* changed significantly in the liquid phase under different redox conditions (Kruskal-Wallis; p -values < 0.0001). Pairwise significant differences were detected in the liquid phase abundances between aerobic and anaerobic conditions and between anoxic and anaerobic (Tukey's comparison; both p -values < 0.01). No significant difference were found between aerobic and anoxic samples. Whereas, pRP4-*gfp* levels were similar in biofilm samples between redox conditions during Stage 2 (Kruskal-Wallis; p -values > 0.05), with no statistically significance difference observed for all redox conditions. The trend in biofilms were similar with pseudo-stable concentrations suggesting pRP4-*gfp* host preferentially survived and persisted in biofilms when continuously seeded, which was less dependent on redox levels.

Table 5-5 *P-values, showing significant differences of pRP4-gfp levels for comparisons between suspended and biofilm samples at different redox conditions in sequencing batch reactors during Phase 2 experiments.*

Bioreactor	Samples	Games-Howell/Tukey post-hoc test
Stage 1 Seeding		
Aerobic - Anaerobic	Liquid phase	0.03*
Aerobic - Anoxic	Liquid phase	0.06
Anaerobic - Anoxic	Liquid phase	0.94
Aerobic - Anaerobic	Biofilm	0.02*
Aerobic - Anoxic	Biofilm	0.56
Anaerobic - Anoxic	Biofilm	0.18
Stage 2 Seeding		
Aerobic - Anaerobic	Liquid phase	$< 0.01^{**}$
Aerobic - Anoxic	Liquid phase	0.29
Anaerobic - Anoxic	Liquid phase	$< 0.01^{**}$
Aerobic - Anaerobic	Biofilm	0.18
Aerobic - Anoxic	Biofilm	0.81
Anaerobic - Anoxic	Biofilm	0.48

Note: Asterisks represent p -values; * denotes $p \leq 0.05$; ** denotes $p \leq 0.01$.

It is important to note that “exposure time” also impacted the changes in pRP4-*gfp* levels within the bioreactors, and differed slightly between seeding frequencies and

sample matrixes. Under both seeding frequencies (Stage 1 and Stage 2), host numbers fluctuated significantly across time points in both the liquid phase (two-way ANOVA; p -values ≤ 0.001) and in biofilms (two-way ANOVA; $0.0098 \leq p$ -values** ≤ 0.004), with less impact seen in the biofilms. This indicates that pRP4-*gfp* levels in the non-biofilm phase disappears faster with time compared biofilm cells.

Relative pRP4-*gfp* host abundances (Figure C-2, Appendix C) roughly mirrored absolute pRP4-*gfp* levels. In summary, aerobic conditions always exhibited the lowest relative pRP4-*gfp* levels when compared to the other redox conditions, both after a single seeding or during semi-continuous seeding. Data suggest host cells are disappearing much more rapidly in aerobic conditions. In contrast, pRP4-*gfp* hosts persisted longer under anoxic and especially anaerobic conditions, both in biofilms and the liquid phase.

Overall, the results suggest that the fate of pRP4-*gfp* involves a sequence of rate-related ecophysiological events including migration, colonisation, and maintenance of the *E. coli* *EcoFJ2* host levels prior to transfer. However, other ecological phenomena, including possibly predation, are also likely to be important and influenced by oxygen conditions (i.e., redox).

5.3.3 *Transfer frequencies estimated by selective plate count*

Detecting presumptive transconjugants that have received pRP4-*gfp* was performed using microbial culturing on nutrient media containing selective antibiotics. The number of indigenous potential recipients (N_r) was determined using FCM prior to the seeding experiment. The number of the original *EcoFJ2* donor strain (N_d) was enumerated using nutrient agar medium amended with the three pRP4-mediated antibiotic markers: ampicillin (Amp), kanamycin (Km) and tetracycline (Tc), plus the chromosomally-mediated nalidixic acid (Nal). The number of bacteria carrying pRP4-*gfp* (N_p) was determined by culturing on nutrient agar plates containing Amp, Km, and Tc. The transfer frequency (f) at 24 h after inoculation was estimated as the difference between to total number of cells in the population encoding pRP4-*gfp* (i.e., resistant to Amp, Km, Tc and Nal) using the formula in Equation 5-3:

Equation 5-3 The equation used to determine the transfer frequency from original seed organism to potential recipient cells present in the bioreactors (Yang et al., 2013a).

$$f = (N_p - N_d)/N_r$$

Where:

N_p = The number of bacteria carrying plasmid pRP4-*gfp*;

N_d = The number of original donor seed organism; and

N_r = The number of indigenous potential recipients

As expected, the transfer frequency was low in all of the samples, ranging from 10^{-5} - 10^{-3} per recipient during the first 24h (Figure 5-14). The results suggest comparatively low levels of putative HGT. However, redox conditions did appear to influence discrete transfer frequencies. Twenty-four hours after the initial seeding of the reporter strain (Stage 1 – Post 24 h) approximately 1 in 500 recipients in the aerobic and anaerobic reactors had received a copy of pRP4-*gfp*: the transfer frequency was similar in both the biofilm and the liquid phase samples. The transfer frequencies in the anoxic reactor were significantly lower, particularly in the liquid phase samples.

At Stage 2 the reactors were reseeded with the reporter strain every 24 hours and samples taken 24 h after each reseeded were analysed for the presence of transconjugants. Again, the highest numbers of transconjugants were observed in the anaerobic reactor, particularly in the liquid phase samples (7.0×10^{-3} - 8.5×10^{-3}). Whereas, aerobic and anoxic samples showed much low transfer frequencies (2.6×10^{-5} ~ 6.1×10^{-3}). ANOVA analyses indicate transfer in biofilms did not significantly differ among redox conditions (ANOVA, $0.12 < p\text{-values} < 0.56$), whereas significance differences were detected in parallel liquid phase samples, with anaerobic conditions displaying significantly higher transfer frequencies (ANOVA; $p\text{-value} = 0.042$). As shown during Stage 1, the numbers of transconjugants in the aerobic and anoxic reactors were significantly lower than that for the anaerobic reactor.

Biofilm samples showed greater transfer frequencies during the Stage 2 seeding regime when bioreactors were reseeded on a 24-hour cycle and become pseudo-steady with higher background pRP4-*gfp* concentrations. However, at this stage it is

not possible to distinguish between the generation of new transconjugants and the maintenance of pre-existing transconjugants. It is possible that semi-continuous influx of *EcoFJ2* seed provide consistent *EcoFJ2* migration with time that allowed successful colonisation into the biofilms, permitting steady gene transfer to occur.

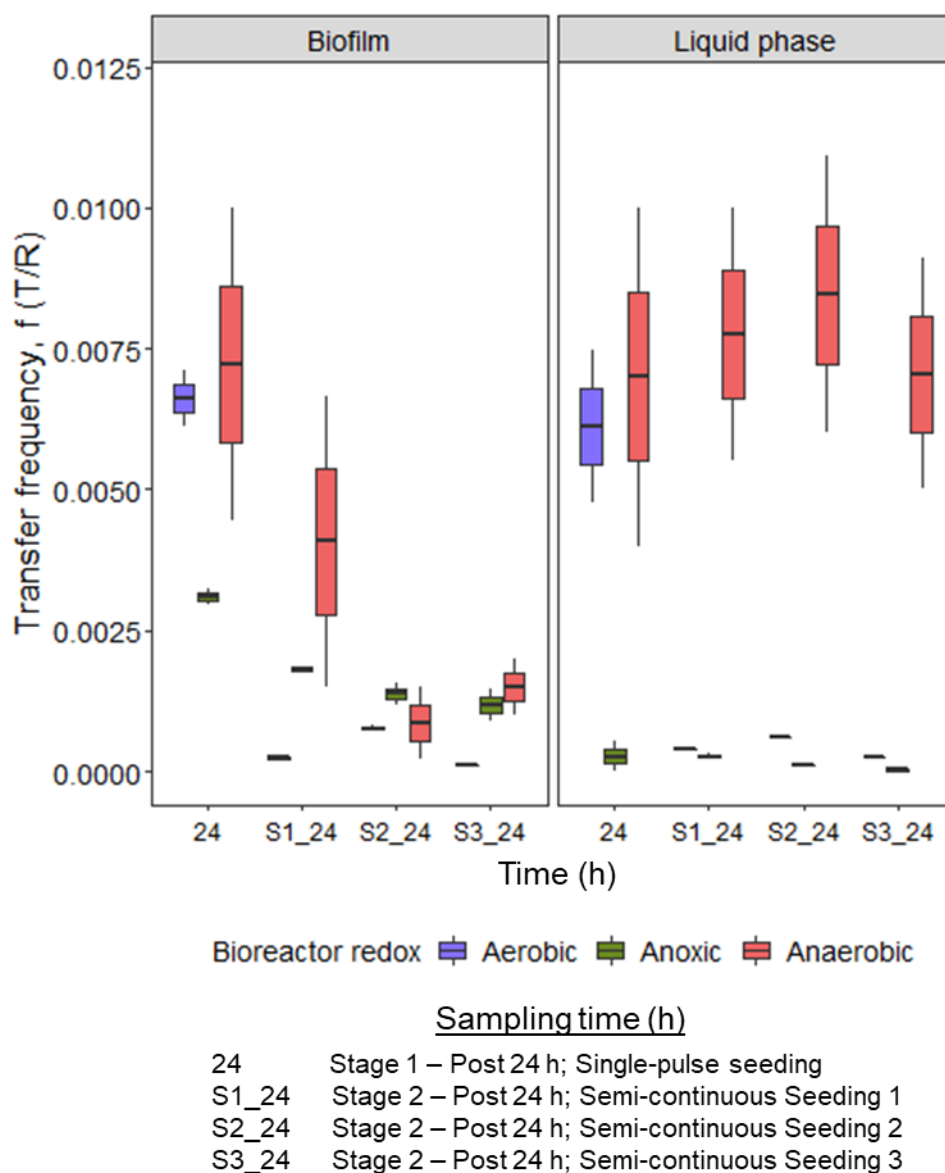


Figure 5-14 Estimated plasmid transfer frequency on recipients (T/R ; putative transconjugant/total recipient cells), in biofilms and the liquid phase during pulse seeding and continuous seeding, taken after each cycle of 24 hours exposure.

5.3.4 Identification and phylogenetic analysis of transconjugants

The 24 putative transconjugants (i.e., one from an aerobic biofilm, one from an anoxic biofilm, six from anaerobic liquid phase, and 16 from anaerobic biofilms) were all identified as strains of *E. coli*, based on 16S rRNA sequence analysis (Table 5-6). A phylogenetic tree was constructed showing the phylogenetic relationships between the isolates and the original *EcoFJ2* host strain (Figure 5-15). *E. coli* strain ATCC 35218, obtained from the NCBI library (GenBank accession number AM980865), was included as a reference strain in the phylogenetic relationship analysis.

The analysis revealed that all of the isolated transconjugants were closely related strains of *E. coli*, indicating that the highest frequency of transfer was between related strains. Much larger number of potential transconjugants (e.g. $> 10^3$) might be needed to be analysed to detect the lower expected frequencies of transfer between unrelated species. Although pRP4 is a broad-host-range plasmid, transfer to other species of the indigenous microbiota within the bioreactors was below the limits of detection in the current system. These reason for this lower level of transfer are likely to involve limitations in the transfer mechanism and the presence of systems (e.g., restriction and modification, CRISPR) that detect and destroy incoming heterologous DNA. Detected transfers appeared low, even in biofilms with greater background conjugative potential. Indigenous microbiota within the different bioreactors, but data strongly indicated that greater HGT happened under anaerobic conditions.

Table 5-6 Significant species detected based on sample DNA sequencing and database sequences in the NCBI nucleotide database.

Sample	Isolate	Identified species (NCBI)	Significant match (%)
Aerobic biofilm	FL1	<i>Escherichia coli</i>	99.8
Anoxic biofilm	FL2	<i>Escherichia coli</i>	99.9
Anaerobic biofilm	FL3	<i>Escherichia coli</i>	99.9
Anaerobic liquid phase	FL4	<i>Escherichia coli</i>	99.9
Anaerobic liquid phase	FL5	<i>Escherichia coli</i>	99.9
Anaerobic liquid phase	FL6	<i>Escherichia coli</i>	99.9
Anaerobic liquid phase	FL7	<i>Escherichia coli</i>	100.0
Anaerobic biofilm	FL8	<i>Escherichia coli</i>	99.9
Anaerobic biofilm	FL9	<i>Escherichia coli</i>	99.9
Anaerobic liquid phase	FL10	<i>Escherichia coli</i>	99.9
Anaerobic biofilm	FL11	<i>Escherichia coli</i>	99.9
Anaerobic biofilm	FL12	<i>Escherichia coli</i>	100.0
Anaerobic biofilm	FL13	<i>Escherichia coli</i>	99.9
Anaerobic biofilm	FL14	<i>Escherichia coli</i>	100.0
Anaerobic biofilm	FL15	<i>Escherichia coli</i>	99.9
Anaerobic biofilm	FL16	<i>Escherichia coli</i>	99.9
Anaerobic biofilm	FL17	<i>Escherichia coli</i>	100.0
Anaerobic liquid phase	FL18	<i>Escherichia coli</i>	99.9
Anaerobic biofilm	FL19	<i>Escherichia coli</i>	99.9
Anaerobic biofilm	FL20	<i>Escherichia coli</i>	99.9
Anaerobic biofilm	FL21	<i>Escherichia coli</i>	99.9
Anaerobic biofilm	FL22	<i>Escherichia coli</i>	99.9
Anaerobic biofilm	FL23	<i>Escherichia coli</i>	99.9
Anaerobic biofilm	FL24	<i>Escherichia coli</i>	99.9

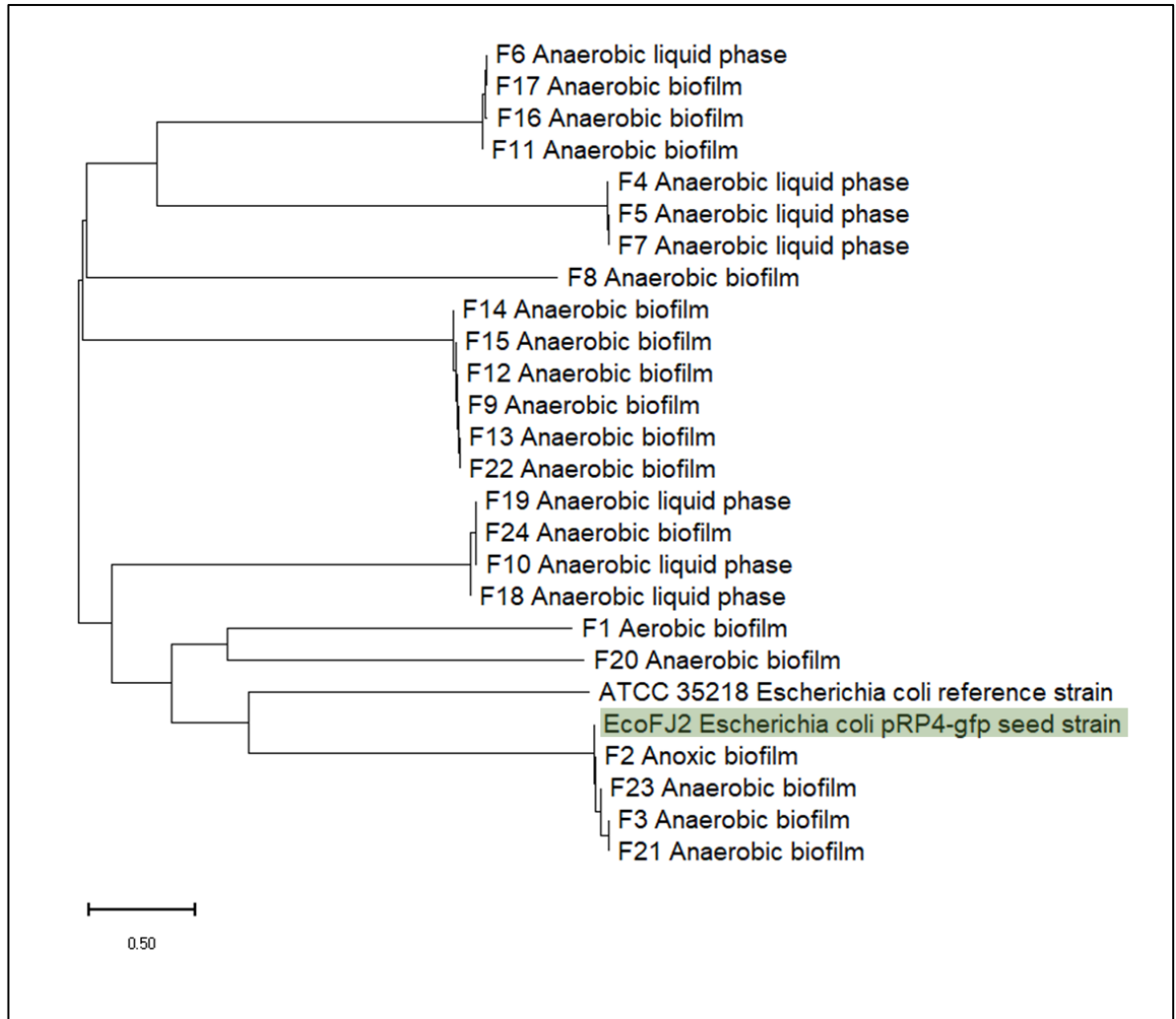


Figure 5-15 Phylogenetic tree based on neighbour-joining (NJ) method showing relationships between the EcoFJ2 seed strain and transconjugants isolated from different samples.

5.3.5 Elevated predation: a possible explanation for the reduced transfer frequencies observed under aerobic conditions

A preliminary microscopic analysis of samples abstracted from the Phase 2 bioreactors had indicated the presence of protozoa in some samples, potentially indicating that higher levels of protozoan grazing under certain conditions might affect the fate of certain group of bacteria (Figure 5-16). Time series samples taken from the Phase 2 experiment were subsampled to quantify presumptive protozoa, using cell counting. The primary goal here was to quantify relative possible predator levels as a function of redox conditions and time. This analysis was only performed at Stage 1, when the reactors has only been seeded once.

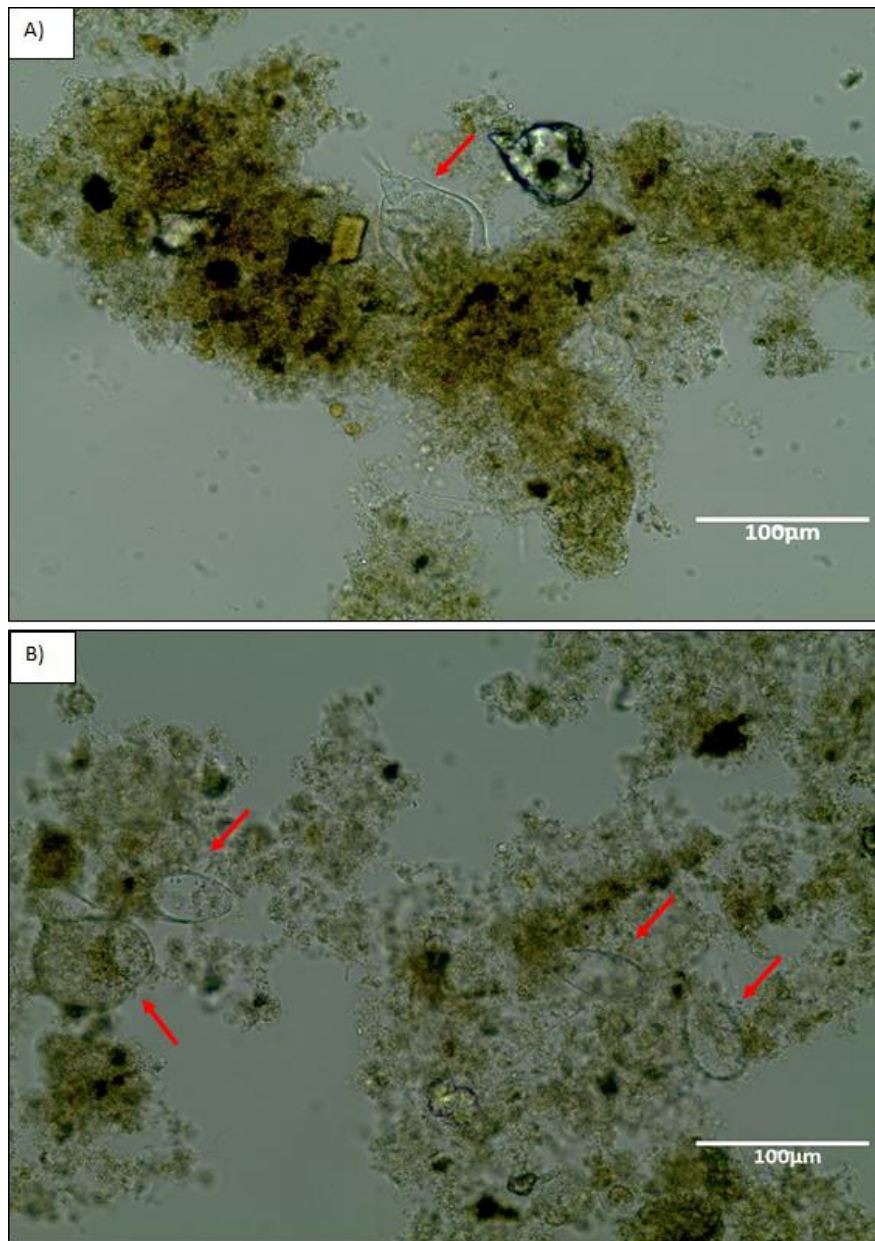


Figure 5-16 Microscopic analysis of samples abstracted from (A) liquid phase; and (B) sponge biofilm from the aerobic SBBR before any seeding. Samples specimens were viewed at 400x magnification and predators were indicated by red arrows.

Given most protozoans are phagocytic heterotrophs that predate and oxidise prey in order to obtain organic nutrients (Bloem *et al.*, 1988), they need oxygen to survive. Therefore, it was hypothesised that higher oxygen levels might support greater predatory activities. This could provide an explanation for why the number of strains encoding pRP4-*gfp* decline most significantly under aerobic conditions (Figure 5-13). In contrast, there were fewer protozoa present under anaerobic conditions, and these are primarily parasitic symbionts rather than bacterial predators.

Haemocytometer counting showed higher abundance of unicellular protists in the aerobic reactors (Figure 5-17), which were significantly higher than the numbers in the anaerobic reactors (both liquid phase and biofilm samples; Wilcoxon test; p-values = 0.0048 and 0.0042). A gradual increase in protozoa numbers within first 24 h hints that increasing predation occurred with seeding, but then declined after 48 h and 72 h, suggesting that protozoan predation might be stimulated by and selective on the pRP4-*gfp* hosts (Figure 5-13). This trend was not seen in the anaerobic reactor samples where protozoa levels were more than an order of magnitude lower.

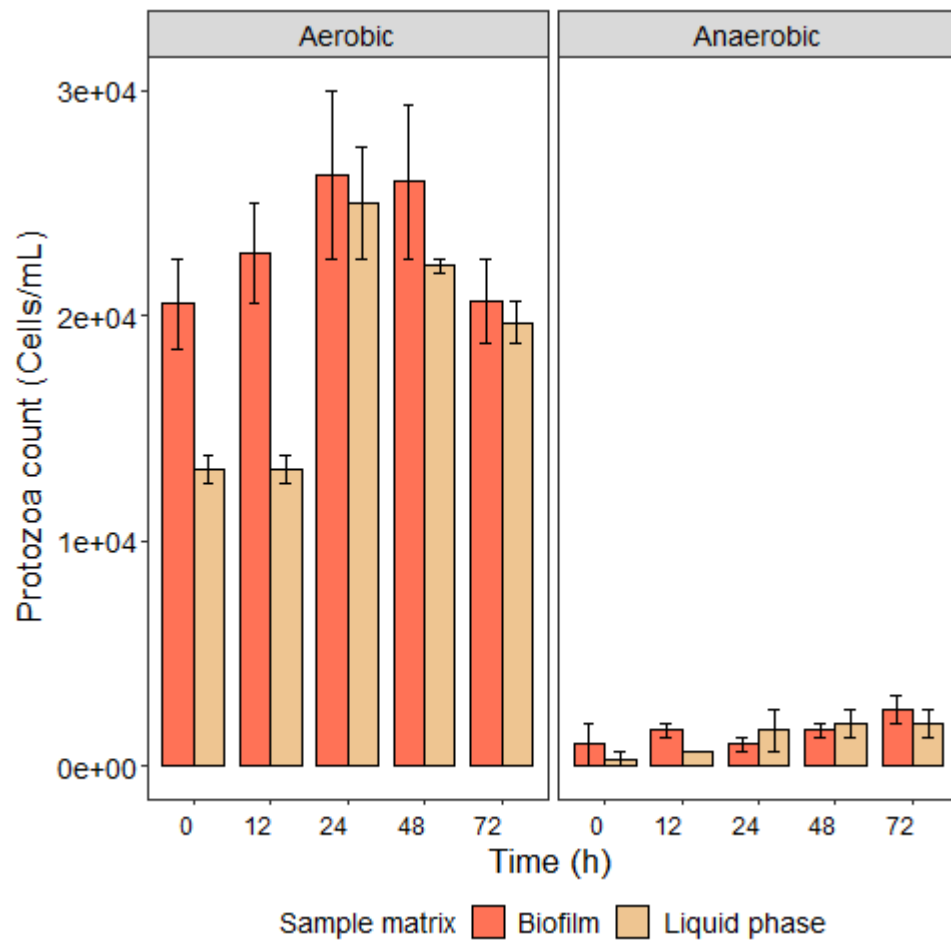


Figure 5-17 Protozoa numbers in samples abstracted from aerobic and anaerobic sponge biofilm and the liquid phase. Error bars indicate standard deviations.

This data parallels higher rates of pRP4-*gfp* host (i.e., reporter strain, *EcoFJ2* and/or putative transconjugants) disappearance under aerobic systems, suggesting predation may be an important suppressor of pRP4-*gfp* *EcoFJ2* survival and, presumptively, subsequent HGT in the reactors. A Pearson correlation test was

performed on the combined data to examine the relationships between protozoa counts and the pRP4-*gfp* host levels (Figure 5-18). A significant negative correlations existed between these two populations, in the liquid phase (Pearson's correlation = -0.71, p-value = 0.00045) and in the biofilms (Pearson's correlation = -0.64, p-value = 0.0024). The strong correlations suggest that *EcoFJ2* numbers might have been reduced by predation.

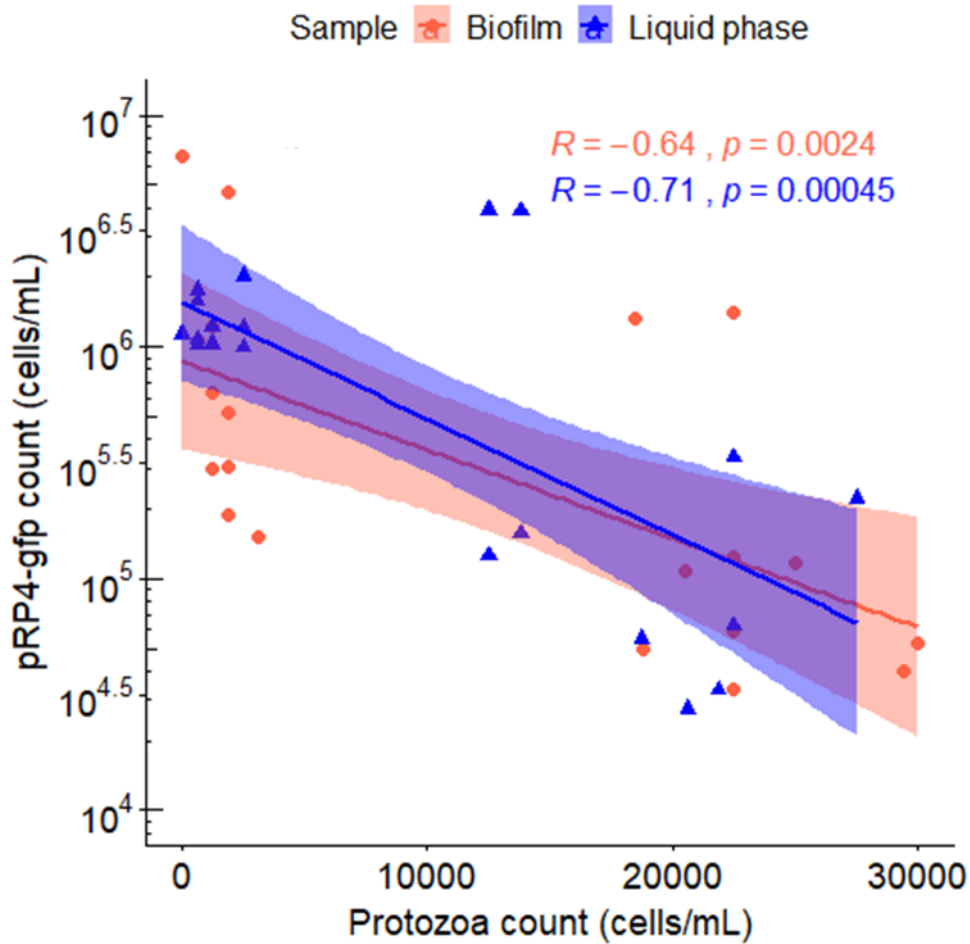


Figure 5-18 Correlations between pRP4-*gfp* levels and protozoa count in liquid phase and biofilm samples. Shaded areas represent the 95% confidence level of the correlation coefficients.

Although not quantitative, further evidence of predation is seen in Figure 5-19. Exploratory screening of the seeded aerobic samples was performed using a Nikon Eclipse Ti fluorescent microscope and GFP fluorescing protozoa were evident in all images assessed, suggesting the ingestion of pRP4-*gfp* host and the retention of GFP signal in the “gut” of the predator.

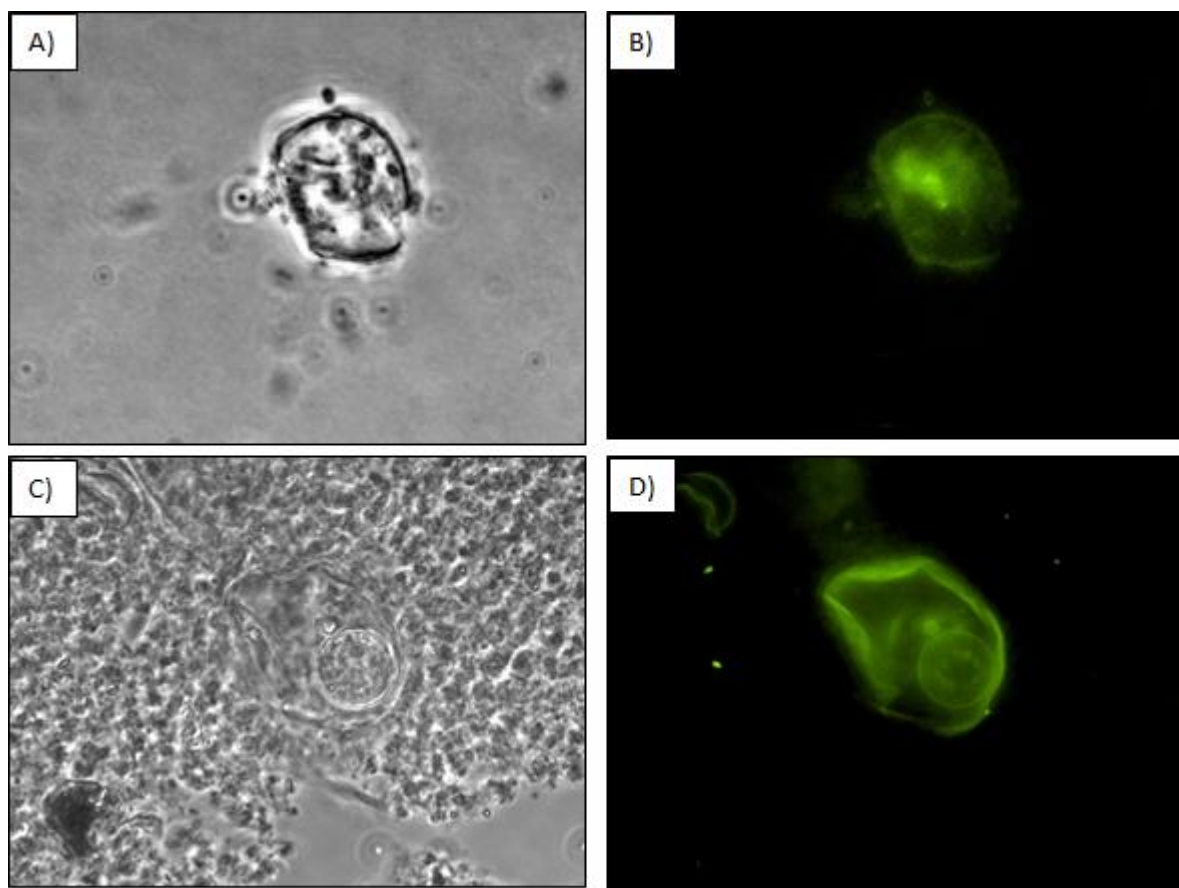


Figure 5-19 Microscopy analysis showing (A & C) Phase contrast, and (B & D) epifluorescence images of food vacuoles expressing GFP fluorescence suggesting pRP4 host cells potentially engulfed by predacious eukaryotes.

5.4 Implications

5.4.1 Tracing AR plasmids in bioreactors

In the past, the migration of conjugal plasmids has been typically estimated through simple mass-action models from liquid broth data (Turner, 2004). The same principle has also been applied when studying horizontal gene flow within environmental samples, including using mating assays on filter mats (Klumper *et al.*, 2015) or on solid agar medium (Geisenberger *et al.*, 1999). However, using these methods, observed mating of donors and recipients neglects the wider influence of environmental and ecological factors, which almost certainly also impact plasmid transfer in the real world.

In contrast, the GFP marker system used here provides a reporter for the presence of pRP4 in manner than quantifies real-time changes of AR plasmid levels and their hosts within more realistic wastewater environments. In both Phase 1 and 2 experiments, discernible changes in pRP4-*gfp* *EcoFJ2* only occurred after 3 hours of inoculation into bioreactor environments (Figure 5-13). This indicates that the colonisation of host cells (donor) and subsequent HGT, was not instantaneous, but nevertheless quite rapid. The results suggest initial acclimation/adaptation of the incoming host occurs first, and this is influenced by biotic and abiotic habitat factors. This need for adaptation was reported previously by Inoue *et al.* (2005) who showed that transfer of pRP4 from *E.coli* C600 to “activated sludge bacteria” by broth mating was affected by temperature, nutrient concentrations, and mixing conditions in the mating environment. One of the reasons that conjugal transfer may be physically inhibited in bioreactors is disruption of mating pairs caused by the shearing forces generated during mixing (Ehlers and Bouwer (1999).

Overall, the experiments described here detected limited *in situ* growth of the seeded *EcoFJ2* strain. The relative abundance of this strain, however, showed that when growth was detected, the GFP percentages were higher in biofilm samples (Figure 5-13). Such an observation suggests that migration into biofilms led to higher AR plasmid detection, which persisted when the seed strain was continuously introduced into the bioreactors (Phase 2; Stage 2). Interestingly, the pRP4-*gfp* encoding bacteria slowly disappeared from the biofilms after 48 h of exposure during single pulse seeding stage (Phase 2; Stage 1), but was retained over longer periods in both the

biofilm and liquid phase samples when semi-continuously seeded (Phase 2; Stage 2). When semi-continuous feeding was stopped, the numbers of pRP4 encoding bacteria dropped in the liquid phase at the final sampling at 168 h, but were still retained in the biofilm (Figure 5-13). These results indicate the location (liquid phase versus biofilms) and seeding pattern impact the time and place where the host survives in the receiving environment which in turn, will impact on the time window over which HGT might occur.

5.4.2 Influence of redox and local niches

In this study the pRP4-*gfp* reporter, *EcoFJ2*, was seeded at a 1:100 donor:presumptive recipient ratio to monitor the frequency of HGT as a function of the redox environments and spatial distribution of the biomass. The survival of the pRP4-*gfp* encoding host strains can be considered from the data (Figure 5-13). Overall, pRP4-*gfp* hosts did not survive well in the aerobic reactors and these strains declined in numbers comparatively rapidly under aerobic conditions. This decline in numbers was more rapid in the liquid phase samples compared with the biofilm samples (e.g., persisted to greater extent) even during semi-continuous seeding. Irrespective to spatial location, pRP4-*gfp* host strains survived longer in the anoxic and anaerobic reactors. This implies the pRP4 host strains was comparatively more fit in reducing environments and potentially less subject to ecological pressures, such as predation, which evidence suggest was more probable under aerobic conditions.

Such aerobic results were comparable with previous studies. In a microcosm experiment, Eberl *et al.* (2006) inoculated $\sim 10^7$ GFP-labelled *Pseudomonas putida* KT2442 into aerobic activated sludge and detected a significant decline by two orders of magnitude after five days. Using *in situ* hybridisation and epifluorescence microscopy, they traced the elimination of the *P. putida* seed culture to protozoan predation. Similarly, work by Yang *et al.* (2013a) showed relatively low frequencies of transfer of pRP4 from *E. coli* K12 in membrane bioreactor mixed liquor, which diminished to nearly zero over 28 days.

Higher gene transfer had been expected in biofilm samples versus the liquid phase samples. This is because for many plasmids, including *Inc-P1* plasmids, conjugation occurs optimally on a mating surface, probably due to higher cell densities, better cell contact and the stabilisation of the mating pairs on a substratum (Bradley *et al.*

(1980). Although pRP4 hosts were retained for longer periods of time in the biofilms of the semi-continuously seeded reactors, data here (Section 5.3.3 and Section 5.3.5), does not reflect greater transfer frequency of pRP4 on a per recipient cell basis. In fact, estimated transfer frequencies were generally lower in the biofilm samples. It is possible that the matrix of the biofilm actually form a barrier that limits the access of donors to potential recipients. In contrast, planktonic donors are free to mate with suitable planktonic recipients. However, this needs to be proven. Another possible explanation is shearing forces present at the biofilm-liquid interface, which may impede mating pair formation (Ehlers and Bouwer, 1999).

Other factors believed to influence overall HGT within complex wastewater ecosystems, including the impact of nutrients and temperature. Bacteria need to consume available nutrients to provide the energy required for conjugation. In a chemically complex bioreactor ecosystem, bacteria need to compete for available substrates. While better adapted species may thrive, greater access to nutrients in the liquid phase may explain why higher transfer frequencies were observed in the liquid phase. Finally, given that antibiotics levels and other possible stressors (i.e., selectors) are probably low in “domestic” wastewater, limited selective pressure exists to drive new acquisition of foreign genetic material, such as would be provided by the pRP4-*gfp* (Devanas *et al.*, 1986).

5.4.3 Removal of pRP4 hosts

The number of bacteria reduced in activated sludge processes is typically in the order of one- to two-log (Kabler, 1959; Vanderdrift *et al.*, 1977). It is believed that predation by ciliated protozoa may be one important mechanism involved in the removal of faecal coliforms from sewage with biological treatment (Madoni, 2011). Protozoa are present in many natural habitats and also proliferate in engineered ecosystems, such as wastewater treatment ponds. They feed on bacteria and organic particulates, and graze on biofilms. Therefore, it is generally assumed that their primary impact in wastewater treatment processes is associated with effluent clarification.

Within any ecosystem, oxygen levels (i.e., redox conditions) greatly influence the abundance of eukaryotes. This was very evident in the experiments described here. Protozoan abundances were 1.0 to 2.0 logs higher in the aerobic versus anaerobic

reactors, both in the liquid phase and biofilms. Levels were slightly higher in biofilms ($\sim 10^4$ cells/mL in aerobic samples), regardless of redox conditions, but always much lower in the anaerobic conditions. One explanation for why protozoa levels were slightly higher in the biofilm could be related to locomotive structures; i.e., most protozoa have appendages that are extended body parts, such as swimming hair, tails, antennae etc. (Yaegar R.G., 1996). As a result, many are prone to attach or associate with surfaces, such as flocs or biofilm carriers. Our results showed that protozoa actively thrived in aerobic environments, apparently grazing in bacteria (including the seeded pRP4-*gfp* *EcoFJ2*), which declined inversely in abundance, in parallel to increases in protozoa levels. This was much less apparent in the anaerobic systems, which had very low protozoan abundances and also lower reductions in pRP4 host levels after seeding.

There is precedence for this observation. Mallory *et al.* (1983) showed that two antibiotic resistant strains, a strain of *Salmonella typhimurium* and a strain of *Klebsiella pneumonia*, declined dramatically in the presence of eukaryotic predators after their addition to sewage mixed liquor. However, no decline was observed when eukaryotic inhibitors were added to the systems, which resulted much lower eukaryote levels. Furthermore, other predatory strains, such as bacteriophages and obligate aerobic *Bdellovibrio* sp, might also have contribute to the reduction of pRP4-*gfp* host strains, although this was not tested here.

5.4.4 Putative HGT in bioreactor

The transfer frequencies (T/R) of pRP4 have been previously reported to range over several orders of magnitudes: from 8.8×10^{-7} to 1.3×10^{-2} /recipient in liquid broth (Inoue *et al.*, 2005), and 4.6×10^{-3} to 7×10^{-2} /recipient on membrane filters (Soda *et al.*, 2008). In this study, putative HGT in the bioreactors ranged from 2.6×10^{-5} /recipient in the anoxic liquid phase to between 7.0×10^{-3} and 8.5×10^{-3} /recipient in the anaerobic liquid phase. These rates are therefore comparable to previous data from liquid and membrane mating assays.

Although higher numbers of the pRP4-*gfp* host strains were retained in the biofilms (Figure 5-13), little *in situ* transfer frequency was evident compared with the liquid phase (Figure 5-14). This indicates that while the pRP4-*gfp* host strain was more associate with biofilms, it was less able to participate in HGT.

One possible assumption is the shielding of biofilm bacteria by its molecular extracellular polymeric substances and the extracellular DNA network within biofilm structure, which protect the encapsulated biofilm bacteria from environmental physical, chemical and biological stresses (Aminov, 2011; Das *et al.*, 2013; Reichhardt *et al.*, 2014). Such protection actually reduced their capacity to access potential donors. The relatively higher frequencies seen in the liquid phase, could be due to their greater access to both suitable recipients and to nutrients, as it is known that transfer and maintenance of plasmids (e.g. pilus formation, plasmid DNA replication) result in metabolic cost, therefore is a nutrient dependent process (Devanas *et al.*, 1986).

Although plasmids can confer beneficial traits on their host, such as antibiotic resistance, they also increase the host's genetic load, and this can impact on survival under nutrient limitation or the absence of a strong positive selective pressure (Devanas *et al.*, 1986; Turner, 2004). Importantly, pRP4-*gfp* host cells survived better within anaerobic systems, therefore long-term exposure may allow incorporation of seeded host cells into indigenous community. This may create increased opportunities for mating pair formation hence increasing evident HGT. Specifically, HGT rates and frequencies in wastewater environments may have little to do with genetic potential and more related to ecological events occurring around cells, which reduce cell-cell exposure and available time between hosts and recipients.

5.5 Conclusions

This study was aimed at determining the survival of a seed culture, *E. coli* EcoFJ2, in the different redox conditions in bioreactors treating domestic wastewater. It also aimed to assess the transmission of AR genes located on a promiscuous conjugal plasmid, pRP4-*gfp*, encoded by the seed culture. Distinct redox environments were sustained using sequencing batch bioreactors, with both biofilm and liquid phase as ideal proxy for the sequential redox stages in the DDHS bioreactors. Local biofilms and liquid phase from aerobic, anoxic and anaerobic redox environments were quantified relative to *in situ* HGT, tracked by a fluorescent-labelled promiscuous AR plasmid seeded into the reactors. Flow cytometry showed that the GFP signal disappeared more rapidly in the aerobic bioreactors, both in biofilms and the liquid phase, whereas host populations did not significantly decline under anoxic and

anaerobic conditions. Survival of the pRP4 host strains, as measured by redox conditions were: anaerobic > anoxic > aerobic.

Host survival was greatest in oxygen-free systems, especially in biofilms and during semi-continuous seeding. However, the frequency of conjugal (i.e., permissiveness) was generally low, albeit slightly higher in biofilms versus the liquid phase. It is possible that although the seeded pRP4-*gfp EcoFJ2* can attach to the sponges and grow on biofilms, this mode of growth may have limited gene exchange. Colonisation and gene exchange was influenced by local obstructions in the biofilms, such as extracellular polymeric substances. Higher eukaryote levels in the aerobic reactors imply protozoan predation may also be critical to reducing AR genes and plasmids, possibly as an effective removal mechanism in aerobic treatment systems.

Overall, multiple environmental factors affect HGT during biological wastewater treatment, which involves multi-step processes and likely to be system specific. Here we show HGT is impacted by the local ecology, including the relative survival of donor strains. It involves the interplay between host migrations, redox conditions, nutrient access and predation, which provides possibilities for manipulating these variables to control microbial HGT during biological wastewater treatment. It is important to appreciate that the fate of plasmid-borne AR genes and host bacteria can differ within different biological systems, operating variables and plasmid types. In reality, it may not be possible to fully understand the myriad factors in biological treatment processes or any ecosystems can affect the persistence and transmission of AR genes and AR plasmids. However, in the current systems, we can conclude that aerobic treatment conditions appear to be superior in reducing AR plasmid exchange, primarily due to increased rates of disappearance of hosts, probably through predation.

Acknowledgement

I would like to thank Andrew Zealand for transporting wastewater samples during the weekly sampling trip at Tudhoe Mill sewage treatment work. I thank Matthew Brown for the loan of submersible magnetic stirring plates, and Andrew Fuller for flow cytometry training. I am grateful to Susanne Pohl for facilitating in the molecular microbiology, and Adrian Blackburn for assisting in the protozoa counting and Marcos for coaching DNA sequences analysis. Many thanks to Nur Abdul Latif who helped out during the Phase 1 experiment when an extra pair of hand was needed during the sampling and processing of sponge cubes.

Chapter 6 Operating and optimising DDHS prototype as a small-scale domestic wastewater treatment technology, in Southern Malaysia

6.1 Introduction

DDHS is a relatively new technology, which is not yet commercialised, but shows promise as a method for wastewater treatment at smaller scales. Lab testing reported in Chapter 3 showed that domestic sewage can be effectively treated to practical levels for both organic pollutants and AR genes (ARGs) using DDHS systems, which are simple and operationally economical. Therefore, the technology may suit decentralised use in sub-urban and rural locations to treat community wastewater and mitigate AR spread, especially in low-to-middle income countries (LMICs).

Chapter 4 provided a more refined picture of DDHS sponge biofilm microbiomes, whereas Chapter 5 examined the fate of an AR plasmid (an MGE) in different redox environments. The next step in the DDHS development, therefore, is to test the technology at larger pilot scales, before potential commercialisation. Work in Chapter 6 arose from Impact Acceleration drivers at Newcastle University (Grant reference: BH171843), which supported a UK collaboration between Newcastle University and overseas counterparts in Southeast Asia.

In this study, a DDHS prototype designed for ten population equivalents (p.e.) was designed, built, and operated for 12 months to validate and semi-optimize the reactor performance in the field. The pilot DDHS was installed at a local sewage treatment in Johor Bahru, Southern Malaysia; an asset owned by the Malaysia water company (Indah Water Konsortium; IWK).

Trialling of the DDHS bioreactor aimed to operationalise the technology in a sub-urban setting to see whether laboratory data can be translated to the real world where less control to external variables existed. Malaysia was chosen as a model LMIC in Asia because of growing local urbanisation, which was ideal for testing the technology. Here, nations including Malaysia, China, Thailand, Cambodia, Indonesia,

etc. were listed within the 'water hotspots' region, where 1.9 billion people do not have access to effective sanitation (United Nations ESCAP, 2013). Johor Bahru is a rapidly developing city (i.e., second largest in Malaysia) with many sub-urban housing areas, which was suitable for testing this technology in smaller, clustered neighbourhoods. The objectives were as follows:

- a) To operate and optimise a pilot-scale DDHS bioreactor for treating community wastewater in peri-urban Johor Bahru, Malaysia.
- b) To assess and compare resistomes of two semi-optimised pilot DDHS configurations using high-throughput qPCR (HTH-qPCR), quantifying the influence of different redox exposures on AR gene and MGE removals.
- c) To evaluate the levels of pharmaceuticals and personal care products (PPCPs; emerging contaminants) in raw wastewater and DDHS effluents.

6.2 Materials and methods

6.2.1 DDHS prototype design

Sizing of the pilot reactor was based on the National Research Council (NRC) equation for trickling filters (also bearing in mind lab data) to determine the volume of the packing media required to meet the specified biochemical oxygen demand (BOD) performance. Whilst the NRC equation is not generally considered appropriate for wide-spread use and cannot be applied to plastic media filter systems (Logan *et al.*, 1987), it provides a suitable guide for sizing the sponge reactor as no model currently exists and the DDHS configuration has not yet been upscaled to provide information on performance beyond lab-scale.

The design BOD removal rates were drawn from the chemical oxygen demand (COD) removal rate data calculated from the laboratory-scale reactors at ambient temperatures (Chapter 3). It was assumed that the rate of removal of BOD would be equivalent to the rate of removal of COD within the aerobic section. It also was assumed that this correlation could be extrapolated through any size of reactor and any strength of wastewater. However, for the current project, whilst the strength of the influent wastewater at pilot scale was unknown, it assumed to be similar to the strength of influent used for the lab-scale reactors; i.e., primary settled, domestic wastewater.

The pilot DDHS bioreactor comprised of aerobic and anoxic treatment zones, constructed with stainless steel, which were columns separated for maintenance purposes. The two columns were coupled to one another by pipe with the anoxic tank placed below and downstream of the aerobic tank. The aerobic reactor was designed with openings (25 mm diameter) every 100 mm along the entire height of the reactor, on four sides, for maximal natural aeration while the anoxic reactor was completely sealed (watertight) to minimise oxygenation. To increase ventilation, the lid of the aerobic tank (5 mm thick steel plate) was perforated. Whereas, a rubber gasket was placed in between the flange and the lid of the anoxic tank, which were tightened with bolt and nuts to ensure it was airtight.

Inside of both reactors was comprised of basket receptacles and each receptacle was configured for stacking to form a receptacle column to allow the flow of wastewater downwards through the column. A simplified schematic of the pilot reactor is provided below (Figure 6-1) and details of reactor specifications are provided in Appendix D-1.

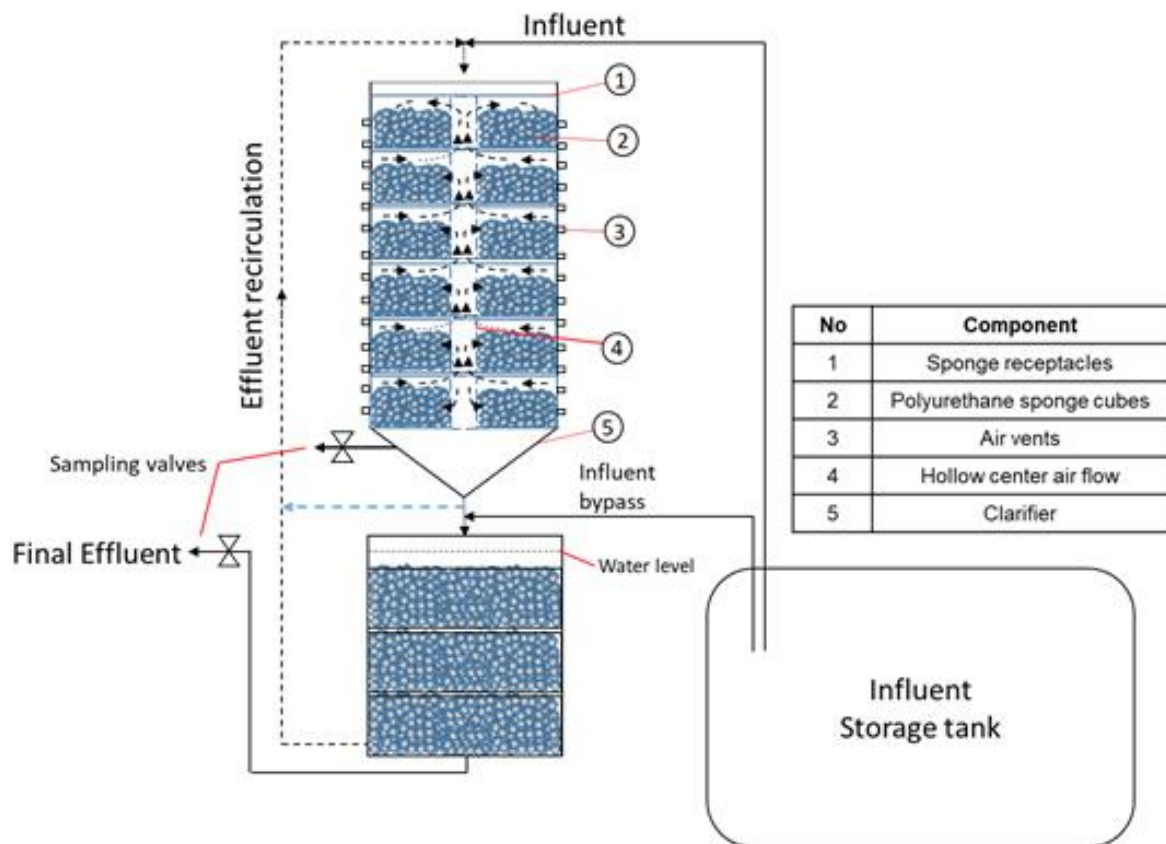


Figure 6-1 A schematic view of the pilot DDHS prototype showing configurations of treatment tanks with major components.

Flow rates to the aerobic zone were defined according to the average per capita water consumption in Malaysia; i.e., mean of 220 L/day (Malaysian Water Association, 2015). The influent flows do not take infiltration or storm flows into consideration since the flow will be controlled through the use of a storage tank and control pumps. The reactor system was equipped with 15 mm PVC pipes for water distribution at the top of the system and sampling ports were included along the reactor column: one at post-aerobic clarifier to sample for post-aerobic effluent and one at the final effluent discharge point.

6.2.2 Bioreactor installation

The pilot plant was located at a local sub-urban community near Johor Bahru in the Southern Malaysia (the Taman Selesa sewage treatment works; STW) (Figure 6-2). The site was selected based on its small population equivalent (with low and variable flows), easy access to power supply, and the space available for placing the pilot bioreactor. Taman Selesa serves a small village of approximately 1,500 people with no major industrial activities around the neighbourhood. The STW was design for treating domestic wastewater from the neighbourhood including stormwater.



Figure 6-2 Photographs of pilot plant installation at Taman Selesa STW, Johor Bahru. (A) DDHS apparatus were manufactured locally according to designed specifications; (B) designated space cleared and levelled for the installation of the pilot; and (C) onsite assembly of the pilot plant by the local contractor.

The pilot plant was housed under a shelter to protect the bioreactor and electrical components from weather, and was operated at ambient tropical climate with no temperature control on the reactor (Figure 6-3). The same packing media polyurethane (PU) sponges with specific porosity (Chapter 3) was used to fill the reactor core, which was comprised of mesh baskets to retain the sponges in place. The coarse sponges (i.e., 20 pres per inch; ppi) were packed in the aerobic core and fine sponges (i.e., 45 ppi) were used in the anoxic tank.

After inoculation with nitrifying activated sludge according to procedures described in (Bundy *et al.*, 2017), the reactor was allowed to flow at the lowest possible recirculation flowrate for overnight before being fed with domestic wastewater from the 1 m³ storage tank that was tapped from influent at the Taman Selesa STW. Continuous wastewater inflow, bypass, and effluent recirculation were controlled by pumps and valves to maintain desired flowrates (see operating regimes; Section 6.2.3).

6.2.3 Operating regimes

The pilot trial was conducted using four sequential operating regimes, performed after acclimatisation of each hydraulic regime. The aim was to assess treatment performance through different redox environments within the bioreactor and especially to test the impact of bypass on overall reactor performance. A submersible pump drew settled wastewater from the primary settling chamber of the Taman Selesa STW into a 1m³ storage tank, for use as influent wastewater feed to the pilot bioreactor. Centrifugal pumps (Potenza, Malaysia) with adequate capacity (maximum rate 11 L/min and head 2.1 m) for the designed hydraulics were used to pump the wastewater:

- i) to the top of the aerobic tank (as influent feed);
- ii) to the top of the anoxic tank (as bypass feed); and
- iii) to recirculate effluent to the top of aerobic tank.

PVC-U pipe with internal diameter of 15 mm was used throughout for the influent, recirculation, and effluent lines. Flexible hose with the same diameter connected influent pumps to the wastewater storage tank and throughout the DDHS system to reduce elbows and kinks that may compromise the flow.



Figure 6-3 Pilot plant set up at Taman Selesa, Johor Bahru. Reactor consisted separate aerobic and anoxic tank with hydraulic operations controlled by pumps and a control panel. Aerobic tank was raised and mounted on a platform supported by steel frame structure with the anoxic tank located at the bottom to create a gravity flow within the system.

Influent and bypass rates were applied according to Table 6-1 as designed for the four operating conditions, with a resulting hydraulic retention time (HRT) of 3.1 hours. The total influent flowrates as 0.80 L/min that equates to a population size of five p.e., according to the average daily water usage per capita in Malaysia (i.e., 220 L/day). It was not possible to increase the wastewater loading, which was originally sized to treat wastewater for up to ten p.e. because no locally available pump could cater to higher flowrates. The pilot organic loading rates (OLRs) ranged from 2.38 – 3.58 kg COD/m³-sponge/day, which were up to nine-fold higher than the lab-scale DDHS as previously tested in Chapter 3 (i.e., ~ 0.4 kg COD/m³-sponge/day).

For the bypass rate, 0.16 L/min was used to provide a bypass ratio of 20% as previously tested to be co-optimal for reducing TN and ARGs (Chapter 3). Final effluent left the DDHS under gravity and was returned to the existing STW process chain. The four operating conditions, designated as OP1, OP2, OP3 and OP4, were as follow:

Table 6-1 Testing of pilot reactor at four hydraulic operating conditions to assess the impact of bypass and recirculation regimes.

Flow regimes (L/min)	OP1	OP2	OP3	OP4
Total flowrate	0.80	0.80	0.80	0.80
Upper influent flowrate	0.80	0.64	0.80	0.64
By-pass flowrate	0.00	0.16	0.00	0.16
Percent bypass (%)	0	20	0	20
Recirculation regime ^a	Aerobic recirculation		Complete recirculation	
Recirculation fraction	Aerobic effluent		Final effluent	
Bypass recirculation ^b	-	NO	-	YES
OLR ^c aerobic sponges	2.43	2.26	2.03	2.00
OLR anoxic sponges	0.44	1.32	0.35	1.18
Total system OLR	2.87	3.58	2.38	3.18

Notes: ^a defines recirculation of liquid through specified redox compartment of DDHS core; ^b describes whether the bypassed wastewater at anoxic tank was recirculated; ^c organic loading rate defines as kg COD/m³-sponge/day and calculated as per COD loading and total working sponge volume in respective reactor cores.

Recirculation is crucial to improve water distribution and to facilitate wetting of the aerobic sponge media. Here, the impact of recirculation on the treatment of bypassed wastewater was assessed. Specifically, two recirculation regimes were configured to evaluate the effect of recirculation on the bypassed wastewater (i.e., not recirculated vs. recirculated through the sequential redox environment). This was done by switching the recirculation liquid between aerobic effluent (aerobic recirculation) and the final effluent (complete recirculation), which in tandem compared the impact of enhanced aerobic exposure of incoming wastewater at the top of the reactor. This scheme has not been assessed previously any sponge type bioreactor.

As redox environment could influence fate of TN, other pollutants, and organisms, we were interested in learning how increased aerobic exposure might alter the fate of

ARG and MGE in the inflow wastewater, especially when aerobic treatment had shown better AR bacteria removal (Chapter 5). Therefore, recirculation rates at 0.8 L/min and 0.64 L/min (i.e., 100% effluent recirculation from either aerobic or anoxic tank) were included. OP1 and OP3 did not use any bypass and were control conditions used to contrast the different recirculation regimes.

Further, a rotating distributor (also made from PVC-U pipe with internal diameter of 15 mm) was placed on the top of the aerobic tank to evenly distribute wastewater throughout a cross-sectional area of the aerobic reactor. The reactor was operated in continuous flow mode throughout the field trial, from July 2017 to July 2018. After which, the reactor was run under alternate conditions. Further monitoring is currently ongoing (but not included herein).

6.2.4 Sample collection and analysis

6.2.4.1 Routine sample collection and analysis

Liquid samples of influent and effluent were collected and analysed once per week to monitor reactor performance. Duplicate samples from each sampling point were collected in sterilised 0.5-L Schott bottles and transported on ice within three to four hours for analysis on the same day. A range of physico-chemical parameters were measured using a Hach test kits and a DR6000 spectrophotometer (Hach Lange, UK).

Total chemical oxygen demand (COD_{Total}) and soluble COD (COD_{Soluble}; filtered through 0.45- μ m filter) were measured in duplicate using Hach COD HR (range 20-1500 mg/L) calorimetric test kits digested with a DR200 laboratory heat block and the DR6000. Ammoniacal nitrogen and total nitrogen were quantified using the salicylate method (NH₃-N (HR); range 0.40 - 50.0 mg/L) and persulfate digestion (N (HR); 2-50 mg/L) methods, respectively. Samples were measured in sample cells for nitrite (NO₂-N; Ferrous sulphate method; range 2-250 mg/L) and nitrate (NO₃-N; Cadmium reduction method; range 0.3-30.0 mg/L). *In situ* pH, dissolved oxygen and temperature were determined using a portable field multimeter HQ40D (Hach, UK).

6.2.4.2 Genomic DNA sampling procedure

Following reactor monitoring over the four different operating regimes, semi-optimised configurations were achieved by operating the reactor with a 20%

wastewater bypass to the anoxic tank; i.e., OP2 and OP4, which effectively removed organic pollutants C and N that satisfied local discharge standards. Sampling campaigns were implemented for two of the operating configurations to collect samples for resistome analysis and for micropollutants. Sample collection for ARG, MGE, and antibiotic resistant bacteria (ARB; i.e., Extended Spectrum Beta Lactamase (ESBL)-producing isolates and meropenem resistant bacteria) quantification was undertaken during quasi-steady-state conditions (based on C and TN removal data) over three weekly sampling regimes. Liquid (aqueous) samples of raw wastewater, post-aerobic treatment effluent and the final effluent were collected in duplicate from the reactor during each sampling campaign using sterile 0.5-L Schott bottles and transported to laboratory on ice in coolers.

Altogether, 18 samples were collected for AR-related analyses per operating condition ($n = 6$ per sampling week), which consisted of raw influent, post-aerobic effluent, and final effluent in duplicates. In parallel, another set of aqueous samples were also collected in duplicates in 0.5-L sterile Schott bottles wrapped with aluminium foil to shield samples from light, for pharmaceutical and personal care products (PPCPs) analysis described later (Section 6.2.4.6).

In addition, to assess the resistome of biofilms along the sequential redox treatment line, sub-samples of biofilms also were collected from sponges during the two sampling campaigns, on the final sampling week. Sponge cubes were sampled at selected locations from the reactor column along sponge depths that included the sequential redox environment.

Prior to sampling sponges, the reactor was stopped and liquid in the anoxic tank was drained at minimum flowrate to a temporary storage container to allow the sponge media to drip dry for two hours. Sponges then were randomly selected from the first (i.e., Top biofilm) and the fourth (i.e. Middle biofilm) sponge baskets in the aerobic section, and from the second level sponge baskets in the anoxic column (i.e., Bottom biofilm). From each location, a total of ten sponge cubes were collected from around the sponge receptacles by evenly distributing the sampling spots to include all sides, the centre, and the depth of each receptacle, all in triplicate ($n = 10$ per replicate). Sponges were kept in sterile containers and transported to lab on ice.

After sampling, the anoxic tank was immediately refilled and reactor operation recommenced to minimise interruption of the system.

6.2.4.3 Extraction of genomic DNA from aqueous and sponge biofilm samples

Aqueous samples. After sampling, liquid samples were processed on the same day by filtering through sterile 0.22- μ m membrane disc filters (Millipore, Billerica, MA, USA) and samples were kept on ice pending filtration to ensure minimum biological activities. After filtering appropriate volumes of samples to allow concentration cell biomass, total genomic DNA was extracted from the membrane discs using the Fast DNA Spin Kit for Soils (MP Biomedicals, USA) according to the manufacturer's instructions and stored in 4 °C prior to subsequent analysis.

Biofilm samples. Sponges were soaked in sterile saline solution (1 x PBS) for two hours at 4 °C and squeezed to elute biofilms from each sponge cubes. Biomass eluted from the ten sponge cubes per replicate were pooled together and centrifuged at 12000 rpm for 30 minutes (supplier, UK). The biomass pellet was recovered for genomic DNA extraction using the Fast DNA Spin Kit for Soils (MP Biomedicals, USA), according to the manufacturer's instructions and stored in 4 °C prior to subsequent analysis.

DNA quality and quantity. Following extraction, the quality of DNA samples and DNA concentrations were determined using a Denovix DS-11 Spectrophotometer (Denovix, UK) and DNA concentrations were quantified by using a Qubit 2.0 Fluorometer (Invitrogen, UK). All genomic DNA was stored at -20 °C prior to subsequent analysis.

6.2.4.4 Antibiotic resistant bacteria (ARB) enumeration

In parallel, aqueous samples that were collected during the two sampling campaigns were screened for total coliforms using the Hicrome coliform agar (Sigma Aldrich, UK). Extended Spectrum Beta Lactamase (ESBL)-producing and meropenem resistant coliforms, using selective media made by Hicrome coliform agar supplemented with ESBL ChromoSelect supplement (Sigma Aldrich, UK), meropenem amended media at 2 μ g/mL also were performed. All antibiotic supplements were filter-sterilised before addition after the media cooled to below 55 °C from autoclaving at 121 °C. A volume of 100- μ L of serially diluted samples (in

sterile PBS) were evenly spread on the three sets of agar plates in triplicate. All plates were incubated at 37 °C for 24 hours. Dilution containing colonies within the range of 30-100 cells were counted to determine respective ARB concentrations.

6.2.4.5 High-throughput quantitative Polymerase Chain Reaction (HTH-qPCR)

To quantify the abundance and diversity of ARGs and MGEs in the bioreactor samples, high-throughput quantitative PCR (HTH-qPCR) of targeted genes was performed using the method developed by Su and colleagues (Su *et al.*, 2015) as described in Chapter 3 (Section 3.2.5). Same as previous, an array of 296 validated primer sets (Zhu *et al.*, 2013) was used to screen for ARGs and MGEs (Table A3), with additional integron-associated target genes as follow:

- i) 283 ARGs, representing potential resistance to nine major classes of antibiotics,
- ii) eight transposase genes,
- iii) four integron genes (i.e., universal class I integron-integrase gene, *intl1*; the clinical class 1 integron-integrase gene, *cintl1*; class II integron-integrase gene, *intl2*; and class III integron-integrase gene, *intl3*); and
- iv) one eubacterial 16S rRNA gene.

Each sample was tested with three technical replicates on the array. HTH-qPCR cycling conditions were according to the procedure in Ouyang *et al.* (2015).

Corroborating 16S rRNA quantification targeting universal eubacteria for the same samples was performed using conventional qPCR on a separate platform using a Roche LightCycler 480 system (Roche Inc., USA). Standard curves and the same 16S rRNA primer sequences were used to quantify 16S gene copies for sample normalisation (Looft *et al.*, 2012; Ouyang *et al.*, 2015).

6.2.4.6 Quantifying antimicrobial agents and other personal care products (PPCPs)

Beyond resistome and microbiology analysis, bioreactor samples were also analysed for micropollutants levels in the influent and treated effluents using solid phase extraction (SPE) coupled with ultrahigh performance liquid chromatography-tandem mass spectrometry (UHPLC-MS/MS) method developed by Tran *et al.* (2016a). This

allowed evaluation of the fate of different PPCPs compounds through DDHS treatment and provide first insights of reactor performance for potential PPCPs removal.

Sample pre-treatment. The 0.5-L of aqueous samples in aluminium-foiled bottles were processed immediately upon arrival in the laboratory by filtering through 1.2- μm glass fiber filters (GF/C, Whatman, UK), followed by 0.45- μm membrane filters (PALL, corporation, US) and adjusted to a pH of between 2.5 and 3.0. Subsequently, acidified filtrate samples were spiked with a constant amount of tetra-sodium EDTA (Na_4EDTA ; 100 mg/mL) and isotope labelled internal/surrogate standards (ILISs; 100-ng). Samples then were stored in the dark at 4 °C until subsequent SPE on the next day (no later than 24 h after the collection to minimise degradation/hydrolysis of target analytes).

Solid phase extraction. Previously developed and optimised SPE protocols were used (Tran *et al.*, 2016a; Tran *et al.*, 2016b) to extract PPCP compounds present in samples. Briefly, SPE cartridges Chromabond HR-X (500-mg, 6-mL) suitable for environmental samples were preconditioned with 5 mL methanol, followed by 5 mL of acidified Milli-Q water (pH 3.0) at a flow rate of 3 mL/min. Subsequently, pre-treated raw wastewater (100-mL) and effluent samples from the post-aerobic step and the final points (250-mL each) were loaded onto the cartridges at a flow rate of 5 mL/min. After all water samples were passed through SPE cartridges, the cartridges were rinsed with 5-mL of acidified Milli-Q water (pH 3.0) to remove weakly bound impurities and Na_4EDTA . SPE cartridges containing PPCPs were stored in the dark in -20 °C until shipping for subsequent UHPLC-MS/MS analysis of the elution at the Department of Civil and Environmental Engineering, National University of Singapore.

6.2.5 Data analysis

6.2.5.1 HTH-qPCR genomic data processing

All data were analysed using R statistical software 3.5.0 (R Core Team, 2013) following normality checks. HTH-qPCR genomic data was initially cleaned to exclude potential false positive amplifications and genes under detection limits as previously described (Ouyang *et al.*, 2015). The cleaned dataset then was processed in the R environment where the relative copy number of ARGs, transposase genes, and

integrase genes were calculated and transformed to absolute copy numbers by normalizing to 16S rRNA gene copy numbers for each sample. Amplifications with at least two positive reactions from the three replicates defined “detection” and used for subsequent analysis.

6.2.5.2 Reactor performance

One-way analysis of variance (ANOVA) sample tests followed by multiple pairwise comparisons using post-hoc Tukey test were performed to compare the differences in reactor performance for:

- i) nutrient removals (C and N),
- ii) AR-related analysis for ARGs and MGEs abundances from HTH-qPCR data, and ARB;
- iii) PPCPs levels between contrasting operating conditions.

When data distributions were not normal, the Kruskal-Wallis and Games-Howell post-hoc tests were used as non-parametric alternatives to the ANOVA and Tukey test, respectively. Unless otherwise noted, differences between data groups with p-values less than or equal to 0.05 were defined as significant.

6.3 Results and Discussion

6.3.1 Acclimatisation of the pilot DDHS system and operational challenges

The initial reactor start-up faced with several operational challenges. Problems primarily related to hydraulic complications caused by the poor wastewater settling prior to entering the DDHS system. Raw wastewater drawn from the primary settling chamber at Taman Selesa STW was high in solids due to its shallow chamber depth and resuspension of solids during the periodical filling of wastewater in the chamber. Coarse solids and debris from the waste stream caused regular blockages in the submersible pump used for drawing wastewater from the settling chamber, pipes, and the distributor of the pilot plant. These issues resulted in poor biofilm formation due to episodic interruptions to influent feeding and therefore slow acclimatisation.

To resolve these issues, a solid screener (Figure 6-4) which had 6 mm apertures was constructed with help from Mr. Nathan at RKT Corporation (M) Sdn. Bhd. The

stainless steel filter was designed to house the submersible pump that was placed inside the STW settling chamber to filter bulky items during wastewater intake. Further, an additional storage tank was retrofitted upstream of the influent holding tank to act as a preliminary clarifier to remove coarse solids such as sand and gravels from storm water runoff. This is crucial to prevent damage of fixtures and the equipment in the pilot plant treatment line. The additional pre-settling tank was included in the system by placement on an adjustable stainless steel base to allow the flow of settled wastewater to the subsequent influent storage tank under gravity.



Figure 6-4 Retrofits to improve system operation in the field. (A) A stainless steel filter; and (B) additional clarifier installed upstream of the influent storage tank at Taman Selesa STW which were designed to prevent clogging of the hydraulic system of the pilot DDHS.

6.3.2 Operational performance: Wastewater bypass versus recirculation regimes

After the system modifications, solids removal improved in the pilot system and the DDHS system regained acclimatisation and began to stabilise. For example, C (soluble COD) and N (ammonia) removals were $58 \pm 8.9\%$ and $70 \pm 9.0\%$, respectively, as defined by percentage load removal (Equation 6-1) during pseudo-steady state operating conditions.

Equation 6-1 The equation used to determine percentage of load removal rate based on pollutants loading onto sponge media.

$$\text{Percentage load removal (\%)} = \frac{\text{Influent pollutants load} - \text{Effluent pollutants load}}{\text{Influent pollutants load}} \times 100$$

Where:

Load is equal to pollutants loading per sponge volume (kg/m³-sponge/day).

Overall, C and N levels in wastewater were reduced in treated effluents in all four regimes, all satisfying Malaysian Environmental Quality (Sewage) Regulations 2009 (Department of Environment Malaysia, 1979) for new sewage treatment systems (Table D-1; Appendix D). Summaries of reactor effluent quality for the monitored parameters and corresponding percentage load removal are provided in Table D-2 (Appendix D). Although the current Malaysian discharge standard do not include guidelines for TN, they use ammonia, nitrite and nitrate to monitor majority of N-species. Specifically, nitrate reductions were enhanced during OP2 and OP4 when wastewater bypass was implemented (from average 17% without bypass to average 43%), which matched removal rates in the lab-scale DDHS bioreactors.

Reactor performance relative to the loading shows different removals among the four conditions operated with different hydraulic schemes (Figure 6-5). COD_{Total}, NH₃-N and NO₂-N removal were similar among operating conditions (ANOVA; p-values > 0.05), which suggest these parameters were not impacted by both recirculation and bypass regimes. This is likely because particulate fraction in COD_{Total} was removed by filtration through the sponge media and NO₂-N usually remains low within biological treatment as it is an unstable intermediate product of the nitrification and denitrification treatment steps, i.e., easily converted to other forms of nitrogen (Metcalf & Eddy, 2003). It also suggests that nitrification was not restricted by how liquid is recirculated within the system and the bypass ratio did not significantly affect the effluent ammonia levels. Importantly, this also affirmed the sizing of the aerobic tank was adequate (i.e. long enough) for nitrifying bacteria's habitation at the lower section (Chapter 4; Section 4.4.2).

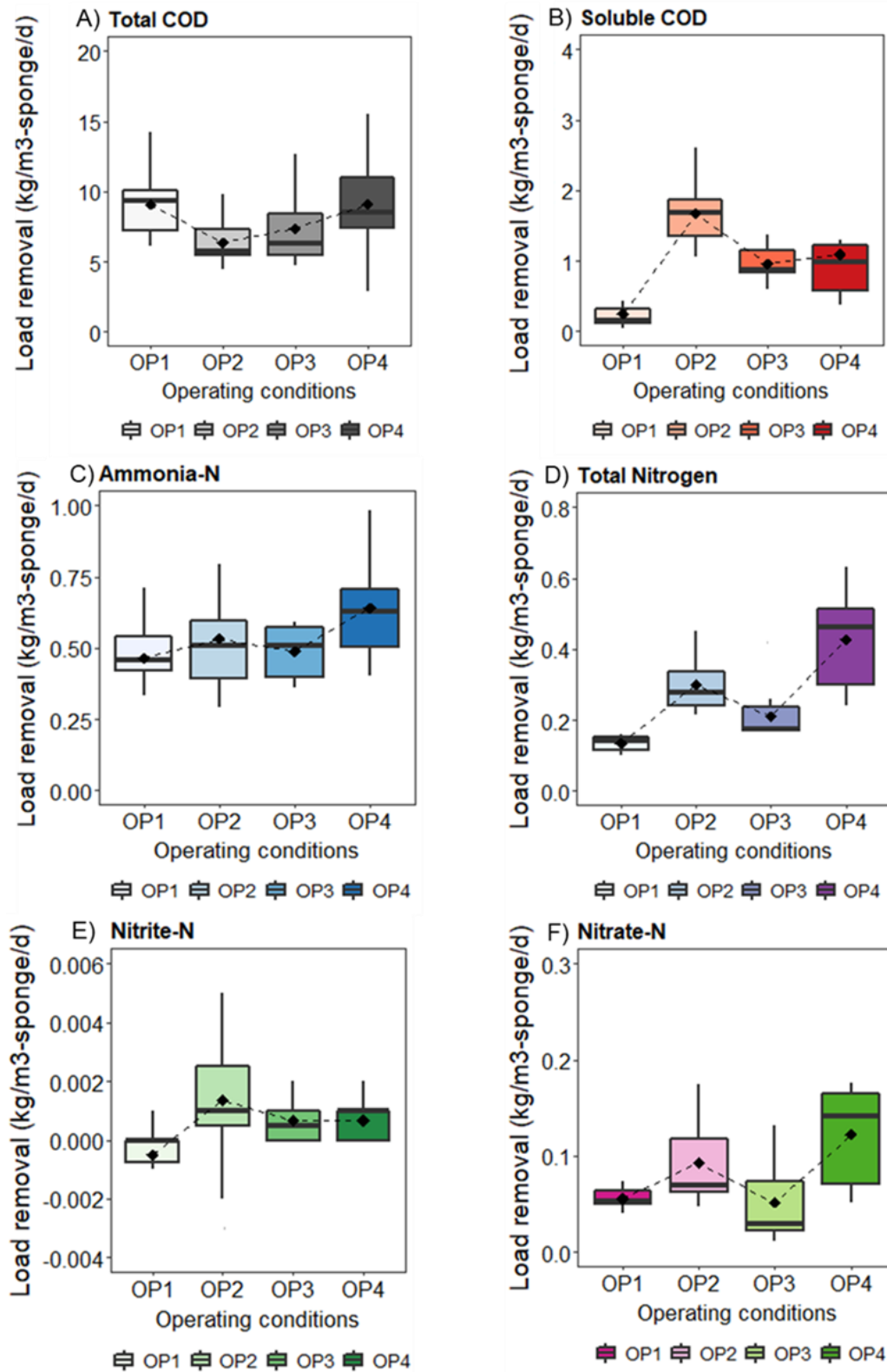


Figure 6-5 Comparisons of pollutants load removals (kg pollutants/m³-sponge/day) through four operating conditions OP1-OP4 using the pilot DDHS. Boxplot ($n = 11$ per operation, except for $n = 8$ for OP3) showing ranges of load removals for (A-B) carbon and (C-F) nitrogen pollutants, with the points inside boxes representing means of removal rates per operation.

Significant differences were seen in $\text{COD}_{\text{Soluble}}$, $\text{NO}_3\text{-N}$ and TN removal rates among the operating conditions (ANOVA; all p-values < 0.05). Subsequent multiple pairwise comparisons confirmed that a 20% bypass significantly enhanced $\text{NO}_3\text{-N}$ and TN removal from the wastewater, which occurred hand in hand. TN load removals were between 0.10 and 0.20 kg TN/m³-sponge/day during OP1 and OP2 (Control operations with no bypass) and displayed a discernible improvement to 0.30 and 0.40 kg TN/m³-sponge/day when bypass was applied during OP2 and OP4 (Tukey's comparisons; OP1 vs. OP2 and OP3 vs. OP4; both p-values < 0.05), respectively. Recirculating from the final effluent further improved TN removal from wastewater, which could be due to some removal by denitrifying heterotrophic bacteria co-presence in the biofilm anoxic zone in the aerobic tank, contributing to higher net TN removal (Tukey's comparisons; OP2 vs. OP4; p-values = 0.01).

It is important to note that DO levels in the final effluents were between 1.50 and 1.90 mg/L (± 0.5), which exceeded ideal DO levels for denitrification of $\text{NO}_3\text{-N}$; i.e., 0.5 to 1.0 mg/L (Tan *et al.*, 2013; Zhao *et al.*, 2017), and this could hamper denitrification that requires anoxia. It is possible that the aerobic filtrate from the preceding aerobic tank was still high in DO upon entering the anoxic tank, which implies a longer buffering zone is needed to adequately lower the DO to allow the reduction of $\text{NO}_3\text{-N}$ to dinitrogen (N_2). As the pilot prototype was sized according to the demand for BOD removal, the sizing of the anoxic tank did not consider the DO buffering zone. Therefore, only a semi-optimised configuration was achieved during this pilot test.

$\text{COD}_{\text{Soluble}}$ removals were slightly higher when bypass was implemented in OP2 and OP4, most likely due to a greater net C consumption when denitrification took place (1.4 to 1.7 kg COD/m³-sponge/day), with no difference detected between contrasting recirculation regimes (Tukey's comparisons; OP2 vs. OP4; p-value=0.24). OP1 had noticeably lower $\text{COD}_{\text{Soluble}}$ and TN removal rates. One possible reason could be due to the release of C and N from previously accumulated solids before the installation of the new solids screen components. Specifically, accumulated solids on the top sponges consists of organic solids, which hydrolysed; adding C and N to the top sponge and may have offset the overall removal efficiencies.

Overall, OP2 and OP4 (with bypass regimes) performed better and all parameters met the local discharge standard (Appendix D; Table D-1). This is encouraging and shows that DDHS reactors are a truly conceivable small-scale treatment technology.

6.3.3 Richness and relative abundance of ARGs and MGEs in wastewater and DDHS effluents

It is important to evaluate the resistome profile of DDHS operations, especially for using the technology to control AR levels in wastewater. Figure 6-6 shows the total abundance and diversity of ARGs and MGEs quantified for both semi-optimised configurations to contrast the impact of redox conditions and recirculation regimes. A total of 105 and 113 unique ARGs and nine MGEs were detected in the raw wastewater used in OP and OP4, respectively (Figure D-1).

Detected ARGs and MGEs in the domestic wastewater from the Taman Selesa community consisted of resistance to nine antibiotic classes, ranging from $3.6 - 4.3 \times 10^8$ gene copies per mL (GC/mL), with highest abundance in ARGs conferring resistance to aminoglycoside (23 -26%), followed by multidrug (20 – 28%), beta-lactams (11 – 15%), and tetracycline (10 – 25%). All eight targeted transposase genes were found at high levels (1.0×10^8 GC/mL; $SD \pm 4.0 \times 10^7$) together with elevated Class 1 integron-integrase genes, *int1* (1.0×10^8 GC/mL; $SD \pm 3.0 \times 10^7$).

Both operating conditions were able to remove ARG and MGE levels in raw influent, which varied across the redox steps (Figure 6-6A). Significantly lower levels were achieved in the OP2 effluents (Kruskal-Wallis; p-value = 0.02) and OP4 effluents (Kruskal-Wallis; p-value = 0.001), although greater removals were achieved in the OP4 configuration. Total ARG abundances were reduced by about 0.8 log after the aerobic treatment step and were further reduced through the reactor anoxic zone to the final effluent.

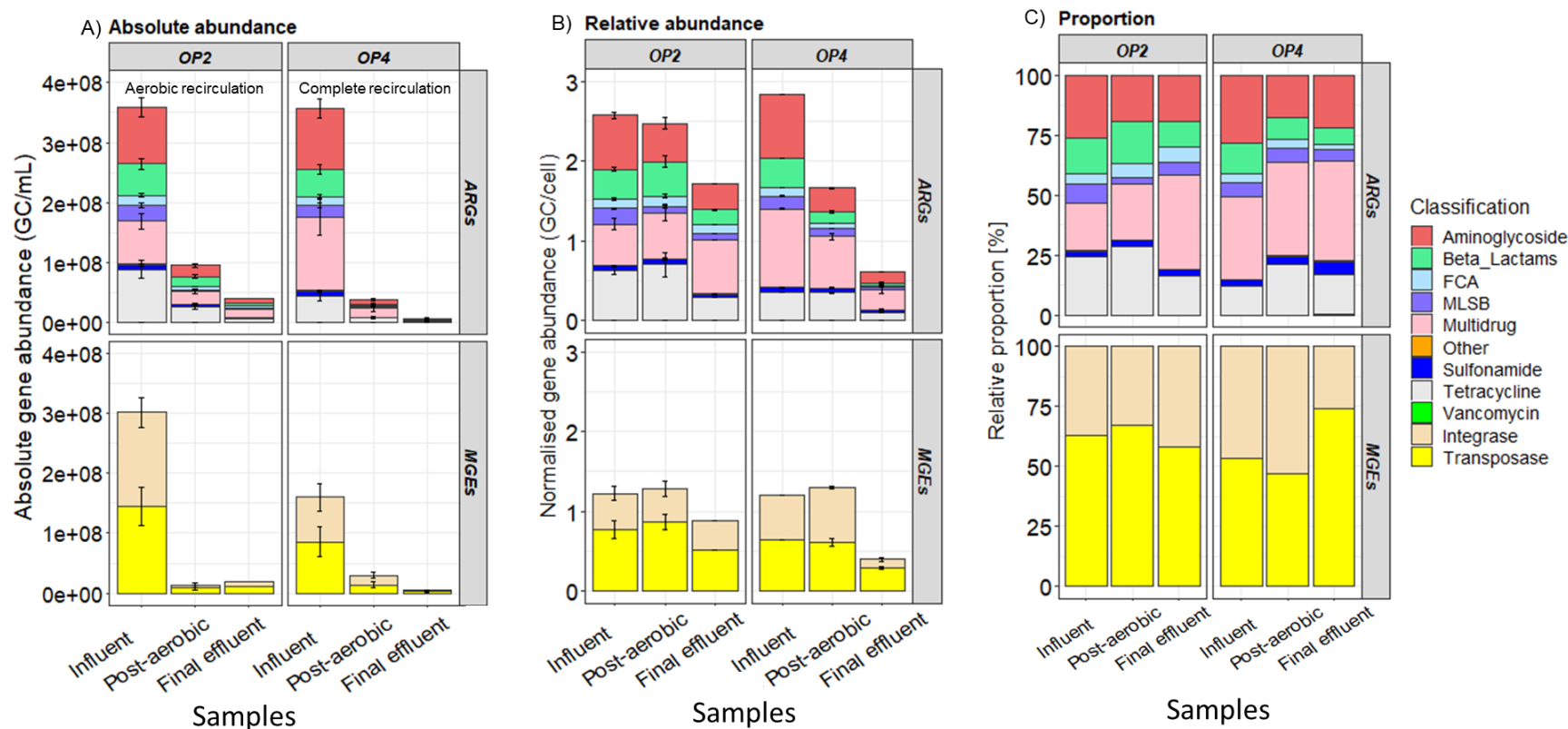


Figure 6-6 Comparisons between OP2 (20% bypass; aerobic recirculation) and OP4 (20% bypass; complete recirculation) over three independent sampling weeks showing (A) absolute gene copies per mL (GC/mL); (B) relative abundance normalised per bacterial genome (GC/cell); and (C) relative percentages of ARG and MGE abundances across samples. Abundance of ARGs and MGEs detected in the raw wastewater and DDHS reactor effluent samples conferring resistance to specific class of antibiotics, including, for ARGs, aminoglycosides, β -lactams, FCA (fluoroquinolone, quinolone, florfenicol, chloramphenicol and amphenicol resistance genes), MLSB (macrolide-lincosamide-streptogramin B), other/efflux (multidrug-efflux pumps or others), sulphonamides; tetracyclines; and vancomycin. Error bars show standard deviation ($n = 6$ per sample per operating regime).

Residual ARGs and MGEs levels ranged from 1.2×10^7 to 6.0×10^7 gene copies per mL (GC/mL), with a 1.0 log net removal achieved in OP2 (Tukey's comparisons; p-value = 0.02) and 1.7 log net removal in OP4 (Tukey's comparisons; p-value = 0.01), which were comparable to laboratory results (Chapter 3; Section 3.3.2).

Aerobic treatment significantly reduced concentrations of ARGs in both operations (Tukey's comparisons; both p-values < 0.05). However, levels of some ARG subtypes were higher during aerobic recirculation (i.e., OP2), namely ARGs conferring resistance to tetracycline, aminoglycoside and β -lactams (Table D-3; Appendix D). These genes were removed more when complete recirculation was implemented during OP4, which suggests they were removed more effectively by sequentially exposing the wastes to aerobic then anoxic conditions. Whilst, they may be selected under the aerobic condition in DDHS core.

This observation is supported by relative abundance data (Figure 6-6B). Higher subtotals of these ARG subtypes were found per bacterial genome, ranging 1.61 ± 0.49 ARGs/cell in the post-aerobic effluent of OP2 as compared to 0.78 ± 0.49 ARGs/cell in OP4. Particularly, ARGs related to β -lactams, tetracycline and multiple drugs (MDR) showed an increase after increased aerobic exposure in OP2 (Table D-4; Appendix D). Greater reductions were seen in OP4. From an average of 2.70 ± 0.12 ARGs/cell in the influent, relative abundance was reduced to 0.61 ± 0.10 ARGs/cell via OP4 versus 1.72 ± 0.04 ARGs/cell ARGs via OP2. This implies bacteria leaving OP2 operations have approximately three-fold more ARGs per genome than those treated in OP4. Further, higher proportion of MDR strains were detected in the final effluent of OP2 (Figure 6-6B), which represents the greatest preponderance in the final effluents (Figure 6-6C).

Here, the level of multidrug resistance type (MDR) was reduced more effectively in OP4 as the relative abundance in raw influent at 0.98 ± 0.01 ARGs/cell was reduced to 0.65 ± 0.07 ARGs/cell and 0.25 ± 0.10 ARGs/cell post-aerobic treatment and final treatment, respectively. Whereas, the relative abundance of MDR ARGs was comparable ($\sim 0.58 \pm 0.07$ ARGs/cell) with the separate redox treatment regime in OP2. This suggests that MDR ARGs are not readily remove by any single redox treatment, but it is more possible through sequential redox exposures, as seen in OP4.

Changes in the levels of integrase and transposase genes were less apparent, with no significant changes detected for both absolute and relative abundance in the final effluents. However, the level of one specific transposase, namely Tn25, was enriched by three-fold after the repeated aerobic exposure in OP2, from 0.15 ± 0.04 GC/cell to 0.45 ± 0.09 GC/cell (see also biofilm core resistome). This may be related to the bacterial SOS responses under 'extreme' aerobic conditions and-or more direct impacts of possible nutrient limitation in the aerobic biofilms (Poole, 2012). It has been shown that carbon starvation stringently stressed bacteria and cued cellular SOS responses can enhance the mobility of transposons (Ilves *et al.*, 2001; Aminov, 2011). When aerobic effluent was recirculated during OP2, the liquid phase passing the aerobic biofilms was diluted by the aerobically treated effluent (i.e., low in C concentration), while influent nutrients were taken up by indigenous biofilm colonised by rapid-growing microbes (Chapter 4; Section 4.3.3). Furthermore, this result also resembled the laboratory results, which showed increased MDR genotypes during the aerobic treatment stage (Chapter 3; Section 3.3.4).

As hypothesised, sequential redox exposure conditions provide effective removals; it is evident that without recirculating the bypassed portion, the ARBs present in the raw influent 'escaped' the aerobic treatment and 'released' via the final discharge. In summary, absolute concentrations for five classes of ARG were reduced through OP4 versus only three in OP2 (Table D-3).

6.3.4 Bacterial and ARBs removals

It is believed that ARG removals during DDHS treatment is due to bacterial removal because ARG removals parallel observed total bacterial removals. Estimated bacterial cell numbers in final treated effluents from both operations showed 0.7 to 1.0 log reductions relative to influent levels (Figure 6-7A), with higher bacterial removals observed in OP4. However, no significant differences were detected between the two effluents (Kruskal-Wallis; p-value = 0.08), which means the bypass level at 20% did not significantly alter the bacterial levels in the system. This is consistent with the previous microbiome data (Chapter 4), which showed the quantified fecal levels in bioreactors (i.e., 0% vs. 20% bypass regime) were relatively lower than in indigenous biofilm microbiota, hence the impact on the DDHS ecosystem was not profound.

Particularly, samples were screened for ESBL-producing and meropenem resistant Enterobacteriaceae (Figure 6-7B). These were chosen because 22% of the Southeast Asia population have fecal colonization with ESBL-producing Enterobacteriaceae (Karanika *et al.*, 2016), therefore was expected to detect higher prevalence of these bacteria in community wastewater here. Further, work in Chapter 3 detected higher concentrations of ESBL-isolates in reactor effluent treated with bypass. Comparing the two operating conditions could show how redox exposure impacts their removal. Statistics again show no difference in total coliforms, ESBL- and meropenem resistant bacteria between the two operations (Kruskal-Wallis; p-value = 0.96).

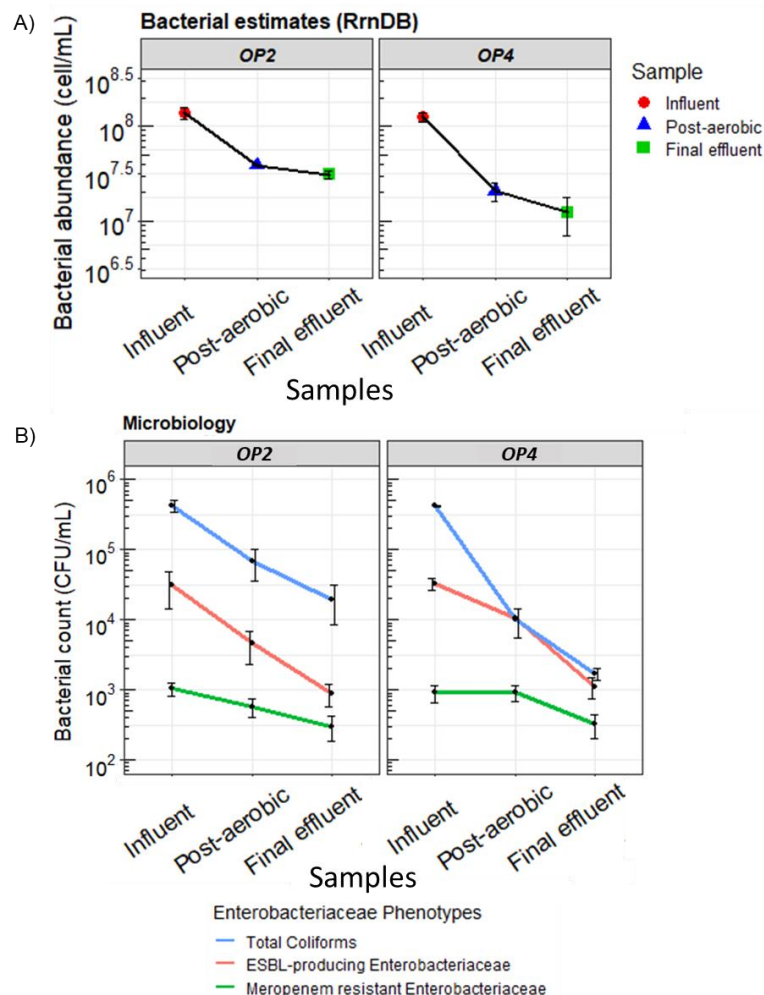


Figure 6-7 Bacterial levels quantified at redox treatment steps during OP2 and OP4, with (A) bacterial cell number estimated from quantified total 16S concentrations of individual sample using the average 16S rRNA-encoding genes per bacteria genome (4.1 copies per genome; RrnDB database); (B) count of enterobacteriaceae colonies cultured on Hicrome coliform media with and without antibiotic supplements ($n = 6$). Error bars show standard deviation around the mean.

Microbiological data imply that bacteria levels introduced via bypass to the anoxic step were within the bypass threshold (previously suggested at 20%), therefore did not negatively impact the overall treatment outcome. Based on this, it is believed that bacteria and ARB removal in the DDHS system was achieved through a series of abiotic and biotic mechanisms. For example, they were first filtered by the sponge media, and then were either outcompeted by native biofilm bacteria (die-off) and/or removed by predation, which previous evidence has indicated may be a genuine ecological removal mechanism in this type of technology. However, further study is required to verify these theories.

6.3.5 *Unique removal patterns and persistent genes*

The influent source consisted an array of 105 to 113 ARGs (measured during OP2 and OP4, respectively), together with nine MGEs comprising eight transposase and one universal class 1 integron-integrase gene, *int1*. Broader observations can be made by overlaying the overall detected ARGs and MGEs among samples. Venn diagram analyses confirmed greater ARGs and MGEs removal via OP4 configuration, with 23 genes removed from the influent to below detected limit versus 15 genes removed via OP2 (Figure 6-8).

Aerobic recirculation indeed enhanced ARGs removal as anticipated, with only four unique genes detected in post-aerobic effluents of OP2. However, more unique genes ($n = 16$) were detected in the final effluent, which suggest the bypassed genes may have 'avoided' the aerobic exposure. When a complete recirculation was applied in OP4, less unique genes were measured in the effluent ($n = 7$), which further hint sequential redox exposure is important for overall gene removal. Further, higher number of genes ($n = 12$) was detected in the post-aerobic effluent here, which confirmed aerobic treatment is effective at reducing ARG and MGEs subtypes.

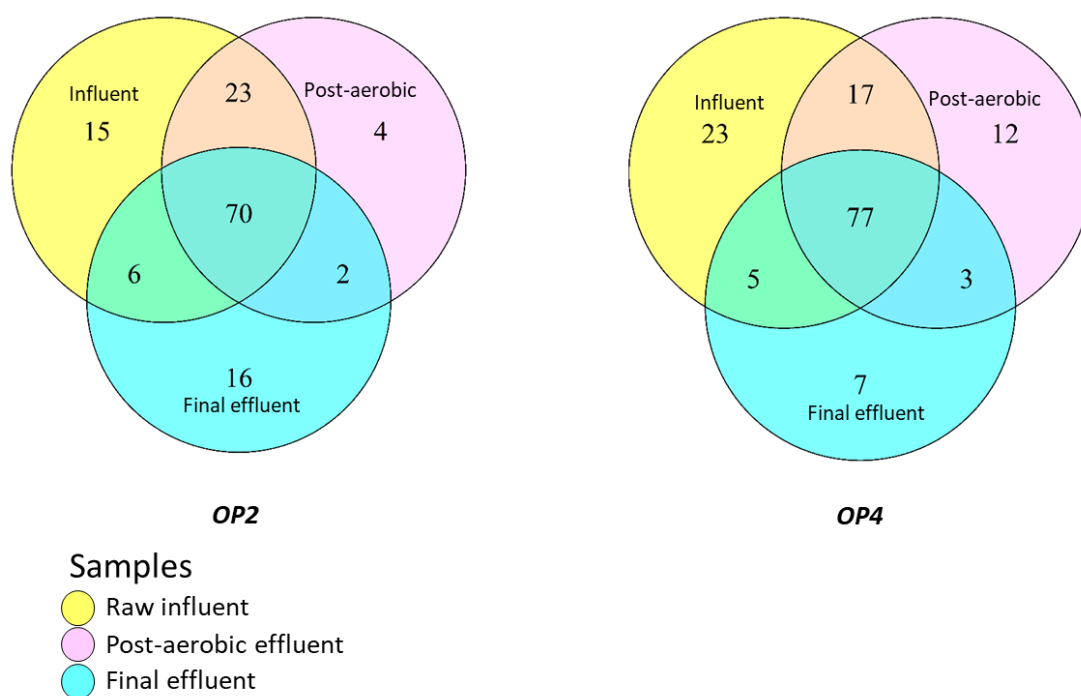


Figure 6-8 Venn diagram showing distribution of detected ARGs and MGEs among influent, post-aerobic effluent and final effluent samples from contrasting operating DDHS configurations, OP2 and OP4. Subsets represent number of unique genes detected in aqueous samples with the central overlap represents the number of persistent ARGs.

Finally, approximately 62% of the detected genes ($n = 70$ and 77) were persistent and not removed by any DDHS configuration. Almost all detected MGEs, except for transposase Tn22, perpetuated in samples. ESBL- (e.g., *bla*_{CTX-M}, *bla*_{SHV}, and *bla*_{TEM}) producing and tetracycline resistance subtypes, including *tetQ*, *tetM*, and *tetR*, were persistent throughout the treatment system. Despite all these, it is important to note that absolute concentrations of these genes were significantly reduced in the final effluent, especially in OP4 (See previous Section 4.2.3). The overall results suggest that some ARGs are persistent, not readily removed biologically (Munir *et al.*, 2011; Zhang *et al.*, 2016), and operating factors such as treatment HRT and OLR affect the degradation of some ARGs during biological treatment (Kim *et al.*, 2007).

6.3.6 DDHS core resistome: Diversity and abundance in biofilms

Total ARGs detected in biofilms samples were 1.6×10^7 GC/mg ($SD \pm 5.7 \times 10^6$), whereas total MGEs levels detected were 1.1×10^7 GC/mg ($SD \pm 8.3 \times 10^6$) (Table D-5). The absolute gene abundances between the two operating configurations were similar (Kruskal-Wallis; p -value = 0.99), with limited differences seen in apparent levels of ARGs and MGEs, regardless of operating regime, which is a clue for a

stable resistome within the sponge biofilm, i.e., the core resistome (Quintela-Baluja *et al.*, 2019). Although, a small variation in richness and relative abundances is seen across bioreactor biofilms, as defined by depths. Figure 6-9A show relative abundances of ARGs and MGEs normalised to the bacterial genome.

The top sponge biofilms (from the first sponge receptacle) reflected the effect of recirculating bypassed wastewater, whereby OP4 top biofilms contained higher abundances of ARGs (1.1×10^7 GC/mg; 1.2 GC/cell). A distinct pattern emerged in OP4 where relative abundance and diversity of ARGs and MGEs reduced with reactor depth in OP4. In OP2, although less ARGs and MGEs were introduced to the top biofilms, their apparent levels increased in the middle and bottom biofilms. Specifically, transposase gene Tn25 was greater in the Middle biofilm (0.13 ± 0.002 GC/cell) compared with the Bottom biofilm (0.97 ± 0.18 GC/cell) under the aerobic recirculation. This was concurrent with elevated relative abundances of MDR and sulphonamide subtypes.

Although changes were not statistically significant among biofilm sites and operating regimes (Kruskal-Wallis; $p > 0.05$), variation between operations are seen in ARG diversity (Figure 6-9B-C). It was found that apparent ARGs diversity increased with sponge depth during OP2 as reactor depth increases, whereas the total number of ARGs increased from 57 ± 4 (Top biofilm) to 74 ± 6 (Bottom biofilm). Whereas, total number of ARGs reduced from 82 ± 4 (Top biofilms) to 66 ± 7 (Bottom biofilms) in OP4, showing less diversity as reactor depth increases.

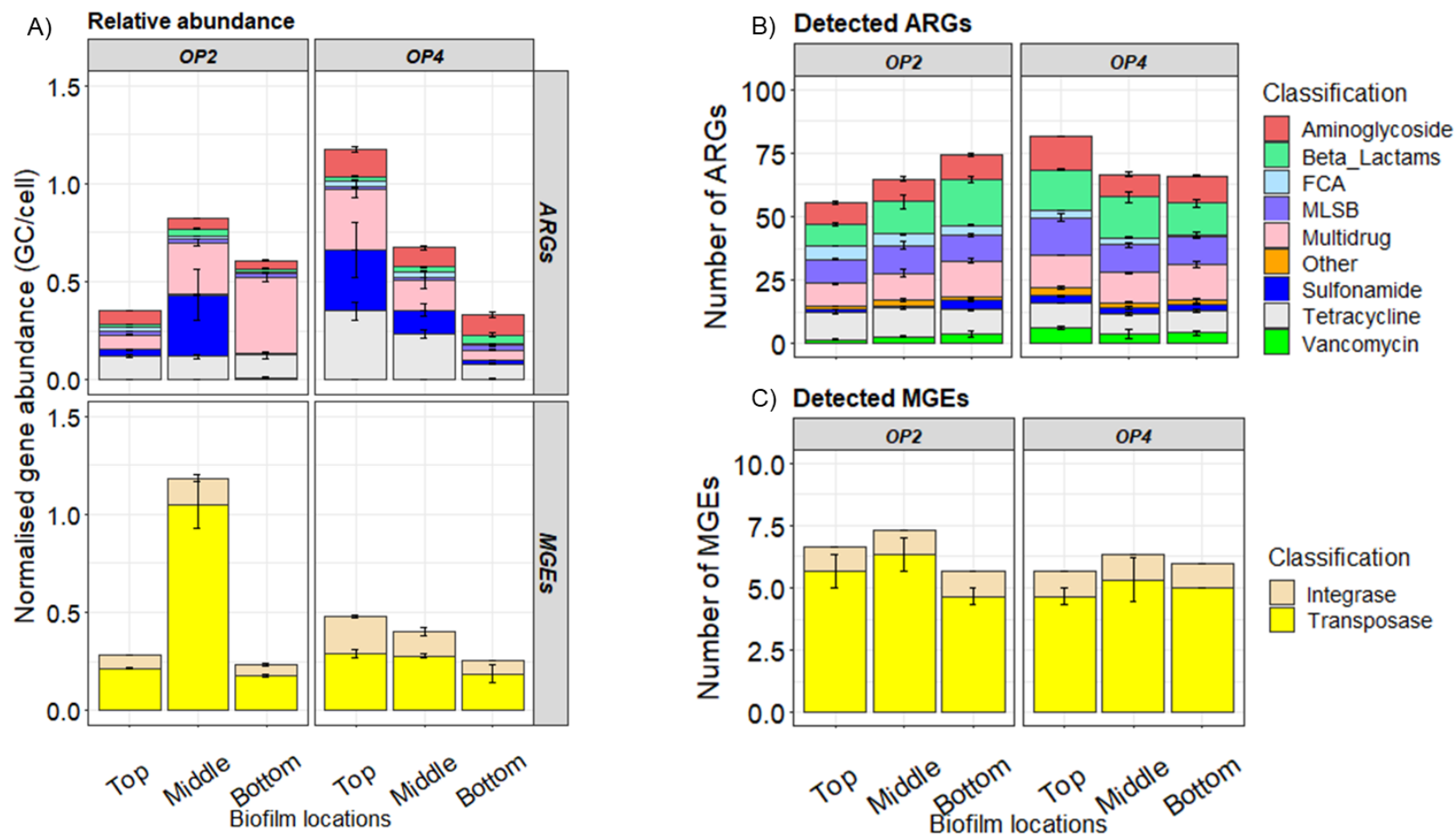


Figure 6-9 Diversity and relative abundance of sponge biofilms abstracted from the aerobic core (Top and Middle) and the anoxic core (Bottom) during operating regimes OP2 and OP4. (A) Relative gene copy per cell (GC/cell) of ARGs and MGEs normalised to bacterial cell numbers derived from 16S-rRNA gene abundances for each sample; (B) number of antibiotic resistance genes (ARGs); and (C) mobile genetic elements (MGEs) at different sites along reactor depths. Error bars show standard deviation around the mean ($n = 3$).

6.3.7 Micropollutants: Fate of antimicrobial agents and other personal care products in DDHS

Pharmaceuticals tend to be used less prudently in many LMICs. It is also reported that on average 70% of antibiotics administered by humans or animals are excreted via urine and feces as a mixture of unchanged antibiotics and metabolite forms (Kümmerer, 2009), i.e., still-active compounds. These compounds can be released into the environment via emissions of untreated sewage and wastewater effluents, sometimes at concentrations higher than the predicted no-effect concentrations (PNECs), which can promote or select for antibiotic resistant bacteria (Kümmerer and Henninger, 2003; Bengtsson-Palme and Larsson, 2016).

Tran *et al.* (2016b) and Polesel *et al.* (2016) showed that pharmaceutical compounds were removed using conventional biological wastewater treatment. However, the fate of antibiotics and other PPCPs in the DDHS systems has not been tested before. In this study, 21 antimicrobials belonging to ten different classes and three contaminants of emerging concerns were investigated, as listed in Table 6-2.

A total of 12 antimicrobial agents and three PCPs traces were detected at total concentrations of approximately 10^4 ng/L in the raw influents, consisting major antibiotics with highest abundance in sulphonamide (i.e., sulfamethoxazole at 48.1 – 65.1 %), followed by β -lactams (i.e., amoxicillin at 19.5 – 22.8 %), and varying levels of tetracycline and macrolides at < 10% (Table D-6). High levels of acetaminophen, a common ingredient for anti-inflammatory products such as ibuprofen and aspirin, was detected at $3.2 - 8.1 \times 10^4$ ng/L in influent samples, which is as expected because such drugs can be purchased across the counter. Many antibiotics, including ceftazidime, meropenem and vancomycin, were not detected during the two sampling campaigns, which implies their environmental half-lives are short or that they are not widely prescribed in the area.

Table 6-2 Array of monitored pharmaceuticals and personal care products (PPCPs) in aqueous phase of reactor samples, during pseudo-steady state sampling campaigns for OP2 and OP4.

Agents Classification	Compound names	MDL	PNEC ¹ (ug/L)
β-lactams	Amoxicillin	15.00	0.250
	Meropenem	1.00	0.064
	Ceftazidime	15.00	0.50
Lincosamides	Lincomycin	0.02	2.000
	Clindamycin	0.02	1.000
Macrolides	Azithromycin	0.02	0.250
	Clarithromycin	0.03	0.250
	Tylosin	0.20	4.000
	Erythromycin-H ₂ O*	0.05	n.a.
Sulfonamides	Sulfamethazine	0.06	n.a.
	Sulfamethoxazole	0.05	16.000
Tetracyclines	Tetracycline	4.50	1.000
	Chlortetracycline	1.00	n.a.
	Minocycline	10.0	1.000
	Oxytetracycline	7.50	0.500
Fluoroquinolone	Ciprofloxacin	0.50	0.064
Glycopeptide	Vancomycin	4.00	8.00
Reductase inhibitor	Trimethoprim	0.06	0.500
Other	Chloramphenicol	0.50	8.000
Antiseptics	Triclocarban	0.60	n.a.
	Triclosan	1.00	n.a.
NSAIDs	Acetaminophen	n.a	n.a.
Beta-blockers	Atenolol	n.a	n.a.
Stimulant	Caffeine	n.a	n.a.

Notes: MDL = method detection limit; n.a. = not available; PNEC¹ = predicted no-effect concentrations (Bengtsson-Palme and Larsson, 2016); NSAIDS = Nonsteroidal Anti-inflammatory Drugs; * Erythromycin-H₂O = anhydroerythromycin is the degradation products of ERY (i.e. ERY-H₂O, with molecular weight of 715 Da) (Tran et al., 2016a).

Although not statistically significant (Kruskal-Wallis; p-value=0.22), fate of different chemicals varied under different redox conditions across the two operating configurations (Figure 6-10). Particularly, sulfamethoxazole appeared more persistent during OP2 under the aerobic recirculation regime, which increased by about 2.7 fold in post-aerobic effluent. The concentration was later reduced by slightly over half in the anoxic treatment step. Conversely, sulfamethoxazole levels

were reduced by 2.6 fold in the post-aerobic effluent during OP4 and remained unchanged in the final effluent after the anoxic step.

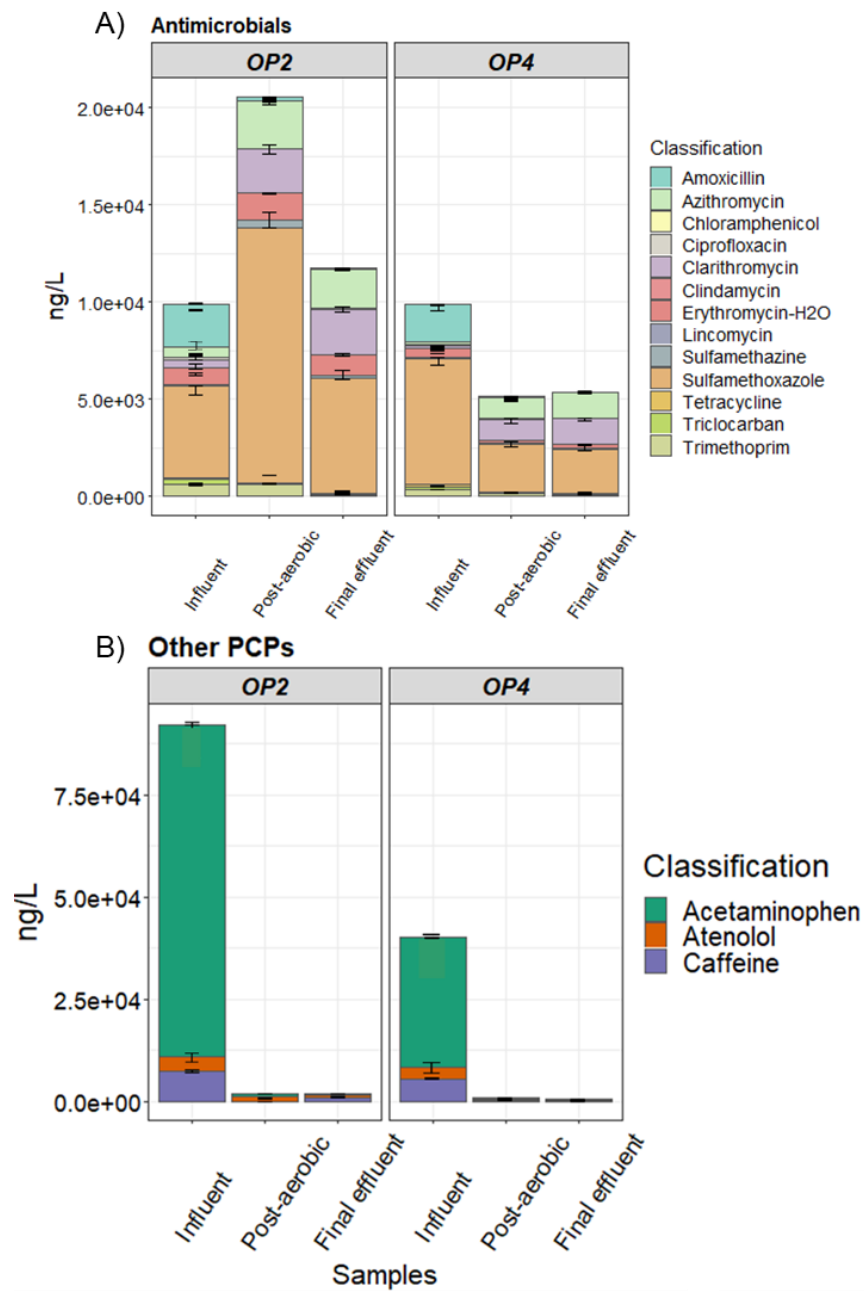


Figure 6-10 Concentrations of the target pharmaceuticals and personal care products (PPCPs) in raw influent, post-aerobic treated effluent and final effluent of DDHS operated at OP2 and OP4, with (A) array of detected antimicrobial agents; (B) other personal care products and caffeine. Error bars show standard deviation around the mean ($n = 6$ per sample per sampling location).

There also were elevated levels of some antibiotics throughout the treatment train in DDHS pilot unit. For example, clarithromycin and azithromycin increased by five to

seven fold relative to the influent concentrations, which resulted in higher discharge concentrations after treatment.

One possible explanation for this anomaly might be that some pharmaceutical compounds (e.g., sulfamethoxazole, clarithromycin and azithromycin) are primarily solid-bound (i.e., faeces and suspended particulates) and were released when the aerobic effluent was recirculated. Greater liquid mixing may have occurred as the wastewater flowed through the aerobic sponge (i.e., 20 PPI), possibly increasing the release of sulfamethoxazole into the aqueous phase. Further, 20% bypass did not negatively change micropollutant levels as no apparent increase was detected in the final discharge after the anoxic treatment. Although the observed quantity for sulfamethoxazole was reduced in the final effluent, soluble azithromycin and clarithromycin remained unchanged, which indicates these compounds may persist thus potentially requiring a longer HRT for removal.

The levels of other PPCPs (i.e., acetaminophen, atenolol and caffeine) were significantly different between OP2 and OP4 (Kruskal-Wallis; p -value=0.02). DDHS was especially good at removing Nonsteroidal Anti-inflammatory Drugs (NSAIDs) with up to 2.6 log reduction in acetaminophen was achieved in final treated effluents during both operating regimes. Major reductions of PPCPs, especially acetaminophen, were achieved by the aerobic step (Tukey's comparisons; p -values < 0.01) with discharge concentrations significantly lowered to $10^2 \sim 10^3$ ng/L.

Generally, antimicrobials and other micropollutants in domestic wastewater can be removed by absorption through DDHS. Polyurethane (PU) with high porosity is an excellent absorbent for wastewater treatment (Elmitwalli *et al.*, 2000). It is hydrophobic and, therefore, can absorb pollutants from water (Nam *et al.*, 2014; Wang *et al.*, 2017b). Therefore, anoxic tank filled with higher porosity (45 PPI) may be generally better at removing micropollutants. Operating parameters such as hydraulic retention time (HRT), type of PU media may influence the overall removal of micropollutants especially those bound to faeces, which may be released during the two-step treatment procedures.

As shown in Figure 6-11, trace concentrations of PPCPs were always lower in OP4. Majority compounds were lower than proposed PNEC limits for resistance selection,

except for clarithromycin and azithromycin. Comparatively, the overall results indicate the OP4 configuration is preferable for controlling some micropollutants.

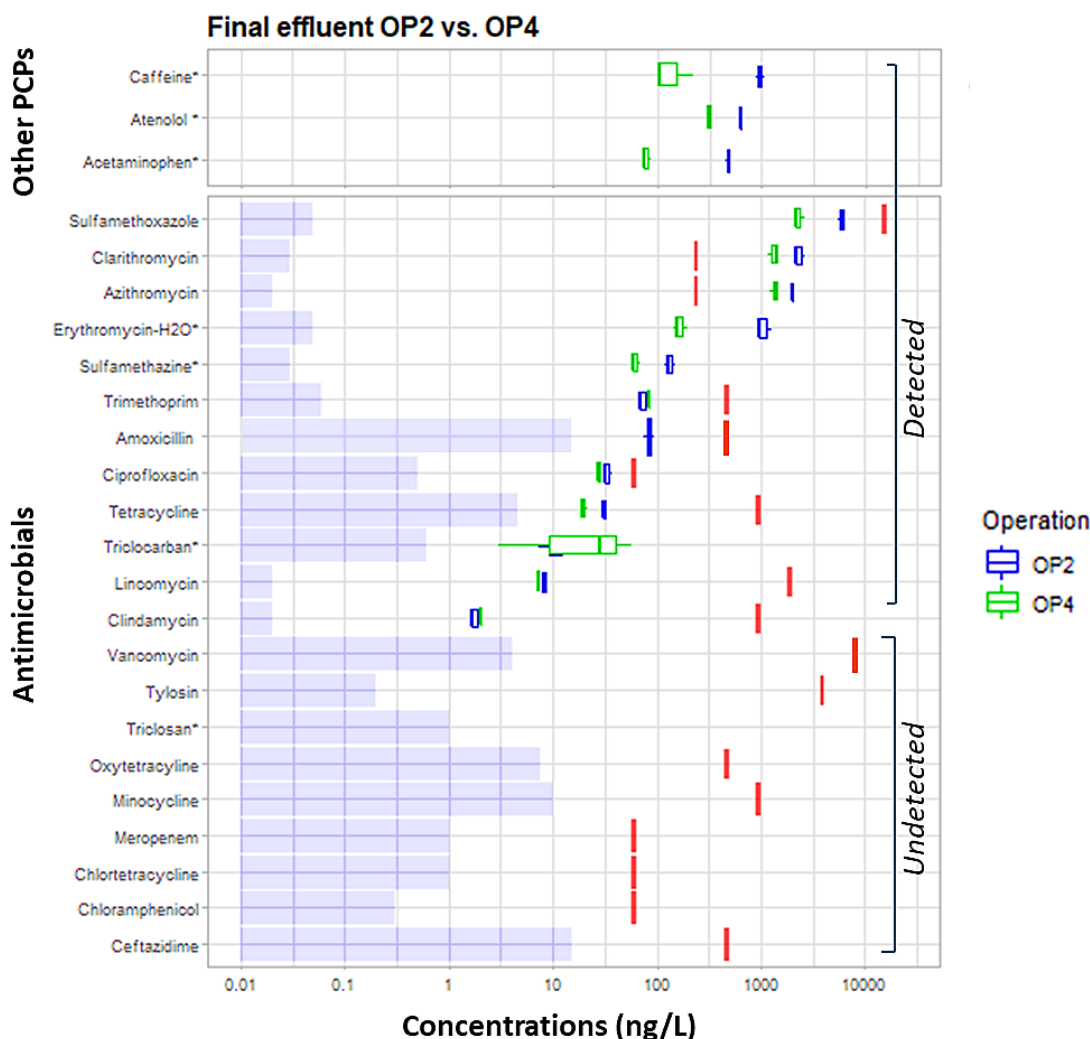


Figure 6-11 Boxplot for antibiotics, antiseptics and personal care products (PCPs) measured and detected in the final effluents of OP2 and OP4. Light purple area represents method detection limit of the SPE-HPLC/MSMS; red lines mark the PNEC (predicted no effect concentration) as proposed by Bengtsson-Palme and Larsson (2016); *no PNEC defined (Bengtsson-Palme and Larsson, 2016).

6.4 Conclusions

A pilot scale DDHS reactor (20% bypass ratio) was operated under different recirculation regimes to treat domestic wastewater. Local Malaysian discharge standards were achieved for new treatment systems (approved post 1999) for COD (< 120 mg/L) at $34.4 \text{ mg/L} \pm 0.85$, ammoniacal-nitrogen (< 10 mg/L) at $7.15 \text{ mg/L} \pm$

2.05, and for nitrate-nitrogen (< 20 mg/L) at $8.95 \text{ mg/L} \pm 0.45$. These are the lower limits set for discharges into rivers located in sensitive catchment areas.

Between 1.0 to 1.7 log-removals in total ARGs and MGEs levels from untreated wastewater were achieved, which were significantly lower than influent levels. ARG removals generated correlated with reductions in bacterial numbers and removed effectively using sequential redox exposures. Biofilm samples consisted 8.2×10^6 – 2.5×10^7 ARGs/mg versus reactor depth. Although slight variations in diversity and relative abundance were seen between the two regimes with recirculation, ARG and MGE levels were statistically similar, signifying a stable core resistome in different DDHS biofilms. Further, pilot DDHS systems operated with 20% bypass and complete recirculation were able reduce some pharmaceuticals and PCPs compounds in the domestic sewage, which most probably attributable to absorption by the sponge media.

Despite promising results, several challenges must be overcome before the commercialisation of DDHS can be considered as a realistic proposition. Primarily, TN removal were not as effective as shown in the lab-scale bioreactors. The main possible reason is the anoxic tank was undersized for sustaining anoxia because the system was allowed to operate naturally, with only hydraulic control, oxygen level in the anoxic tank was above the ideal DO limit for effective denitrification. The anoxic tank was made submerged with nitrified filtrate from the aerobic tank, which was high in DO level. Therefore, a deeper reactor depth is required with the top of the anoxic tank acting as a buffer zone in for reducing DO levels in the aerated filtrate. Improved denitrification should take place at the lower section of the anoxic tank where DO were sufficiently reduced, which is suggested from microbiome data reported in Chapter 4.

Overall, the results were positive for this field test, especially relative to bacterial and ARGs removal. It is believed that the main removal mechanism is via simple bacteria removal with a combined effect of abiotic (i.e., filtration, adsorption, absorption) and biotic mechanisms (i.e., predation, bacterial competition). However, further investigations are needed.

Acknowledgement

The field work would have been impossible without the help of several people. I am thankful to Dr. Ivan Tam from Newcastle University Singapore, and Dr. Mukrizah Othman from Newcastle University Medicine Malaysia (NUMed), for their initial coordination with the Malaysian local contractor for reactor fabrication. I thank Dr. Michaela Goodson, the Dean of research at Numed for her support and assistance during my attachment at Numed. I also thank Joshua Bunce, Mr. Nathan, and Mr. Guna for their help in scaling up and fabricating the pilot DDHS bioreactor. My special thanks to Ms. Mardhiah from NUMed for her tremendous help in setting up a Class 2 water microbiology laboratory, which enabled all reactor monitoring and analyses throughout the field work. I especially thank Jia-Yee and Sylvia for assisting in microbiology and preparation work during the intensive sampling campaigns. I also thank Dr. Ngoc Han Tran and Prof. Karina Gin from National University of Singapore for the UHPLC-MS/MS training and analysis and general support, respectively. Finally, thanks to Hazwan Yusof for assisting during reactor start-up and reactor monitoring.

Chapter 7 Conclusions and future research

7.1 Conclusions

The ultimate goal of this thesis was to study, optimise and operationalise the novel sponge-core bioreactor technology, namely DDHS, for simultaneously reducing antibiotic resistance burden (i.e. AR bacteria and AR genes) and TN levels in domestic wastewater. The core work examined the fate and removal mechanisms of AR genes in sponge biofilms as a function of redox conditions and varied operating regimes.

Four sub-studies were performed, which included resistome profiling in the influent and effluents in bench-scale DDHS bioreactors operated using different hydraulic flow regimes (Chapter 3); 16S microbiomes of DDHS biofilms as a function of redox habitat and operating regimes (Chapter 4); the influence of redox conditions on the fate of a resistance host and a conjugative plasmid in biofilm reactors (Chapter 5); and a field demonstration of the scaled up DDHS prototype (Chapter 6). Each Chapter met the overall aims and objectives set at the start, with the most explanatory results being included in this thesis. Although some experiments have not come to fruition, the work overall addressed key knowledge gaps in operationalising AR removal in small-scale treatment systems, including fate mechanisms under different redox conditions.

Initial work focused on the evaluation and characterisation of bench-scale bioreactors. In Chapter 3, resistomes of raw wastewater and DDHS effluents were quantified using high-throughput qPCR to facilitate the profiling of ARG and TN removal rates using varied operating regimes. The work showed that the DDHS bioreactors were generally very effective at reducing ARGs, i.e., by 2.0 to 3.0 log, although specific ARGs removed and the fate of MGEs differed as a function of wastewater bypass percent. Greater ARG (and ARB) removals were observed in the bioreactors that used a 10-20% wastewater bypass (% of total wastewater by volume). Up to three-log-removal in ARG abundances were achieved in a co-optimal bioreactor operated with 20% wastewater bypass. However, a threshold existed for

wastewater bypass, where an excess bypass (i.e., 30% bypass) releases higher traced levels of ARGs and MGEs, although better TN removal was possible. It is possible that this is due to more influent organisms ‘escaping’ the aerobic treatment step, which data in Chapter 5 suggest might be due to lower levels of host predation under oxygen-free conditions. Nonetheless, overall ARG and MGE levels were reduced significantly in all reactor units, including the bioreactor without any wastewater bypass. Interestingly, more unique ARGs also passed through the DDHS unit without bypass, which contained slightly higher MDR genotypes and MGE levels per cell. Microbial evidence showed that anoxic conditions in the second stage of the reactors with a bypass facilitated greater denitrification (Chapter 4). This confirms systemic microbial characterisation can be helpful in explaining bioreactor performance, i.e., ‘stronger’ microbial community performed better.

Indeed, microbial communities differed between bioreactors with and without 20% bypass, apparently being shaped by both redox and operating conditions. The 16S microbiome assessment in Chapter 4 showed that sponge core communities was locally influenced by receiving OLR, which was impacted by percent wastewater bypass. Counterintuitively, a greater community shift was apparent in aerobic zone biofilms, resulting from the wastewater bypass. The aerobic zone received a higher OLR in the non-bypassed bioreactor, which resulted in lower abundances and microbial diversity, selecting for fewer dominant species. In contrast, the 20% bypass reactor had greater diversity in the aerobic zone and a more equal biofilm community throughout the whole reactor. Further, the bypass appeared to select for known denitrifying species in the anoxic zone, namely *Flavobacterium* and *Shewanella*, which corroborated with enriched the *nirS* genotypes, hence highly TN removals. However, the 20% bypass did not select for greater putative faecal genotypes, suggesting that ARG levels were not altered at this ‘safe’ bypass ratio, corroborated with results in Chapter 3. Regardless, the most appropriate bypass ratio needs to be carefully chosen in actual operations to prevent elevated ARG and-or faecal discharges due to bypassed wastewater ‘avoiding’ the aerobic treatment step.

Based on the promising results in Chapters 3 and 4, we were keen to determine more specifically how redox conditions influenced ARG fate in DDHS bioreactors, particularly the spatial and temporal fate of mobile AR elements. To investigate the fate of AR plasmid and host bacteria in different redox conditions, an independent

experiment was performed using a recombinant strain and plasmid (Chapter 5). The study used a reporter *E. coli* strain cloned with fluorescent-labelled AR plasmid to seed and then track the migration and putative HGT under different redox conditions maintained in sequencing batch biofilm reactors (SBBR), treating settled domestic wastewater. The SBBR were operated to simulate redox environments used in the DDHS bioreactor, but with stricter control over the collection of biofilm and liquid-phase samples under a designed timeline. This was not possible in the DDHS bioreactor itself.

Work in Chapter 5 revealed that *in situ* HGT in the bioreactor ecosystems involved multiple steps and it was impacted hugely by the local ecology, with the survival of donor strain as a critical requisite for gene exchange in the reactors. It was found that HGT was not rapid or occurred under most conditions, although greater levels of AR plasmid were maintained in biofilms particularly in the anaerobic conditions and under pseudo-persistent host loading conditions. One very important finding is that seeded AR plasmid host consistently disappeared in the aerobic bioreactors, both in the biofilm and liquid phase. Further investigation confirmed that the survival of seeded AR plasmids in the bioreactors was oxygen-related, which strong evidence showed is linked to eukaryotic abundance and probably predation that prevails under the aerobic condition. It is suspected extracellular polymeric substances in biofilms also may be a local obstruction to HGT because relatively lower transfer frequencies seen despite greater background AR plasmid levels; i.e., conjugal transfer of genetic elements (i.e., permissiveness) was limited into native biofilm communities. The broad conclusion of this work is that aerobic conditions are far superior for bacteria removal (i.e. plasmid-bearing AR host or other AR bacteria) and in turn ARG removal (compared with anoxic and anaerobic conditions), although putative HGT is a dynamic process effected by both ecological and genetic factors.

Chapter 6 validated DDHS technology at a field-scale. Semi-optimised configurations were achieved because the anoxic reactor sizing omitted the DO buffering zone, hence undersized. This is confirmed by the results in Chapter 4 where denitrifying species were predominant in the bottom of the lab anoxic unit. Therefore, a longer anoxic column is required to reduce DO level from the aerobically pretreated effluent, to facilitate denitrification to occur at the bottom of the anoxic zone. However, broader ARG removal in aqueous samples can be observed. Resistome data in the

field reactor were similar to laboratory results; i.e., 1.0 to 2.0 log removal in ARG levels. Sequential redox exposure is important to reduce influent ARG (i.e., by total bacterial removal), so that microbial content in the bypassed wastewater is safely treated via full effluent recirculation. Although aerobic conditions favour bacterial removal (Chapter 5), results here show that large aerobic zone may not be entirely beneficial, as it may enrich bacterial genetic plasticity due to SOS response to nutrient constraints. Certain MGE were enriched under aerobic conditions, which coincided with increased putative MDR strains. This is an implication that the increased in unique ARG subtypes passed through the non-bypassed reactor in Chapter 3 is caused by diluted wastewater in the aerobic core, which Chapter 4 found is primarily utilised by dominant fast growing bacteria. Finally, our DDHS treatment system consisted of a pseudo-stable core resistome, which was not significantly affected by varied operating regimes. Within this context, our findings confirm previous studies that showed stable WWTP resistomes can exist at conventional scales.

In summary, the overall conclusion from this thesis is that DDHS systems are a viable technology for use in underserved LMICs regions because it is both effective and affordable. The sequential redox treatment regime and designated hydraulic design enhance bacteria removals, and overall reactor performance is influenced by biofilm stability defined by local redox and the operating bypass-cum-OLR regimes. Although high bacterial densities in biofilm-based system provide cell-to-cell contact deemed for greater HGT, gene exchanges appear to be multi-step and dependent on ecological factors, such as protozoan predation, seem to be most important for ARG removal.

7.2 Potential future work

DDHS is a novel technology for wastewater treatment and the unique sequential redox exposure idea for ARG removal is new, but effective. Therefore, further research is worthwhile to continue refining the technology for possible uptake in the future. In terms of future development, new work is possible and each piece of research reported herein can be refined to provide more in-depth answers.

7.2.1 *Sponge-core at molecular scale*

Laboratory experiments provided valuable groundwork and increased our understanding of how sequential redox conditions can enhance a wastewater treatment unit, which is apparent at the microbial scale. Therefore, deeper molecular microbial analysis is justified using metagenomics. Such information help study the microbial dynamics of sequential redox exposures, including specific ARGs, MGEs, and constituent microbiomes within the sponge-core biofilms. Such ecogenomics data would allow more definitive conclusions as to how AR organisms and-or genes could be treated (or persist), refining relationships among environmental parameters, such as micropollutants, and how levels along the sponge column are impacted by redox conditions and operating regimes. Such additional analysis could be done using the preserved samples from both laboratory and the pilot bioreactors. From there, it would possible to model the fate of specific ARGs (and ARBs) as per operating regimes, which help delineates 'optimised' operating conditions for the technology.

7.2.2 *Understanding the role and extent of horizontal gene transfer*

Based on early data in Chapter 5 (i.e., tracking an AR plasmid using a reporter *E. coli* strain; i.e., *EcoFJ2*), many new experiments are conceivable. Firstly, further genetic engineering to improve the differentiation of reporter organism could be done by cloning additional antibodies, such as mCherry red fluorescent proteins, to the chromosome of *EcoFJ2*. This would allow a more exact estimation of HGT frequency using culture independent fluorescence-activated cell sorting (FACS), which could be sorted into particular bins based on different light scattering. Coupling DAPI (blue-fluorescent DNA stain) staining, samples can be further sorted to total bacteria (blue bin), reporter bacteria (red bin), and transconjugants (green bin) via fluorescent flow cytometry, which is more efficient and higher throughput. This work could be extended by performing the HGT experiment between reporter organisms and specific consortia (i.e. isolated biofilm or wastewater bacteria) using microbioreactor set-ups. Specifically, the microfluidic Biolector system is an ideal option for real-time, high-throughput measurement of the impact of redox on HGT as it consists both fluorescent and oxygen modules, that can maintain different redox conditions through oxygen regulation in the microbioreactors and detect fluorescent flux (via changes in

intensity). However, one should bear in mind that such a microfluidic experiment does not include ecological aspects, which appear critical in the real ecosystems, although it would provide crucial *in vivo* data.

7.2.3 Understanding ARG removal mechanisms

DDHS systems are clearly good at removing ARGs, which we believe occurs by simply removing bacteria in an efficient manner. Chapter 5 strongly suggests aerobic conditions are superior because of eukaryotic predation, which deserves further investigation. However, understanding other environmental factors relative to ARG bacterial removal is key, such as operating HRT, SRT, bacterial predation, and physical removal mechanisms, such as membrane filtration. Therefore, the next valuable work is to quantify eukaryotic predation on concert with bacterial predation in sequential redox conditions, using molecular approaches, such as targeted 18S quantitative PCR and for known bacterial predators. For example, understanding the role of parasitic phage and predatory bacteria (e.g. *Bdellovibrio* spp.) as a function of redox conditions is key. Moreover, studying of the role of polyurethane sponge media in removing target micropollutants should be explored, to determine how absorption and adsorption on sponge media with different porosity might be optimised to help enhance ARG and ARB removal.

7.2.4 Reiterating prototype: modularity in design

We propose two major actions to move the development of DDHS technology to the next phase. Engineering models for design calculations do not exist for sizing reactors and are needed. However, field data at larger scales is now available to start building models. Firstly, a design model specific for the sequential redox sponge-core bioreactor can be created, but with reference to more data from the pilot system. Specifically sizing of the anoxic reactor for denitrification can be done by extrapolating the performance of the pilot reactor for the removal of NO₃-N, with dissolved oxygen as additional parameter to include a buffer zone to the sizing.

Secondly, we propose to adopt a modular design for future DDHS prototype, which allows one to customise the DDHS core to local wastewater characteristics (i.e., strength) and discharge standards. For example, aerobic and anoxic tank can be modularised by sponge receptacles, whereby the size (i.e. height) of each core can be adjusted depending on operating variables. A modular design also permits

flexibility in implementing the system on-site, conveniently integrated to any existing treatment works to polish partially treated effluent. This would galvanise the adoption of the technology.

7.3 Final thoughts

Basic principles of pollutants removal, including AR factors, using DDHS sequential redox systems have been shown at a small scale for decentralised applications. This is the first study for such a technology; one designed for simultaneously reducing AR genes and bacteria and TN through sequential biological redox exposure. Although faced with many difficulties in the initial development phase, we are positive that DDHS systems are possible for LMICs applications, especially locations deserted from centralised sewage treatment systems.

Clemenceau famously said “War is too important to be left to the generals”. In this context, our war against AMR is too important to be left to the clinicians because AMR is not only a problem in the medical realm; it is a multi-sectoral and cross-countries health challenge. There are too many aspects of infection management and all experts from the world ought to participate as a global coalition to design concerted strategies. Our aims remain unchanged: to use a simple, affordable, and practical technology to limit transmission of waste- and wastewater-borne antibiotic resistance in the environment in locations with inadequate sanitation.

Appendices

Appendix A

Table A-1. Summary of wastewater characteristics and reactor performance as a function of percent wastewater bypass.

Parameter (mg/L) ^a	Influent	R-S0		R-S10		R-S20		R-S30	
		Effluent	R%	Effluent	R%	Effluent	R%	Effluent	R%
COD_{Total}	353.3 (146) ^b	43.4 (24.8)	83.1	34.0 (24.2)	88.6	35.1 (26.8)	88.2	45.7 (25.4)	84.3
COD_{Soluble}	198 (61.0)	33.8 (24.9)	79.1	30.7 (22.3)	82.8	29.8 (25.1)	85.1	38.3 (29.4)	81.0
TN	37.7 (12.8)	25.4 (9.8)	28.5	22.1 (8.8)	37.6	12.4 (8.0)	64.5	10.9 (7.1)	71.0
NH₄-N	22.6 (6.7)	1.0 (1.9)	95.7	0.4 (0.6)	97.7	1.6 (2.5)	93.2	3.4 (3.7)	84.2
NO₂-N	BDL ^c	0.4 (0.5)	-	0.2 (0.3)	-	0.2 (0.3)	-	0.1 (0.3)	-
NO₃-N	BDL	28.4 (22.8)	-	27.5 (18.9)	-	8.5 (6.8)	-	1.6 (1.6)	-
TSS	162 (70.2)	12.3 (10.7)	90.6	7.7 (9.8)	92.8	8.9 (10.2)	92.1	7.3 (7.2)	93.5
VSS	130 (66.2)	8.3 (7.0)	91.9	7.8 (8.1)	91.5	7.9 (8.9)	91.7	9 (6.3)	90.8
pH	7.1 (0.2)	6.8 (0.4)	-	6.9 (0.1)	-	6.7 (0.2)	-	6.9 (0.3)	-
Temp	Room temperature (20 – 23 °C)								

Notes: ^a Except pH and temperature; R-S0 = 0.0 wastewater by-pass; R-S10 = 10% wastewater by-pass; R-S20 = 20% wastewater by-pass; R-S30 = 30% wastewater by-pass;

^b Values within parenthesis represent standard deviations (n = 12); ^c BDL = Below detection limit.

Table A-2: Primer sets used in this study and their target classification. Quantitative PCR primer sets, assay target, and gene classification by target drug and mechanism of resistance. Target gene designations were found by BLAST on the ARDB or National Center for Biotechnology Information (NCBI) databases. FCA = fluoroquinolone, quinolone, florfenicol, chloramphenicol, and amphenicol resistance genes. MLSB = Macrolide-Lincosamide-Streptogramin B resistance. IS = Insertion sequence.

Gene Name	Forward Primer	Reverse Primer	Gene Classification	Resistance Mechanism
16S rRNA	GGGTTGCGCTCGTTGC	ATGGYTGTCTCGTCAGCTCGTG	16S rRNA	NA
<i>catB3</i>	GCACTCGATGCCTTCCAAAA	AGAGCCGATCCAAACGTCAT	FCA	deactivate
<i>cfr</i>	GCAAAATTCAGAGCAAGTTACGAA	AAAATGACTCCCAACCTGCTTTAT	FCA	deactivate
<i>floR</i>	ATTGTCTTCACGGTGTCCGTTA	CCGCGATGTCGTCTGAAC	FCA	efflux
<i>yidY/mdtL</i>	GCAGTTGCATATCGCCTTCTC	CTTCCCGGCAAACAGCAT	FCA	efflux
<i>yidY/mdtL</i>	TGCTGATCGGGATTCTGATTG	CAGGCGCGACGAACATAAT	FCA	efflux
<i>cmlA1</i>	TAGGAAGCATCGGAACGTTGAT	CAGACCGAGCAGCACTGTTG	FCA	efflux
<i>cmlA1</i>	AGGAAGCATCGGAACGTTGA	ACAGACCGAGCAGCACTGTTG	FCA	efflux
<i>cmx(A)</i>	GCGATCGCCATCCTCTGT	TCGACACGGAGCCTTGGT	FCA	efflux
<i>catA1</i>	GGGTGAGTTTCACCAAGTTTGATT	CACCTTGTCGCTTGCGTATA	FCA	deactivate
<i>mexE</i>	GGTCAGCACCGACAAGGTCTAC	AGCTCGACGTACTTGAGGAACAC	FCA	efflux
<i>mexF</i>	CCGCGAGAAGGCCAAGA	TTGAGTTCGGCGGTGATGA	FCA	efflux
<i>emrB/qacA</i>	CTTTTCTCTAACCGTACATTATCTACGATAAA	AGAACGTAGCGACTGATAAAATGCT	FCA	efflux
<i>pmrA</i>	TTTGCAGGTTTTGTTCTAATGC	GCAGAGCCTGATTTCTCCTTG	FCA	efflux
<i>qnrA</i>	AGGATTTCTCACGCCAGGATT	CCGCTTTCAATGAAACTGCAA	FCA	unknown
<i>acrB</i>	AGTCGGTGTTGCGCGTTAAC	CAAGGAAACGAACGCAATACC	FCA	efflux
<i>acrB</i>	TGGTAGTGGGCGTCATTAACAC	GGCAACGTAATCCGAAATATCC	FCA	efflux
<i>acrF</i>	GCGGCCAGGCACAAAA	TACGCTCTTCCCACGGTTTC	FCA	efflux
<i>adeA</i>	CAGTTCGAGCGCCTATTTCTG	CGCCCTGACCGACCAAT	FCA	efflux
<i>cmeA</i>	GCAGCAAAGAAGAAGCACCAA	AGCAGGGTAAGTAAACTAAGTGGTAAATCT	FCA	efflux
<i>acrA</i>	CAACGATCGGACGGGTTTC	TGGCGATGCCACCGTACT	FCA	efflux
<i>acrA</i>	GGTCTATCACCTACGCGCTATC	GCGCGCACGAACATACC	FCA	efflux
<i>mexA</i>	AGGACAACGCTATGCAACGAA	CCGGAAGGGCCGAAAT	FCA	efflux
<i>mexD</i>	TTGCCACTGGCTTTCATGAG	CACTGCGGAGAACTGTCTGTAGA	FCA	efflux
<i>oprJ</i>	ACGAGAGTGGCGTCGACAA	AAGGCGATCTCGTTGAGGAA	FCA	efflux
<i>acrA</i>	CAGACCCGCATCGCATATT	CGACAATTTGCGGCTCATG	FCA	efflux

<i>acrA</i>	TACTTTGCGCGCCATCTTC
<i>acrA</i>	CGTGCGCGAACGAACA
<i>aac</i>	CCCTGCGTTGTGGCTATGT
<i>aacC1</i>	GGTCGTGAGTTCGGAGACGTA
<i>aacC2</i>	ACGGCATTCTCGATTGCTTT
<i>aacC4</i>	CGGCGTGGGACACGAT
<i>aac(6')I1</i>	GACCGGATTAAGGCCGATG
<i>aacA/aphD</i>	AGAGCCTTGGGAAGATGAAGTTT
<i>aac(6')-Iy</i>	GCTTTGCGGATGCCTCAAT
<i>aac(6')-II</i>	CGACCCGACTCCGAACAA
<i>aacC</i>	CGTCACTTATTCGATGCCCTTAC
<i>aac(6')-Ib</i>	GTTTGAGAGGCAAGGTACCGTAA
<i>aac(6')-Ib</i>	CGTCGCCGAGCAACTTG
<i>aadA5</i>	ATCACGATCTTGCGATTTTGCT
<i>aadA5</i>	GTTCTTGCTCTTGCTCGCATT
<i>aac(6')-Ib</i>	AGAAGCACGCCCGACACTT
<i>aadA1</i>	AGCTAAGCGCGAACTGCAAT
<i>aadA2</i>	ACGGCTCCGCAGTGGAT
<i>aadA</i>	GTTGTGCACGACGACATCATT
<i>aadA2</i>	CTTGTCGTGCATGACGACATC
<i>aadD</i>	CCGACAACATTTCTACCATCCTT
<i>aadA2</i>	CAATGACATTCTTGCGGGTATC
<i>aadA9</i>	CGCGGCAAGCCTATCTTG
<i>aadA</i>	CGAGATTCTCCGCGCTGTA
<i>aadA9</i>	GGATGCACGCTTGGATGAA
<i>aadE</i>	TACCTTATTGCCCTTGGAAGAGTTA
<i>spcN</i>	AAAAGTTCGATGAAACACGCCTAT
<i>spcN</i>	CAGAATCTTCCTGAAAAGTTTGATGAA
<i>aphA3</i>	AAAAGCCCGAAGAGGAACTTG
<i>aph6ia</i>	CCCATCCCATGTGTAAGGAAA
<i>aph(2')-Id</i>	TGAGCAGTATCATAAGTTGAGTGAAAAAG
<i>aph(2')-Id</i>	TAAGGATATACCGACAGTTTTGGAAA
<i>aph</i>	TTTCAGCAAGTGGATCATGTAAAAAT

CGTGC GCGCAACGAACT
ACTTTGCGCGCCATCTTC
TTGGCCACGCCAATCC
GCAAGTTCCCCGAGGTAATCG
CCGAGCTTCACGTAAGCATTT
AGGGAACCTTTGCCATCAACT
CTTGCCTTGATATTCACTTTTATAACCA
TTGATCCATACCATAGACTATCTCATCA
GGAGAACAAAAATACCTTCAAGGAAA
GCACGAATCCTGCCTTCTCA
GTCGGGCGCGGCATA
GAATGCCTGGCGTGTTGA
CGGTACCTTGCTCTCAAACC
CTGCGGATGGGCCTAGAAG
GATGCTCGGCAGGCAAAC
GCTCTCCATTCAAGATTGCA
TGGCTCGAAGATACCTGCAA
GGCCACAGTAACCAACAAATCA
GGCTCGAAGATACCTGCAAGAA
TCGAAGATACCCGCAAGAATG
ACCGAAGCGCTCGTCGTATA
GACCTACCAAGGCAACGCTATG
CAAATCAGCGACCGCAGACT
GCTGCCATTCTCAAATTGC
CCTCTAGCGGCCGAGTATT
GGAATATGTCCCTTTTAATTCTACAATCT
TCCAGTGGTAGTCCCCGAATC
CGCAGACACGCCGAATC
CATCTTTCACAAAGATGTTGCTGTCT
GCCACCGCTTCTGCTGTAC
GACAGAACAAATCAATCTCTATGGAATG
TTTAATCCCTCTTCATACCAATCCATA
CCAAGCTGTTTCCACTGTTTTTC

[illegible]

<i>aphA1</i>	TGAACAAGTCTGGAAAGAAATGCA	CCTATTAATTTCCCCTCGTCAAAAA	Aminoglycoside	deactivate
<i>aphA3</i>	CGGAATTGAAAAAACTGATCGAA	ATACCGGCTGTCCGTCATTT	Aminoglycoside	deactivate
<i>str</i>	AATGAGTTTTGGAGTGTCTCAACGTA	AATCAAAACCCCTATTAAAGCCAAT	Aminoglycoside	deactivate
<i>strA</i>	CCGGTGGCATTGTGAGAAAAA	GTGGCTCAACCTGCGAAAAAG	Aminoglycoside	deactivate
<i>strB</i>	GCTCGGTGCTGAGAACAATCT	CAATTTGCGTGCCTGGTAGT	Aminoglycoside	deactivate
<i>blaSHV</i>	TCCCATGATGAGCACCTTTAAA	TTCGTCACCGGCATCCA	Beta Lactamase	deactivate
<i>blaVEB</i>	CCCGATGCAAAGCGTTATG	GAAAGATTCCCTTTATCTATCTCAGACAA	Beta Lactamase	deactivate
<i>bla1</i>	GCAAGTTGAAGCGAAAGAAAAAGA	TACCAGTATCAATCGCATATACACCTAA	Beta Lactamase	deactivate
<i>blaOKP</i>	GCCGCCATCACCATGAG	GGTGACGTTGTCACCGATCTG	Beta Lactamase	deactivate
<i>blaROB</i>	GCAAAGGCATGACGATTGC	CGCGCTGTTGTCGCTAAA	Beta Lactamase	deactivate
<i>blaOXY</i>	CGTTCAGGCGGCAGGTT	GCCGCGATATAAGATTGAGAATT	Beta Lactamase	deactivate
<i>blaPSE</i>	TTGTGACCTATTTCCCTGTAATAGAA	TGCGAAGCACGCATCATC	Beta Lactamase	deactivate
<i>cfxA</i>	TCATTCTCGTTCAAGTTTTCAGA	TGCAGCACCAAGAGGAGATGT	Beta Lactamase	deactivate
<i>cepA</i>	AGTTGCGCAGAACAGTCCCTCTT	TCGTATCTTGCCCGTCGATAAT	Beta Lactamase	deactivate
<i>blaCTX-M</i>	GGAGGCGTGACGGCTTTT	TTCAGTGCGATCCAGACGAA	Beta Lactamase	deactivate
<i>blaCTX-M</i>	GCCGCGGTGCTGAAGA	ATCGGATTATAGTTAACCAGGTCAGATTT	Beta Lactamase	deactivate
<i>blaCTX-M</i>	CGATACCACCACGCCGTTA	GCATTGCCAACGTCAGATT	Beta Lactamase	deactivate
<i>blaCTX-M</i>	CTTGCGGTTGCGCTGAT	CGTTCATCGGCACGGTAGA	Beta Lactamase	deactivate
<i>blaGES</i>	GCAATGTGCTCAACGTTCAAG	GTGCCTGAGTCAATTCTTTCAAAG	Beta Lactamase	deactivate
<i>blaSFO</i>	CCGCCGCCATCCAGTA	GGGCCGCCAAGATGCT	Beta Lactamase	deactivate
<i>blaTLA</i>	ACACTTTGCCATTGCTGTTTATGT	TGCAAAATTTGCGCAATAATCTTT	Beta Lactamase	deactivate
<i>blaZ</i>	GGAGATAAAGTAACAAATCCAGTTAGATATGA	TGCTTAATTTTCCATTTGCGATAAG	Beta Lactamase	deactivate
<i>Pbp5</i>	GGCGAACTTCTAATTAATCCTATCCA	CGCCGATGACATTCTTCTTATCTT	Beta Lactamase	protection
<i>pbp</i>	CCGGTGCCATTGGTTTAGA	AAAATAGCCGCCCAAGATT	Beta Lactamase	protection
<i>blaCTX-M</i>	GCGATAACGTGGCGATGAAT	GTCGAGACGGAACGTTTCGT	Beta Lactamase	deactivate
<i>blaSHV</i>	CTTTCCCATGATGAGCACCTTT	TCCTGCTGGCGATAGTGGAT	Beta Lactamase	deactivate
<i>blaTEM</i>	AGCATCTTACGGATGGCATGA	TCCTCCGATCGTTGTCAGAAGT	Beta Lactamase	deactivate
<i>blaCTX-M</i>	CACAGTTGGTGACGTGGCTTAA	CTCCGCTGCCGGTTTTATC	Beta Lactamase	deactivate
<i>penA</i>	AGACGGTAACGTATAACTTTTTGAAAGA	GCGTGTAGCCGGCAATG	Beta Lactamase	protection
<i>pbp2x</i>	TTTCATAAGTATCTGGACATGGAAGAA	CCAAAGGAAACTTGCTTGAGATTAG	Beta Lactamase	protection
<i>blaPER</i>	TGCTGGTTGCTGTTTTGTGA	CCTGCGCAATGATAGCTTCAT	Beta Lactamase	deactivate
<i>cfiA</i>	GCAGCGTTGCTGGACACA	GTTCCGGGATAAACGTGGTGACT	Beta Lactamase	deactivate
<i>cphA</i>	GCGAGCTGCACAAGCTGAT	CGGCCAGTCGCTCTTC	Beta Lactamase	deactivate

<i>cphA</i>	GTGCTGATGGCGAGTTTCTG	GGTGTGGTAGTTGGTGTGATCAC	Beta Lactamase	deactivate
<i>bla-L1</i>	CACCGGGTTACCAGCTGAAG	GCGAAGCTGCGCTTGTAGTC	Beta Lactamase	deactivate
<i>blaVIM</i>	GCACTTCTCGCGGAGATTG	CGACGGTGATGCGTACGTT	Beta Lactamase	deactivate
<i>blaIMP</i>	AACACGGTTTGGTGGTTCTTGTA	GCGCTCCACAAACCAATTG	Beta Lactamase	deactivate
<i>blaIMP</i>	AAGGCAGCATTTCTCTCATTTT	GGATAGATCGAGAATTAAGCCACTCT	Beta Lactamase	deactivate
<i>bla-ACC-1</i>	CACACAGCTGATGGCTTATCTAAAA	AATAAACGCGATGGGTTC	Beta Lactamase	deactivate
<i>ampC</i>	TGGCGTATCGGGTCAATGT	CTCCACGGGCCAGTTGAG	Beta Lactamase	deactivate
<i>ampC</i>	GCAGCACGCCCCGTAA	TGTACCCATGATGCGCGTACT	Beta Lactamase	deactivate
<i>ampC</i>	AACAAAAGATCCCCGGTATGG	ACGCCCCGTAAATGTTTTGCT	Beta Lactamase	deactivate
<i>blaCMY</i>	CCGCGGCGAAATTAAGC	GCCACTGTTTGCCTGTCAGTT	Beta Lactamase	deactivate
<i>ampC</i>	TCCGGTGACGCGACAGA	CAGCACGCCGGTGAAAGT	Beta Lactamase	deactivate
<i>blaMOX/blaCMY</i>	CTATGTCAATGTGCCGAAGCA	GGCTTGTCCTCTTTCGAATAGC	Beta Lactamase	deactivate
<i>blaOCH</i>	GGCGACTTGCGCCGTAT	TTTTCTGCTCGGCCATGAG	Beta Lactamase	deactivate
<i>blaPAO</i>	CGCCGTACAACCGGTGAT	GAAGTAATGCGGTTCTCCTTTCA	Beta Lactamase	deactivate
<i>blaCMY2</i>	AAAGCCTCAT GGGTGCATAAA	ATAGCTTTTGTGGCCAGCATCA	Beta Lactamase	deactivate
<i>ampC</i>	CTGTTTCGAGCTGGGTCTATAAGTAA	CAGTATCTGGTCACCGGATCGT	Beta Lactamase	deactivate
<i>ampC</i>	CCGCTCAAGCTGGACCATAC	CCATATCCTGCACGTTGGTTT	Beta Lactamase	deactivate
<i>blaCMY2</i>	GCGAGCAGCCTGAAGCA	CGGATGGGCTTGTCCTCTT	Beta Lactamase	deactivate
<i>ampC/blaDHA</i>	TGGCCGCGAGCAGAAAGA	CCGTTTTATGCACCCAGGAA	Beta Lactamase	deactivate
<i>fox5</i>	GGTTTGCCGCTGCAGTTC	GCGGCCAGGTGACCAA	Beta Lactamase	deactivate
<i>ampC</i>	CCGCCCAGAGCAAGGACTA	GCTCGACTTCACGCCGTAAG	Beta Lactamase	deactivate
<i>ampC</i>	GCAGCGAAGCGTCAGTCA	AGATCCGTGGCCGCATAA	Beta Lactamase	deactivate
<i>ampC</i>	CAGCCGCTGATGAAAAAATATG	CAGCGAGCCCACTTCGA	Beta Lactamase	deactivate
<i>blaOXA10</i>	CGCAATTATCGGCCTAGAAACT	TTGGCTTTCCGTCCCATTT	Beta Lactamase	deactivate
<i>blaOXA10</i>	CGCAATTATCGGCCTAGAAACT	TTGGCTTTCCGTCCCATTT	Beta Lactamase	deactivate
<i>blaOXA1/blaOXA30</i>	CGGATGGTTTGAAGGGTTTATTAT	TCTTGGCTTTTATGCTTGATGTTAA	Beta Lactamase	deactivate
<i>mecA</i>	GGTTACGGACAAGGTGAAATACTGAT	TGTCTTTTAATAAGTGAGGTGCGTTAATA	Beta Lactamase	protection
<i>msrC</i>	TCAGACCGGATCGGTTGTC	CCTATTTTTTGGAGTCTTCTCTCTAATGTT	MLSB	efflux
<i>matA/mel</i>	TAGTAGGCAAGCTCGGTGTTGA	CCTGTGCTATTTTAAGCCTTGTTTCT	MLSB	efflux
<i>msrA</i>	CTGCTAACACAAGTACGATTCCAAAT	TCAAGTAAAGTTGTCTTACCTACACCATT	MLSB	efflux
<i>msrC</i>	GAATCACTTGTCCGAGTTTGTT	CGTACACAACGGTTTCGTCAGA	MLSB	efflux
<i>vgaA</i>	CGAGTATTGTGGAAGCAGCTAGTT	CCCGTACCGTTAGAGCCGATA	MLSB	efflux
<i>vgaB</i>	TAAAAGAGAATAAGGCGCAAGGA	TGTTTAGTAGCATGTTGCATTTTCC	MLSB	efflux

<i>lmrA</i>	TCGACGTGACCGTAGTGAACA	CGTGACTACCCAGGTGAGTTGA	MLSB	efflux
<i>vgaB</i>	GAATGATTAAGCCCCCTTCAAAA	ATTCGTGTTTCCAACGATTTTCG	MLSB	efflux
<i>vgaA</i>	GACGGGTATTGTGGAAAGCAA	TTTCCTGTACCATTAGATCCGATAATT	MLSB	efflux
<i>vgbB</i>	CAGCCGGATTCTGGTCCTT	TACGATCTCCATTCAATTGGGTAAA	MLSB	efflux
<i>msrA</i>	AACGAAATCAAGCGCAACAA	CAACCGTGCCTTTTTCTTTTG	MLSB	efflux
<i>oleC</i>	CCCGGAGTCGATGTTCGA	GCCGAAGACGTACACGAACAG	MLSB	efflux
<i>carB</i>	GGAGTGAGGCTGACCGTAGAAG	ATCGGCGAAACGCACAAA	MLSB	efflux
<i>ermK</i>	GTTTGATATTGGCATTGTCAGAGAAA	ACCATTGCCGAGTCCACTTT	MLSB	protection
<i>ermJ/ermD</i>	GGACTCGGCAATGGTCAGAA	CCCCGAAACGCAATATAATGTT	MLSB	protection
<i>ermK</i>	GAGCCGCAAGCCCCCTT	GTGTTTCATTTGACGCGGAGTAA	MLSB	protection
<i>erm(35)</i>	TTGAAAACGATGTTGCATTAAGTCA	TCTATAATCACAATAACCACTTGAACGT	MLSB	protection
<i>ermF</i>	CAGCTTTGGTTGAACATTTACGAA	AAATTCTCTAAAATCACAACCGACAA	MLSB	protection
<i>erm(36)</i>	GGCGGACCGACTTGCAT	TCTGCGTTGACGACGGTTAC	MLSB	protection
<i>ermB</i>	TAAAGGGCATTAAACGACGAAACT	TTTATACCTCTGTTTGTTAGGGAATTGAA	MLSB	protection
<i>ermT</i>	GTTCACTAGCACTATTTTTAATGACAGAAGT	GAAGGGTGTCTTTTTAATACAATTAACGA	MLSB	protection
<i>ermX</i>	GCTCAGTGGTCCCCATGGT	ATCCCCCGTCAACGTTT	MLSB	protection
<i>ermT</i>	GTAAAATCCCTAGAGAATACTTTCATCCA	TGAGTGATATTTTTGAAGGGTGTCTT	MLSB	protection
<i>ermY</i>	TTGTCTTTGAAAGTGAAGCAACAGT	TAACGCTAGAGAACGATTTGTATTGAG	MLSB	protection
<i>ermA</i>	TTGAGAAGGGATTTGCGAAAAG	ATATCCATCTCCACCATTAATAGTAAACC	MLSB	protection
<i>ermC</i>	TTTGAAATCGGCTCAGGAAAA	ATGGTCTATTTCAATGGCAGTTACG	MLSB	protection
<i>ermA/ermTR</i>	ACATTTTACCAAGGAACCTGTGGAA	GTGGCATGACATAAACCTTCATCA	MLSB	protection
<i>pikR1</i>	TCGACATGCGTGACGAGATT	CCGCGAATTAGGCCAGAA	MLSB	protection
<i>pikR2</i>	TCGTGGGCCAGGTGAAGA	TTCCCCCTTGCCGGTGAA	MLSB	protection
<i>ereA</i>	CCTGTGGTACGGAGAATTCATGT	ACCGCATTCGCTTTTGCTT	MLSB	deactivate
<i>vgb</i>	AGGGAGGGTATCCATGCAGAT	ACCAAATGCGCCCGTTT	MLSB	deactivate
<i>vgb</i>	CCACGATGGCTGCCTTTG	GGCCATGCAGGACGGATAT	MLSB	deactivate
<i>vgbB</i>	ATACGAGCTGCCTAATAAAGGATCTT	TGTGAACCACAGGGCATTATCA	MLSB	deactivate
<i>mdtA</i>	CCTAACGGGCGTGACTTCA	TTCACCTGTTTCAAGGGTCAAA	MLSB	efflux
<i>erm(34)</i>	GCGCGTTGACGACGATTT	TGGTCATACTCGACGGCTAGAAC	MLSB	protection
<i>lmrA</i>	TTCAGATGCAATGGCGTTTG	ATAATCGGGAACATAATGAGCATAACTAC	MLSB	efflux
<i>mefA</i>	CCGTAGCATTGGAACAGCTTTT	AAACGGAGTATAAGAGTGCTGCAA	MLSB	efflux
<i>mphA</i>	CTGACGCGCTCCGTGTT	GGTGGTGCATGGCGATCT	MLSB	deactivate
<i>mphB</i>	CGCAGCGCTTGATCTTGAG	TTACTGCATCCATACGCTGCTT	MLSB	deactivate

<i>mphA</i>	TGATGACCCTGCCATCGA	TTGCGAGCCCCCTCTTC	MLSB	deactivate
<i>mphC</i>	CGTTTGAAGTACCGAATTGGAAA	GCTGCGGGTTTGCCTGTA	MLSB	deactivate
<i>InuB</i>	TGAACATAATCCCCTCGTTTAAAGAT	TAATTGCCCTGTTTCATCGTAAATAA	MLSB	deactivate
<i>InuB</i>	AAAGGAGAAGGTGACCAATACTCTGA	GGAGCTACGTCAAACAACCAAGT	MLSB	deactivate
<i>vatD</i>	TGCAATAGTAGCTGCTAATTCTGTTGTT	TGTTTTATTTCGTTAGCAGGATTTCC	MLSB	deactivate
<i>vatE</i>	GGTGCCATTATCGGAGCAAAT	TTGGATTGCCACCGACAAT	MLSB	deactivate
<i>vatB</i>	GGAAAAAGCAACTCCATCTCTTGA	TCCTGGCATAACAGTAACATTCTGA	MLSB	deactivate
<i>vatC</i>	CGGAAATTGGGAACGATGTT	GCAATAATAGCCCCGTTTCCTA	MLSB	deactivate
<i>InuA</i>	TGACGCTCAACACACTCAAAAA	TTCATGCTTAAGTTCCATACGTGAA	MLSB	deactivate
<i>vatE</i>	GACCGTCCTACCAGGCGTAA	TTGGATTGCCACCGACAATT	MLSB	deactivate
<i>vatB</i>	TTGGGAAAAAGCAACTCCATCT	CAATCCACACATCATTTCCAACA	MLSB	deactivate
<i>vatC</i>	CGATGTTTGGATTGGACGAGAT	GCTGCAATAATAGCCCCGTTT	MLSB	deactivate
<i>InuA</i>	AGAATGAAAAAGAAGCTGAGCTTCTT	AAGGTGGCAATTACGTTTTTCAAA	MLSB	deactivate
<i>InuC</i>	TGGTCAATATAACAGATGTAAACCAGATTT	CACCCCAGCCACCATCAA	MLSB	deactivate
<i>tnpA</i>	AATTGATGCGGACGGCTTAA	TCACCAAACCTGTTTATGGAGTCGTT	IS6 Group	transposase
<i>IS613</i>	AGGTTCCGACTCAATGCAACA	TTCAGCACATAACCGCCTTGAT	IS613	transposase
<i>tnpA</i>	CATCATCGGACGGACAGAATT	GTCGGAGATGTGGGTGTAGAAAGT	IS21 Group	transposase
<i>tnpA</i>	CCGATCACGGAAGCTCAAG	GGCTCGCATGACTTCAATC	IS6 Group	transposase
<i>tnpA</i>	GAAACCGATGCTACAATATCCAATTT	CAGCACCGTTTGCAGTGTAAG	ISEcp1B	transposase
<i>tnpA</i>	GCCGCACTGTCGATTTTTATC	GCGGGATCTGCCACTTCTT	IS6 Group	transposase
<i>Tp614</i>	GGAAATCAACGGCATCCAGTT	CATCCATGCGCTTTTGTCTCT	Tp614	transposase
<i>tnpA</i>	GGGCGGGTCGATTGAAA	GTGGGCGGGATCTGCTT	IS4 Group	transposase
<i>tnpA</i>	TGCAGATGGTTTAACCTTGGATATT	TCGGTTCATCAAACCTGCTTCAC	IS6 Group	transposase
<i>marR</i>	GCGGCGTACTGGTGAAGCTA	TGCCCTGGTCGTTGATGA	other/efflux	efflux
<i>marR</i>	TCTGGCGTTAGCTTACCAGTAC	GTGCAAAGGCTGGATCGAA	other/efflux	efflux
<i>catB8</i>	CACTCGACGCCTTCCAAAG	CCGAGCCTATCCAGACATCATT	other/efflux	deactivate
<i>dfrA1</i>	GGAATGGCCCTGATATTCCA	AGTCTTGCGTCCAACCAACAG	other/efflux	deactivate
<i>dfrA12</i>	CCTCTACCGAACCGTCACACA	GCGACAGCGTTGAAACAACACTAC	other/efflux	deactivate
<i>folA</i>	CGAGCAGTTCCTGCCAAAG	CCCAGTCATCCGGTTCATAATC	other/efflux	deactivate
<i>bexA</i>	GCGGATCTCTGGTCAGCAA	TGATTGATGGTTCCCCGTACA	other/efflux	efflux
<i>cmr</i>	CGGCATCGTCAGTGGAATT	CGGTTCCGAAAAAGATGGAA	other/efflux	efflux
<i>sdeB</i>	CACTACCGCTTCCGCACTTAA	TGAAAAAACGGGAAAAAGTCCAT	other/efflux	efflux
<i>ereB</i>	GCTTTATTTACAGGAGGCGGAAT	TTTTAAATGCCACAGCACAGAATC	other/efflux	deactivate

<i>fosX</i>	GATTAAGCCATATCACTTTAATTGTGAAAG	TCTCCTTCCATAATGCAAATCCA	other/efflux	deactivate
<i>mepA</i>	ATCGGTCGCTCTTCGTTTAC	ATAAATAGGATCGAGCTGCTGGAT	other/efflux	efflux
<i>emrD</i>	CTCAGCAGTATGGTGGTAAGCATT	ACCAGGCGCCGAAGAAC	other/efflux	efflux
<i>mdet11</i>	ATACAGCAGTGGATATTGGTTTAATTGT	TGCATAAGGTGAATGTTCCATGA	other/efflux	efflux
<i>yceE/mdtG</i>	TGGCACAAAATATCTGGCAGTT	TTGTGTGGCGATAAGAGCATTAG	other/efflux	efflux
<i>yceE/mdtG</i>	TTATCTGTTTTCTGCTCACCTTCTTTT	GCGTGGTGACAAACAGGCTTA	other/efflux	efflux
<i>yceL/mdtH</i>	TCGGGATGGTGGGCAAT	CGATAACCGAGCCGATGTAGA	other/efflux	efflux
<i>yceL/mdtH</i>	CGCGTGAAACCTTAAGTGCTT	AGACGGCTAAACCCCATATAGCT	other/efflux	efflux
<i>yceL/mdtH</i>	CTGCCGTTAAATGGATGTATGC	ACTCCAGCGGGCGATAGG	other/efflux	efflux
<i>rarD</i>	GCGGGTGTGGTCACTACGAT	AGCGTTGGGCCGATATACTG	other/efflux	efflux
<i>rarD</i>	TGACGCATCGCGTGATCT	AAATTTTCTGTGGCGTCTGAATC	other/efflux	efflux
<i>qacA/qacB</i>	TTTAGGCAGCCTCGCTTCA	CCGAATCCAAATAAAACCCAATAA	other/efflux	efflux
<i>yjaR</i>	CCGTTGCAAGAAGATTATAGAAAAA	CAAGCATAAGACCGCATAAATGAT	other/efflux	deactivate
<i>fosB</i>	TCACTGTAATAATGAAGCATTAGACCAT	CCATCTGGATCTGTAAAGTAAAGAGATC	other/efflux	deactivate
<i>bacA</i>	CGGCTTCGTGACCTCGTT	ACAATGCGATAACCAGGCAAAT	other/efflux	deactivate
<i>bacA</i>	TTCCACGACACGATTAAGTCATTG	CGGCTCTTTCGGCTTCAG	other/efflux	deactivate
<i>nimE</i>	TGCGCCAAGATAGGGCATA	GTCGTGAATTCGGCAGGTTTA	other/efflux	unknown
<i>imiR</i>	CCGGACTAGAGCTTCATGTAAGC	CCCACGCGGTACTCTTGTA	other/efflux	unknown
<i>nisB</i>	GGGAGAGTTGCCGATGTTGTA	AGCCACTCGTTAAAGGGCAAT	other/efflux	unknown
<i>ttgB</i>	TCGCCCTGGATGTACACCTT	ACCATTGCCGACATCAACAAC	other/efflux	efflux
putative multidrug	AATTTTGCCGATTATTGCTGAAA	GATTGTCATCATTGTTTTATCACCAA	other/efflux	efflux
<i>pica</i>	GCAATCGAGGCGGTGTTT	TTGCCGCAGCCAATTCA	other/efflux	unknown
<i>fabK</i>	TTTCAGCTCAGCACTTTGGTCAT	AAGGCATCTTTTTCAGCCAGTTC	other/efflux	deactivate
<i>ceoA</i>	ATCAACACGGACCAGGACAAG	GGAAAGTCCGCTCACGATGA	other/efflux	efflux
<i>mdtE/yhiU</i>	CGTCGGCGCACTCGTT	TCCAGACGTTGTACGGTAACCA	other/efflux	efflux
<i>acrR</i>	GCGCTGGAGACACGACAAC	GCCTTGCTGCGAGAACAAA	other/efflux	efflux
<i>acrR</i>	GATGATACCCCTGCTGTGAGA	ACCAAACAAGAAGCGCAAGAA	other/efflux	efflux
<i>mtrD</i>	TGCGCGTAGTCGTTTCATCTC	CGTTCCAATTTCTGATGATTG	other/efflux	efflux
<i>mtrE</i>	CGATGTGTCGTTTTGGAAGGT	CCTGCACCATGATTCTCAATA	other/efflux	efflux
<i>mtrD</i>	GGTCGGCACGCTCTTGTC	TGAAGAATTTGCGCACCCTAC	other/efflux	efflux
<i>mtrD</i>	CCGCCAAGCCGATATAGACA	GGCCGGGTTGCCAAA	other/efflux	efflux
<i>oprD</i>	ATGAAGTGGAGCGCCATTG	GGCCACGGCGAACTGA	other/efflux	efflux
<i>ttgA</i>	ACGCCAATGCCAAACGATT	GTCACGGCGCAGCTTGA	other/efflux	efflux

<i>mtrC</i>	GGACGGGAAGATGGTCCAA	CGTAGCGTTCGGGTTGAT	other/efflux	efflux
<i>mtrC</i>	CGGAGTCCATCGACCATTTG	ATCGTCGGCAAGGAGAATCA	other/efflux	efflux
<i>tolC</i>	GGCCGAGAACCTGATGCA	AGACTTACGCAATTCCGGGTTA	other/efflux	efflux
<i>tolC</i>	CAGGCAGAGAACCTGATGCA	CGCAATTCCGGGTTGCT	other/efflux	efflux
<i>tolC</i>	GCCAGGCAGAGAACCTGATG	CGCAATTCCGGGTTGCT	other/efflux	efflux
<i>qacH</i>	GTGGCAGCTATCGCTTGAT	CCAACGAACGCCACAA	other/efflux	efflux
<i>qacH</i>	CATCGTGCTTGTCGAGCTA	TGAACGCCCAGAAGTCTAGTTTT	other/efflux	efflux
<i>qacEΔ1</i>	TCGCAACATCCGCATTAATA	ATGGATTTTCAAGACCAGAGAAAGAAA	other/efflux	efflux
<i>qacEΔ1</i>	CCCCTTCCGCCGTTGT	CGACCAGACTGCATAAGCAACA	other/efflux	efflux
<i>qac</i>	CAATAATAACCGAAATAATAGGGACAAGTT	AATAAGTGTTCTAGTGTTGGCCATAG	other/efflux	efflux
<i>qacA</i>	TGGCAATAGGAGCTATGGTGTTT	AAGGTAACACTATTTTCGGTCCAAATC	other/efflux	efflux
<i>sat4</i>	GAATGGGCAAAGCATAAAAACTTG	CCGATTTTGAAACCACAATTATGATA	other/efflux	deactivate
<i>speA</i>	GCAAGAGGTATTTGCTCAACAAGA	CAGGGTCACCCTCATAAAGAAAA	other/efflux	unknown
<i>sul2</i>	TCATCTGCCAAACTCGTCGTTA	GTCAAAGAACGCCGCAATGT	Sulfonamide	protection
<i>sul1</i>	CAGCGCTATGCGCTCAAG	ATCCCGCTGCGCTGAGT	Sulfonamide	protection
<i>sulA/foIP</i>	CAGGCTCGTAAATTGATAGCAGAAG	CTTTCCTTGCGAATCGCTTT	Sulfonamide	protection
<i>sulA/foIP</i>	GCGATTGCAAGGAAAAGTGA	CACATGGGCCATTTTTTCATC	Sulfonamide	protection
<i>sulA/foIP</i>	CACGGCTTCGGCTCATGT	TGCCATCCTGTGACTAGCTACGT	Sulfonamide	protection
<i>tetU</i>	GTGGCAAAGCAACGGATTG	TGCGGGCTTGCAAACTATC	Tetracycline	unknown
<i>tetU</i>	AACAGCGGGTTAAGTGTCAA	ATGGTATCATTAGTTTTCCGACAAT	Tetracycline	unknown
<i>tetX</i>	AAATTTGTTACCGACACGGAAGTT	CATAGCTGAAAAAATCCAGGACAGTT	Tetracycline	unknown
<i>tet(37)</i>	GAGAACGTTGAAAAGGTGGTGAA	AACCAAGCCTGGATCAGTCTCA	Tetracycline	unknown
<i>tet(35)</i>	ACCCCATGACGTACCTGTAGAGA	CAACCCACACTGGCTACCAGTT	Tetracycline	unknown
<i>tet(34)</i>	CTTAGCGCAAACAGCAATCAGT	CGGTGATACAGCGCGTAAACT	Tetracycline	unknown
<i>tet(36)</i>	AGAATACTCAGCAGAGGTCAGTTCCT	TGGTAGGTCGATAACCCGAAAAT	Tetracycline	protection
<i>tet(32)</i>	CCATTACTTCGGACAACGGTAGA	CAATCTCTGTGAGGGCATTAAACA	Tetracycline	protection
<i>tetO</i>	ATGTGGATACTACAACGCATGAGATT	TGCCTCCACATGATATTTTCCT	Tetracycline	protection
<i>tetQ</i>	CGCCTCAGAAGTAAGTTCATACACTAAG	TCGTTTCATGCGGATATTATCAGAAT	Tetracycline	protection
<i>tetM</i>	CATCATAGACACGCCAGGACATAT	CGCCATCTTTTGCAGAAATCA	Tetracycline	protection
<i>tetW</i>	ATGAACATTCCCACCGTTATCTTT	ATATCGGCGGAGAGCTTATCC	Tetracycline	protection
<i>tetO</i>	CAACATTAACGGAAAGTTTATTGTATACCA	TTGACGCTCCAAATTCATTGTATC	Tetracycline	protection
<i>tetM</i>	TAATATTGGAGTTTTAGCTCATGTTGATG	CCTCTCTGACGTTCTAAAAGCGTATTAT	Tetracycline	protection
<i>tetS</i>	TTAAGGACAACTTTCTGACGACATC	TGTCTCCCATTGTTCTGGTTCA	Tetracycline	protection

<i>tetPB</i>	ACACCTGGACACGCTGATTTT	ACCGTCTAGAACGCGGAATG	Tetracycline	protection
<i>tetPB</i>	TGATACACCTGGACACGCTGAT	CGTCCAAAACGCGGAATG	Tetracycline	protection
<i>tetPB</i>	TGGGCGACAGTAGGCTTAGAA	TGACCCTACTGAAACATTAGAAATATACCT	Tetracycline	protection
<i>tetPB</i>	AGTGGTGCAAATACTGAAAAAGTTGT	TTTGTTCCCTTCGTTTTGGACAGA	Tetracycline	protection
<i>tetPB</i>	CTGAAGTGGAGCGATCATTCC	CCCTCAACGGCAGAAATAACTAA	Tetracycline	protection
<i>tetT</i>	CCATATAGAGGTTCCACCAAATCC	TGACCCTATTGGTAGTGGTTCTATTG	Tetracycline	protection
<i>tet(36)</i>	TGCAGGAAAGACCTCCATTACAG	CTTTGTCCACACTTCCACGTACTATG	Tetracycline	protection
<i>tetA</i>	GCTGTTTGTCTGCCGAAAA	GGTTAAGTTCTTGAACGCAAAC	Tetracycline	efflux
<i>tetPA</i>	AGTTGCAGATGTGTATAGTCGTAACTATCTATT	TGCTACAAGTACGAAAAACAACTAGAA	Tetracycline	efflux
<i>tetD</i>	TGCCGCGTTTGATTACACA	CACCAGTGATCCCGGAGATAA	Tetracycline	efflux
<i>tetR</i>	ATGAGTTCGGCCAGAAATTTCC	GGTTGTGCGCGAAATGATT	Tetracycline	efflux
<i>tetA</i>	CTCACCAGCCTGACCTCGAT	CACGTTGTTATAGAAGCCGCATAG	Tetracycline	efflux
<i>tetB</i>	AGTGCGCTTTGGATGCTGTA	AGCCCCAGTAGCTCCTGTGA	Tetracycline	efflux
<i>tetC</i>	CATATCGCAATACATGCGAAAAA	AAAGCCGCGGTAAATAGCAA	Tetracycline	efflux
<i>tetG</i>	TCAACCATTGCCGATTCGA	TGGCCCGGCAATCATG	Tetracycline	efflux
<i>tetK</i>	CAGCAGTCATTGGAAAATTATCTGATTATA	CCTTGTAATAACCTACCAAAAATCAAAATA	Tetracycline	efflux
<i>tetH</i>	TTTGGGTCATCTTACCAGCATTAA	TTGCGCATTATCATCGACAGA	Tetracycline	efflux
<i>tetD</i>	TGTCATCGCGCTGGTGATT	CATCCGCTTCCGGGAGAT	Tetracycline	efflux
<i>tetG</i>	CATCAGCGCCGGTCTTATG	CCCCATGTAGCCGAACCA	Tetracycline	efflux
<i>tetB</i>	GCCCAGTGCTGTTGTTGTCAT	TGAAAGCAAACGGCCTAAATACA	Tetracycline	efflux
<i>tetL</i>	AGCCCGATTTATTCAAGGAATTG	CAAATGCTTTCCCCCTGTTCT	Tetracycline	efflux
<i>tetL</i>	ATGGTTGTAGTTGCGCGCTATAT	ATCGCTGGACCGACTCCTT	Tetracycline	efflux
<i>tetR</i>	CGCGATAGACGCCTTCGA	TCCTGACAACGAGCCTCCTT	Tetracycline	efflux
<i>tetR</i>	CGCGATGGAGCAAAAAGTACAT	AGTGAAAAACCTTGTTGGCATAAAA	Tetracycline	efflux
<i>tetC</i>	ACTGGTAAGGTAAACGCCATTGTC	ATGCATAAACCCAGCCATTGAGTAAG	Tetracycline	efflux
<i>tetV</i>	GCGGGAACGACGATGTATATC	CCGCTATCTCACGACCATGAT	Tetracycline	efflux
<i>tetJ</i>	GGGTGCCGCATTAGATTACCT	TCGTCCAATGTAGAGCATCCATA	Tetracycline	efflux
<i>tet(38)</i>	TTAATGTGGCGGTATCTGTAGGTATT	TTGCCTGGGAAATTTAATGCTTT	Tetracycline	efflux
<i>tetE</i>	TTGGCGCTGTATGCAATGAT	CGACGACCTATGCGATCTGA	Tetracycline	efflux
<i>vanA</i>	AAAAGGCTCTGAAAACGCAGTTAT	CGGCCGTTATCTTGTAACAAACAT	Vancomycin	protection
<i>vanRA</i>	CCCTTACTCCCACCGAGTTTT	TTCGTGCCCCATATCTCAT	Vancomycin	protection
<i>vanRA</i>	CCACTCCGGCCTTGTTCATT	GCTAACCACATTCCCCTTGTTTT	Vancomycin	protection
<i>vanSA</i>	CGCGTCATGCTTTCAAATTC	TCCGCAGAAAGCTCAATTTGTT	Vancomycin	protection

vanXA	CGCTAAATATGCCACTTGGGATA	TCAAAAGCGATTGAGCCAACT	Vancomycin	protection
vanB	TTGTCGGCGAAGTGGATCA	AGCCTTTTTCCGGCTCGTT	Vancomycin	protection
vanB	CCGGTCGAGGAACGAAATC	TCCTCCTGCAAAAAAGATCAAC	Vancomycin	protection
vanHB	GAGGTTTCCGAGGCGACAA	CTCTCGGCGGCAGTCGTAT	Vancomycin	protection
vanWB	CGGACAAAGATACCCCTATAAAG	AAATAGTAAATTGCTCATCTGGCACAT	Vancomycin	protection
vanXB	AGGCACAAAATCGAAGATGCTT	GGGTATGGCTCATCAATCAACTT	Vancomycin	protection
vanRB	GCCCTGTCGGATGACGAA	TTACATAGTCGTCTGCCTCTGCAT	Vancomycin	protection
vanSB	GCGCGGCAAAATGACAAC	TTTGCCATTTTATTCGCACTGT	Vancomycin	protection
vanYB	GGCTAAAGCGGAAGCAGAAA	GATATCCACAGCAAGACCAAGCT	Vancomycin	protection
vanC	ACAGGGATTGGCTATGAACCAT	TGACTGGCGATGATTTGACTATG	Vancomycin	protection
vanC	CCTGCCACAATCGATCGTT	CGGCTTCATTCCGGCTTGATA	Vancomycin	protection
vanC	AAATCAATACTATGCCGGGCTTT	CCGACCGCTGCCATCA	Vancomycin	protection
vanTC	CACACGCATTTTTTCCCATCTAG	CAGCCAACAGATCATCAAAACAA	Vancomycin	protection
vanC1	AGGCGATAGCGGGTATTGAA	CAATCGTCAATTGCTCATTTCC	Vancomycin	protection
vanC2/vanC3	TTTGA CTGTCGGTGCTTGTA	TCAATCGTTTTCAGGCAATGG	Vancomycin	protection
vanRC	TGCGGGAAAACTGAACGA	CCCCCATAACGGTTTTGATTA	Vancomycin	protection
vanRC4	AGTGCTTTGGCTTATCTCGAAAA	TCCGGCAGCATCACATCTAA	Vancomycin	protection
vanSC	ATCAACTGCGGGAGAAAACTCT	TCCGCTGTTCCGCTTCTT	Vancomycin	protection
vanSC	GCCATCAGCGAGTCTGATGA	CAGCTGGGATCGTTTTTCCTT	Vancomycin	protection
vanTC	ACAGTTGCCGCTGGTGAAG	CGTGGCTGGTCGATCAAAA	Vancomycin	protection
vanD	CAGAGGAACATAATGTTTCGATAAAATCT	GCCGGATTTTGTGATTCCAA	Vancomycin	protection
vanHD	GTGGCCGATTATACCGTCATG	CGCAGGTCATTGAGGCAAT	Vancomycin	protection
vanXD	TAAACCGTGTTATGGGAACGAA	GCGATAGCCGTCCCATAAGA	Vancomycin	protection
vanRD	TTATAATGGCAAGGATGCACTAAAGT	CGTCTACATCCGGAAGCATGA	Vancomycin	protection
vanYD	AAGGCGATACCCTGACTGTCA	ATTGCCGGACGGAAGCA	Vancomycin	protection
vanYD	CAAACGGAAGAGAGGTCACTTACA	CGGACGGTAATAGGGACTGTTC	Vancomycin	protection
vanSE	TGGCCGAAGAAGCAGGAA	CAATAATACTCGTCAAAGGAGTTCTCA	Vancomycin	protection
vanTE	GTGGTGCCAAGGAAGTTGCT	CGTAGCCACCGCAAAAAAAT	Vancomycin	protection
vanWG	ACATTTTCATTTTGGCAGCTTGAC	CCGCCATAAGAGCCTACAATCT	Vancomycin	protection
vanG	ATTTGAATTGGCAGGTATACAGGTTA	TGATTTGTCTTTGTCCATACATAATGC	Vancomycin	protection
vanTG	CGTGTAGCCGTTCCGTTCTT	CGGCATTACAGGTATATCTGGAAA	Vancomycin	protection

Table A-3 Absolute abundance of ARGs and MGEs detected in wastewater and DDHS effluents and their corresponding removal rates. Blue shading shows persistent ARG in samples; yellow shading shows unique ARG in particular sample.

ARDB gene name	Classification	Influent (copies/L)	R-S0 (copies/L)	Removal (%)	R-S10 (copies/L)	Removal (%)	R-S20 (copies/L)	Removal (%)	R-S30 (copies/L)	Removal (%)
<i>aac6ib</i>	Aminoglycoside	6.38E+07	0.00E+00	100.0	4.80E+04	99.9	0.00E+00	100.0	0.00E+00	100.0
<i>aac6ie</i>	Aminoglycoside	5.87E+06	0.00E+00	100.0	0.00E+00	100.0	0.00E+00	100.0	0.00E+00	100.0
<i>aac3ia</i>	Aminoglycoside	2.31E+09	3.58E+06	99.8	3.15E+06	99.9	2.30E+06	99.9	0.00E+00	100.0
<i>ant3ia</i>	Aminoglycoside	3.13E+07	0.00E+00	100.0	0.00E+00	100.0	0.00E+00	100.0	4.65E+07	-48.6
<i>aph3iia</i>	Aminoglycoside	4.14E+08	1.61E+06	99.6	6.17E+05	99.9	7.99E+05	99.8	0.00E+00	100.0
<i>ant2ia</i>	Aminoglycoside	7.86E+08	5.14E+06	99.3	0.00E+00	100.0	0.00E+00	100.0	1.38E+07	98.2
<i>aadA5</i>	Aminoglycoside	2.88E+08	2.73E+05	99.9	0.00E+00	100.0	1.14E+05	100.0	1.77E+07	93.9
<i>ant6ia</i>	Aminoglycoside	9.27E+06	0.00E+00	100.0	1.38E+04	99.9	0.00E+00	100.0	3.00E+06	67.7
<i>aph3ia</i>	Aminoglycoside	0.00E+00	0.00E+00	-	0.00E+00	-	1.20E+04	-	0.00E+00	-
<i>aph33ib</i>	Aminoglycoside	5.14E+06	0.00E+00	100.0	0.00E+00	100.0	0.00E+00	100.0	0.00E+00	100.0
<i>aph6id</i>	Aminoglycoside	1.08E+09	1.93E+06	99.8	7.32E+05	99.9	5.34E+05	100.0	0.00E+00	100.0
Summary:		4.99E+09	1.25E+07	-	4.56E+06	-	3.23E+06	-	8.11E+07	-
<i>bl1_ampC</i>	β _Lactamase	0.00E+00	0.00E+00	-	3.37E+04	-	0.00E+00	-	0.00E+00	-
<i>bl1_ec</i>	β _Lactamase	0.00E+00	0.00E+00	-	0.00E+00	-	0.00E+00	-	7.55E+05	-
<i>bl1_ec(ampC)</i>	β _Lactamase	0.00E+00	2.27E+05	-	0.00E+00	-	0.00E+00	-	0.00E+00	-
<i>bl1_ampc</i>	β _Lactamase	9.22E+06	0.00E+00	100.0	0.00E+00	100.0	0.00E+00	100.0	0.00E+00	100.0
<i>bl2a_iii</i>	β _Lactamase	0.00E+00	0.00E+00	-	3.49E+04	-	0.00E+00	-	0.00E+00	-
<i>bl1_cmy2</i>	β _Lactamase	3.64E+07	0.00E+00	100.0	0.00E+00	100.0	0.00E+00	100.0	0.00E+00	100.0
<i>bl2be_ctxm</i>	β _Lactamase	2.93E+07	0.00E+00	100.0	0.00E+00	100.0	0.00E+00	100.0	0.00E+00	100.0
<i>bl2_ges</i>	β _Lactamase	4.21E+07	0.00E+00	100.0	0.00E+00	100.0	0.00E+00	100.0	4.18E+05	99.0
<i>bl2d_oxa1/bl2d_oxa30</i>	β _Lactamase	1.72E+08	5.85E+05	99.7	3.49E+04	100.0	8.86E+04	99.9	4.68E+06	97.3
<i>bl2d_oxa10</i>	β _Lactamase	1.08E+09	3.65E+06	99.7	1.38E+06	99.9	1.46E+06	99.9	2.92E+07	97.3
<i>blaSFO</i>	β _Lactamase	3.98E+07	0.00E+00	100.0	0.00E+00	100.0	0.00E+00	100.0	0.00E+00	100.0

<i>bl2be_shv2</i>	β_Lactamase	1.21E+07	0.00E+00	100.0	0.00E+00	100.0	0.00E+00	100.0	0.00E+00	100.0
<i>bl2b_tem1</i>	β_Lactamase	6.58E+07	0.00E+00	100.0	0.00E+00	100.0	0.00E+00	100.0	0.00E+00	100.0
<i>bl2_veb</i>	β_Lactamase	8.55E+06	0.00E+00	100.0	0.00E+00	100.0	0.00E+00	100.0	0.00E+00	100.0
<i>bl2e_cfxa</i>	β_Lactamase	4.15E+08	1.52E+06	99.6	0.00E+00	100.0	4.58E+05	99.9	1.17E+07	97.2
<i>bl3_cpha</i>	β_Lactamase	5.25E+07	7.18E+06	86.3	8.78E+04	99.8	0.00E+00	100.0	7.12E+05	98.6
<i>fox5</i>	β_Lactamase	1.05E+08	4.04E+06	96.2	0.00E+00	100.0	0.00E+00	100.0	0.00E+00	100.0
Summary:		2.06E+09	1.72E+07	99.2	1.57E+06	99.9	2.01E+06	99.9	4.75E+07	97.7
<i>cata1</i>	FCA	2.62E+06	0.00E+00	100.0	0.00E+00	100.0	0.00E+00	100.0	0.00E+00	100.0
<i>catb3</i>	FCA	1.31E+07	0.00E+00	100.0	1.26E+04	99.9	0.00E+00	100.0	0.00E+00	100.0
<i>catb8</i>	FCA	3.03E+06	0.00E+00	100.0	0.00E+00	100.0	0.00E+00	100.0	0.00E+00	100.0
<i>cml_e1</i>	FCA	0.00E+00	4.15E+05	-	0.00E+00	-	0.00E+00	-	0.00E+00	-
<i>cmx(A)</i>	FCA	0.00E+00	0.00E+00	-	1.62E+06	-	0.00E+00	-	1.86E+06	-
<i>cml_e3</i>	FCA	0.00E+00	1.20E+06	-	2.38E+05	-	2.43E+05	-	3.79E+06	-
Summary:		1.87E+07	1.62E+06	91.4	1.87E+06	90.0	2.43E+05	98.7	5.65E+06	69.9
<i>erea</i>	MLSB	0.00E+00	0.00E+00	-	0.00E+00	-	3.36E+04	-	0.00E+00	-
<i>erm36</i>	MLSB	0.00E+00	5.01E+05	-	0.00E+00	-	0.00E+00	-	0.00E+00	-
<i>ermb</i>	MLSB	7.04E+08	2.33E+05	100.0	3.50E+04	100.0	2.99E+04	100.0	3.21E+06	99.5
<i>ermf</i>	MLSB	1.64E+08	0.00E+00	100.0	1.85E+05	99.9	0.00E+00	100.0	6.47E+06	96.1
<i>lnub</i>	MLSB	4.35E+08	0.00E+00	100.0	4.11E+04	100.0	0.00E+00	100.0	0.00E+00	100.0
<i>matA/mel</i>	MLSB	1.47E+09	7.26E+05	100.0	4.52E+05	100.0	3.62E+05	100.0	8.53E+06	99.4
<i>mpha</i>	MLSB	0.00E+00	2.86E+06	-	0.00E+00	-	0.00E+00	-	2.11E+06	-
<i>msrC</i>	MLSB	1.67E+06	0.00E+00	100.0	0.00E+00	100.0	0.00E+00	100.0	0.00E+00	100.0
<i>pikR2</i>	MLSB	0.00E+00	0.00E+00	-	0.00E+00	-	5.24E+04	-	0.00E+00	-
<i>vate</i>	MLSB	0.00E+00	3.42E+05	-	0.00E+00	-	0.00E+00	-	0.00E+00	-
Summary:		2.77E+09	4.66E+06	99.8	7.13E+05	100.0	4.78E+05	100.0	2.03E+07	99.3

<i>acrA</i>	Multidrug	4.75E+07	0.00E+00	100.0	0.00E+00	100.0	0.00E+00	100.0	8.43E+05	98.2
<i>acrA</i>	Multidrug	0.00E+00	3.19E+05	-	0.00E+00	-	1.41E+05	-	0.00E+00	-
<i>acrb</i>	Multidrug	6.82E+07	0.00E+00	100.0	0.00E+00	100.0	0.00E+00	100.0	4.01E+05	99.4
<i>acrF</i>	Multidrug	0.00E+00	0.00E+00	-	3.89E+04	-	0.00E+00	-	0.00E+00	-
<i>acrR</i>	Multidrug	5.21E+07	0.00E+00	100.0	0.00E+00	100.0	0.00E+00	100.0	0.00E+00	100.0
<i>adea</i>	Multidrug	0.00E+00	9.52E+04	-	0.00E+00	-	0.00E+00	-	0.00E+00	-
<i>emrd</i>	Multidrug	4.60E+07	0.00E+00	100.0	0.00E+00	100.0	0.00E+00	100.0	0.00E+00	100.0
<i>marR</i>	Multidrug	0.00E+00	7.41E+05	-	0.00E+00	-	0.00E+00	-	0.00E+00	-
<i>mdtE/yhiU</i>	Multidrug	0.00E+00	0.00E+00	-	0.00E+00	-	3.34E+04	-	0.00E+00	-
<i>mexf</i>	Multidrug	0.00E+00	2.71E+07	-	0.00E+00	-	0.00E+00	-	0.00E+00	-
<i>mtrC</i>	Multidrug	1.31E+06	0.00E+00	100.0	0.00E+00	100.0	0.00E+00	100.0	0.00E+00	100.0
<i>oprj</i>	Multidrug	0.00E+00	2.19E+06	-	6.09E+05	-	0.00E+00	-	0.00E+00	-
<i>qacEdelta1</i>	Multidrug	5.64E+09	9.24E+07	98.4	3.05E+07	99.5	1.42E+07	99.7	1.78E+08	96.8
<i>qacH</i>	Multidrug	1.12E+09	1.60E+06	99.9	9.01E+05	99.9	0.00E+00	100.0	6.18E+06	99.5
<i>rarD</i>	Multidrug	4.42E+07	0.00E+00	100.0	0.00E+00	100.0	0.00E+00	100.0	0.00E+00	100.0
<i>tolc</i>	Multidrug	0.00E+00	0.00E+00	-	0.00E+00	-	0.00E+00	-	4.83E+06	-
<i>ttgB</i>	Multidrug	0.00E+00	0.00E+00	-	4.43E+04	-	0.00E+00	-	7.59E+06	-
<i>yceE/mdtG</i>	Multidrug	5.85E+07	0.00E+00	100.0	0.00E+00	100.0	0.00E+00	100.0	0.00E+00	100.0
<i>yceL/mdtH</i>	Multidrug	1.17E+08	1.44E+05	99.9	2.53E+04	100.0	2.96E+04	100.0	5.75E+05	99.5
<i>yidy/mdtI</i>	Multidrug	8.17E+07	2.49E+05	99.7	4.22E+04	99.9	4.71E+04	99.9	2.21E+05	99.7
Summary:		7.28E+09	1.25E+08	98.3	3.22E+07	99.6	1.44E+07	99.8	1.99E+08	97.3
<i>baca</i>	other	7.07E+07	0.00E+00	100.0	2.88E+04	100.0	0.00E+00	100.0	1.29E+06	98.2
<i>pncA</i>	other	0.00E+00	1.30E+06	-	0.00E+00	-	0.00E+00	-	0.00E+00	-
<i>sat</i>	other	1.12E+07	0.00E+00	100.0	0.00E+00	100.0	0.00E+00	100.0	0.00E+00	100.0
Summary:		8.20E+07	1.30E+06	98.4	2.88E+04	100.0	0.00E+00	100.0	1.29E+06	98.4

<i>dfra1</i>	Sulfa	7.17E+07	0.00E+00	100.00	0.00E+00	100.00	0.00E+00	100.00	0.00E+00	100.00
<i>folA</i>	Sulfa	3.57E+06	0.00E+00	100.00	0.00E+00	100.00	0.00E+00	100.00	0.00E+00	100.00
	Summary:	7.53E+07	0.00E+00	100.00	0.00E+00	100.00	0.00E+00	100.00	0.00E+00	100.00
<i>tete</i>	Tet	1.07E+08	0.00E+00	100.0	1.91E+05	99.8	1.67E+05	99.8	0.00E+00	100.0
<i>tetg</i>	Tet	0.00E+00	7.99E+06	-	0.00E+00	-	8.67E+05	-	2.09E+07	-
<i>teth</i>	Tet	2.74E+06	0.00E+00	100.0	0.00E+00	100.0	8.64E+03	99.7	0.00E+00	100.0
<i>tetl</i>	Tet	5.43E+08	0.00E+00	100.0	1.35E+05	100.0	2.81E+05	99.9	3.29E+06	99.4
<i>tetm</i>	Tet	1.74E+09	5.36E+05	100.0	7.17E+05	100.0	4.66E+05	100.0	1.55E+07	99.1
<i>teto</i>	Tet	7.43E+08	5.23E+05	99.9	2.12E+05	100.0	0.00E+00	100.0	8.02E+06	98.9
<i>tetpa</i>	Tet	1.48E+07	0.00E+00	100.0	8.30E+04	99.4	0.00E+00	100.0	0.00E+00	100.0
<i>tetpb</i>	Tet	3.29E+07	5.58E+05	98.3	1.06E+04	100.0	0.00E+00	100.0	0.00E+00	100.0
<i>tetq</i>	Tet	8.82E+08	3.74E+06	99.6	6.96E+05	99.9	1.63E+06	99.8	4.32E+07	95.1
<i>tetR</i>	Tet	0.00E+00	0.00E+00	-	2.55E+05	-	2.39E+05	-	0.00E+00	-
<i>tets</i>	Tet	1.08E+07	0.00E+00	100.0	0.00E+00	100.0	0.00E+00	100.0	0.00E+00	100.0
<i>tett</i>	Tet	9.73E+06	0.00E+00	100.0	0.00E+00	100.0	0.00E+00	100.0	0.00E+00	100.0
<i>tetx</i>	Tet	1.23E+08	4.50E+05	99.6	7.67E+04	99.9	3.05E+05	99.8	6.02E+06	95.1
	Summary:	4.21E+09	1.38E+07	99.7	2.38E+06	99.9	3.96E+06	99.9	9.69E+07	97.7
<i>vanb</i>	Vancomycin	0.00E+00	1.73E+05	-	0.00E+00	-	0.00E+00	-	0.00E+00	-
<i>vanhb</i>	Vancomycin	1.40E+07	4.00E+05	97.1	1.63E+04	99.9	2.04E+05	98.5	0.00E+00	100.0
<i>vanwg</i>	Vancomycin	8.18E+06	0.00E+00	100.0	0.00E+00	100.0	0.00E+00	100.0	0.00E+00	100.0
<i>vanxd</i>	Vancomycin	0.00E+00	7.07E+04	-	0.00E+00	-	0.00E+00	-	0.00E+00	-
<i>vanyd</i>	Vancomycin	0.00E+00	0.00E+00	-	0.00E+00	-	3.44E+04	-	0.00E+00	-
	Summary:	2.22E+07	6.44E+05	97.1	1.63E+04	99.9	2.39E+05	98.9	0.00E+00	100.0

MGE		Influent (copies/L)	R-S0 (copies/L)	Removal (%)	R-S10 (copies/L)	Removal (%)	R-S20 (copies/L)	Removal (%)	R-S30 (copies/L)	Removal (%)
<i>CIntI</i>	Integrase	2.86E+09	7.97E+07	97.2	2.39E+07	99.2	8.83E+06	99.7	1.74E+08	93.9
<i>IntI</i>	Integrase	1.11E+09	0.00E+00	100.0	0.00E+00	100.0	0.00E+00	100.0	0.00E+00	100.0
<i>transposase</i>	Transposase	1.11E+09	0.00E+00	100.0	0.00E+00	100.0	0.00E+00	100.0	0.00E+00	100.0
<i>Tn21</i>	Transposase	9.17E+08	2.76E+06	99.7	4.60E+05	99.9	0.00E+00	100.0	2.69E+07	97.1
<i>Tn22</i>	Transposase	0.00E+00	2.14E+06	-	2.92E+06	-	1.95E+06	-	1.25E+07	-
<i>tnpA</i>	Transposase	2.77E+09	0.00E+00	100.0	0.00E+00	100.0	0.00E+00	100.0	4.78E+06	99.8
<i>Tn25</i>	Transposase	0.00E+00	1.41E+08	-	8.81E+06	-	3.98E+06	-	0.00E+00	-
<i>Tn24</i>	Transposase	3.06E+09	8.44E+06	99.7	4.17E+06	99.9	2.16E+06	99.9	3.59E+07	98.8
<i>tp614</i>	Transposase	3.70E+08	1.41E+06	99.6	3.05E+05	99.9	6.90E+05	99.8	1.59E+07	95.7
Summary:		1.22E+10	2.36E+08	98.1	4.06E+07	99.7	1.76E+07	99.9	2.70E+08	97.8

Table A-4 Unique ARGs found in the effluents from each DDHS reactor and also ARGs persistent among the influent and all effluents. General gene classes are noted as well as the primary resistance mechanism associated with each ARG.

Resistance gene ^a	Resistance target or class	Resistance Mechanism
Unique ARGs in R-S0 Effluents		
<i>cml_e1</i>	Chloramphenicol	Efflux
<i>adea</i>	Multidrug	Efflux
<i>marR</i>	Multidrug	Efflux
<i>mexf</i>	Multidrug	Efflux
<i>mphA</i>	MLSB	Deactivate
<i>vate</i>	MLSB	Deactivate
<i>erm36</i>	MLSB	Protection
<i>vanb</i>	Vancomycin	Protection
<i>vanxd</i>	Vancomycin	Protection
<i>pncA</i>	Other	Unknown
Unique ARGs in R-S10 Effluents		
<i>aac6ib</i>	Aminoglycoside	Deactivate
<i>acrF</i>	Multidrug	Efflux
<i>bl2a_iii</i>	β -Lactam	Deactivate
Unique ARGs in R-S20 Effluents		
<i>aph3ia</i>	Aminoglycoside	Deactivate
<i>erea</i>	MLSB	Deactivate
<i>mdtE/yhiU</i>	Multidrug	Efflux
<i>pikR2</i>	MLSB	Protection
<i>vanyd</i>	Vancomycin	Protection
Unique ARGs in R-S30 Effluents		
<i>bl1_ec</i>	β -Lactam	Deactivate
<i>tolc</i>	Multidrug	Efflux
Persistent ARGs in Influent and Effluents		
<i>ant3ia</i>	Aminoglycoside	Deactivate
<i>ant2ia</i>	Aminoglycoside	Deactivate
<i>bl2d_oxa10</i>	β -Lactam	Deactivate
<i>bl2d_oxa1/bl2d_oxa30</i>	β -Lactam	Deactivate
<i>ermb</i>	MLSB	Protection
<i>matA/mel</i>	MLSB	Efflux
<i>qacEdelta1</i>	Multidrug	Efflux
<i>tetm</i>	Tetracycline	Protection
<i>tetq</i>	Tetracycline	Protection
<i>tetx</i>	Tetracycline	Unknown

Table A-5 Spearman's bivariate correlation matrix between ARGs and MGEs that are persistent in all DDHS reactor configurations (*r* values are provided). Significant correlations are noted in bold (*p*-values < 0.05; values provided in brackets). Green shading indicates significant correlations between ARGs and transposase genes, whereas blue shading indicates correlations between ARGs and integron-associated genes.

Genes	<i>ant2ia</i>	<i>bl2d_oxa10</i>	<i>bl2d_oxa/bl2d_oxa30</i>	<i>ermb</i>	<i>matA.mel</i>	<i>qacE_delta1_01</i>	<i>tetM</i>	<i>tetQ</i>	<i>tetX</i>	<i>int1</i>	<i>Cint1</i>	Tn24	tp614
<i>ant3ia</i>	0.900 (0.037)	0.800 (0.104)	0.900 (0.037)	0.700 (0.188)	0.900 (0.037)	0.100 (0.873)	0.900 (0.037)	0.900 (0.037)	0.900 (0.037)	-0.300 (0.624)	0.000 (1.00)	0.600 (0.285)	0.900 (0.037)
<i>ant2ia</i>		0.600 (0.285)	0.700 (0.188)	0.400 (0.505)	0.700 (0.188)	-0.400 (0.505)	0.700 (0.188)	0.700 (0.188)	0.700 (0.188)	-0.500 (0.391)	-0.400 (0.505)	0.300 (0.624)	0.700 (0.188)
<i>bl2d_oxa10</i>			0.900 (0.037)	0.700 (0.188)	0.900 (0.037)	0.100 (0.873)	0.900 (0.037)	0.900 (0.037)	0.900 (0.037)	-0.200 (0.747)	0.200 (0.747)	0.400 (0.505)	0.900 (0.037)
<i>bl2d_oxa.bl2d_oxa30</i>				0.900 (0.037)	1.000	0.100 (0.873)	1.000	1.000	1.000	-0.400 (0.505)	0.100 (0.873)	0.700 (0.188)	1.000
<i>ermb</i>					0.900 (0.037)	0.300 (0.624)	0.900 (0.037)	0.900 (0.037)	0.900 (0.037)	-0.300 (0.624)	0.300 (0.624)	0.900 (0.037)	0.900 (0.037)
<i>matA.mel</i>						0.100 (0.873)	1.000	1.000	1.000	-0.400 (0.505)	0.100 (0.873)	0.700 (0.188)	1.000
<i>qacEdelta1</i>							0.000 (1.00)	0.000 (1.00)	0.000 (1.00)	0.900 (0.037)	0.900 (0.037)	0.300 (0.624)	0.000 (1.00)
<i>tetM</i>								1.000	1.000	-0.400 (0.505)	0.100 (0.873)	0.700 (0.188)	1.000
<i>tetQ</i>									1.000	-0.400 (0.505)	0.100 (0.873)	0.700 (0.188)	1.000
<i>tetX</i>										-0.400 (0.505)	0.100 (0.873)	0.700 (0.188)	1.000
<i>int1</i>											0.800 (0.104)	-0.100 (0.873)	-0.400 (0.505)
<i>Cint1</i>												0.400 (0.505)	0.100 (0.873)
Tn24													0.700 (0.188)

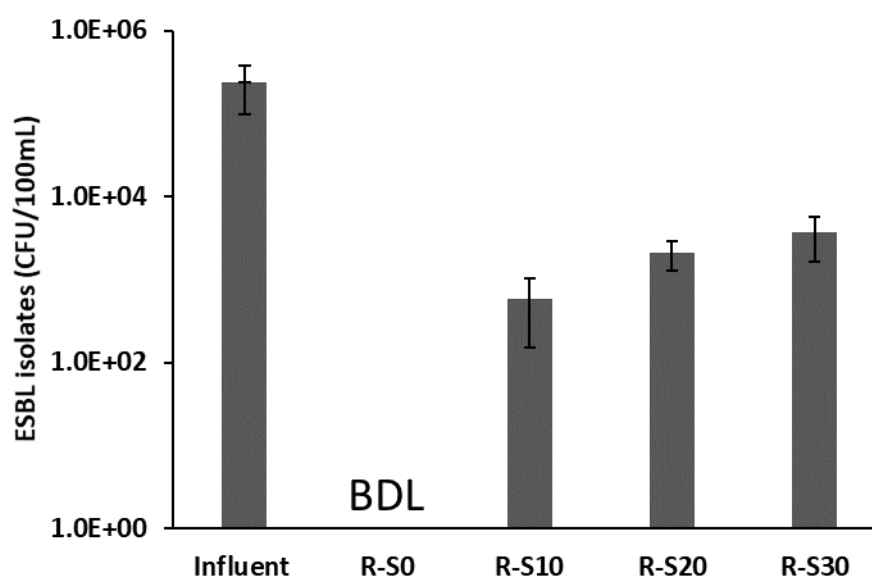
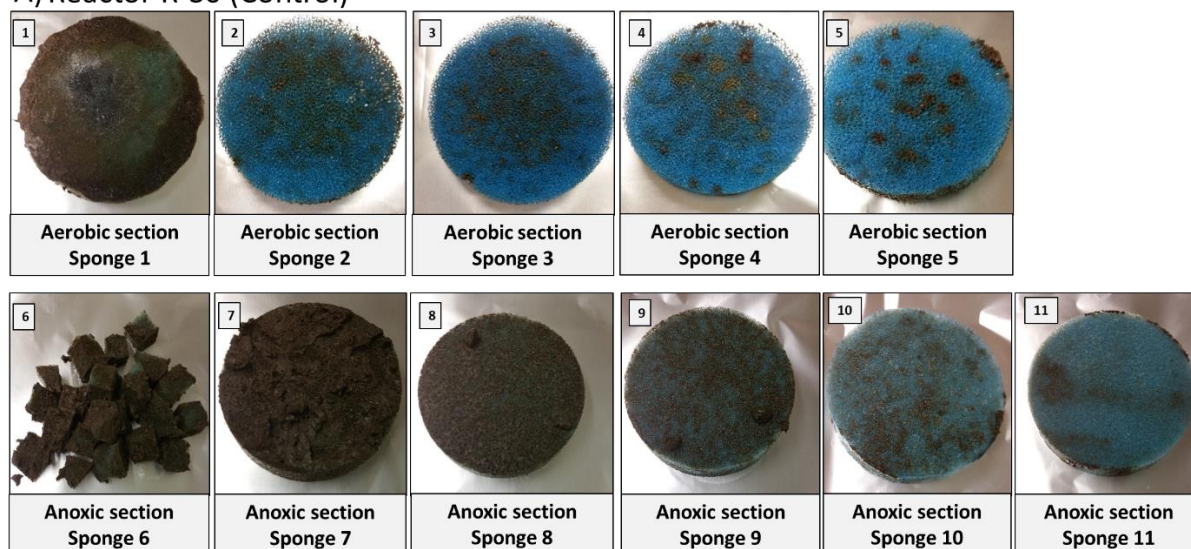


Figure A-1 ESBL *Enterobacteriaceae* isolate abundances in the reactor influent and effluents with different bypass percentages using ChromID ESBL selective chromogenic media (Biomérieux, UK). Presumptive *E.coli* and KESC (*Klebsiella*, *Enterobacter*, *Serratia* and *Citrobacter*) isolates are distinguishable by colour on the chromogenic media. The figure shows CFU concentrations for ESBL-producing *E.coli* plus KESC isolates in influent and treated effluents for different levels of by-pass (R-S0 = 0%, R-S10 = 10%, R-S20 = 20% and R-S30 = 30%). Influent levels are for settled domestic wastewater from a local wastewater treatment plant. BDL denotes below detection limit. Error bars are standard deviations ($n = 4$).

Appendix B

A) Reactor R-S0 (Control)



B) Reactor R-S20 (Co-optimal)

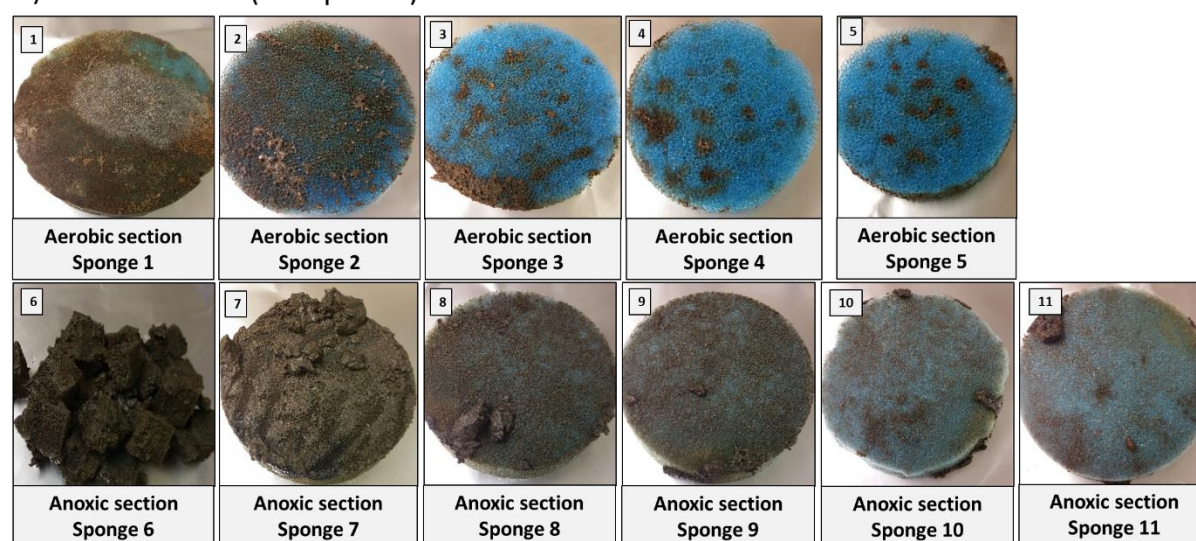


Figure B-1 Sponge discs collected during deconstruction of bench-scale DDHS bioreactors from (A) the Control bioreactor; R-S0 and (B) the Co-optimal bioreactor; R-S20. A total of eleven semi-dried sponge discs were sterilely retrieved from each bioreactor and wrapped in pre-sterile aluminium foil and stored in -80 °C until DNA extraction.

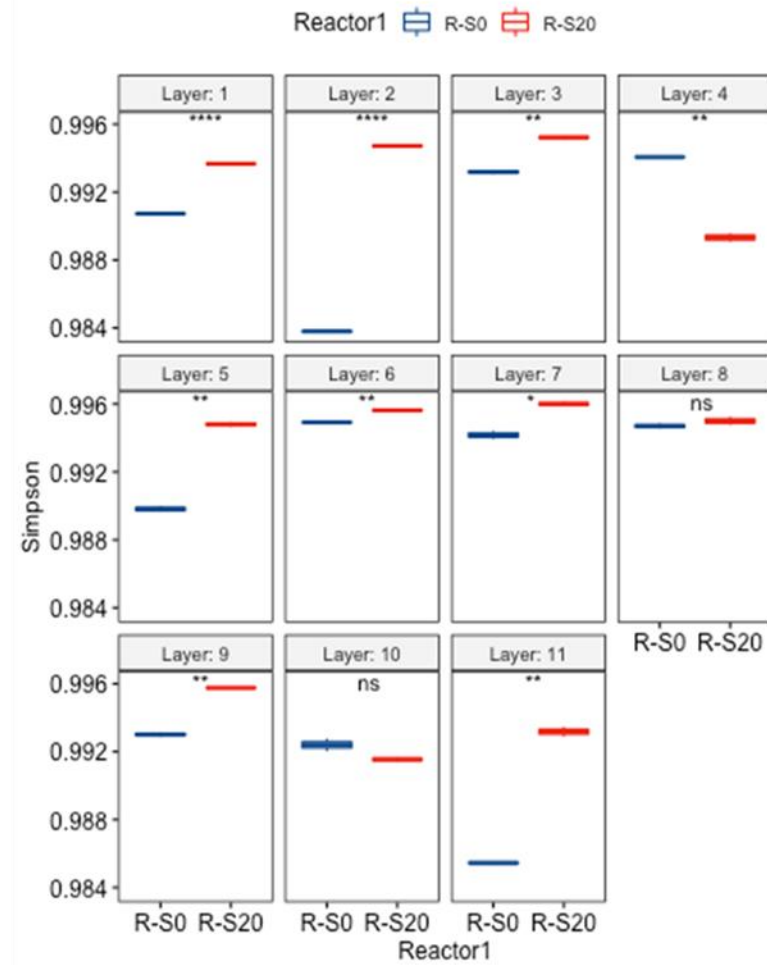
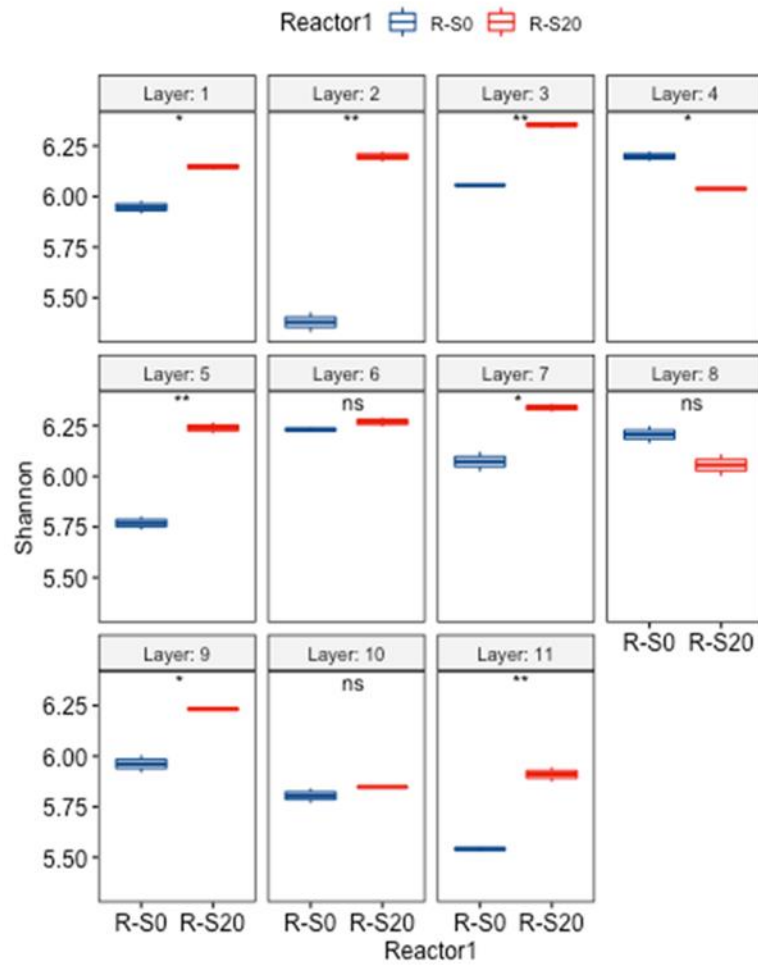


Figure B-2 Shannon and Simpson indices comparisons (i.e., Alpha diversity) by sponge layers and unpaired T-tests between DDHS biofilm samples; a) Shannon indices comparisons; b) Simpson indices comparisons. Asterisk * denotes $p \leq 0.05$; ** denotes $p \leq 0.01$; *** denotes $p \leq 0.001$, **** denotes $p \leq 0.0001$ ns denotes $p > 0.05$.

Table B-1 Relative abundance of core bacterial flora throughout sponge layers along sequential redox habitats

		Bacterial Genera relative abundance (%)							
		<i>Acinetobacter</i>	<i>Pseudomonas</i>	<i>Aeromonas</i>	<i>Chryseobacterium</i>	<i>Nitrosomonas</i>	<i>Nitrospira</i>	<i>Flavobacterium</i>	<i>Shewanella</i>
R-S0 ^a	Aerobic biofilm								
	Sponge 1	7.8	11.1	13.1	4.1	2.0	4.6	1.4	2.2
	Sponge 2	26.3	12.6	7.3	10.2	1.2	5.4	2.7	0.2
	Sponge 3	14.1	9.5	2.4	7.4	1.0	3.9	8.2	0.3
	Sponge 4	5.9	10.2	2.1	6.3	2.1	9.0	3.6	0.1
R-S0 ^a	Anoxic biofilm								
	Sponge 5	14.9	16.2	3.0	5.5	2.1	7.4	4.6	0.4
	Sponge 6	0.4	6.4	1.4	1.3	0.5	2.9	0.2	0.1
	Sponge 7	0.3	3.1	0.6	0.2	0.3	1.8	0.1	0.2
	Sponge 8	0.6	5.7	0.9	0.4	0.4	2.0	0.3	0.1
	Sponge 9	2.9	6.2	0.4	1.0	0.1	1.0	0.9	0.0
	Sponge 10	5.2	5.7	0.1	0.7	0.1	0.2	8.2	0.9
	Sponge 11	15.7	10.8	1.0	2.2	0.2	1.0	11.8	1.0
R-S20 ^b	Aerobic biofilm								
	Sponge 1	1.9	6.9	8.2	0.3	1.7	4.2	0.8	0.9
	Sponge 2	2.6	7.3	2.9	0.7	1.7	3.6	5.5	0.2
	Sponge 3	1.2	5.2	0.7	0.5	2.3	5.6	6.7	0.5
	Sponge 4	2.7	4.6	2.5	1.5	3.4	8.2	16.1	0.6
R-S20 ^b	Anoxic biofilm								
	Sponge 5	0.7	5.8	0.8	0.6	2.3	8.1	4.5	0.4
	Sponge 6	0.8	5.8	1.1	0.0	0.4	2.5	1.5	1.3
	Sponge 7	0.5	4.2	1.2	0.1	0.3	0.8	1.5	0.5
	Sponge 8	1.3	6.0	0.8	0.0	0.2	0.1	1.4	0.1
	Sponge 9	1.2	6.0	0.8	0.2	0.2	0.6	2.9	0.8
	Sponge 10	2.1	5.4	1.3	2.1	0.1	0.1	15.6	0.9
	Sponge 11	2.1	14.1	2.2	0.2	0.2	0.1	12.0	5.9

Notes: ^aR-S0 = Biofilm samples from reactor Control without any bypass; ^bR-S20 = Biofilm samples from reactor Co-optimal with 20% wastewater bypass into the anoxic sponge layers (grey shading).

Appendix C



Health and Safety
Executive

The Genetically Modified Organisms (Contained Use) Regulations 2000

Activity Notification

Notification of intention to conduct individual contained use activities

<ul style="list-style-type: none"> If the activity involves working with a biological agent that is listed on schedule 5 of the Anti-terrorism, Crimes and Security Act 2001, this form should not be e-mailed to HSE because it contains sensitive information. Please print the completed form and send it by post to the Notification Officer, Health & Safety Executive, Building 1.2 Redgrave Court, Merton Road, Bootle, Merseyside L20 7HS. The Schedule 5 list can be found at www.opsi.gov.uk/acts/acts2001/ukpga_20010024_en_18#sch5. The public register sections MUST be understandable without reference to the risk assessment or other supporting documents. Please return your completed form to the Health and Safety Executive at the address given in Notes for Guidance. Please do not feel constrained by the box sizes - expand them or continue on separate sheets if necessary. Important - please refer to Notes for Guidance where identified. Fields marked with an asterisk (*) must be completed before the form is submitted to HSE. 									
FOR HSE USE ONLY									
GM centre reference: GM				Date notification acknowledged:			Date activity ceased:		
Dates on which additional information submitted									
Date on which accident notification submitted									
<input type="checkbox"/> Consent granted (Class 3/4) (to be completed by HSE)									
1. Organisation Details									
* Name of organisation (note 1)				Newcastle University					
* Address				Occupational Health and Safety Service, Newcastle University, King's Gate, Newcastle upon Tyne, NE1 7RU					
* Telephone Number				+44 (0) 191 208 3184		Fax Number			
Email Address				samantha.dainty@ncl.ac.uk					
Address(es) of premises where the activities will actually be conducted (if different from that at Section 1) (note 1a)									
Baddileys-Clark Building, Newcastle University, Rooms 2.26/2.21/1.09 and associated instrument and constant temperature rooms & the Bioreactor Site, Cassie Building, Newcastle University.									
2. Date of premises notification (note 2)									
15/11/93									
* HSE Centre Number									
GM 540									
3. <input type="checkbox"/> Please check if notifying a connected programme of work (note 3)									
4. * Class(es) of activity - check all relevant boxes (note 4)									
<input checked="" type="checkbox"/> Class 2 <input type="checkbox"/> Class 3 <input type="checkbox"/> Class 4 <input type="checkbox"/> Activity involving notifiable non-micro-organisms									

Public Register

Public Register

Public Register

☐ For Class 3 or 4, check box if GMOs are likely to be imported from or exported outside the EC

Activity Notification

5. * Please give a short descriptive title of the activity (or activities)

Use of fluorescent tagged plasmid with known sequence in an E.coli strain isolated from wastewater to assess transmission of mobile genetic elements in a closed wastewater treatment bioreactor.

Public Register

6. * Purpose of the contained use (note 5)

Six wastewater treatment bioreactors have been established to monitor the dissemination of an antibiotic resistance plasmid throughout the reactors from a strain of E. coli to be seeded into the incoming wastewater stream. To distinguish antibiotic resistance genes that occur naturally in the wastewater, the seeded strain will carry a copy of plasmid RP4 into which the gene encoding the green fluorescent protein (GFP) has been cloned (Musovic et al., AEM, 76, 4813-4818 (2010) & EM Rpt 6, 125-130 (2014)).

It will be transferred by conjugation to a wild type E. coli strain isolated from wastewater as the seed organism to investigate the fate of broad host range IncP-1 plasmid during wastewater treatment. The work will be performed in tandem with an on-going bioreactor experiment to study the dynamic of antibiotic resistance genes (ARGs) associated with mobile genetic elements (MGEs) during treatment processes. pRP4 encodes resistance genes for ampicillin, tetracycline and kanamycin. Mass balance of gfp-labelled pRP4- Plac::gfp plasmid will be quantified using flow cytometry (Medical School Flow Cytometry Core Facility) to monitor the conjugal transfer kinetics of the plasmid and the harboured ARGs between commensal bacterial. The experiment will involve the seeding of E. coli donor strain into six wastewater treatment bioreactors to track the transmission of the RP4 plasmid over a time series within the operating treatment cycle. Additionally, the prevalence of the antibiotic resistances encoded by pRP4 will be monitored by plate counts. The frequencies of the target resistances and the GFP signal will provide the required data from horizontal transfer in the bacterial cell population of the individual reactors.

Public Register

7. * Characteristics of the GMO(s) including the evaluation of foreseeable effects (note 6)

Recipient or parental organism

An E.coli strain isolated from domestic wastewater will be used as the seed organism to host the GFP-tagged pRP4 plasmid. The identity of the E. coli was confirmed by the Microbiology Department at the Freeman Hospital and is susceptible to 17 clinical antibiotics including major classes of beta-lactams antibiotics (e.g. Aztreonam, Meropenam, Ertapenam), trimethoprim, ciprofloxacin, etc. A serotype test has also been carried out and has confirmed that the strain is not of the O157 serotype and therefore not shiga toxigenic.

Public Register

* Host / vector system

Plasmid RP4::Plac::gfp (Musovic et al., 2010) has a molecular size 56.4 kb, and encodes resistance against the antibiotics ampicillin, tetracycline and kanamycin. The used of the native pRP4 (ie without the gfp gene) is not subject to GM regulations or other restrictions.

Public Register

* Origins and intended functions of the genetic material involved

The gfp gene has been introduced onto pRP4 to facilitate the monitoring of the transfer of the antibiotic resistance genes associated with pRP4 within the population of cells within the bioreactor. The gfp gene, obtained originally from *Aequorea victoria*, is widely used as a visual and quantifiable reporter gene and is not associated with any toxicity. Its role here is to monitor transfer to other cells in the bioreactor population. Plasmid RP4, subgroup alpha (Thomas, 1981) and tagged with a mini Tn5 insertion of a gfpmut3b gene, is derived from *Pseudomonas putida* KT2440 (Barth et al., 2015). The complete nucleotide sequence pRP4 has been published (Pansegrau et al., 1994). The plasmid will be obtained from Dr Musovic, Technical University of Denmark. The gfp gene will be expressed from the Plac promoter at a medium level of expression.

Plate mating assays will be used to transfer the gfp-labelled plasmid to the indigenous *E. coli*. The resulting transconjugant will be used as the donor strain for the subsequent seeding experiments to track the fate and migration of the plasmid and the associated resistance genes to other indigenous bacteria found in wastewater treatment system. This is a natural process that occurs in wastewater treatment processes. The gfp-labelled pRP4 plasmid will not be subjected to any further modifications.

Public Register

Activity Notification

7. Characteristics of the GMO(s) including the evaluation of foreseeable effects (*cont'd*)

* Evaluation of foreseeable effects

pRP4 is a well-characterised resistance plasmid belonging to the IncP-1 group, which is a promiscuous conjugal plasmid with the ability transfer and replicate in broad range of hosts especially to Gram-negative bacteria. The ability of the pRP4 to replicate and to be maintained in the recipient organisms poses a potential environmental and health risk if released. However, the work will be restricted to Containment Level 2 laboratories in both the Baddiley-Clark and Cassie Buildings. RP4 vector will be introduced in a closed bioreactor systems under contained use and all remnant materials, including the reactor outflow, will be inactivated by autoclaving. The only exception will be small (millilitre volumes) samples taken for FACS and DNA extraction, which will be inactivated during processing.

The primary hazard is the potential of the commensal *E. coli* isolated from domestic wastewater being a pathogenic strain (ACDP Hazard Group 2), which may be carried through the biotreatment processes (activated sludge, secondary treatment biofilms and final effluent) but at much lower concentrations, equivalent to ACDP Hazard Group 2 (Compendium of Guidance). Prof David Graham has an internationally recognised reputation for running bioreactors using wastewater input streams, and the only variation in the proposed experiments is the presence of the gfp gene. As a result there will be no increase in the risk to human health. Ms Jong also has more than two year of experience running wastewater bioreactors. Therefore, under the proposed contained use, the recombinant organism is unlikely to represent an increased risk to human health.

Level of risk is predicted to be low/medium.

Public Register

8. Containment and control measures for GMOs that are not micro-organisms (eg GM animals and plants) (*note 7*)

Not applicable

Public Register

Activity Notification

9. Maximum culture volumes per experiment - for GMMs only (note 8)

(i) Class 2 activities, state approximate culture volume

The maximum volume will be approximately 1 litre.

Public Register

(ii) for Class 3 or Class 4 activities, specify the culture volume

Public Register

10. For GMMs only, indicate the level of containment that will be applied (please check the appropriate box(es)) (note 9)

	Level 2	Level 3	Level 4
Laboratory activities	<input checked="" type="checkbox"/>	<input type="checkbox"/>	<input type="checkbox"/>
Glasshouses	<input type="checkbox"/>	<input type="checkbox"/>	<input type="checkbox"/>
Growthrooms	<input type="checkbox"/>	<input type="checkbox"/>	<input type="checkbox"/>
Animal Units	<input type="checkbox"/>	<input type="checkbox"/>	<input type="checkbox"/>

Public Register

Large scale activities (ie activities to which Table 2, Schedule 8 containment is appropriate)	<input type="checkbox"/>	<input type="checkbox"/>	<input type="checkbox"/>
Human clinical applications	<input type="checkbox"/>	<input type="checkbox"/>	<input type="checkbox"/>

11. For GMMs only - application for any derogation from full containment for the Class of activity (measures and justification) (note 10)

Not applicable

Public Register

Activity Notification

12. * Describe the waste management measures which you will apply to the activity (including the type and form, treatment, degree of kill, proposed process testing / monitoring measures, ultimate form and fate) (note 11)

All contaminated materials, including waste destined for incineration, will be inactivated by autoclaving (100% kill) prior to disposal of waste or cleaning and recycling of reusable laboratory equipment, such as glassware. Autoclaves will be validated by annual thermocouple mapping and each run will be monitored using TST (Time, Steam, and Temperature) test strips (Albert Browne Ltd., TST class 6 emulating indicator 121°C for 20 min). Contaminated materials used in laboratory during the experiment and waste will be disposed of via an appropriate route e.g. sharps in sharps bins, bulk materials in autoclaves. All outflow from bioreactors will be inactivated by means of autoclaving. A limited number of samples will be used for analytical studies (PCR, FACS etc), and these will be inactivated during processing and autoclaved after use.

Public Register

13. * Is an emergency plan required according to regulation 20?

☐ Yes ☒ No

Public Register

☐ If 'Yes', please check to confirm that it is attached to this form

14. ☒ * Please check to confirm that you have attached a risk assessment to this form (note 12)

☐ Please check if you are claiming exemption from disclosure for sections of the risk assessment

Public
Register

15. * Please enter comments of the genetic modification safety committee on the risk assessment (note 13)

The only comment was "My only issue with the risk assessment is that it does not mention the possibility of the strain being HG3. Since it is an unknown strain, it would be useful to have some kind of assurance that it is not verocytotoxicogenic (ie HG3). They may already know this from the identification that was done at the Freeman, but it would be worth stating it explicitly in the risk assessment." The confirmation that the strain was tested at the Freeman Hospital Microbiology Department to confirm it was not verocytotoxicogenic was added to the GMM risk assessment form as requested.

Public Register

Activity Notification

16. Personal Information

* Name of person responsible for supervision and safety of GM activities at the premises

Professor Colin Harwood

Training and qualifications

Professor Harwood, PhD, has more than 35 years experience of working with recombinant strains and will oversee the GM aspects of the work. He has been a member of the local GM committee and has acted as departmental Safety and Radiation protection officers. He has regularly attended GM and biohazard safety courses at the University.

NON DISCLOSURE OF INFORMATION

17. Enter in this section any information required in sections 1-15 which you do not wish disclosed, together with full justification (note 14)

Not applicable

18. Declaration

I am notifying an intention to carry out an activity involving contained use of genetically modified organisms with the authority and approval of the person (organisation or individual) named in section 1 of this form

Name	Professor Colin Harwood		
Position in	Professor of Molecular Microbiology, Newcastle University		
Signed (<i>note 15</i>)		Date	15 th March 2017

If the activity involves working with a biological agent that is listed on schedule 5 of the Anti-terrorism, Crimes and Security Act 2001, this form should not be e-mailed to HSE because it contains sensitive information. Please print the completed form and send it by post to the Notification Officer, Health & Safety Executive, Building 1.2 Redgrave Court, Merton Road, Bootle, Merseyside L20 7HS. The Schedule 5 list can be found at www.opsi.gov.uk/acts/acts2001/ukpga_20010024_en_18#sch5.

**THE GENETICALLY MODIFIED ORGANISMS (CONTAINED USE) REGULATIONS 2000
NOTIFICATION OF INTENTION TO CONDUCT INDIVIDUAL CONTAINED USE ACTIVITIES****NOTES FOR GUIDANCE****Data Protection Act 1998**

This Act requires the Health and Safety Executive (HSE) to inform you that this form may include information about you (this is called "personal data" in the Act) and that we are a "data controller" for the purposes of the Act. HSE will process the data for health, safety and environmental purposes. HSE may disclose these data to any person or organisation for the purposes for which it was collected or where the Act allows disclosure. As data subject, you have the right to ask for a copy of the data and to ask for any inaccurate data to be corrected.

All the information given in sections 1-15 of this form will be placed on HSE's public register of notifications within 14 days of receipt. You may consider that there is information relevant to these sections whose disclosure would adversely affect your organisation's competitive position, intellectual property rights or which you do not wish disclosed on other grounds referred to in the Environmental Information Regulations (EIR) 2004, regulation 12. If so, you should enter such information in section 17 with a full justification for its exemption from disclosure. However, it should always be possible to provide some information in these sections for the public register. The Competent Authority will decide whether the information in section 17 will be exempt from disclosure and will notify you of its decision in writing.

Personal information will not be disclosed unless the individual concerned has given his or her explicit written permission.

Compliance with other legislation

It is important to note that compliance with the provisions of the Contained Use Regulations does not constitute compliance with other relevant legislation. For example, you may also need to apply separately for licences or permits under legislation controlling the plant health, animal scientific procedures, or the introduction of non-indigenous species. For clinical trials involving gene therapy, you will need approval from the Gene Therapy Advisory Committee.

Even if you have fulfilled the requirements of the Contained Use Regulations, and have any necessary consents or approvals under that legislation, you **cannot begin** the activity unless you also have the relevant licences / permits under any other applicable legislation.

Note 1

This will normally be the University, Institution, Company or Organisation. Only rarely will it be necessary to include an individual's name.

Note 1a

If you intend to carry out activities involving GMMs, you must not leave this section blank unless you are claiming exemption from disclosure. If you are claiming that the precise address of the premises where activities with GM animals or plants are to be carried out should not be disclosed, you must include this, together with the justification, in section 17.

Note 2

If you have previously notified your premises, indicate the date of the notification and the HSE reference number assigned (eg GM111). If you have not notified your premises, you will not have a reference number so please contact the notification officer (see note 15) or email notificationofficer@hse.gsi.gov.uk for a GM centre reference number. Note that if not previously notified, you will also have to complete a premises application notification - using the CU1 form provided if you wish - and submit it at the same time as this activity notification. The fee payable in such cases will only be that related to the activity notification.

Note 3

It is permissible to notify a connected programme of work using this form. However, you must include details of all of the component activities in sections 4-15. The fee payable in relation to connected programmes is the fee for the highest Class of activity involved. (notifiable activities involving GM animals and plants are equivalent to Class 2 for this purpose).

Note 4

Please check all applicable boxes. For class 3 and 4: The EC Regulation on transboundary movements of GMOs requires Member States to inform the Biological Clearing House and the European Commission of any decisions on class 3 and class 4 contained use activities involving GMMs that are likely to be subject to transboundary movements. Transboundary movements are those entering or leaving the EC. In order for this information to be collected, please check the box if your class is 3 or 4 GMMs are likely

to be subject to such transboundary movements. Any information you do not wish disclosed should be entered in section 17 together with the justification.

Note 5

Any information you do not wish disclosed should be entered in section 17 together with full justification.

Note 6

For activities involving GMMs, this section **cannot** be left blank unless you have a justified request for non-disclosure in respect of protection of intellectual property rights (IPR). If you are not making a request for non-disclosure in respect of IPR, you must at least include general characteristics of the GMMs involved in the intended activity. Where there are no justifiable requests for non-disclosure, you must include precise details. An evaluation of the foreseeable effects must also be included, in as precise detail as possible. The evaluation of foreseeable effects should include the identity and characteristics of the GMMs indicated by the risk assessment. Include information on hazards to human health and the environment with particular reference to those arising from the modification as opposed to being inherent properties of the host micro-organism (a fuller account of these details will be included in the risk assessment).

For activities involving GMOs which are not micro-organisms (eg GM animals and plants), it is permissible to request non-disclosure for any of the required information, but the second section should still be completed in as precise detail as possible taking into account it may be disclosed. The evaluation of foreseeable effects is required to consider only human health and safety aspects. Any information you do not wish disclosed should be entered in section 17 together with the justification.

Note 7

For activities involving GMOs which are not micro-organisms (eg GM animals and plants), describe the containment and control measures which you will apply to the activity. These should be justified by reference to the risk assessment. Any information you do not wish disclosed should be entered in section 17 together with the justification.

Note 8

Any information you do not wish disclosed should be entered in section 17 together with the justification.

Note 9

You must not leave this section blank.

Note 10

For activities involving GMMs, you will normally need to apply all the measures specified as requirements for the relevant containment level. If, however, your risk assessment indicates that any of those measures are unnecessary, you may ask for permission to omit them by requesting a derogation(s). Indicate any such measures with a brief justification for the derogation that includes references to the relevant parts of the risk assessment. You **cannot** request non-disclosure for the actual containment measures (unless your intellectual property rights might be affected) BUT you may wish to request exemption for the justification. If a request is made for non-disclosure, the exempt information must be included in section 17 together with the justification.

Note 11

Waste management measures which will be applied to the activity must be described. You should take into consideration only the waste consisting of or containing viable GM material. You must specify the type and form of waste(s) generated, their treatment and proposals for testing / monitoring the inactivation process. For activities involving GMMs, this section cannot be left blank unless you are claiming protection for reasons of intellectual property rights. Even if this is not the case, it is permissible not to give precise details if claims for non-disclosure can be justified. For instance, you could say that inactivation is by heat treatment to give 100% kill, but the precise detail of how this is achieved may be commercially confidential information. If a request is made for non-disclosure, the information must be included in section 17 together with the justification.

Note 12

You must attach the risk assessment of the activity to this form. The risk assessment will not be placed on the public register, but will be open to disclosure to members of the public on request (subject to exemption provisions).

If you wish to claim exemption from disclosure for any sections of the risk assessment, please indicate those sections clearly on the risk assessment and set out a full justification for exemption. If a request for information is received and your justification for non-disclosure is accepted, the risk assessment will be disclosed with the exempt sections removed. You are advised to submit a second version of the risk assessment from which those sections have already been removed. If it is decided, in the public's interest, to release the information, you will be informed of this decision in writing.

Note 13

NB Remember that, as well as consulting the genetic modification safety committee on the risk assessment, you must also comply with the Safety Representatives and Safety Committees Regulations 1977 and, where any employees are not in groups covered by trade union safety representatives, you must consult such employees according to the Health and Safety (Consultation with Employees) Regulations 1996. If you do not wish some of the information to be disclosed, the exempt information must be included in section 17 together with the justification.

Note 14

Please enter in this section any information, required in sections 1-15, which you wish to be exempt from public disclosure on grounds that:

- (a) disclosure would harm your organisation's competitive position;
- (b) disclosure would compromise your intellectual property rights; or
- (c) the information falls into one of the other categories for exemption in the EIR Regulations, regulation 12, state which.

For each piece of information entered you must:

- (a) state clearly which the grounds applies. In particular, state which category of exemption allowed by the Environmental Information Regulations 2004 applies, namely disclosure would adversely effect:
 - international relations, defence, national security or public safety
 - the course of justice
 - confidentiality of proceedings
 - commercial / industrial confidentiality
 - intellectual property
 - protection of the environment
- (b) indicate the section of the form to which it is relevant; and
- (c) provide a full justification, explaining why the stated ground for exemption applies

You do not need to enter any personal information as this information is covered by the Data Protection Act and will automatically be treated as confidential.

Note 15

Send the completed form by email to:

notificationofficer@hse.gsi.gov.uk

Or alternatively by post to the address below:

Notifications Officer
Health and Safety Executive
Building 1.2, Redgrave Court
Merton Road
Bootle
Merseyside
L20 7HS

Tel: 0151 951 4718
Fax: 0151 951 3474

Note 16

If the activity involves working with a biological agent that is listed on schedule 5 of the Anti-terrorism, Crimes and Security Act 2001, this form should not be e-mailed to HSE because it contains sensitive information. Please print the completed form and send it by post to the Notification Officer, Health & Safety Executive, Building 1.2 Redgrave Court, Merton Road, Bootle, Merseyside L20 7HS. The Schedule 5 list can be found at www.opsi.gov.uk/acts/acts2001/ukpga_20010024_en_18#sch5.

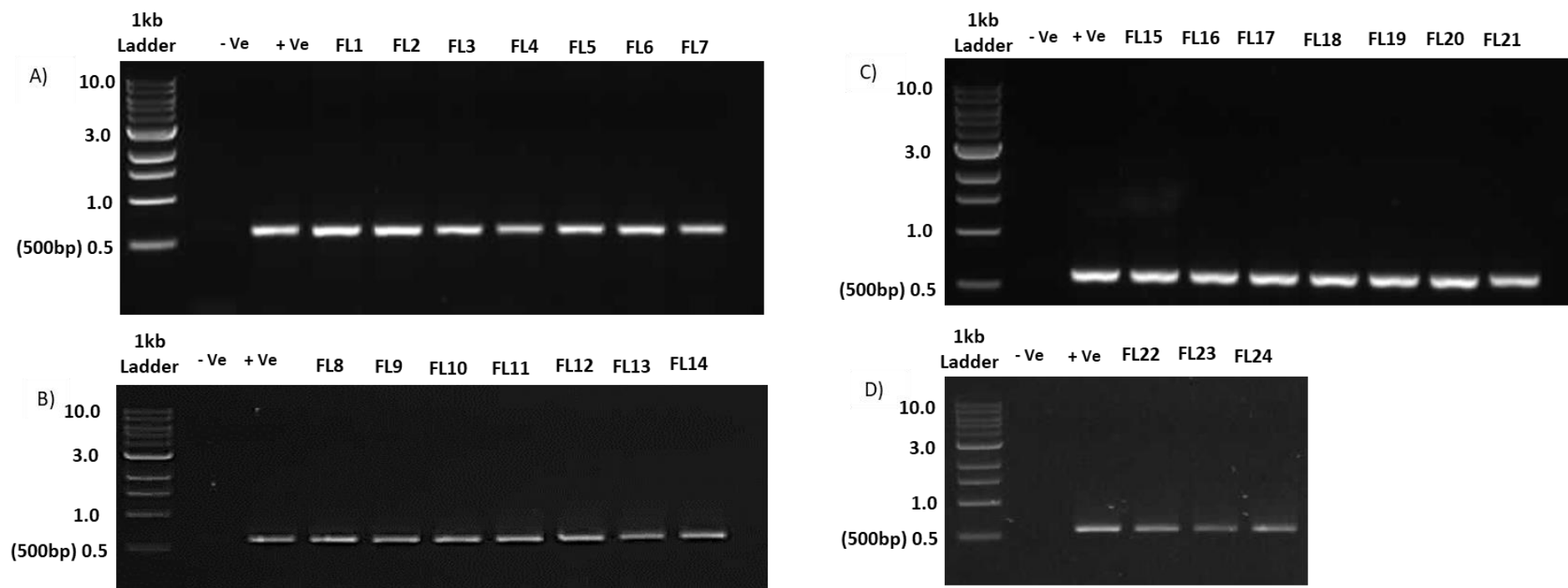


Figure C-1: Electrophoresis gel analysis of PCR products from the *gfpmut3b* gene amplification performed on the 24 presumptive transconjugants, (A) FL1-FL7; (B) FL8-FL14; (C) FL15-FL21; (D) FL22-FL23. Negative control was the environmental *E. coli* strain, *EcoFJ1-Nal^r* and positive control was the *E. coli* reporter strain (*EcoFJ2*) harbouring the *gfpmut3b* gene on the *pRP4-gfp* plasmid. Bands confirmed the presence of *gfpmut3b* gene in the presumptive transconjugants with an expected band size of 593bp.

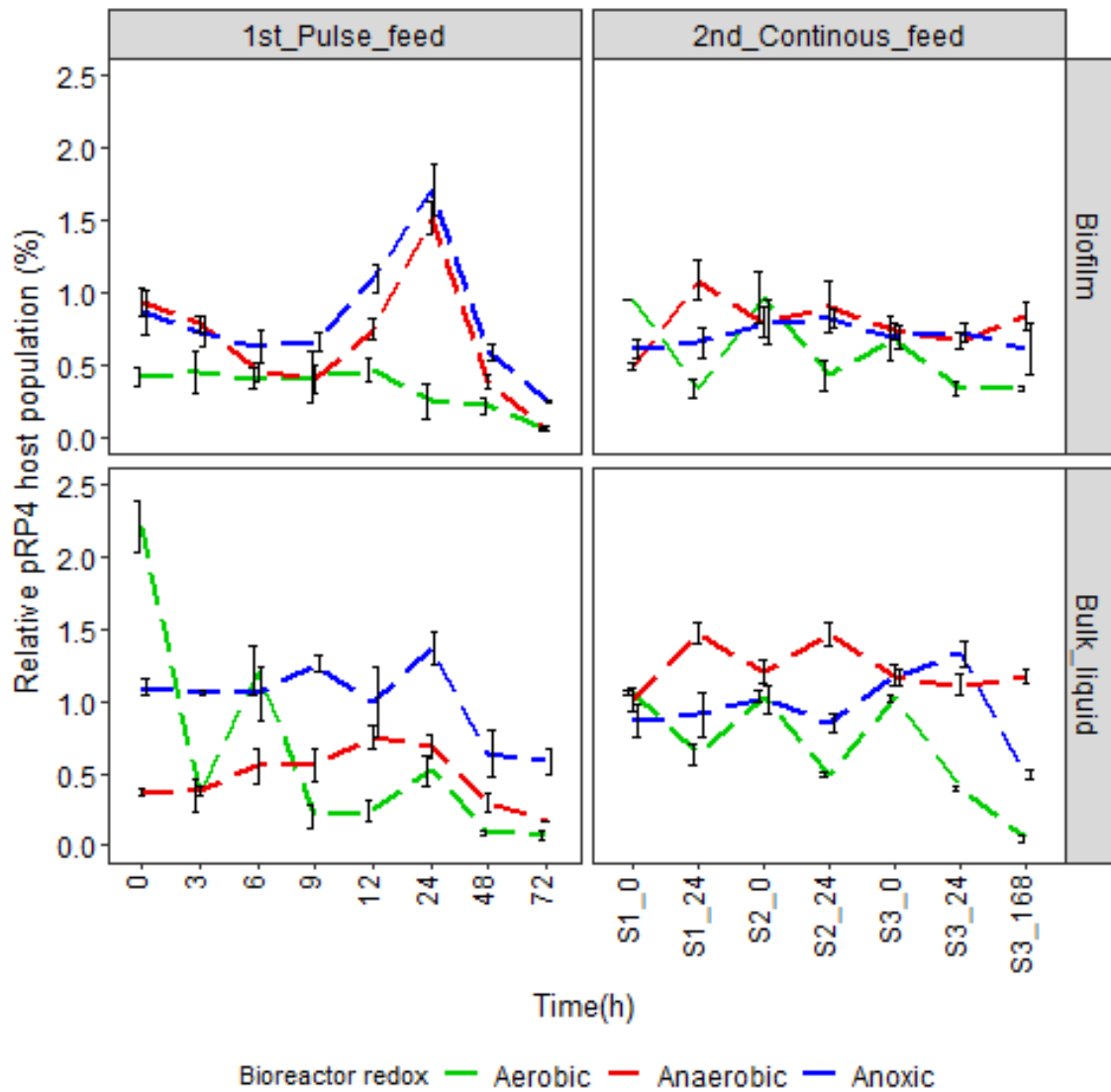
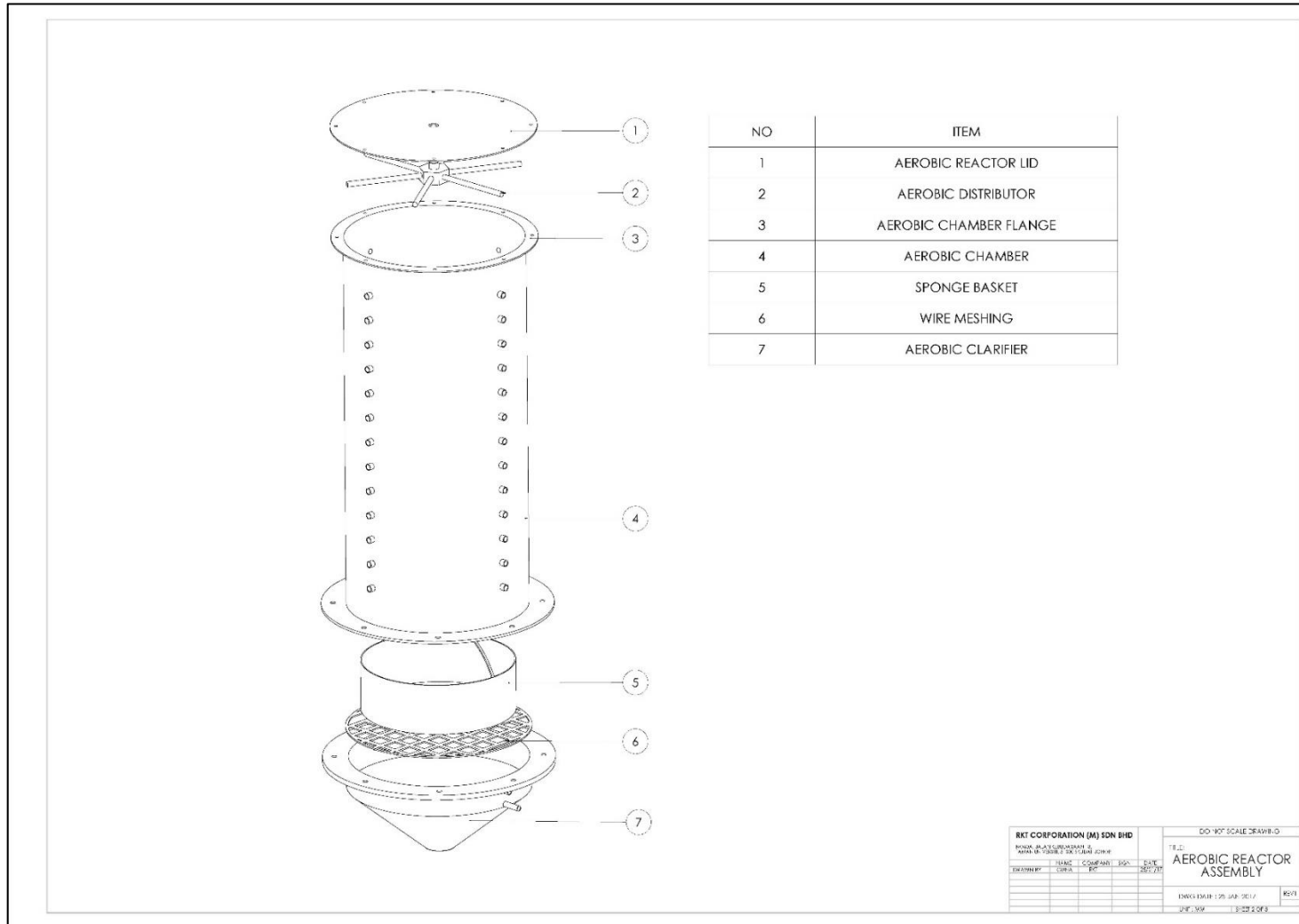
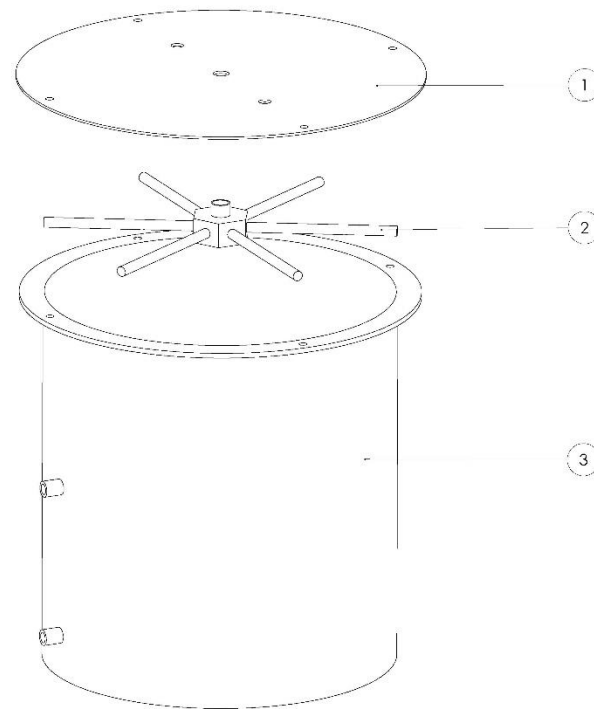


Figure C-2: Spatial and temporal pattern of relative GFP densities across contrasting redox conditions in biofilms and suspended liquid during the pulse feed seeding and continuous feed seeding.

Appendix D

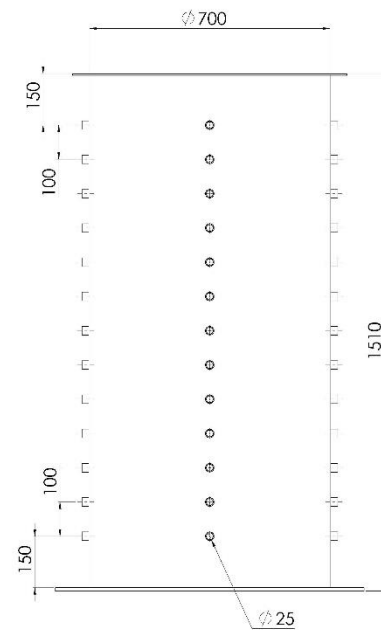
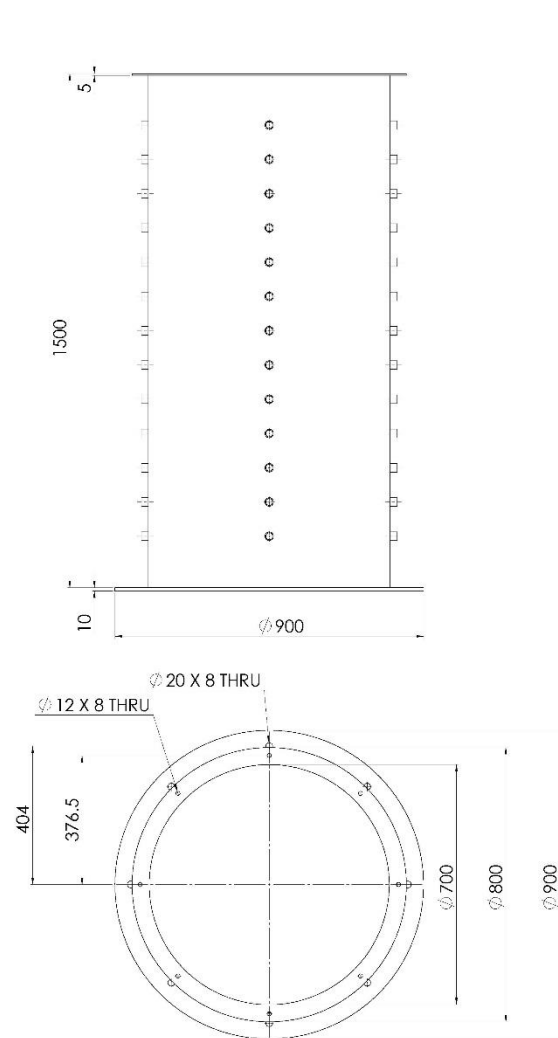
D-1 Sponge core reactor design





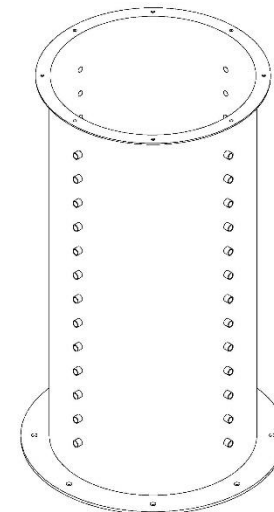
NO	ITEM
1	ANOXIC CHAMBER LID
2	ANOXIC DISTRIBUTOR
3	ANOXIC CHAMBER

RKT CORPORATION (M) SDN BHD					DO NOT SCALE DRAWING	
KORPORASI TEKNOLOGI KIMIA PAMAH UNIVERSITI SINGAPORE, JOHORE					TITLE	
					ANOXIC REACTOR ASSEMBLY	
DESIGNED BY	PLANT	COMPANY	SIGN	DATE	DWG DATE: 25 JAN 2017	
	05-15	19		2020/12	(REV)	
					UNIT: MM	
					1:1000 3/2018	

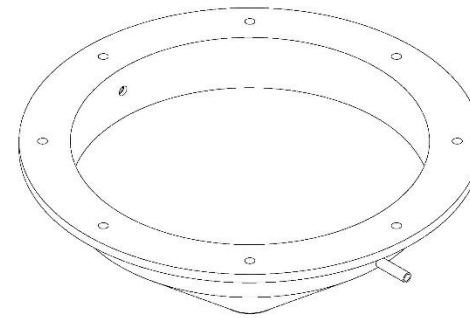
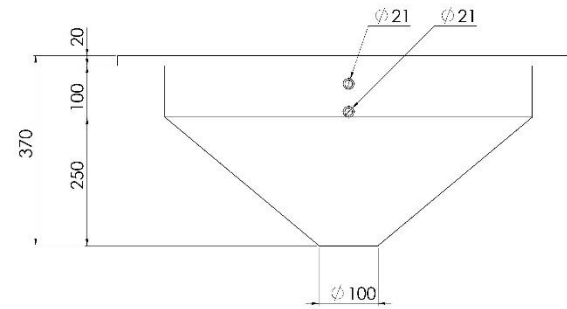
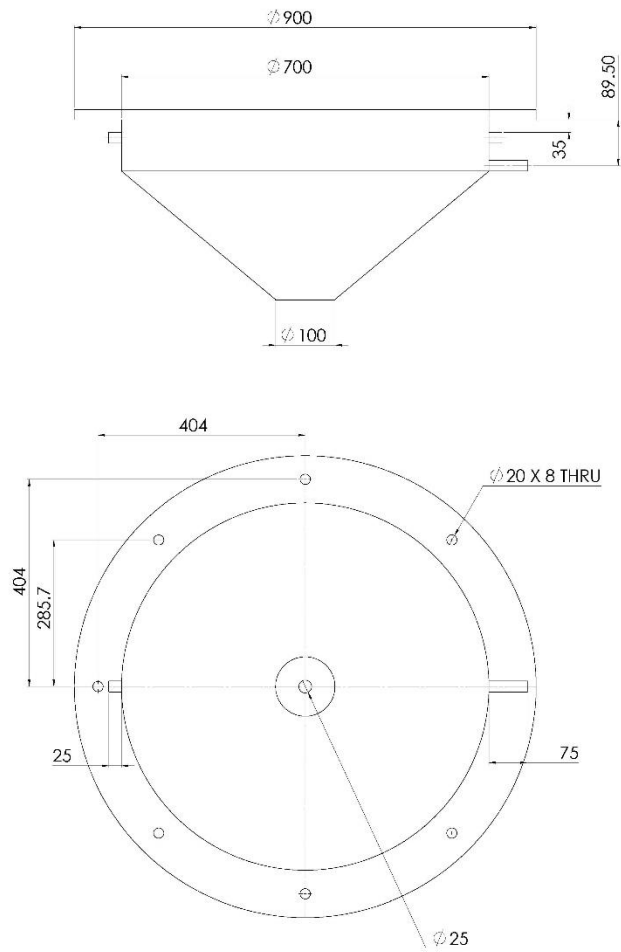


NOTE:

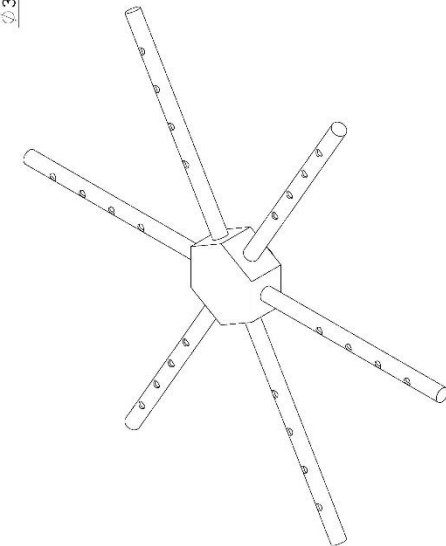
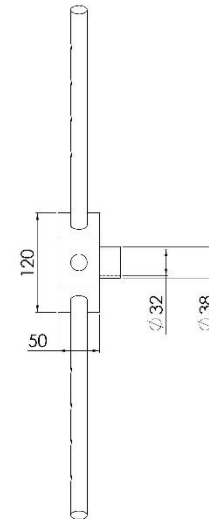
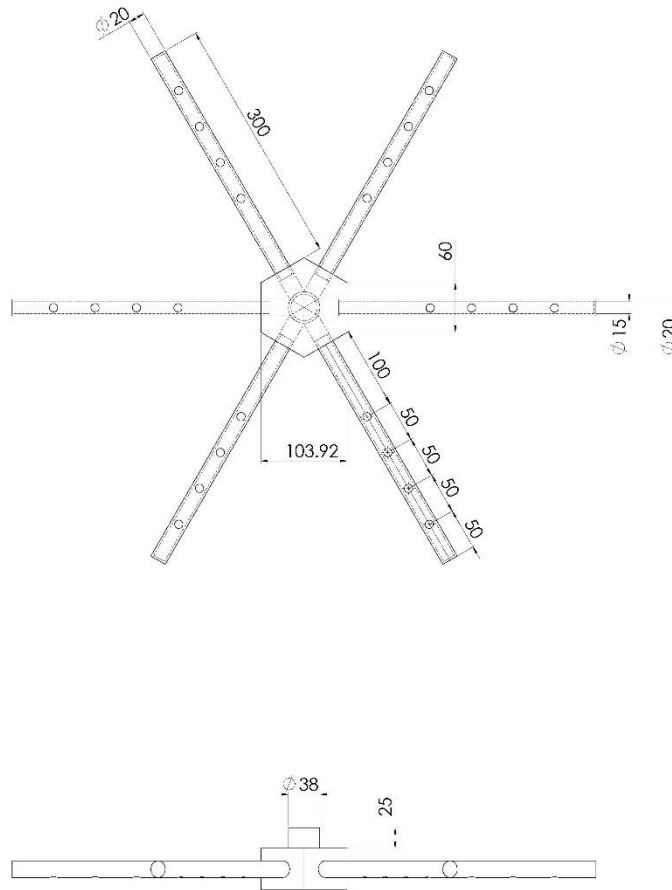
1. 13X4 NOS D25MM SOCKETS WELDED WITH 100MM INTERVAL



RKT CORPORATION (M) SDN BHD					DO NOT SCALE DRAWING	
REKHA P. ANANDARAMAN, B. ENG. & ARCHT. (HONORARY) ENGINEER					TITLE	
DESIGNED BY	NAME	COMPANY	DATE	DATE	AEROBIC REACTOR	
DRAWN BY	ORINA	REI	20/1/17			
					DWG DATE: 25 JAN 2017	
					SHEET 4 OF 5	

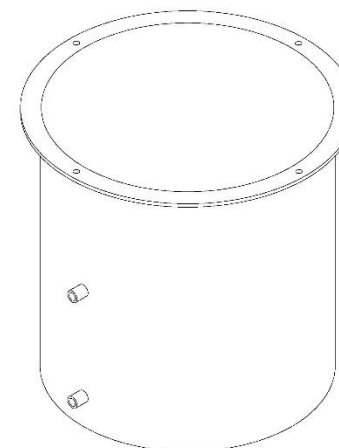
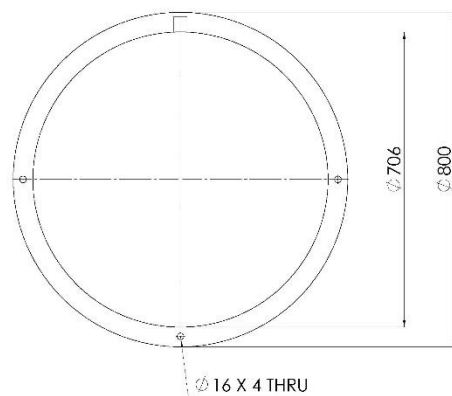
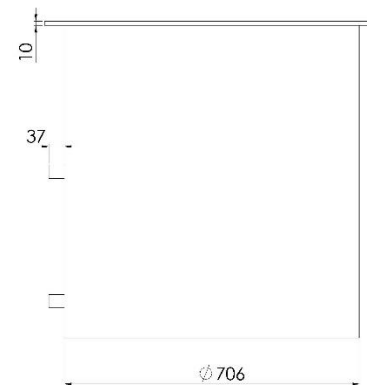
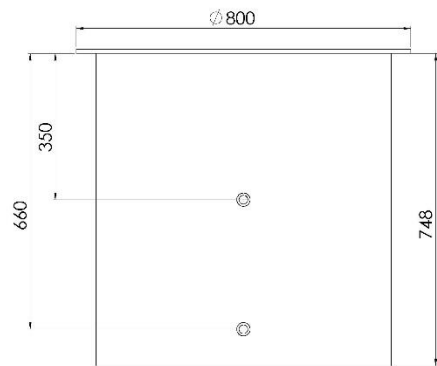


RKT CORPORATION (M) SDN BHD					DO NOT SCALE DRAWING	
PUSAT INSAN & BINA BANGSA TANAH ENDAH, 41000 BUKIT JALOH					TITLE:	
DRAWN BY:	NAME:	COMPANY:	DATE:		AEROBIC CLARIFIER	
	SHARAH	RKT	25/01/17			
					DWG. DATE: 25 JAN 2017	
					DATE: MM /	
					SHEET 5 OF 8	



NOTE: THE SIZE OF ANOXIC DISTRIBUTOR IS SIMILAR TO THE SIZE OF AEROBIC DISTRIBUTOR

RKT CORPORATION (M) SDN BHD					DO NOT SCALE DRAWING	
NOOR ALAM GIBRANAH B. TAJAR UNIVERSITI AIR ITAM, JOHOR					TITLE: AEROBIC DISTRIBUTOR	
DRAWN BY	NAME	COMPANY	DATE	REV	DWG DATE: 25 JAN 2017	
	UAE-A	90	2017/1/2		REV:	
					DATE: MAY 1 2017	
					SHEET 6 OF 6	



RKT CORPORATION (M) SDN BHD						DO NOT SCALE DRAWING	
NO. 22, JALAN KEDAHAN 8, TAMAN JALAN KEDAHAN 8, JOHOR						TITLE	
DESIGNER	DATE	COMPANY	REV.	DATE	26/07/17	ANOXIC REACTOR	
						DWG. DATE: 25 JAN 2017	
						REV.	
						SHEET 2 OF 8	

Table D-1 Effluent discharge standard for new Malaysian sewage treatment system

APPENDIX K1

Extracted from Environmental Quality (Sewage) Regulations 2009 (PU(A) 432)

SECOND SCHEDULE

(Regulation 7)

ACCEPTABLE CONDITIONS OF SEWAGE DISCHARGE OF STANDARDS A AND B

(i) New sewage treatment system

Parameter		Unit	Standard	
(1)	(2)		A (3)	B (4)
(a)	Temperature	°C	40	40
(b)	pH Value	-	6.0-9.0	5.5-9.0
(c)	BOD5 at 20°C	mg/L	20	50
(d)	COD	mg/L	120	200
(e)	Suspended Solids	mg/L	50	100
(f)	Oil and Grease	mg/L	5.0	10.0
(g)	Ammonical Nitrogen (enclosed water body)	mg/L	5.0	5.0
(h)	Ammonical Nitrogen (river)	mg/L	10.0	20.0
(i)	Nitrate – Nitrogen (river)	mg/L	20.0	50.0
(j)	Nitrate – Nitrogen (enclosed water body)	mg/L	10.0	10.0
(k)	Phosphorous (enclosed water body)	mg/L	5.0	10.0

Note : Standard A is applicable to discharges into any inland waters within catchment areas listed in the Third Schedule, while Standard B is applicable to any other inland waters or Malaysian waters.

Table D-2 Summary of pollutants concentrations in raw wastewater and DDHS treated effluents across the four operating conditions with corresponding percentage load removals.

Parameter (mg/L)	Influent	Treated effluents							
		OP1	R ^a (%)	OP2	R ^a (%)	OP3	R ^a (%)	OP4	R ^a (%)
COD _{Total}	339.8 (49.2)	47.9 (4.1)	89.0 (1.1)	33.5 (2.3)	86.6 (1.2)	22.0 (4.9)	94.2 (1.0)	35.2 (8.4)	89.9 (2.1)
COD _{soluble}	79.4 (9.2)	42.9 (2.8)	45.1 (4.5)	32.9 (1.6)	61.9 (1.5)	23.3 (4.2)	69.3 (5.4)	31.8 (7.2)	54.9 (5.5)
NH ₃ -N	24.2 (1.7)	5.4 (3.6)	77.1 (5.9)	9.2 (2.3)	60.6 (3.4)	5.8 (2.4)	60.8 (13.0)	5.1 (3.5)	79.9 (3.6)
NO ₂ -N ^b	0.2 (0.1)	0.2 (0.1)	-28.4 (24.5)	0.2 (0.0)	-16.4 (28.0)	0.1 (0.0)	10.7 (2.1)	0.1 (0.0)	-21.4 (7.3)
NO ₃ -N ^b	0.2 (0.1)	16.0 (2.2)	21.3 (2.6)	8.5 (1.1)	38.9 (5.1)	11.8 (1.2)	22.2 (4.4)	9.4 (1.4)	47.0 (3.4)
TN	34.3 (3.9)	24.9 (1.7)	25.2 (1.9)	24.2 (1.6)	36.5 (5.5)	27.5 (1.7)	27.9 (4.6)	20.8 (1.5)	53.1 (4.5)
DO (mg/L)	0.7 (0.5)	1.5 (0.5)		1.9 (0.5)		1.5 (0.3)		1.6 (0.1)	
pH	7.0 (0.1)	6.7 (0.3)		6.7 (0.3)		6.0 (0.4)		6.3 (0.4)	
Temp	28.1 (1.3)	27.8 (1.6)		28.6 (1.2)		28.6 (2.7)		28.3 (1.6)	

Note: ^a Percentage load removal calculated using Equation 6.1 representing removal rate as per waste loading and sponge volume; ^b Nitrite and nitrate concentrations incorporated secondary loading generated internally from the aerobic treatment step.

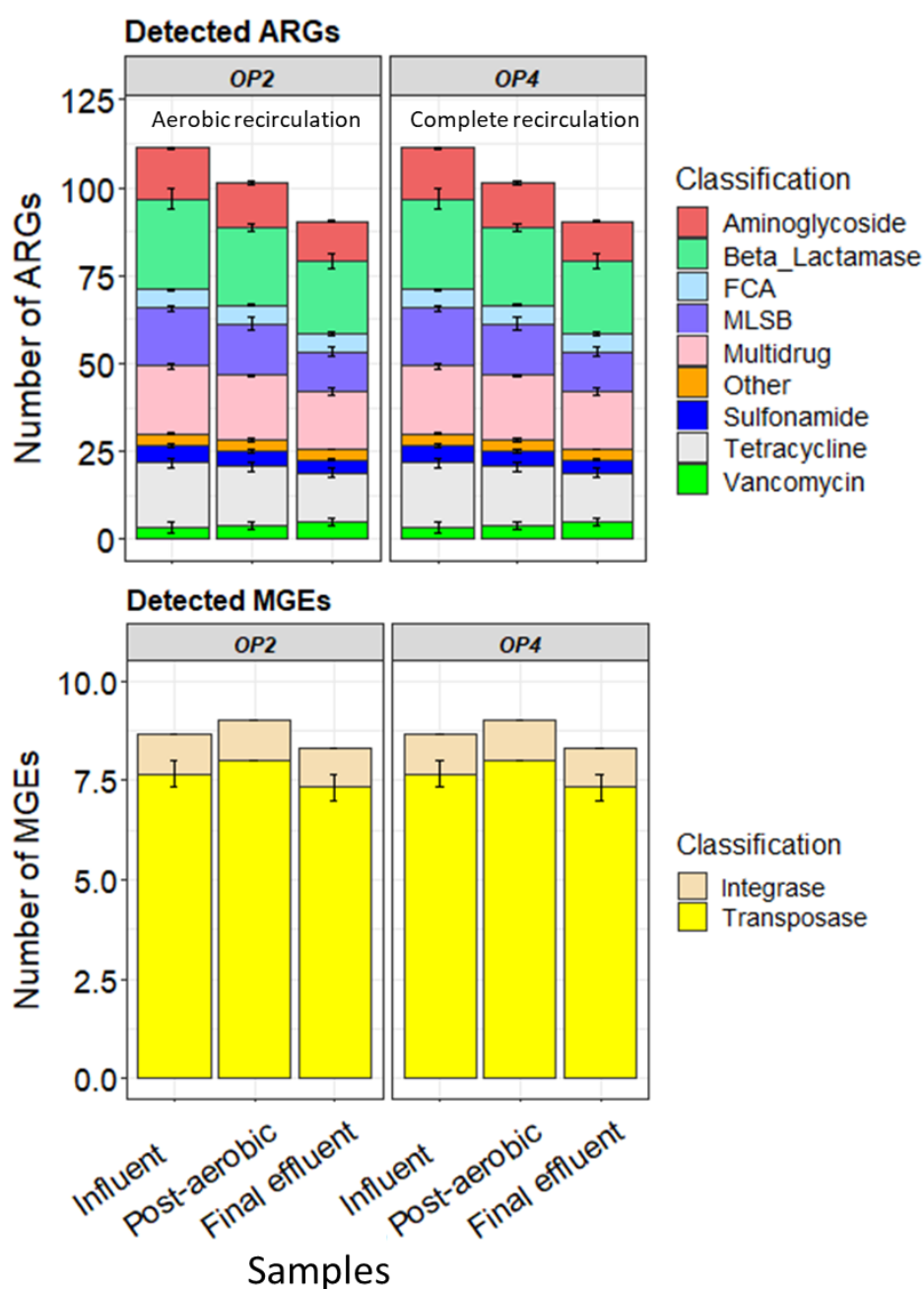


Figure D-1 Number of antibiotic resistance genes (ARGs) and mobile genetic elements (MGEs) detected in the aqueous samples during OP2 and OP4. Resistance genes are classified based on the antibiotics to which they confer resistance. They include aminoglycosides, b-lactams, FCA (fluoroquinolone, quinolone, florfenicol, chloramphenicol and amphenicol resistance genes), MLSB (macrolide-lincosamide-streptogramin B), other/efflux (multidrug-efflux pumps or others), sulphonamides; tetracyclines; and vancomycin.

Table D-3 Comparison of the absolute abundance, gene copies per mL (log concentrations; GC/mL) in DDHS influent and effluents during OP2 and OP4. Significant differences between influent and final effluent were tested in pairwise comparisons using the two sample T-test (normal distributed data) or Wilcoxon test (non-normal distributed data). The asterisk in the p-value column indicates the level of significance (0.05*, 0.001**, 0.001***). The trend column indicates if the concentration increased (↑), decreased (↓), or was not significantly different (-) in the final effluent.

Log GC/mL	OP2					OP4				
	Influent	Post-aerobic	Final effluent	P-value	Trend	Influent	Post-aerobic	Final effluent	P-value	Trend
Aminoglycoside	7.97 ± 0.12	7.27 ± 0.10	6.88 ± 0.01	0.051	-	8.00 ± 0.13	6.81 ± 0.31	6.17 ± 0.23	0.039*	↓
Beta_Lactams	7.72 ± 0.13	7.22 ± 0.10	6.62 ± 0.00	0.047*	↓	7.66 ± 0.15	6.52 ± 0.34	5.69 ± 0.35	0.043*	↓
FCA	7.20 ± 0.20	6.72 ± 0.11	6.39 ± 0.03	0.085	-	7.15 ± 0.17	6.15 ± 0.44	5.23 ± 0.38	0.065	-
MLSB	7.44 ± 0.09	6.45 ± 0.11	6.32 ± 0.01	0.029*	↓	7.31 ± 0.16	6.36 ± 0.34	5.56 ± 0.32	0.048*	↓
Multidrug	7.85 ± 0.16	7.35 ± 0.12	7.19 ± 0.01	0.072	-	8.09 ± 0.19	7.17 ± 0.39	6.45 ± 0.25	0.086	-
Other	6.19 ± 0.16	5.10 ± 0.08	4.64 ± 0.01	0.077	-	5.94 ± 0.12	5.00 ± 0.37	4.40 ± 0.31	0.040*	↓
Sulfonamide	6.85 ± 0.13	6.41 ± 0.13	6.00 ± 0.05	0.046*	↓	6.90 ± 0.17	6.12 ± 0.56	5.48 ± 0.26	0.067	-
Tetracycline	7.95 ± 0.14	7.43 ± 0.14	6.82 ± 0.00	0.051	-	7.65 ± 0.16	6.90 ± 0.36	6.11 ± 0.34	0.050*	↓
Vancomycin	5.06 ± 0.17	3.62 ± 0.10	4.15 ± 0.05	0.100	-	5.34 ± 0.23	4.46 ± 0.24	4.40 ± 0.33	0.160	-
Integrase	8.19 ± 0.25	6.48 ± 0.15	6.93 ± 0.00	0.180	-	7.87 ± 0.32	7.20 ± 0.41	6.20 ± 0.84	0.120	-
Transposase	8.16 ± 0.20	6.99 ± 0.08	7.07 ± 0.01	0.120	-	7.93 ± 0.31	7.14 ± 0.36	6.55 ± 0.28	0.110	-
Total ARG	8.55 ± 0.12	7.98 ± 0.12	7.60 ± 0.00	0.046*	↓	8.55 ± 0.15	7.57 ± 0.08	6.84 ± 0.13	0.046*	↓
Total MGE	8.48 ± 0.21	7.11 ± 0.10	7.31 ± 0.00	0.140	-	8.20 ± 0.31	7.47 ± 0.08	6.71 ± 0.20	0.110	-

Table D-4 Comparison of the relative abundance, gene copies per cell (normalised per bacterial genome; GC/cell) in DDHS influent and effluents during OP2 and OP4. Significant differences between influent and final effluent were tested in pairwise comparisons using the two sample T-test (normal distributed data) or Wilcoxon test (non-normal distributed data). The asterisk in the p-value column indicates the level of significance (0.05*, 0.001**, 0.001***). The trend column indicates if the concentration increased (↑), decreased (↓), or was not significantly different (-) in the final effluent. Red shaded boxes denote the increase of abundance per bacterial cell after the aerobic treatment.

GC/cell Classification	OP2					OP4				
	Influent	Post-aerobic	Final effluent	P-value	Trend	Influent	Post-aerobic	Final effluent	P-value	Trend
Aminoglycoside	0.67 ± 0.07	0.48 ± 0.01	0.33 ± 0.01	0.019*	↓	0.80 ± 0.06	0.29 ± 0.11	0.13 ± 0.02	0.003**	↓
Beta_Lactams	0.38 ± 0.05	0.43 ± 0.01	0.18 ± 0.008	0.031*	↓	0.36 ± 0.06	0.14 ± 0.05	0.04 ± 0.01	0.016*	↓
FCA	0.11 ± 0.04	0.14 ± 0.01	0.11 ± 0.02	0.76	-	0.11 ± 0.03	0.06 ± 0.03	0.01 ± 0.004	0.059	-
MLSB	0.20 ± 0.01	0.07 ± 0.04	0.09 ± 0.004	0.003**	↓	0.16 ± 0.02	0.10 ± 0.04	0.03 ± 0.008	0.014*	↓
Multidrug	0.51 ± 0.12	0.58 ± 0.03	0.67 ± 0.01	0.19	-	0.98 ± 0.38	0.65 ± 0.28	0.25 ± 0.04	0.11	-
Other	0.01 ± 0.002	0.00 ± 0.002	0.00 ± 0.009	0.68	-	0.01 ± 0.001	0.00 ± 0.002	0.00 ± 0.001	0.029*	↓
Sulfonamide	0.05 ± 0.02	0.07 ± 0.10	0.04 ± 0.008	0.79	-	0.06 ± 0.02	0.06 ± 0.03	0.03 ± 0.01	0.14	-
Tetracycline	0.63 ± 0.01	0.70 ± 0.02	0.29 ± 0.01	0.031*	↓	0.35 ± 0.07	0.35 ± 0.14	0.10 ± 0.02	0.038*	↓
Vancomycin	0.00 ± 0.00	0.00 ± 0.00	0.00 ± 0.00	0.73	-	0.00 ± 0.002	0.00 ± 0.00	0.00 ± 0.003	0.47	-
Integrase	0.45 ± 0.15	0.42 ± 0.15	0.37 ± 0.01	0.60	-	0.57 ± 0.27	0.69 ± 0.32	0.10 ± 0.07	0.13	-
Transposase	0.77 ± 0.19	0.86 ± 0.21	0.51 ± 0.08	0.29	-	0.64 ± 0.26	0.61 ± 0.24	0.30 ± 0.01	0.20	-
Total ARG	2.57 ± 0.23	2.47 ± 0.23	1.72 ± 0.04	0.035*	↓	2.83 ± 0.61	1.66 ± 0.69	0.61 ± 0.10	0.033*	↓
Total MGE	1.22 ± 0.33	1.29 ± 0.43	0.89 ± 0.001	0.30	-	1.21 ± 0.52	1.30 ± 0.57	0.40 ± 0.07	0.16	-

Table D-5 Comparison of concentrations, gene copies per mg (GC/mg) in DDHS biofilm samples taken from different depths of the sponge core (i.e., Top, Middle, Bottom), during OP2 and OP4.

Classification	OP2			OP4		
	Top	Middle	Bottom	Top	Middle	Bottom
Aminoglycoside	2.9×10^6 (7.7×10^5)	2.1×10^6 (8.6×10^5)	2.6×10^6 (9.2×10^5)	2.2×10^6 (7.8×10^4)	1.4×10^6 (1.9×10^5)	1.0×10^6 (2.2×10^5)
β _Lactams	4.8×10^5 (1.4×10^5)	5.0×10^5 (2.5×10^5)	1.1×10^6 (4.1×10^5)	4.7×10^5 (1.4×10^4)	8.8×10^5 (1.6×10^5)	4.9×10^5 (2.3×10^5)
FCA	6.6×10^5 (1.1×10^5)	6.6×10^5 (1.7×10^5)	2.0×10^5 (3.8×10^4)	6.9×10^5 (6.6×10^4)	3.8×10^5 (4.9×10^4)	1.4×10^5 (1.1×10^5)
MLSB	2.5×10^5 (8.8×10^4)	2.4×10^5 (1.0×10^5)	5.7×10^5 (1.8×10^4)	5.5×10^5 (4.8×10^4)	4.5×10^5 (3.8×10^4)	4.6×10^5 (3.7×10^4)
Multidrug	6.4×10^6 (1.8×10^5)	3.6×10^6 (2.4×10^6)	1.3×10^6 (2.3×10^5)	2.3×10^6 (2.3×10^5)	7.1×10^6 (2.5×10^6)	9.6×10^6 (8.5×10^5)
Other	5.7×10^3 (3.3×10^3)	1.4×10^4 (1.4×10^4)	4.1×10^3 (1.2×10^3)	7.0×10^4 (4.6×10^3)	3.6×10^4 (3.2×10^3)	3.1×10^4 (2.6×10^4)
Sulfonamide	7.1×10^6 (6.1×10^6)	2.8×10^6 (1.9×10^6)	3.8×10^5 (9.2×10^4)	1.0×10^6 (1.2×10^5)	7.5×10^6 (4.7×10^6)	2.4×10^5 (2.9×10^4)
Tetracycline	7.3×10^6 (2.0×10^6)	5.1×10^6 (2.2×10^6)	1.9×10^6 (1.7×10^5)	3.6×10^6 (3.2×10^5)	2.9×10^6 (4.1×10^5)	2.8×10^6 (8.3×10^5)
Vancomycin	2.9×10^4 (9.8×10^3)	3.4×10^4 (7.7×10^5)	9.6×10^4 (2.1×10^4)	5.2×10^4 (1.1×10^3)	7.6×10^4 (2.6×10^4)	2.6×10^5 (1.1×10^5)
Integrase	4.0×10^6 (6.1×10^5)	2.8×10^6 (7.7×10^5)	1.7×10^6 (4.0×10^5)	2.1×10^6 (1.2×10^5)	3.3×10^6 (3.9×10^5)	1.4×10^6 (2.3×10^5)
Transposase	5.9×10^6 (6.7×10^5)	5.8×10^6 (7.7×10^5)	4.4×10^6 (1.3×10^6)	6.6×10^6 (2.0×10^5)	2.6×10^7 (4.0×10^6)	4.4×10^6 (2.3×10^5)
Total ARG	2.5×10^7 (5.6×10^6)	1.5×10^7 (7.7×10^5)	8.2×10^6 (1.5×10^5)	1.1×10^7 (7.7×10^6)	2.1×10^7 (6.9×10^6)	1.5×10^7 (3.7×10^7)
Total MGE	9.9×10^6 (3.2×10^5)	8.5×10^6 (7.7×10^5)	6.1×10^6 (7.9×10^5)	8.6×10^6 (1.3×10^5)	3.0×10^7 (7.7×10^7)	5.8×10^6 (2.7×10^6)
Sum	3.5×10^7 (8.7×10^6)	2.4×10^7 (7.7×10^6)	1.4×10^7 (6.3×10^6)	2.0×10^7 (6.2×10^6)	3.0×10^7 (7.5×10^7)	2.1×10^7 (1.6×10^7)

Table D-6 Concentrations in ng/L for antibiotics, antiseptics and personal care products (PCPs) measured and detected in the raw wastewater, post-aerobic effluent and final effluent of OP2 and OP4.

ng/L	OP2			OP4		
Classification	Influent	Post-aerobic	Final effluent	Influent	Post-aerobic	Final effluent
Sulfamethoxazole	4757.7 ± 414.2	13118.3 ± 740.4	5980.9 ± 390.3	6419.8 ± 379	2461.7 ± 229.8	2293.3 ± 220.6
Clarithromycin	414.1 ± 207.0	2244.7 ± 364.9	2328.7 ± 250.4	144.1 ± 42.2	1069.5 ± 190.2	1337.8 ± 125.9
Azithromycin	487.6 ± 294.9	2454.0 ± 247.0	2026.3 ± 18.4	115.5 ± 34.4	1081.2 ± 153.3	1339.1 ± 73.7
Ery-H2O	853.7 ± 134.1	1380.3 ± 77.9	1061.6 ± 148.8	423.9 ± 2.7	153.0 ± 25.9	164.4 ± 21.3
Sulfamethazine	54.4 ± 15.8	450.6 ± 18.8	131.7 ± 13.1	67.3 ± 10.5	47.8 ± 11.3	63.2 ± 4.8
Trimethoprim	577.2 ± 25.9	607.8 ± 30.9	74.3 ± 8.9	313.7 ± 7.0	120.7 ± 21.5	84.6 ± 1.6
Chloramphenicol	25.8 ± 7.1	0.0 ± 0.0	0.0 ± 0.0	0.0 ± 0.0	0.0 ± 0.0	0.0 ± 0.0
Amoxicilin	2256.0 ± 108.2	156.0 ± 25.1	84.0 ± 7.3	1926.0 ± 293.8	76.3 ± 6.6	0.0 ± 0.0
Ciprofloxacin	105.5 ± 3.7	47.5 ± 0.7	33.8 ± 2.4	82.7 ± 0.7	34.7 ± 1.1	27.8 ± 0.5
Tetracycline	33.7 ± 10.7	32.3 ± 1.4	30.8 ± 0.8	142.2 ± 2.5	25.6 ± 0.9	19.7 ± 1.5
Triclocarban	320.2 ± 74.6	19.2 ± 1.9	10.4 ± 2.2	177.1 ± 41.6	59.4 ± 29.6	29.5 ± 21.9
Lincomycin	4.8 ± 0.20	7.8 ± 0.0	8.3 ± 0.5	36.8 ± 30.9	6.8 ± 0.9	7.2 ± 0.1
Clindamycin	4.0 ± 0.40	2.2 ± 0.2	1.8 ± 0.2	6.6 ± 1.6	2.3 ± 0.4	2.0 ± 0.0
Caffeine	7353.7 ± 582.3	145.7 ± 4.9	956.0 ± 72.0	5629.7 ± 214.9	253.7 ± 19.6	142.3 ± 57.7
Atenolol	3687.6 ± 76.7	1058.0 ± 56.2	629.5 ± 15.6	2747.0 ± 186.2	381.7 ± 19.7	312.0 ± 13.1
Acetaminophen	81160.0 ± 7461.3	722.0 ± 273.0	472.0 ± 17.7	31807.7 ± 4264.7	224.3 ± 40.5	78.7 ± 6.6

References

- Agrawal, L.K., Ohashi, Y., Mochida, E., Okui, H., Ueki, Y., Harada, H. and Ohashi, A. (1997) 'Treatment of raw sewage in a temperate climate using a UASB reactor and the hanging sponge cubes process', *Water Science and Technology*, 36(6-7), pp. 433-440.
- Ahammad, S.Z., Zealand, A., Dolfing, J., Mota, C., Armstrong, D.V. and Graham, D.W. (2013) 'Low-energy treatment of colourant wastes using sponge biofilters for the personal care product industry', *Bioresour Technol*, 129, pp. 634-8.
- Ahammad, Z.S., Sreekrishnan, T.R., Hands, C.L., Knapp, C.W. and Graham, D.W. (2014) 'Increased Waterborne bla(NDM-1) Resistance Gene Abundances Associated with Seasonal Human Pilgrimages to the Upper Ganges River', *Environmental Science & Technology*, 48(5), pp. 3014-3020.
- Akinbowale, O.L., Peng, H. and Barton, M.D. (2006) 'Antimicrobial resistance in bacteria isolated from aquaculture sources in Australia', *Journal of Applied Microbiology*, 100(5), pp. 1103-1113.
- Alonso, A., Sánchez, P. and Martínez, J.L. (2001) 'Environmental selection of antibiotic resistance genes', *Environmental Microbiology*, 3(1), pp. 1-9.
- Alouache, S., Estepa, V., Messai, Y., Ruiz, E., Torres, C. and Bakour, R. (2014) 'Characterization of ESBLs and Associated Quinolone Resistance in Escherichia coli and Klebsiella pneumoniae Isolates from an Urban Wastewater Treatment Plant in Algeria', *Microbial Drug Resistance*, 20(1), pp. 30-8.
- Amann, R., Fuchs, B.M. and Behrens, S. (2001) 'The identification of microorganisms by fluorescence in situ hybridisation', *Current Opinion in Biotechnology*, 12(3), pp. 231-236.
- Amann, R.I., Ludwig, W. and Schleifer, K.H. (1995) 'PHYLOGENETIC IDENTIFICATION AND IN-SITU DETECTION OF INDIVIDUAL MICROBIAL-CELLS WITHOUT CULTIVATION', *Microbiological Reviews*, 59(1), pp. 143-169.
- Ambus, P. and Zechmeister-Boltenstern, S. (2007) 'Chapter 22 - Denitrification and N-Cycling in Forest Ecosystems', in Bothe, H., Ferguson, S.J. and Newton, W.E. (eds.) *Biology of the Nitrogen Cycle*. Amsterdam: Elsevier, pp. 343-358.
- Aminov, R. (2011) 'Horizontal Gene Exchange in Environmental Microbiota', *Frontiers in Microbiology*, 2(158).

Amos, G.C.A., Zhang, L., Hawkey, P.M., Gaze, W.H. and Wellington, E.M. (2014) 'Functional metagenomic analysis reveals rivers are a reservoir for diverse antibiotic resistance genes', *Veterinary Microbiology*, 171(3-4), pp. 441-447.

Andersen, J.B., Sternberg, C., Poulsen, L.K., Bjørn, S.P., Givskov, M. and Molin, S. (1998) 'New Unstable Variants of Green Fluorescent Protein for Studies of Transient Gene Expression in Bacteria', *Applied and Environmental Microbiology*, 64(6), p. 2240.

Araki, N., Ohashi, A., Machdar, I. and Harada, H. (1999) 'Behaviors of nitrifiers in a novel biofilm reactor employing hanging sponge-cubes as attachment site', *Water Science and Technology*, 39(7), pp. 23-31.

Ashbolt, N.J., Grabow, W.O.K. and Snozzi, M. (2001) 'Indicators of microbial water quality', in Lorna Fewtrell and Bartram, J. (eds.) *Water quality: Guidelines, standards and health*. Cornwall, UK: IWA Publishing, pp. 289-316.

AVMA (2008) *One Health: A new professional imperative. One Health Initiative Task Force Final Report*. Schaumburg: American Veterinary Medical Association.

Ayukekbong, J.A., Ntemgwa, M. and Atabe, A.N. (2017) 'The threat of antimicrobial resistance in developing countries: causes and control strategies', *Antimicrobial Resistance and Infection Control*, 6, p. 8.

Baharoglu, Z., Bikard, D. and Mazel, D. (2010) 'Conjugative DNA Transfer Induces the Bacterial SOS Response and Promotes Antibiotic Resistance Development through Integron Activation', *Plos Genetics*, 6(10), p. 10.

Bahl, M.I., Burmølle, M., Meisner, A., Hansen, L.H. and Sørensen, S.J. (2009a) 'All IncP-1 plasmid subgroups, including the novel ϵ subgroup, are prevalent in the influent of a Danish wastewater treatment plant', *Plasmid*, 62(2), pp. 134-139.

Bahl, M.I., Oregaard, G., Sørensen, S.J. and Hansen, L.H. (2009b) 'Construction and Use of Flow Cytometry Optimized Plasmid-Sensor Strains', in Gogarten, M.B., Gogarten, J.P. and Olendzenski, L.C. (eds.) *Horizontal Gene Transfer: Genomes in Flux*. Totowa, NJ: Humana Press, pp. 257-268.

Baker-Austin, C., Wright, M.S., Stepanauskas, R. and McArthur, J.V. (2006) 'Co-selection of antibiotic and metal resistance', *Trends in Microbiology*, 14(4), pp. 176-182.

Baquero, F., Martínez, J.-L. and Cantón, R. (2008) 'Antibiotics and antibiotic resistance in water environments', *Current Opinion in Biotechnology*, 19(3), pp. 260-265.

- Bengtsson-Palme, J. and Larsson, D.G.J. (2016) 'Concentrations of antibiotics predicted to select for resistant bacteria: Proposed limits for environmental regulation', *Environment International*, 86, pp. 140-149.
- Bennett, P.M. (2008) 'Plasmid encoded antibiotic resistance: acquisition and transfer of antibiotic resistance genes in bacteria', *British Journal of Pharmacology*, 153(S1), pp. S347-57.
- Blaak, H., de Kruijf, P., Hamidjaja, R.A., van Hoek, A.H.A.M., de Roda Husman, A.M. and Schets, F.M. (2014) 'Prevalence and characteristics of ESBL-producing *E. coli* in Dutch recreational waters influenced by wastewater treatment plants', *Veterinary Microbiology*, 171(3), pp. 448-459.
- Blaak, H., Lynch, G., Italiaander, R., Hamidjaja, R.A., Schets, F.M. and Husman, A.M.D. (2015) 'Multidrug-Resistant and Extended Spectrum Beta-Lactamase-Producing *Escherichia coli* in Dutch Surface Water and Wastewater', *Plos One*, 10(6), p. 16.
- Blázquez, E., Bezerra, T., Lafuente, J. and Gabriel, D. (2017) 'Performance, limitations and microbial diversity of a biotrickling filter for the treatment of high loads of ammonia', *Chemical Engineering Journal*, 311, pp. 91-99.
- Bloem, J., Starink, M., Bär-Gilissen, M.J. and Cappenberg, T.E. (1988) 'Protozoan grazing, bacterial activity, and mineralization in two-stage continuous cultures', *Applied and environmental microbiology*, 54(12), pp. 3113-3121.
- Bouki, C., Venieri, D. and Diamadopoulos, E. (2013) 'Detection and fate of antibiotic resistant bacteria in wastewater treatment plants: A review', *Ecotoxicology and Environmental Safety*, 91, pp. 1-9.
- Bradley, D.E., Taylor, D.E. and Cohen, D.R. (1980) 'Specification of surface mating systems among conjugative drug resistance plasmids in *Escherichia coli* K-12', *Journal of bacteriology*, 143(3), pp. 1466-1470.
- Brown, J., Cairncross, S. and Ensink, J.H.J. (2013) 'Water, sanitation, hygiene and enteric infections in children', *Archives of Disease in Childhood*, 98(8), pp. 629-634.
- Brown, L. and Murray, V. (2013) 'Examining the relationship between infectious diseases and flooding in Europe: A systematic literature review and summary of possible public health interventions', *Disaster health*, 1(2), pp. 117-127.

- Brown, M.R., Camézuli, S., Davenport, R.J., Petelenz-Kurdziel, E., Øvreås, L. and Curtis, T.P. (2015) 'Flow cytometric quantification of viruses in activated sludge', *Water Research*, 68, pp. 414-422.
- Brunton, L.A., Desbois, A.P., Garza, M., Wieland, B., Mohan, C.V., Häsler, B., Tam, C.C., Le, P.N.T., Phuong, N.T., Van, P.T., Nguyen-Viet, H., Eltholth, M.M., Pham, D.K., Duc, P.P., Linh, N.T., Rich, K.M., Mateus, A.L.P., Hoque, M.A., Ahad, A., Khan, M.N.A., Adams, A. and Guitian, J. (2019) 'Identifying hotspots for antibiotic resistance emergence and selection, and elucidating pathways to human exposure: Application of a systems-thinking approach to aquaculture systems', *Science of The Total Environment*, 687, pp. 1344-1356.
- Bu, Q., Shi, X., Yu, G., Huang, J. and Wang, B. (2016) 'Assessing the persistence of pharmaceuticals in the aquatic environment: Challenges and needs', *Emerging Contaminants*, 2(3), pp. 145-147.
- Bundy, C.A., Wu, D., Jong, M.-C., Edwards, S.R., Ahammad, Z.S. and Graham, D.W. (2017) 'Enhanced denitrification in Downflow Hanging Sponge reactors for decentralised domestic wastewater treatment', *Bioresource Technology*, 226, pp. 1-8.
- Burch, T.R., Sadowsky, M.J. and LaPara, T.M. (2016) 'Modeling the fate of antibiotic resistance genes and class 1 integrons during thermophilic anaerobic digestion of municipal wastewater solids', *Applied Microbiology and Biotechnology*, 100(3), pp. 1437-1444.
- Burgmann, H., Frigon, D., Gaze, W.H., Manaia, C.M., Pruden, A., Singer, A.C., Smets, B.F. and Zhang, T. (2018) 'Water and sanitation: an essential battlefield in the war on antimicrobial resistance', *Fems Microbiology Ecology*, 94(9), p. 14.
- Butler, M.S. and Cooper, M.A. (2011) 'Antibiotics in the clinical pipeline in 2011', *The Journal Of Antibiotics*, 64, p. 413.
- Byerley, L.O., Samuelson, D., Blanchard, E., Luo, M., Lorenzen, B.N., Banks, S., Ponder, M.A., Welsh, D.A. and Taylor, C.M. (2017) 'Changes in the gut microbial communities following addition of walnuts to the diet', *Journal of Nutritional Biochemistry*, 48, pp. 94-102.
- Callahan, B.J., McMurdie, P.J., Rosen, M.J., Han, A.W., Johnson, A.J.A. and Holmes, S.P. (2016a) 'DADA2: High-resolution sample inference from Illumina amplicon data', *Nature Methods*, 13(7), pp. 581-+.
- Callahan, B.J., Sankaran, K., Fukuyama, J.A., McMurdie, P.J. and Holmes, S.P. (2016b) 'Bioconductor Workflow for Microbiome Data Analysis: from raw reads to community analyses', *F1000Res*, 5, p. 1492.

Canica, M., Manageiro, V., Jones-Dias, D., Clemente, L., Gomes-Neves, E., Poeta, P., Dias, E. and Ferreira, E. (2015) 'Current perspectives on the dynamics of antibiotic resistance in different reservoirs', *Research in Microbiology*, 166(7), pp. 594-600.

Cantas, L., Shah, S.Q.A., Cavaco, L.M., Manaia, C., Walsh, F., Popowska, M., Garelick, H., Bürgmann, H. and Sørum, H. (2013) 'A brief multi-disciplinary review on antimicrobial resistance in medicine and its linkage to the global environmental microbiota', *Frontiers in Microbiology*, 4.

Caporaso, G. (2018) 'Qiime2'. Available at: <https://qiime2.org/>.

Caporaso, J.G., Kuczynski, J., Stombaugh, J., Bittinger, K., Bushman, F.D., Costello, E.K., Fierer, N., Peña, A.G., Goodrich, J.K., Gordon, J.I., Huttley, G.A., Kelley, S.T., Knights, D., Koenig, J.E., Ley, R.E., Lozupone, C.A., McDonald, D., Muegge, B.D., Pirrung, M., Reeder, J., Sevinsky, J.R., Turnbaugh, P.J., Walters, W.A., Widmann, J., Yatsunenko, T., Zaneveld, J. and Knight, R. (2010) 'QIIME allows analysis of high-throughput community sequencing data', *Nature Methods*, 7, p. 335.

Chalfie, M., Tu, Y., Euskirchen, G., Ward, W.W. and Prasher, D.C. (1994) 'GREEN FLUORESCENT PROTEIN AS A MARKER FOR GENE-EXPRESSION', *Science*, 263(5148), pp. 802-805.

Chan, Y.J., Chong, M.F., Law, C.L. and Hassell, D.G. (2009) 'A review on anaerobic-aerobic treatment of industrial and municipal wastewater', *Chemical Engineering Journal*, 155(1-2), pp. 1-18.

Chen, J., Wei, X.D., Liu, Y.S., Ying, G.G., Liu, S.S., He, L.Y., Su, H.C., Hu, L.X., Chen, F.R. and Yang, Y.Q. (2016a) 'Removal of antibiotics and antibiotic resistance genes from domestic sewage by constructed wetlands: Optimization of wetland substrates and hydraulic loading', *Science of the Total Environment*, 565, pp. 240-248.

Chen, Q.L., An, X.L., Li, H., Su, J.Q., Ma, Y.B. and Zhu, Y.G. (2016b) 'Long-term field application of sewage sludge increases the abundance of antibiotic resistance genes in soil', *Environment International*, 92-93, pp. 1-10.

Chen, Y. and Wang, F. (2015) 'Insights on nitrate respiration by *Shewanella*', *Frontiers in Marine Science*, 1(80).

Chereau, F., Opatowski, L., Tourdjman, M. and Vong, S. (2017) 'Risk assessment for antibiotic resistance in South East Asia', *Bmj-British Medical Journal*, 358, pp. 2-8.

Chim, H., Tan, B.H. and Song, C. (2007) 'Five-year review of infections in a burn intensive care unit: High incidence of *Acinetobacter baumannii* in a tropical climate', *Burns*, 33(8), pp. 1008-1014.

Christgen, B., Yang, Y., Ahammad, S.Z., Li, B., Rodriguez, D.C., Zhang, T. and Graham, D.W. (2015) 'Metagenomics Shows That Low-Energy Anaerobic-Aerobic Treatment Reactors Reduce Antibiotic Resistance Gene Levels from Domestic Wastewater', *Environmental Science & Technology*, 49(4), p. 2577.

Chuang, H.P., Ohashi, A., Imachi, H., Tandukar, M. and Harada, H. (2007) 'Effective partial nitrification to nitrite by down-flow hanging sponge reactor under limited oxygen condition', *Water Research*, 41(2), pp. 295-302.

Clark, D.P. and Pazdernik, N.J. (2013) 'Chapter e20 - Plasmids', in Clark, D.P. and Pazdernik, N.J. (eds.) *Molecular Biology (Second Edition)*. Boston: Academic Press, pp. e473-e478.

Cole, J.R., O'Sullivan, O., O'Toole, P.W., Wang, Q., Ross, R.P., Greene-Diniz, R. and Claesson, M.J. (2010) 'Comparison of two next-generation sequencing technologies for resolving highly complex microbiota composition using tandem variable 16S rRNA gene regions', *Nucleic Acids Research*, 38(22), pp. e200-e200.

Collignon, P., Beggs, J.J., Walsh, T.R., Gandra, S. and Laxminarayan, R. (2018) 'Anthropological and socioeconomic factors contributing to global antimicrobial resistance: a univariate and multivariable analysis', *The Lancet Planetary Health*, 2(9), pp. e398-e405.

Cousins, S. (2018) 'Extremely drug-resistant typhoid in south Asia', *The Lancet Infectious Diseases*, 18(9), p. 950.

Crowdy, J.P. (1984) 'Sanitation and Disease: Health Aspects of Excreta and Wastewater Management. Feachem, R. G., Bradley, D. J., Garelick, H. & Mara, D. D. Chichester, UK: John Wiley & Sons, 1983. 501 pp., illus. Price: £33.50. ISBN: 0 47190094X', *Transactions of The Royal Society of Tropical Medicine and Hygiene*, 78(6), pp. 760-760.

Cydzik-Kwiatkowska, A., Rusanowska, P., Zielinska, M., Bernat, K. and Wojnowska-Baryla, I. (2014) 'Structure of nitrogen-converting communities induced by hydraulic retention time and COD/N ratio in constantly aerated granular sludge reactors treating digester supernatant', *Bioresource Technology*, 154, pp. 162-170.

Czekalski, N., Berthold, T., Caucci, S., Egli, A. and Bürgmann, H. (2012) 'Increased Levels of Multiresistant Bacteria and Resistance Genes after Wastewater Treatment and Their Dissemination into Lake Geneva, Switzerland', *Frontiers in Microbiology*, 3, p. 106.

Czekalski, N., Sigdel, R., Birtel, J., Matthews, B. and Bürgmann, H. (2015) 'Does human activity impact the natural antibiotic resistance background? Abundance of antibiotic resistance genes in 21 Swiss lakes', *Environment International*, 81, pp. 45-55.

Das, T., Sehar, S. and Manefield, M. (2013) 'The roles of extracellular DNA in the structural integrity of extracellular polymeric substance and bacterial biofilm development', *Environmental Microbiology Reports*, 5(6), pp. 778-786.

Daughton, C.G. (2003) 'Cradle-to-cradle stewardship of drugs for minimizing their environmental disposition while promoting human health. II. Drug disposal, waste reduction, and future directions', *Environmental Health Perspectives*, 111(5), pp. 775-785.

Davies, J. (1994) 'Inactivation of antibiotics and the dissemination of resistance', *Science*, 264(5157), p. 375.

Davies, J. and Davies, D. (2010) 'Origins and Evolution of Antibiotic Resistance', *Microbiology and Molecular Biology Reviews : MMBR*, 74(3), pp. 417-433.

Davison, J. (1999) 'Genetic Exchange between Bacteria in the Environment', *Plasmid*, 42(2), pp. 73-91.

De Briyne, N., Atkinson, J., Pokludová, L. and Borriello, S.P. (2014) 'Antibiotics used most commonly to treat animals in Europe', *The Veterinary record*, 175(13), pp. 325-325.

de Oliveira, A.J.F.C. and Watanabe Pinhata, J.M. (2008) 'Antimicrobial resistance and species composition of Enterococcus spp. isolated from waters and sands of marine recreational beaches in Southeastern Brazil', *Water Research*, 42(8), pp. 2242-2250.

Del Casale, A., Flanagan, P.V., Larkin, M.J., Allen, C.C.R. and Kulakov, L.A. (2011) 'Analysis of transduction in wastewater bacterial populations by targeting the phage-derived 16S rRNA gene sequences', *Fems Microbiology Ecology*, 76(1), pp. 100-108.

Department of Environment Malaysia (1979) *Environmental Quality (Sewage and Industrial Effluents) Regulations, 1979*. Malaysia.

Devanas, M.A., Rafaelieshkol, D. and Stotzky, G. (1986) 'SURVIVAL OF PLASMID-CONTAINING STRAINS OF ESCHERICHIA-COLI IN SOIL - EFFECT OF PLASMID SIZE AND NUTRIENTS ON SURVIVAL OF HOSTS AND MAINTENANCE OF PLASMIDS', *Current Microbiology*, 13(5), pp. 269-277.

Dong, B., Tan, J., Yang, Y., Pang, Z.S., Li, Z.T. and Dai, X.H. (2016) 'Linking nitrification characteristic and microbial community structures in integrated fixed film activated sludge reactor by high-throughput sequencing', *Water Science and Technology*, 74(6), pp. 1354-1364.

EAWAG (2015) *Spread of antibiotic resistance in the aquatic environment*. Available at: <http://www.eawag.ch> (Accessed: 28 September).

Eberl, L., Schulze, R., Ammendola, A., Geisenberger, O., Erhart, R., Sternberg, C., Molin, S. and Amann, R. (2006) 'Use of green fluorescent protein as a marker for ecological studies of activated sludge communities', *FEMS Microbiology Letters*, 149(1), pp. 77-83.

Ehlers, L.J. and Bouwer, E.J. (1999) 'Rp4 plasmid transfer among species of pseudomonas in a biofilm reactor', *Water Science and Technology*, 39(7), pp. 163-171.

El-Hifnawi, L.C.B.a.M.B. (2014) *Facilitating Trade through Competitive, Low-carbon Transport: The Case for Vietnam's Inland and Coastal Waterways*. Washington DC: The World Bank.

Elmitwalli, T.A., van Dun, M., Bruning, H., Zeeman, G. and Lettinga, G. (2000) 'The role of filter media in removing suspended and colloidal particles in an anaerobic reactor treating domestic sewage', *Bioresource Technology*, 72(3), pp. 235-242.

Fang, W., Yan, D., Wang, X., Huang, B., Wang, X., Liu, J., Liu, X., Li, Y., Ouyang, C., Wang, Q. and Cao, A. (2018) 'Responses of Nitrogen-Cycling Microorganisms to Dazomet Fumigation', *Frontiers in Microbiology*, 9(2529).

FAO (2016) *Drivers, dynamics and epidemiology of antimicrobial resistance in animal production*. Rome: Food and Agriculture Organization of the United Nations. [Online]. Available at: www.fao.org/publications.

Farkas, A., Bocos, B. and Butiuc-Keul, A. (2016) 'Antibiotic Resistance and int1 Carriage in Waterborne Enterobacteriaceae', *Water Air and Soil Pollution*, 227(7), p. 11.

Fernández, A., Huang, S., Seston, S., Xing, J., Hickey, R., Criddle, C. and Tiedje, J. (1999) 'How stable is stable? Function versus community composition', *Applied and environmental microbiology*, 65(8), pp. 3697-3704.

Finley, R.L., Collignon, P., Larsson, D.G.J., McEwen, S.A., Li, X.-Z., Gaze, W.H., Reid-Smith, R., Timinouni, M., Graham, D.W. and Topp, E. (2013) 'The scourge of antibiotic resistance: the important role of the environment', *Clinical infectious diseases : an official publication of the Infectious Diseases Society of America*, 57(5), pp. 704-710.

Fleifle, A., Tawfik, A., Saavedra, O., Yoshimura, C. and Elzeir, M. (2013a) 'Modeling and profile analysis of a down-flow hanging sponge system treating agricultural drainage water', *Separation and Purification Technology*, 116, pp. 87-94.

Fleifle, A., Tawfik, A., Saavedra, O.C. and Elzeir, M. (2013b) 'Treatment of agricultural drainage water via downflow hanging sponge system for reuse in agriculture', *Water Science and Technology-Water Supply*, 13(2), pp. 403-412.

Fletcher, S. (2015) 'Understanding the contribution of environmental factors in the spread of antimicrobial resistance', *Environmental Health and Preventive Medicine*, 20(4), pp. 243-252.

Founou, L.L., Founou, R.C. and Essack, S.Y. (2016) 'Antibiotic Resistance in the Food Chain: A Developing Country-Perspective', *Frontiers in Microbiology*, 7, p. 19.

Fredrickson, J.K., Romine, M.F., Beliaev, A.S., Auchtung, J.M., Driscoll, M.E., Gardner, T.S., Neilson, K.H., Osterman, A.L., Pinchuk, G., Reed, J.L., Rodionov, D.A., Rodrigues, J.L.M., Saffarini, D.A., Serres, M.H., Spormann, A.M., Zhulin, I.B. and Tiedje, J.M. (2008) 'Towards environmental systems biology of *Shewanella*', *Nature Reviews Microbiology*, 6(8), pp. 592-603.

Geisenberger, O., Ammendola, A., Christensen, B.B., Molin, S., Schleifer, K.-H. and Eberl, L. (1999) 'Monitoring the conjugal transfer of plasmid RP4 in activated sludge and in situ identification of the transconjugants', *FEMS Microbiology Letters*, 174(1), pp. 9-17.

Ghaderpour, A., Ho, W.S., Chew, L.L., Bong, C.W., Chong, V.C., Thong, K.L. and Chai, L.C. (2015) 'Diverse and abundant multi-drug resistant E-coli in Matang mangrove estuaries, Malaysia', *Frontiers in Microbiology*, 6, p. 13.

Gillings, M.R., Gaze, W.H., Pruden, A., Smalla, K., Tiedje, J.M. and Zhu, Y.-g. (2015) 'Using the class 1 integron-integrase gene as a proxy for anthropogenic pollution', *The ISME Journal*, 9(6), pp. 1269-1279.

Givan, A.L. (2011) 'Flow Cytometry: An Introduction', in Hawley, T.S. and Hawley, R.G. (eds.) *Flow Cytometry Protocols*. Totowa, NJ: Humana Press, pp. 1-29.

Gomez, M.A., Rodelas, B., Saez, F., Pozo, C., Martinez-Toledo, M.V., Hontoria, E. and Gonzalez-Lopez, J. (2005) 'Denitrifying activity of Xanthobacter autotrophicus strains isolated from a submerged fixed-film reactor', *Applied Microbiology and Biotechnology*, 68(5), pp. 680-685.

Gould, I.M. and Bal, A.M. (2013) 'New antibiotic agents in the pipeline and how they can help overcome microbial resistance', *Virulence*, 4(2), pp. 185-191.

Graham, D.W., Bergeron, G., Bourassa, M.W., Dickson, J., Gomes, F., Howe, A., Kahn, L.H., Morley, P.S., Scott, H.M., Simjee, S., Singer, R.S., Smith, T.C., Storrs, C. and Wittum, T.E. (2019a) 'Complexities in understanding antimicrobial resistance across domesticated animal, human, and environmental systems', *Annals of the New York Academy of Sciences*, 1441(1), pp. 17-30.

Graham, D.W., Collignon, P., Davies, J., Larsson, D.G.J. and Snape, J. (2014) 'Underappreciated Role of Regionally Poor Water Quality on Globally Increasing Antibiotic Resistance', *Environmental Science & Technology*, 48(20), pp. 11746-11747.

Graham, D.W., Giesen, M.J. and Bunce, J.T. (2019b) 'Strategic Approach for Prioritising Local and Regional Sanitation Interventions for Reducing Global Antibiotic Resistance', *Water*, 11(1), p. 21.

Graham, D.W., Olivares-Rieumont, S., Knapp, C.W., Lima, L., Werner, D. and Bowen, E. (2011) 'Antibiotic Resistance Gene Abundances Associated with Waste Discharges to the Almendares River near Havana, Cuba', *Environmental Science & Technology*, 45(2), pp. 418-424.

Gray, N.F. (2004) *Biology of wastewater treatment*. London: Imperial College Press.

Hanssen, A.-M., Kjeldsen, G. and Sollid, J.U.E. (2004) 'Local Variants of Staphylococcal Cassette Chromosome *mec* in Sporadic Methicillin-Resistant *Staphylococcus aureus* and Methicillin-Resistant Coagulase-Negative Staphylococci: Evidence of Horizontal Gene Transfer?', *Antimicrobial Agents and Chemotherapy*, 48(1), pp. 285-296.

Hawkey, P.M. and Jones, A.M. (2009) 'The changing epidemiology of resistance', *Journal of Antimicrobial Chemotherapy*, 64(suppl_1), pp. i3-i10.

Henze, M., Loosdrecht, M.C.M.V., Ekama, G.A. and Damir Brdjanovic (2008) *Biological wastewater treatment: Principles, Modelling and Design*. 1st Edition edn. London: IWA Publishing.

Hong, C., Si, Y.X., Xing, Y. and Li, Y. (2015) 'Illumina MiSeq sequencing investigation on the contrasting soil bacterial community structures in different iron mining areas', *Environmental Science and Pollution Research*, 22(14), pp. 10788-10799.

Horn, M.A., Ihssen, J., Matthies, C., Schramm, A., Acker, G. and Drake, H.L. (2005) 'Dechloromonas denitrificans sp nov., Flavobacterium denitrificans sp nov., Paenibacillus anaericanus sp. nov and Paenibacillus terrae strain MH72, N₂O-producing bacteria isolated from the gut of the earthworm *Aporrectodea caliginosa*', *International Journal of Systematic and Evolutionary Microbiology*, 55, pp. 1255-1265.

Horton, R.A., Randall, L.P., Snary, E.L., Cockrem, H., Lotz, S., Wearing, H., Duncan, D., Rabie, A., McLaren, I., Watson, E., La Ragione, R.M. and Coldham, N.G. (2011) 'Fecal carriage and shedding density of CTX-M extended-spectrum {beta}-lactamase-producing *Escherichia coli* in cattle, chickens, and pigs: implications for environmental contamination and food production', *Applied and environmental microbiology*, 77(11), pp. 3715-3719.

Huang, X.-Z., Frye, J.G., Chahine, M.A., Glenn, L.M., Ake, J.A., Su, W., Nikolich, M.P. and Lesho, E.P. (2012) 'Characteristics of plasmids in multi-drug-resistant Enterobacteriaceae isolated during prospective surveillance of a newly opened hospital in Iraq', *PloS one*, 7(7), pp. e40360-e40360.

Hugenholtz, P., Goebel, B.M. and Pace, N.R. (1998) 'Impact of culture-independent studies on the emerging phylogenetic view of bacterial diversity', *Journal of bacteriology*, 180(18), pp. 4765-4774.

Huysman, F., Verstraete, W. and Brookes, P.C. (1994) 'EFFECT OF MANURING PRACTICES AND INCREASED COPPER CONCENTRATIONS ON SOIL MICROBIAL-POPULATIONS', *Soil Biology & Biochemistry*, 26(1), pp. 103-110.

Ikeda, N., Natori, T., Okubo, T., Sugo, A., Aoki, M., Kimura, M., Yamaguchi, T., Harada, H., Ohashi, A. and Uemura, S. (2013) 'Enhancement of denitrification in a down-flow hanging sponge reactor by effluent recirculation', *Water Sci Technol*, 68(3), pp. 591-8.

Ilves, H., H rak, R. and Kivisaar, M. (2001) 'Involvement of sigma(S) in starvation-induced transposition of *Pseudomonas putida* transposon Tn4652', *Journal of bacteriology*, 183(18), pp. 5445-5448.

Inoue, D., Sei, K., Soda, S., Ike, M. and Fujita, M. (2005) 'Potential of predominant activated sludge bacteria as recipients in conjugative plasmid transfer', *Journal of Bioscience and Bioengineering*, 100(6), pp. 600-605.

- Isaacs, S.H. and Henze, M. (1995) 'Controlled carbon source addition to an alternating nitrification denitrification wastewater treatment process including biological P-removal', *Water Research*, 29(1), pp. 77-89.
- James, J.P. (1999) 'The mechanisms and the spread of antibiotic resistance', *Pediatric Annals*, 28(7), pp. 446-452.
- Jechalke, S., Dealtry, S., Smalla, K. and Heuer, H. (2013) 'Quantification of IncP-1 Plasmid Prevalence in Environmental Samples', *Applied and Environmental Microbiology*, 79(4), p. 1410.
- Jiang, X., Ma, M., Li, J., Lu, A. and Zhong, Z. (2008) 'Bacterial Diversity of Active Sludge in Wastewater Treatment Plant', *Earth Science Frontiers*, 15(6), pp. 163-168.
- Johnson, T.J., Wannemuehler, Y.M., Johnson, S.J., Logue, C.M., White, D.G., Doetkott, C. and Nolan, L.K. (2007) 'Plasmid Replicon Typing of Commensal and Pathogenic Escherichia coli Isolates', *Applied and environmental microbiology AEM.*, 73(6), pp. 1976-1983.
- Joly, D. and Faure, D. (2015) 'Next-generation sequencing propels environmental genomics to the front line of research', *Heredity*, 114(5), pp. 429-430.
- Jong, M.-C., Su, J.-Q., Bunce, J.T., Harwood, C.R., Snape, J.R., Zhu, Y.-G. and Graham, D.W. (2018) 'Co-optimization of sponge-core bioreactors for removing total nitrogen and antibiotic resistance genes from domestic wastewater', *Science of The Total Environment*, 634, pp. 1417-1423.
- Ju, F., Li, B., Ma, L., Wang, Y., Huang, D. and Zhang, T. (2016) 'Antibiotic resistance genes and human bacterial pathogens: Co-occurrence, removal, and enrichment in municipal sewage sludge digesters', *Water Research*, 91, pp. 1-10.
- Kabler, P. (1959) 'Removal of Pathogenic Microorganisms by Sewage Treatment Processes', *Sewage and Industrial Wastes*, 31(12), pp. 1373-1382.
- Kain, S.R., Adams, M., Kondepudi, A., Yang, T.T., Ward, W.W. and Kitts, P. (1995) 'GREEN FLUORESCENT PROTEIN AS A REPORTER OF GENE-EXPRESSION AND PROTEIN LOCALIZATION', *Biotechniques*, 19(4), pp. 650-655.
- Karanika, S., Karantanos, T., Arvanitis, M., Grigoras, C. and Mylonakis, E. (2016) 'Fecal Colonization With Extended-spectrum Beta-lactamase-Producing Enterobacteriaceae and Risk Factors Among Healthy Individuals: A Systematic Review and Metaanalysis', *Clinical Infectious Diseases*, 63(3), pp. 310-318.

Katoh, K., Misawa, K., Kuma, K. and Miyata, T. (2002) 'MAFFT: a novel method for rapid multiple sequence alignment based on fast Fourier transform', *Nucleic Acids Research*, 30(14), pp. 3059-3066.

Khan, A.U., Maryam, L. and Zarrilli, R. (2017) 'Structure, Genetics and Worldwide Spread of New Delhi Metallo- β -lactamase (NDM): a threat to public health', *BMC Microbiology*, 17(1), p. 101.

Kim, N.-K., Oh, S. and Liu, W.-T. (2016) 'Enrichment and characterization of microbial consortia degrading soluble microbial products discharged from anaerobic methanogenic bioreactors', *Water Research*, 90, pp. 395-404.

Kim, S., Jensen, J.N., Aga, D.S. and Weber, A.S. (2007) 'Fate of tetracycline resistant bacteria as a function of activated sludge process organic loading and growth rate', *Water Science and Technology*, 55(1-2), pp. 291-297.

Kittinger, C., Lipp, M., Folli, B., Kirschner, A., Baumert, R., Galler, H., Grisold, A.J., Luxner, J., Weissenbacher, M., Farnleitner, A.H. and Zarfel, G. (2016) 'Enterobacteriaceae Isolated from the River Danube: Antibiotic Resistances, with a Focus on the Presence of ESBL and Carbapenemases', *PLOS ONE*, 11(11), p. e0165820.

Klappenbach, J.A., Saxman, P.R., Cole, J.R. and Schmidt, T.M. (2001) 'rrndb: the Ribosomal RNA Operon Copy Number Database', *Nucleic Acids Research*, 29(1), pp. 181-184.

Klein, E.Y., Van Boeckel, T.P., Martinez, E.M., Pant, S., Gandra, S., Levin, S.A., Goossens, H. and Laxminarayan, R. (2018) 'Global increase and geographic convergence in antibiotic consumption between 2000 and 2015', *Proceedings of the National Academy of Sciences*, 115(15), pp. E3463-E3470.

Klumper, U., Riber, L., Dechesne, A., Sannazzarro, A., Hansen, L.H., Sorensen, S.J. and Smets, B.F. (2015) 'Broad host range plasmids can invade an unexpectedly diverse fraction of a soil bacterial community', *Isme Journal*, 9(4), pp. 934-945.

Knapp, C.W., Lima, L., Olivares-Rieumont, S., Bowen, E., Werner, D. and Graham, D.W. (2012) 'Seasonal variations in antibiotic resistance gene transport in the Almendares River, Havana, Cuba', *Frontiers in Microbiology*, 3, p. 11.

Knapp, C.W., McCluskey, S.M., Singh, B.K., Campbell, C.D., Hudson, G. and Graham, D.W. (2011) 'Antibiotic Resistance Gene Abundances Correlate with Metal and Geochemical Conditions in Archived Scottish Soils', *PLoS One*, 6(11).

Kobayashi, N., Oshiki, M., Ito, T., Segawa, T., Hatamoto, M., Kato, T., Yamaguchi, T., Kubota, K., Takahashi, M., Iguchi, A., Tagawa, T., Okubo, T., Uemura, S., Harada, H., Motoyama, T., Araki, N. and Sano, D. (2017) 'Removal of human pathogenic viruses in a down-flow hanging sponge (DHS) reactor treating municipal wastewater and health risks associated with utilization of the effluent for agricultural irrigation', *Water Research*, 110, pp. 389-398.

Koczura, R., Krysiak, N., Taraszewska, A. and Mokracka, J. (2015) 'Coliform bacteria isolated from recreational lakes carry class 1 and class 2 integrons and virulence-associated genes', *Journal of Applied Microbiology*, 119(2), pp. 594-603.

Kozich, J.J., Westcott, S.L., Baxter, N.T., Highlander, S.K. and Schloss, P.D. (2013) 'Development of a Dual-Index Sequencing Strategy and Curation Pipeline for Analyzing Amplicon Sequence Data on the MiSeq Illumina Sequencing Platform', *Applied and Environmental Microbiology*, 79(17), pp. 5112-5120.

Kubota, K., Hayashi, M., Matsunaga, K., Iguchi, A., Ohashi, A., Li, Y.Y., Yamaguchi, T. and Harada, H. (2014) 'Microbial community composition of a down-flow hanging sponge (DHS) reactor combined with an up-flow anaerobic sludge blanket (UASB) reactor for the treatment of municipal sewage', *Bioresource Technology*, 151, pp. 144-150.

Kumarasamy, K.K., Toleman, M.A., Walsh, T.R., Bagaria, J., Butt, F., Balakrishnan, R., Chaudhary, U., Doumith, M., Giske, C.G., Irfan, S., Krishnan, P., Kumar, A.V., Maharjan, S., Mushtaq, S., Noorie, T., Paterson, D.L., Pearson, A., Perry, C., Pike, R., Rao, B., Ray, U., Sarma, J.B., Sharma, M., Sheridan, E., Thirunarayan, M.A., Turton, J., Upadhyay, S., Warner, M., Welfare, W., Livermore, D.M. and Woodford, N. (2010) 'Emergence of a new antibiotic resistance mechanism in India, Pakistan, and the UK: a molecular, biological, and epidemiological study', *The Lancet. Infectious diseases*, 10(9), pp. 597-602.

Kümmerer, K. (2009) 'Antibiotics in the aquatic environment – A review – Part I', *Chemosphere*, 75(4), pp. 417-434.

Kümmerer, K. and Henninger, A. (2003) 'Promoting resistance by the emission of antibiotics from hospitals and households into effluent', *Clinical Microbiology and Infection*, 9(12), pp. 1203-1214.

Lamba, M., Gupta, S., Shukla, R., Graham, D.W., Sreekrishnan, T.R. and Ahammad, S.Z. (2018) 'Carbapenem resistance exposures via wastewaters across New Delhi', *Environment International*, 119, pp. 302-308.

Lata, P., Ram, S., Agrawal, M. and Shanker, R. (2009) 'Enterococci in river Ganga surface waters: Propensity of species distribution, dissemination of antimicrobial-resistance and virulence-markers among species along landscape', *Bmc Microbiology*, 9, p. 10.

Laxminarayan, R., Duse, A., Wattal, C., Zaidi, A.K.M., Wertheim, H.F.L., Sumpradit, N., Vlieghe, E., Hara, G.L., Gould, I.M., Goossens, H., Greko, C., So, A.D., Bigdeli, M., Tomson, G., Woodhouse, W., Ombaka, E., Peralta, A.Q., Qamar, F.N., Mir, F., Kariuki, S., Bhutta, Z.A., Coates, A., Bergstrom, R., Wright, G.D., Brown, E.D. and Cars, O. (2013) 'Antibiotic resistance-the need for global solutions', *The Lancet. Infectious diseases*, 13(12), pp. 1057-1098.

Leavitt, A., Chmelnitsky, I., Colodner, R., Ofek, I., Carmeli, Y. and Navon-Venezia, S. (2009) 'Ertapenem Resistance among Extended-Spectrum- β -Lactamase-Producing *Klebsiella pneumoniae* Isolates', *Journal of Clinical Microbiology*, 47(4), pp. 969-974.

Leonard, A.F.C., Zhang, L., Balfour, A.J., Garside, R. and Gaze, W.H. (2015) 'Human recreational exposure to antibiotic resistant bacteria in coastal bathing waters', *Environment International*, 82, pp. 92-100.

Lessard, P. and Le Bihan, Y. (2003) '19 - Fixed film processes', in Mara, D. and Horan, N. (eds.) *Handbook of Water and Wastewater Microbiology*. London: Academic Press, pp. 317-336.

Leverstein-van Hall, M.A., Blok, H.E.M., Donders, A.R.T., Paauw, A., Fluit, A.C. and Verhoef, J. (2003) 'Multidrug resistance among Enterobacteriaceae is strongly associated with the presence of integrons and is independent of species or isolate origin', *Journal of Infectious Diseases*, 187(2), pp. 251-259.

Li, B., Qiu, Y., Zhang, J., Liang, P. and Huang, X. (2019) 'Conjugative potential of antibiotic resistance plasmids to activated sludge bacteria from wastewater treatment plants', *International Biodeterioration & Biodegradation*, 138, pp. 33-40.

Li, Y., Lv, Y., Xue, F., Zheng, B., Liu, J. and Zhang, J. (2015) 'Antimicrobial resistance surveillance of doripenem in China', *The Journal Of Antibiotics*, 68, p. 496.

Liao, J.H., Fang, C., Yu, J., Sathyagal, A., Willman, E. and Liu, W.T. (2017) 'Direct treatment of high-strength soft drink wastewater using a down-flow hanging sponge reactor: performance and microbial community dynamics', *Applied Microbiology and Biotechnology*, 101(14), pp. 5925-5936.

- Liu, B.B., Liu, H., Zhang, B. and Bi, J. (2013) 'Modeling Nutrient Release in the Tai Lake Basin of China: Source Identification and Policy Implications', *Environmental Management*, 51(3), pp. 724-737.
- Liu, Y.-Y., Wang, Y., Walsh, T.R., Yi, L.-X., Zhang, R., Spencer, J., Doi, Y., Tian, G., Dong, B., Huang, X., Yu, L.-F., Gu, D., Ren, H., Chen, X., Lv, L., He, D., Zhou, H., Liang, Z., Liu, J.-H. and Shen, J. (2015) 'Emergence of plasmid-mediated colistin resistance mechanism MCR-1 in animals and human beings in China: a microbiological and molecular biological study', *The Lancet Infectious Diseases*.
- Logan, B.E., Hermanowicz, S.W. and Parker, D.S. (1987) 'A Fundamental Model for Trickling Filter Process Design', *Journal (Water Pollution Control Federation)*, 59(12), pp. 1029-1042.
- Logan, L.K. and Weinstein, R.A. (2017) 'The Epidemiology of Carbapenem-Resistant Enterobacteriaceae: The Impact and Evolution of a Global Menace', *Journal of Infectious Diseases*, 215, pp. S28-S36.
- Looft, T., Johnson, T.A., Allen, H.K., Bayles, D.O., Alt, D.P., Stedtfeld, R.D., Sul, W.J., Stedtfeld, T.M., Chai, B.L., Cole, J.R., Hashsham, S.A., Tiedje, J.M. and Stanton, T.B. (2012) 'In-feed antibiotic effects on the swine intestinal microbiome', *Proceedings of the National Academy of Sciences of the United States of America*, 109(5), pp. 1691-1696.
- Loosdrecht, M.C.M.v., Nielsen, P.H., Lopez-Vazquez, C.M. and Damir Brdjanovic (2016) *Experimental methods in wastewater treatment* London: IWA Publishing.
- Lowbury, E.J.L., Lilly, H.A., Kidson, A., Ayliffe, G.A.J. and Jones, R.J. (1969) 'SENSITIVITY OF PSEUDOMONAS AERUGINOSA TO ANTIBIOTICS: EMERGENCE OF STRAINS HIGHLY RESISTANT TO CARBENICILLIN', *The Lancet*, 294(7618), pp. 448-452.
- Lu, S.Y., Zhang, Y.L., Geng, S.N., Li, T.Y., Ye, Z.M., Zhang, D.S., Zou, F. and Zhou, H.W. (2010) 'High Diversity of Extended-Spectrum Beta-Lactamase-Producing Bacteria in an Urban River Sediment Habitat', *Applied and Environmental Microbiology*, 76(17), pp. 5972-5976.
- Lüddecke, F., Heß, S., Gallert, C., Winter, J., Güde, H. and Löffler, H. (2015) 'Removal of total and antibiotic resistant bacteria in advanced wastewater treatment by ozonation in combination with different filtering techniques', *Water Research*, 69, pp. 243-251.
- Luo, Y., Yang, F.X., Mathieu, J., Mao, D.Q., Wang, Q. and Alvarez, P.J.J. (2014) 'Proliferation of Multidrug-Resistant New Delhi Metallo-beta-lactamase Genes in Municipal Wastewater Treatment Plants in Northern China', *Environmental Science & Technology Letters*, 1(1), pp. 26-30.

Mac Conell, E.F.A., Almeida, P.G.S., Martins, K.E.L., Araujo, J.C. and Chernicharo, C.A.L. (2015) 'Bacterial community involved in the nitrogen cycle in a down-flow sponge-based trickling filter treating UASB effluent', *Water Science and Technology*, 72(1), pp. 116-122.

MacFadden, D.R., McGough, S.F., Fisman, D., Santillana, M. and Brownstein, J.S. (2018) 'Antibiotic resistance increases with local temperature', *Nature Climate Change*, 8(6), pp. 510-514.

Machdar, I., Harada, H., Ohashi, A., Sekiguchi, Y., Okui, H. and Ueki, K. (1997) 'A novel and cost-effective sewage treatment system consisting of UASB pre-treatment and aerobic post-treatment units for developing countries', *Water Science and Technology*, 36(12), pp. 189-197.

Machdar, I., Muhammad, S., Onodera, T. and Syutsubo, K. (2018) 'A pilot-scale study on a down-flow hanging sponge reactor for septic tank sludge treatment', *Environmental Engineering Research*, 23(2), pp. 195-204.

Madoni, P. (2011) 'Protozoa in wastewater treatment processes: A minireview', *Italian Journal of Zoology*, 78(1), pp. 3-11.

Malaysian Water Association (2015) *Water Malaysia*.

Mallory, L.M., Yuk, C.S., Liang, L.N. and Alexander, M. (1983) 'Alternative prey: a mechanism for elimination of bacterial species by protozoa', *Applied and Environmental Microbiology*, 46(5), p. 1073.

Manaia, C.M., Macedo, G., Fatta-Kassinos, D. and Nunes, O.C. (2016) 'Antibiotic resistance in urban aquatic environments: can it be controlled?', *Applied Microbiology and Biotechnology*, 100(4), pp. 1543-1557.

Manti, A., Boi, P., Falcioni, T., Canonico, B., Ventura, A., Sisti, D., Pianetti, A., Balsamo, M. and Papa, S. (2008) 'Bacterial cell monitoring in wastewater treatment plants by flow cytometry', *Water Environment Research*, 80(4), pp. 346-354.

Mao, D.Q., Luo, Y., Mathieu, J., Wang, Q., Feng, L., Mu, Q.H., Feng, C.Y. and Alvarez, P.J.J. (2014) 'Persistence of Extracellular DNA in River Sediment Facilitates Antibiotic Resistance Gene Propagation', *Environmental Science & Technology*, 48(1), pp. 71-78.

Mara, D., Lane, J., Scott, B. and Trouba, D. (2010) 'Sanitation and Health', *Plos Medicine*, 7(11), p. 7.

Mara, D.D. (2003) 'Water, sanitation and hygiene for the health of developing nations', *Public Health*, 117(6), pp. 452-456.

Marshall, J., Molloy, R., Moss, G.W.J., Howe, J.R. and Hughes, T.E. (1995) 'THE JELLYFISH GREEN FLUORESCENT PROTEIN - A NEW TOOL FOR STUDYING ION-CHANNEL EXPRESSION AND FUNCTION', *Neuron*, 14(2), pp. 211-215.

Martínez, J.L. (2008) 'Antibiotics and antibiotic resistance genes in natural environments', *Science*, 321(5887), pp. 365-367.

Massoud, M.A., Tarhini, A. and Nasr, J.A. (2009) 'Decentralized approaches to wastewater treatment and management: Applicability in developing countries', *Journal of Environmental Management*, 90(1), pp. 652-659.

Mazel, D. (2006) 'Integrins: agents of bacterial evolution', *Nature Reviews Microbiology*, 4(8), pp. 608-620.

McMurdie, P.J. and Holmes, S. (2013) 'phyloseq: An R Package for Reproducible Interactive Analysis and Graphics of Microbiome Census Data', *Plos One*, 8(4), p. 11.

Metcalf & Eddy (2003) *Wastewater Engineering Treatment and Reuse*. New York: McGraw-Hill

Ministry of Environmental Protection (2002) *Discharge standard of pollutants for municipal wastewater treatment plant (GB18918-2002)*. Ministry of Environmental Protection of the People's Republic of China: People's Republic of China.

Ministry of Natural Resources and Environment (1992) *The enhancement and conservation of national environmental quality act 1992 (B.E. 2535)*. Thailand.

Mokracka, J., Koczura, R. and Kaznowski, A. (2012) 'Multiresistant Enterobacteriaceae with class 1 and class 2 integrons in a municipal wastewater treatment plant', *Water Research*, 46(10), pp. 3353-3363.

Moura, A., Pereira, C., Henriques, I. and Correia, A. (2012) 'Novel gene cassettes and integrons in antibiotic-resistant bacteria isolated from urban wastewaters', *Research in Microbiology*, 163(2), pp. 92-100.

Munck, C., Albertsen, M., Telke, A., Ellabaan, M., Nielsen, P.H. and Sommer, M.O.A. (2015) 'Limited dissemination of the wastewater treatment plant core resistome', *Nat Commun*, 6.

- Munir, M., Wong, K. and Xagorarakis, I. (2011) 'Release of antibiotic resistant bacteria and genes in the effluent and biosolids of five wastewater utilities in Michigan', *Water Research*, 45(2), pp. 681-693.
- Munita, J.M. and Arias, C.A. (2016) 'Mechanisms of Antibiotic Resistance', *Microbiology spectrum*, 4(2), pp. 10.1128/microbiolspec.VMBF-0016-2015.
- Musovic, S., Dechesne, A., Sørensen, J. and Smets, B.F. (2010) 'Novel Assay To Assess Permissiveness of a Soil Microbial Community toward Receipt of Mobile Genetic Elements', *Applied and Environmental Microbiology*, 76(14), p. 4813.
- Musovic, S., Oregaard, G., Kroer, N. and Sørensen, S.J. (2006) 'Cultivation-Independent Examination of Horizontal Transfer and Host Range of an IncP-1 Plasmid among Gram-Positive and Gram-Negative Bacteria Indigenous to the Barley Rhizosphere', *Applied and Environmental Microbiology*, 72(10), pp. 6687-6692.
- Muyzer, G. (1999) 'DGGE/TGGE a method for identifying genes from natural ecosystems', *Current Opinion in Microbiology*, 2(3), pp. 317-322.
- Nam, S.-W., Choi, D.-J., Kim, S.-K., Her, N. and Zoh, K.-D. (2014) 'Adsorption characteristics of selected hydrophilic and hydrophobic micropollutants in water using activated carbon', *Journal of Hazardous Materials*, 270, pp. 144-152.
- Nelson, R. (2003) 'Antibiotic development pipeline runs dry', *The Lancet*, 362(9397), pp. 1726-1727.
- Nikaido, H. (2009) 'Multidrug resistance in bacteria', *Annual review of biochemistry*, 78, pp. 119-146.
- Nishiyama, M., Ogura, Y., Hayashi, T. and Suzuki, Y. (2017) 'Antibiotic Resistance Profiling and Genotyping of Vancomycin-Resistant Enterococci Collected from an Urban River Basin in the Provincial City of Miyazaki, Japan', *Water*, 9(2), p. 17.
- Nogales, B., Timmis, K.N., Nedwell, D.B. and Osborn, A.M. (2002) 'Detection and Diversity of Expressed Denitrification Genes in Estuarine Sediments after Reverse Transcription-PCR Amplification from mRNA', *Applied and Environmental Microbiology*, 68(10), p. 5017.
- Novo, A. and Manaia, C.M. (2010) 'Factors influencing antibiotic resistance burden in municipal wastewater treatment plants', *Applied Microbiology and Biotechnology*, 87(3), pp. 1157-66.

Oh, J. and Silverstein, J. (1999) 'Oxygen inhibition of activated sludge denitrification', *Water Research*, 33(8), pp. 1925-1937.

Okaka, F.O. and Odhiambo, B.D.O. (2018) 'Relationship between Flooding and Out Break of Infectious Diseases in Kenya: A Review of the Literature', *Journal of environmental and public health*, 2018, pp. 5452938-5452938.

Onodera, T., Kanaya, G., Syutsubo, K., Miyaoka, Y., Hatamoto, M. and Yamaguchi, T. (2015) 'Spatial changes in carbon and nitrogen stable isotope ratios of sludge and associated organisms in a biological sewage treatment system', *Water Research*, 68, pp. 387-393.

Onodera, T., Matsunaga, K., Kubota, K., Taniguchi, R., Harada, H., Syutsubo, K., Okubo, T., Uemura, S., Araki, N., Yamada, M., Yamauchi, M. and Yamaguchi, T. (2013) 'Characterization of the retained sludge in a down-flow hanging sponge (DHS) reactor with emphasis on its low excess sludge production', *Bioresource Technology*, 136, pp. 169-175.

Onodera, T., Yoochatchaval, W., Sumino, H., Mizuochi, M., Okadera, T., Fujita, T., Banjongproo, P. and Syutsubo, K. (2014) 'Pilot-scale experiment of down-flow hanging sponge for direct treatment of low-strength municipal wastewater in Bangkok, Thailand', *Bioprocess Biosyst Eng*, 37(11), pp. 2281-7.

Osaka, T., Shirotani, K., Yoshie, S. and Tsuneda, S. (2008) 'Effects of carbon source on denitrification efficiency and microbial community structure in a saline wastewater treatment process', *Water Research*, 42(14), pp. 3709-3718.

Ouyang, W.-Y., Huang, F.-Y., Zhao, Y., Li, H. and Su, J.-Q. (2015) 'Increased levels of antibiotic resistance in urban stream of Jiulongjiang River, China', *Applied Microbiology and Biotechnology*, 99(13), pp. 5697-5707.

Pal, C., Papp, B. and Lercher, M.J. (2005) 'Adaptive evolution of bacterial metabolic networks by horizontal gene transfer', *Nature Genetics*, 37(12), pp. 1372-1375.

Pangare, G., Das, B., Arriens, W.L. and Makin, I. (2014) *Waterwealth? Investing in basin management in Asia and the Pacific*. International Union for Conservation of Nature and Asian Development Bank Academic Foundation, N.D., India.

Park, E., Mancl, K.M., Tuovinen, O.H., Bisesi, M.S. and Lee, J. (2016) 'Ensuring safe reuse of residential wastewater: reduction of microbes and genes using peat biofilter and batch chlorination in an on-site treatment system', *Journal of Applied Microbiology*, 121(6), pp. 1777-1788.

Parkinson, J. (2005) *Decentralised domestic wastewater and faecal sludge management in Bangladesh*.

Parkinson, J. and Tayler, K. (2003) 'Decentralized wastewater management in peri-urban areas in low-income countries', *Environment and Urbanization*, 15(1), pp. 75-89.

Partridge, S.R., Tsafnat, G., Coiera, E. and Iredell, J.R. (2009) 'Gene cassettes and cassette arrays in mobile resistance integrons', *Fems Microbiology Reviews*, 33(4), pp. 757-784.

Pauli, W., Jax, K. and Berger, S. (2001) 'Protozoa in Wastewater Treatment: Function and Importance', in Beek, B. (ed.) *Biodegradation and Persistence*. Berlin, Heidelberg: Springer Berlin Heidelberg, pp. 203-252.

Pimentel, D., Cooperstein, S., Randell, H., Filiberto, D., Sorrentino, S., Kaye, B., Nicklin, C., Yagi, J., Brian, J., O'Hern, J., Habas, A. and Weinstein, C. (2007) 'Ecology of Increasing Diseases: Population Growth and Environmental Degradation', *Human Ecology*, 35(6), pp. 653-668.

Polesel, F., Andersen, H.R., Trapp, S. and Plósz, B.G. (2016) 'Removal of Antibiotics in Biological Wastewater Treatment Systems—A Critical Assessment Using the Activated Sludge Modeling Framework for Xenobiotics (ASM-X)', *Environmental Science & Technology*, 50(19), pp. 10316-10334.

Poole, K. (2012) 'Bacterial stress responses as determinants of antimicrobial resistance', *Journal of Antimicrobial Chemotherapy*, 67(9), pp. 2069-2089.

Popowska, M. and Krawczyk-Balska, A. (2013) 'Broad-host-range IncP-1 plasmids and their resistance potential', *Frontiers in Microbiology*, 4, p. 8.

Price, M.N., Dehal, P.S. and Arkin, A.P. (2010) 'FastTree 2-Approximately Maximum-Likelihood Trees for Large Alignments', *Plos One*, 5(3), p. 10.

Prim, N., Rivera, A., Rodriguez-Navarro, J., Espanol, M., Turbau, M., Coll, P. and Mirelis, B. (2016) 'Detection of mcr-1 colistin resistance gene in polyclonal Escherichia coli isolates in Barcelona, Spain, 2012 to 2015', *Euro surveillance : bulletin Europeen sur les maladies transmissibles = European communicable disease bulletin*, 21(13).

Pruden, A., Larsson, D.G.J., Amézquita, A., Collignon, P., Brandt, K.K., Graham, D.W., Lazorchak, J.M., Suzuki, S., Silley, P., Snape, J.R., Topp, E., Zhang, T. and Yong-Guan, Z. (2013) 'Management Options for Reducing the Release of Antibiotics and Antibiotic

Resistance Genes to the Environment', *Environmental Health Perspectives (Online)*, 121(8), p. 878.

Pruden, A., Pei, R., Storteboom, H. and Carlson, K.H. (2006) 'Antibiotic Resistance Genes as Emerging Contaminants: Studies in Northern Colorado', *Environmental Science & Technology*, 40(23), pp. 7445-7450.

Quintela-Baluja, M., Abouelnaga, M., Romalde, J., Su, J.-Q., Yu, Y., Gomez-Lopez, M., Smets, B., Zhu, Y.-G. and Graham, D.W. (2019) 'Spatial ecology of a wastewater network defines the antibiotic resistance genes in downstream receiving waters', *Water Research*, 162, pp. 347-357.

Quintela-Baluja, M., Chan, C.W., Ezzat Alnakip, M., Abouelnaga, M. and Graham, D.W. (2015) 'Sanitation, water quality and antibiotic resistance dissemination', in *The Battle Against Microbial Pathogens: Basic Science, Technological Advances and Educational Programs*. Spain: Formatex, pp. 965-975.

R Core Team (2013) *R: A language and environment for statistical computing* [Computer program]. Available at: <http://www.R-project.org/>.

Rahube, T.O. and Yost, C.K. (2010) 'Antibiotic resistance plasmids in wastewater treatment plants and their possible dissemination into the environment', *African Journal of Biotechnology*, 9(54), pp. 9183-9190.

Ramette, A. (2007) 'Multivariate analyses in microbial ecology', *FEMS Microbiology Ecology*, 62(2), pp. 142-160.

Reichhardt, C., Lim, J.Y., Rice, D., Fong, J.N. and Cegelski, L. (2014) 'Structure and Function of Bacterial Biofilms by Solid-State NMR', *Biophysical Journal*, 106(2), pp. 192A-192A.

Review on AMR (2014) *Antimicrobial resistance: Tackling a crisis for the health and wealth of nations*. Available at: https://amr-review.org/sites/default/files/AMR%20Review%20Paper%20-%20Tackling%20a%20crisis%20for%20the%20health%20and%20wealth%20of%20nations_1.pdf (Accessed: 28 September).

Review on AMR (2015) 'Antimicrobial in agriculture and the environment: Reducing unnecessary use and waste'.

Review on AMR (2016a) *Infection prevention, control and surveillance: Limiting the development and spread of drug resistance*. Available at: <https://amr-review.org>.

Review on AMR (2016b) *Tackling drug-resistant infections globally: Final report and recommendations*. Available at: <https://amr-review.org>.

Robinson, T.P., Bu, D.P., Carrique-Mas, J., Fevre, E.M., Gilbert, M., Grace, D., Hay, S.I., Jiwakanon, J., Kakkar, M., Kariuki, S., Laxminarayan, R., Lubroth, J., Magnusson, U., Ngoc, P.T., Van Boeckel, T.P. and Woolhouse, M.E.J. (2016) 'Antibiotic resistance is the quintessential One Health issue', *Transactions of the Royal Society of Tropical Medicine and Hygiene*, 110(7), pp. 377-380.

Roura, E., Homedes, J. and Klasing, K.C. (1992) 'Prevention of Immunologic Stress Contributes to the Growth-Permitting Ability of Dietary Antibiotics in Chicks', *The Journal of Nutrition*, 122(12), pp. 2383-2390.

Rysz, M., Mansfield, W.R., Fortner, J.D. and Avarez, P.J.J. (2013) 'Tetracycline Resistance Gene Maintenance under Varying Bacterial Growth Rate, Substrate and Oxygen Availability, and Tetracycline Concentration', *Environmental Science & Technology*, 47(13), pp. 6995-7001.

Saminathan, S.K.M., Galvez-Cloutier, R. and Kamal, N. (2013) 'Performance and Microbial Diversity of Aerated Trickling Biofilter Used for Treating Cheese Industry Wastewater', *Applied Biochemistry and Biotechnology*, 170(1), pp. 149-163.

Schipper, L.A., Robertson, W.D., Gold, A.J., Jaynes, D.B. and Cameron, S.C. (2010) 'Denitrifying bioreactors—An approach for reducing nitrate loads to receiving waters', *Ecological Engineering*, 36(11), pp. 1532-1543.

Schloss, P.D., Westcott, S.L., Ryabin, T., Hall, J.R., Hartmann, M., Hollister, E.B., Lesniewski, R.A., Oakley, B.B., Parks, D.H., Robinson, C.J., Sahl, J.W., Stres, B., Thallinger, G.G., Van Horn, D.J. and Weber, C.F. (2009) 'Introducing mothur: Open-Source, Platform-Independent, Community-Supported Software for Describing and Comparing Microbial Communities', *Applied and Environmental Microbiology*, 75(23), pp. 7537-7541.

Schluter, A., Szczepanowski, R., Puhler, A. and Top, E.M. (2007) 'Genomics of IncP-1 antibiotic resistance plasmids isolated from wastewater treatment plants provides evidence for a widely accessible drug resistance gene pool', *Fems Microbiology Reviews*, 31(4), pp. 449-477.

- Seiler, C. and Berendonk, T.U. (2012) 'Heavy metal driven co-selection of antibiotic resistance in soil and water bodies impacted by agriculture and aquaculture', *Frontiers in Microbiology*, 3, p. 10.
- Shackle, V.J., Freeman, C. and Reynolds, B. (2000) 'Carbon supply and the regulation of enzyme activity in constructed wetlands', *Soil Biology & Biochemistry*, 32(13), pp. 1935-1940.
- Shaikh, S., Fatima, J., Shakil, S., Rizvi, S.M.D. and Kamal, M.A. (2015) 'Antibiotic resistance and extended spectrum beta-lactamases: Types, epidemiology and treatment', *Saudi Journal of Biological Sciences*, 22(1), pp. 90-101.
- Shannon, C.E. (1948) 'A mathematical theory of communication', *The Bell System Technical Journal*, 27(3), pp. 379-423.
- Silver, L.L. (2011) 'Challenges of Antibacterial Discovery', *Clinical Microbiology Reviews*, 24(1), pp. 71-109.
- Simpson, E.H. (1949) 'Measurement of Diversity', *Nature*, 163(4148), pp. 688-688.
- Singer, A.C., Shaw, H., Rhodes, V. and Hart, A. (2016) 'Review of Antimicrobial Resistance in the Environment and Its Relevance to Environmental Regulators', *Frontiers in Microbiology*, 7, p. 22.
- Singh, P.K. (2017) 'One Health approach to tackle antimicrobial resistance in South East Asia', *BMJ*, 358.
- Smith, M.S., Yang, R.K., Knapp, C.W., Niu, Y., Peak, N., Hanfelt, M.M., Galland, J.C. and Graham, D.W. (2004) 'Quantification of tetracycline resistance genes in feedlot lagoons by real-time PCR', *Applied and environmental microbiology*, 70(12), pp. 7372-7377.
- Soda, S., Otsuki, H., Inoue, D., Tsutsui, H., Sei, K. and Ike, M. (2008) 'Transfer of Antibiotic Multiresistant Plasmid RP4 from Escherichia coli to Activated Sludge Bacteria', *Journal of Bioscience and Bioengineering*, 106(3), pp. 292-296.
- Soki, J., Edwards, R., Hedberg, M., Fang, H., Nagy, E., Nord, C.E. and Res, E.S.G.A. (2006) 'Examination of *cfiA*-mediated carbapenem resistance in *Bacteroides fragilis* strains from a European antibiotic susceptibility survey', *International Journal of Antimicrobial Agents*, 28(6), pp. 497-502.

- Song, K., Harper, W.F., Hori, T., Riya, S., Hosomi, M. and Terada, A. (2015) 'Impact of carbon sources on nitrous oxide emission and microbial community structure in an anoxic/oxic activated sludge system', *Clean Technologies and Environmental Policy*, 17(8), pp. 2375-2385.
- Stephenson, T., Reid, E., Avery, L.M. and Jefferson, B. (2013) 'Media surface properties and the development of nitrifying biofilms in mixed cultures for wastewater treatment', *Process Safety and Environmental Protection*, 91(4), pp. 321-324.
- Stokes, H.W. and Gillings, M.R. (2011) 'Gene flow, mobile genetic elements and the recruitment of antibiotic resistance genes into Gram-negative pathogens', *Fems Microbiology Reviews*, 35(5), pp. 790-819.
- Stokes, H.W., Holmes, A.J., Nield, B.S., Holley, M.P., Nevalainen, K.M.H., Mabbutt, B.C. and Gillings, M.R. (2001) 'Gene cassette PCR: Sequence-independent recovery of entire genes from environmental DNA', *Applied and Environmental Microbiology*, 67(11), pp. 5240-5246.
- Stretton, S., Techkarnjanaruk, S., McLennan, A.M. and Goodman, A.E. (1998) 'Use of green fluorescent protein to tag and investigate gene expression in marine bacteria', *Applied and environmental microbiology*, 64(7), pp. 2554-2559.
- Su, J.Q., Wei, B., Ou-Yang, W.Y., Huang, F.Y., Zhao, Y., Xu, H.J. and Zhu, Y.G. (2015) 'Antibiotic Resistome and Its Association with Bacterial Communities during Sewage Sludge Composting', *Environmental Science & Technology*, 49(12), pp. 7356-7363.
- Sustainable sanitation alliance (2008) 'Towards more sustainable sanitation solutions'. Available at: <https://www.susana.org/>.
- Tan, C., Ma, F., Li, A., Qiu, S. and Li, J. (2013) 'Evaluating the Effect of Dissolved Oxygen on Simultaneous Nitrification and Denitrification in Polyurethane Foam Contact Oxidation Reactors', *Water Environment Research*, 85(3), pp. 195-202.
- Tandukar, M., Uemura, S., Machdar, I., Ohashi, A. and Harada, H. (2005) 'A low-cost municipal sewage treatment system with a combination of UASB and the "fourth-generation" downflow hanging sponge reactors', *Water Science and Technology*, 52(1-2), pp. 323-329.
- Tanikawa, D., Yamashita, S., Kataoka, T., Sonaka, H., Hirakata, Y., Hatamoto, M. and Yamaguchi, T. (2019) 'Non-aerated single-stage nitrogen removal using a down-flow hanging sponge reactor as post-treatment for nitrogen-rich wastewater treatment', *Chemosphere*, 233, pp. 645-651.

Taucer-Kapteijn, M., Hoogenboezem, W., Heiligers, L., de Bolster, D. and Medema, G. (2016) 'Screening municipal wastewater effluent and surface water used for drinking water production for the presence of ampicillin and vancomycin resistant enterococci', *International Journal of Hygiene and Environmental Health*, 219(4-5), pp. 437-442.

Tendencia, E.A. and de la Peña, L.D. (2001) 'Antibiotic resistance of bacteria from shrimp ponds', *Aquaculture*, 195(3), pp. 193-204.

Tennstedt, T., Szczepanowski, R., Braun, S., Puhler, A. and Schluter, A. (2003) 'Occurrence of integron-associated resistance gene cassettes located on antibiotic resistance plasmids isolated from a wastewater treatment plant', *Fems Microbiology Ecology*, 45(3), pp. 239-252.

The Guardian (2019) 'Antibiotic resistance as big a threat as climate change', *The Guardian newspaper*edn). [Online] Available at: <https://www.theguardian.com>.

Thomas, C.M. (1981) 'Molecular genetics of broad host range plasmid RK2', *Plasmid*, 5(1), pp. 10-19.

Tran, N.H., Chen, H.J., Do, T.V., Reinhard, M., Ngo, H.H., He, Y.L. and Gin, K.Y.H. (2016a) 'Simultaneous analysis of multiple classes of antimicrobials in environmental water samples using SPE coupled with UHPLC-ESI-MS/MS and isotope dilution', *Talanta*, 159, pp. 163-173.

Tran, N.H., Chen, H.J., Reinhard, M., Mao, F. and Gin, K.Y.H. (2016b) 'Occurrence and removal of multiple classes of antibiotics and antimicrobial agents in biological wastewater treatment processes', *Water Research*, 104, pp. 461-472.

Tsien, R.Y. (1998) 'THE GREEN FLUORESCENT PROTEIN', *Annual Review of Biochemistry*, 67(1), pp. 509-544.

Turner, P.E. (2004) 'Phenotypic Plasticity in Bacterial Plasmids', *Genetics*, 167(1), p. 9.

Uemura, S., Suzuki, S., Abe, K., Kubota, K., Yamaguchi, T., Ohashi, A., Takemura, Y. and Harada, H. (2010) 'Removal of organic substances and oxidation of ammonium nitrogen by a down-flow hanging sponge (DHS) reactor under high salinity conditions', *Bioresource Technology*, 101(14), pp. 5180-5185.

Uemura, S., Suzuki, S., Maruyama, Y. and Harada, H. (2012) 'Direct Treatment of Settled Sewage by DHS Reactors with Different Sizes of Sponge Support Media', *International Journal of Environmental Research*, 6(1), pp. 25-32.

UNICEF (2012) *Pneumonia and diarrhoea: Tackling the deadliest diseases for the world's poorest children*. New York: United Nations Children's Fund Nations, U. [Online]. Available at: <https://data.unicef.org>.

United Nations (2015a) *A 10 year story the water for life decade decade 2005-2015*. United Nations Office. [Online]. Available at: <https://www.un.org/waterforlifedecade/pdf/WaterforLifeENG.pdf>.

United Nations (2015b) *Sustainable Development Goals (SDGs)*. New York: United Nations publishing, U.N.

United Nations (2016) *The Sustainable Development Goals Report 2016*. New York: United Nations Department of Public Information. [Online]. Available at: <http://unstats.un.org/sdgs/report/2016>.

United Nations (2018) *Antimicrobial Resistance in the Environment*. Available at: <http://www.fao.org/3/BU656en/bu656en.pdf>.

United Nations ESCAP (2013) *The Status of the Water-Food-Energy Nexus in Asia and the Pacific*. Thailand: United Nations publication, U.N. [Online]. Available at: <https://www.unescap.org>.

Valentín-Vargas, A., Toro-Labrador, G. and Massol-Deyá, A.A. (2012) 'Bacterial Community Dynamics in Full-Scale Activated Sludge Bioreactors: Operational and Ecological Factors Driving Community Assembly and Performance', *PLOS ONE*, 7(8), p. e42524.

van Hoek, A.H.A.M., Mevius, D., Guerra, B., Mullany, P., Roberts, A.P. and Aarts, H.J.M. (2011) 'Acquired Antibiotic Resistance Genes: An Overview', *Frontiers in Microbiology*, 2, p. 203.

Vanderdrift, C., Vanseggelen, E., Stumm, C., Hol, W. and Tuinte, J. (1977) 'REMOVAL OF ESCHERICHIA-COLI IN WASTEWATER BY ACTIVATED-SLUDGE', *Applied and Environmental Microbiology*, 34(3), pp. 315-319.

Vaz-Moreira, I., Nunes, O.C. and Manaia, C.M. (2011) 'Diversity and antibiotic resistance patterns of Sphingomonadaceae isolates from drinking water', *Applied and environmental microbiology*, 77(16), pp. 5697-5706.

Ventola, C.L. (2015) 'The Antibiotic Resistance Crisis: Part 1: Causes and Threats', *Pharmacy and Therapeutics*, 40(4), pp. 277-283.

Verraes, C., Van Boxtael, S., Van Meervenne, E., Van Coillie, E., Butaye, P., Catry, B., de Schaetzen, M.-A., Van Huffel, X., Imberechts, H., Dierick, K., Daube, G., Saegerman, C., De Block, J., Dewulf, J. and Herman, L. (2013) 'Antimicrobial resistance in the food chain: a review', *International journal of environmental research and public health*, 10(7), pp. 2643-2669.

Viswanathan, P. and Bahinipati, C.S. (2016) *Water Security Challenges of South and South East Asia: Mainstreaming Local Governance Institutions*.

Wagner, M., Loy, A., Nogueira, R., Purkhold, U., Lee, N. and Daims, H. (2002) 'Microbial community composition and function in wastewater treatment plants', *Antonie van Leeuwenhoek*, 81(1), pp. 665-680.

Wales, A.D. and Davies, R.H. (2015) 'Co-Selection of Resistance to Antibiotics, Biocides and Heavy Metals, and Its Relevance to Foodborne Pathogens', *Antibiotics-Basel*, 4(4), pp. 567-604.

Walsh, T.R., Weeks, J., Livermore, D.M. and Toleman, M.A. (2011) 'Dissemination of NDM-1 positive bacteria in the New Delhi environment and its implications for human health: an environmental point prevalence study', *The Lancet Infectious Diseases*, 11(5), pp. 355-362.

Wang, J., Gong, B., Huang, W., Wang, Y. and Zhou, J. (2017a) 'Bacterial community structure in simultaneous nitrification, denitrification and organic matter removal process treating saline mustard tuber wastewater as revealed by 16S rRNA sequencing', *Bioresource Technology*, 228, pp. 31-38.

Wang, R., van Dorp, L., Shaw, L.P., Bradley, P., Wang, Q., Wang, X., Jin, L., Zhang, Q., Liu, Y., Rieux, A., Dorai-Schneiders, T., Weinert, L.A., Iqbal, Z., Didelot, X., Wang, H. and Balloux, F. (2018) 'The global distribution and spread of the mobilized colistin resistance gene *mcr-1*', *Nature communications*, 9(1), pp. 1179-1179.

Wang, Z., Ma, H., Chu, B. and Hsiao, B.S. (2017b) 'Super-hydrophobic polyurethane sponges for oil absorption', *Separation Science and Technology*, 52(2), pp. 221-227.

Wang, Z., Zhang, X.-X., Huang, K., Miao, Y., Shi, P., Liu, B., Long, C. and Li, A. (2013) 'Metagenomic Profiling of Antibiotic Resistance Genes and Mobile Genetic Elements in a Tannery Wastewater Treatment Plant', *PLoS One*, 8(10).

Watari, T., Mai, T.C., Tanikawa, D., Hirakata, Y., Hatamoto, M., Syutsubo, K., Fukuda, M., Nguyen, N.B. and Yamaguchi, T. (2017) 'Development of downflow hanging sponge (DHS) reactor as post treatment of existing combined anaerobic tank treating natural rubber processing wastewater', *Water Science and Technology*, 75(1), pp. 57-68.

Watari, T., Thanh, N.T., Tsuruoka, N., Tanikawa, D., Kuroda, K., Huong, N.L., Tan, N.M., Hai, H.T., Hatamoto, M., Syutsubo, K., Fukuda, M. and Yamaguchi, T. (2016) 'Development of a BR-UASB-DHS system for natural rubber processing wastewater treatment', *Environmental Technology*, 37(4), pp. 459-465.

Wen, Q., Yang, L., Zhao, Y., Huang, L. and Chen, Z. (2018) 'Insight into effects of antibiotics on reactor performance and evolutions of antibiotic resistance genes and microbial community in a membrane reactor', *Chemosphere*.

White, P.A., McIver, C.J. and Rawlinson, W.D. (2001) 'Integrins and gene cassettes in the Enterobacteriaceae', *Antimicrobial Agents and Chemotherapy*, 45(9), pp. 2658-2661.

Whitman, W.B., Rainey, F., Kämpfer, P., Trujillo, M., Chun, J., DeVos, P., Hedlund, B., Dedysh, S., Bernardet, J.-F. and Bowman, J.P. (2015) 'Flavobacterium', in *Bergey's Manual of Systematics of Archaea and Bacteria*. pp. 1-75.

WHO (2001) *WHO Global Strategy for Containment of Antimicrobial Resistance*. Available at: <http://www.who.int> (Accessed: 29 December).

WHO (2014) *Antimicrobial resistance: An emerging water, sanitation and hygiene issue*. Available at: <http://www.who.int> (Accessed: 4 Jan).

WHO (2015a) *Global action plan on antimicrobial resistance*. Available at: <https://www.who.int/antimicrobial-resistance/publications/global-action-plan/en/>.

WHO (2015b) *Progress on sanitation and drinking water*.

WHO (2017) *Progress on drinking water, sanitation and hygiene*. Available at: <http://www.unwater.org/publications/whounicef-joint-monitoring-program-water-supply-sanitation-hygiene-jmp-2017-update-sdg-baselines/>.

WHO and UNICEF (2006) *Meeting the MDG drinking water and sanitation target the urban and rural challenge of the decade*. Switzerland: World Health Organisation and UNICEF.

Willemsen, I., Oome, S., Verhulst, C., Pettersson, A., Verduin, K. and Kluytmans, J. (2015) 'Trends in Extended Spectrum Beta-Lactamase (ESBL) Producing Enterobacteriaceae and ESBL Genes in a Dutch Teaching Hospital, Measured in 5 Yearly Point Prevalence Surveys (2010-2014)', *Plos One*, 10(11), p. 10.

William, H.G., Stephen, M.K., Larsson, D.G.J., Xian-Zhi, L., Joseph, A.R., Pascal, S., Kornelia, S., Mohammed, T., Ed, T., Elizabeth, M.W., Gerard, D.W. and Yong-Guan, Z. (2013) 'Influence of Humans on Evolution and Mobilization of Environmental Antibiotic Resistome', *Emerging Infectious Disease journal*, 19(7).

World Bank (2018) 'Decline of Global Extreme Poverty Continues but Has Slowed: World Bank' Howton, E. The World Bank. Available at: <https://www.worldbank.org/en/news>.

Wright, G.D. (2010) 'Antibiotic resistance in the environment: a link to the clinic?', *Current Opinion in Microbiology*, 13(5), pp. 589-594.

Wright, G.D. (2014) 'Something old, something new: revisiting natural products in antibiotic drug discovery', *Canadian Journal of Microbiology*, 60(3), pp. 147-154.

Wu, Y., Cui, E., Zuo, Y., Cheng, W., Rensing, C. and Chen, H. (2016) 'Influence of two-phase anaerobic digestion on fate of selected antibiotic resistance genes and class I integrons in municipal wastewater sludge', *Bioresource Technology*, 211, pp. 414-421.

Xu, Z.S. and Chai, X.L. (2017) 'Effect of weight ratios of PHBV/PLA polymer blends on nitrate removal efficiency and microbial community during solid-phase denitrification', *International Biodeterioration & Biodegradation*, 116, pp. 175-183.

Yaegar R.G. (1996) 'Protozoa: Structure, Classification, Growth, and Development', in *Medical Microbiology*. Univeristy of Texas Medical Branch. Available at: <https://www.ncbi.nlm.nih.gov/books/NBK8325/>.

Yang, D., Wang, J., Qiu, Z., Jin, M., Shen, Z., Chen, Z., Wang, X., Zhang, B. and Li, J.-W. (2013a) 'Horizontal transfer of antibiotic resistance genes in a membrane bioreactor', *Journal of Biotechnology*, 167(4), pp. 441-447.

Yang, F.X., Mao, D.Q., Zhou, H., Wang, X.L. and Luo, Y. (2016) 'Propagation of New Delhi Metallo-beta-lactamase Genes (bla(NDM-1)) from a Wastewater Treatment Plant to Its Receiving River', *Environmental Science & Technology Letters*, 3(4), pp. 138-143.

Yang, X.-e., Wu, X., Hao, H.-l. and He, Z.-l. (2008) 'Mechanisms and assessment of water eutrophication', *Journal of Zhejiang University. Science. B*, 9(3), pp. 197-209.

Yang, Y., Li, B., Ju, F. and Zhang, T. (2013b) 'Exploring Variation of Antibiotic Resistance Genes in Activated Sludge over a Four-Year Period through a Metagenomic Approach', *Environmental Science & Technology*, 47(18), p. 10197.

Yates, T., Allen, J., Leandre Joseph, M. and Lantagne, D. (2017) *WASH interventions in disease outbreak response*. United Kingdom: Oxfam.

Yaya, S., Hudani, A., Udenigwe, O., Shah, V., Ekholuenetale, M. and Bishwajit, G. (2018) 'Improving Water, Sanitation and Hygiene Practices, and Housing Quality to Prevent Diarrhea among Under-Five Children in Nigeria', *Tropical medicine and infectious disease*, 3(2), p. 41.

Yoon, S., Sanford, R.A. and Löffler, F.E. (2013) 'Shewanella spp. Use Acetate as an Electron Donor for Denitrification but Not Ferric Iron or Fumarate Reduction', *Applied and Environmental Microbiology*, 79(8), pp. 2818-2822.

Yuan, Q.B., Guo, M.T., Wei, W.J. and Yang, J. (2016) 'Reductions of bacterial antibiotic resistance through five biological treatment processes treated municipal wastewater', *Environmental Science and Pollution Research*, 23(19), pp. 19495-19503.

Zhang, S.H., Lv, X., Han, B., Gu, X., Wang, P.F., Wang, C. and He, Z. (2015) 'Prevalence of antibiotic resistance genes in antibiotic-resistant Escherichia coli isolates in surface water of Taihu Lake Basin, China', *Environmental Science and Pollution Research*, 22(15), pp. 11412-11421.

Zhang, X.-x., Zhang, T. and Fang, H.H. (2009a) 'Antibiotic resistance genes in water environment', *Applied Microbiology and Biotechnology*, 82(3), pp. 397-414.

Zhang, X.X., Zhang, T., Zhang, M., Fang, H.H.P. and Cheng, S.P. (2009b) 'Characterization and quantification of class 1 integrons and associated gene cassettes in sewage treatment plants', *Applied Microbiology and Biotechnology*, 82(6), pp. 1169-1177.

Zhang, Y., Marrs, C.F., Simon, C. and Xi, C. (2009c) 'Wastewater treatment contributes to selective increase of antibiotic resistance among Acinetobacter spp', *Science of The Total Environment*, 407(12), pp. 3702-3706.

Zhang, Y.Y., Zhuang, Y., Geng, J.J., Ren, H.Q., Xu, K. and Ding, L.L. (2016) 'Reduction of antibiotic resistance genes in municipal wastewater effluent by advanced oxidation processes', *Science of the Total Environment*, 550, pp. 184-191.

Zhao, J., Wu, J., Li, X., Wang, S., Hu, B. and Ding, X. (2017) 'The Denitrification Characteristics and Microbial Community in the Cathode of an MFC with Aerobic Denitrification at High Temperatures', *Frontiers in microbiology*, 8, pp. 9-9.

Zhu, Y.-G., Johnson, T.A., Su, J.-Q., Qiao, M., Guo, G.-X., Stedtfeld, R.D., Hashsham, S.A. and Tiedje, J.M. (2013) 'Diverse and abundant antibiotic resistance genes in Chinese swine farms', *Proceedings of the National Academy of Sciences of the United States of America*, 110(9), p. 3435.

Zhu, Y.-G., Zhao, Y., Li, B., Huang, C.-L., Zhang, S.-Y., Yu, S., Chen, Y.-S., Zhang, T., Gillings, M.R. and Su, J.-Q. (2017) 'Continental-scale pollution of estuaries with antibiotic resistance genes', *Nature Microbiology*, 2, p. 16270.

Zhuang, Y., Ren, H., Geng, J., Zhang, Y., Zhang, Y., Ding, L. and Xu, K. (2015) 'Inactivation of antibiotic resistance genes in municipal wastewater by chlorination, ultraviolet, and ozonation disinfection', *Environmental Science and Pollution Research*, 22(9), pp. 7037-7044.